# Repair of DNA Interstrand Crosslinks as a Mechanism of Clinical Resistance to Platinum Drugs in Ovarian Cancer

*Pamela Win Shamai*

Thesis Submitted for the Degree of Doctor of Philosophy

Department of Oncology
University College London

2006





ProQuest LLC
789 East Eisenhower Parkway
P.O. Box 1346
Ann Arbor, MI 48106-1346

**Abstract**

Despite improvements in tumour response and survival following platinum based therapy in ovarian cancer, both intrinsic and acquired drug resistance remain a significant problem. Mechanisms of acquired drug resistance have been studied extensively in ovarian cancer cells in culture following repeated drug exposure however the relevance of these mechanisms to the clinical situation still needs to be clearly defined. Studies in clinical material have been hampered by the unavailability of sensitive methods to detect the critical drug-induced effects in individual cells. Recently, a modification of the single cell gel electrophoresis (comet) assay has been developed which allows for the first time the sensitive detection of DNA interstrand crosslinks in both tumour and normal cells derived directly from clinical material. In this study the role of DNA crosslink repair as a potential mechanism of clinical resistance to platinum drugs has been examined. Methods for isolating ovarian tumour cells and mesothelial (normal) cells from ascitic fluid, and to prepare a single cell suspension from primary ovarian tumour tissue from surgery have been established. Cells treated *ex vivo* with cisplatin were examined for crosslink formation and repair (unhooking) using the comet assay. No significant difference in the peak level of crosslinking was observed between tumour and mesothelial cells from an individual patient, or between patients either untreated or previously treated with platinum-based therapy. In the majority of tumours from nine untreated patients little or no repair of crosslinks was evident at 24 hours (mean of 13.6% repair) with seven patients showing less than 10% repair. In contrast, in the majority of ten treated patients a high level of repair was observed in tumour cells (mean 46.5%), with greater than 70% repair in four at 24 hours. Increased interstrand crosslink repair was also observed in a cisplatin acquired resistant human ovarian tumour cell line. Differences in gene expression pattern between the sensitive and resistant cell lines were compared using microarray analysis. The expression of a number of genes, including ERCC1, were consistently elevated in the resistant cell line, which was confirmed using RT-PCR.

**Table of Contents**

**Dedication**

I would like to dedicate my thesis to my twin sister, Trish, and her brilliant thesis on Weapons of Mass Destruction. Also to my parents whose help and support know no bounds. Thank you.

In remembrance of Andrew Boss and E.P.

**Acknowledgments**

I would like to thank the following people for their help in producing this research;

Dr Victoria Spanswick, Dr Peter Clingen, Mrs Janet Hartley and Mr John Bingham for their continuous support within the Riding House Laboratory. Dr Claire Newton, for collating patient information, discussion of cases and comet photos. Dr Minal Kotecha for PCR support. Dr Alan Entwistle (The Ludwig institute for Cancer Research, London) for help with microscopy. Dr Stephen Henderson for his analysis of the microarray data. Mr Tim Milne for his help in accessing patient notes. Miss Philippa Munson (UCL, Department of Pathology) for her guidance with the immunocytochemistry experiments. Professor Mike O'Hare for teaching me a novel technique for processing ascites and for use of his lab equipment.

I would especially like to thank Mr Tim Mould, Ms Adeola Olaitan and their team for welcoming me into their operating theatres, for collecting patient samples, and for discussion of cases. In addition, I would like to thank Mr Tim Mould for his encouragement and positive attitude.

Thank you to Professor John Hartley and Dr Jonathan Ledermann for supervising this project and for making it all possible. Thank you to the Carol Middleweek Fund for supporting this research.

Most importantly, thank you to the women who took part in this study. Your altruism and generosity were essential, and much appreciated.

PWS May 2006

**List of Figures**

**Page Number**

**List of Tables**

**List of Abbreviations**

| | |
|---|---|
| 4-HC | 4 hydroperoxy-cyclophosphamide |
| 5-FU | 5-fluorouracil |
| 6-4PPs | Pyrimidine (6-4) photoproducts |
| 6-MP | Mercaptopurine |
| γGCS | γ- glutamyl cysteine synthetase |
| $A_{260}$ | Absorbance at 260nm |
| $A_{280}$ | Absorbance at 280nm |
| A2M | Alpha-2-macroglobulin |
| AAS | Atomic absorption spectroscopy |
| ABC | ATP-binding cassette |
| ABCC2 | ATP-binding cassette subfamily C member 1 |
| ACNU | 1-(4-amino-2-methyl-5-pyrimidinyl)-methyl-3-(2-chloroethyl)-3-nitrosoureahydrochloride |
| ADEPT | Antibody directed enzyme pro-drug therapy |
| ADR | Adriamycin/doxorubicin |
| AIF | Apoptosis inducing factor |
| ALDH | Aldehyde dehydrogenase |
| ALLnL | N-acetyl leucyl-leucyl norlucinal |
| Apaf-1 | Apoptotic peptidase activating factor |
| APES | 3-amino-propyltriethoxysilone |
| APRT | Adenine phosphoribosyltransferase |
| Ara-C | Arabinofuranosylcytosine |
| ARL4 | ADP-ribosylation like-4 |
| ATP | Adenosine triphosphate |
| AUA1 | Arklies unknown antibody 1 |
| AUC | Area under the curve |
| BAM | 4-[bis(2-chloroethyl)amine]benzoic acid |
| Bad | Bcl-associated death promoter |
| Bak | Bcl-2 antagonist/killer 1 |
| Bax | Bcl-2 associated X protein |
| Bcl-2 | B-cell CLL/lymphoma 2 |
| Bcl-XL | B-cell leukaemia/lymphoma X |

| | |
|---|---|
| BCNU | 1,3-bis(2-chloroethyl)-1-nitrosourea |
| BCRP | Breast cancer resistance protein |
| BER | Base excision repair |
| BLAST | Basic local alignment search tool |
| bp | Base pair |
| BRCA | Breast cancer |
| BSO | L-buthionine sulfoximine |
| CAM-DR | Cell adhesion mediated drug resistance |
| CAPZB | Capping protein (actin filament) muscle Z-line beta |
| CBL | Chlorambucil |
| CCNU | 1,(2-chloroethyl)-3-cyclohexyl-1-nitrosurea |
| CDDP | Cis-diamminodichloroplatinum(II) (cisplatin) |
| cDNA | Complementary DNA |
| CENU | Chloroethylnitrosoureas |
| CGH | Comparative genomic hybridisation |
| CHO | Chinese hamster ovarian cell lines |
| cMOAT | Multispecific organic anion transporter |
| COL6A3 | Collagen 6 alpha 3 |
| CPD | Cyclobutane pyrimidine dimer |
| CSA | Cockayne's syndrome A |
| CSB | Cockayne's syndrome B |
| DAB | 3,3`diaminobenzidinetetrahydrochloride |
| DACH | 1,2-diaminocyclohexane |
| DEPC | Diethyl pyrocarbonate |
| DF | Dilution factor |
| DHFR | Dihydrofolate reductase |
| DMEM | Dulbecco's Modified Eagle's Medium |
| DMSO | Dimethyl sulphoxide |
| DSB | Double strand break |
| DTT | Dithiothreitol |
| ECM | Extracellular matrix |
| EDTA | Ethylenediaminetetraacetic acid |
| ELISA | Enzyme linked immunosorbent assay |
| EOC | Epithelial ovarian carcinoma |

| | |
|---|---|
| EP-CAM | Epithelial-cell adhesion molecule |
| ERCC1 | Excision repair cross complementing 1 |
| ES | Embryonic stem cells |
| EVI1 | Ectropic viral integration site 1 |
| F11782 | (a novel catalytic inhibitor of topoisomerases I and II) |
| FA | Fanconi's anaemia |
| FANC | Fanconi's anaemia |
| FAK | Focal adhesion kinase |
| FCS | Fetal calf serum |
| FDA | Food and Drug Administration |
| FDR | False discovery rate |
| FEN1 | Flap structure specific endonuclease 1 |
| FIGO | International Federation of Gynaecology and Obstetrics |
| GDEPT | Gene-directed enzyme pro-drug therapy |
| GF211 | Gene filter from Research Genetics (ResGen) |
| GG-NER | Global genomic-nucleotide excision repair |
| GGT | γ-glutamyl transpeptidase |
| GS- | Glutathione thiolate anion |
| GSH | Glutathione |
| GST | Glutathione s-transferase |
| GSTT2 | GST theta 2 |
| HMG | High mobility group |
| hMLH1 | Human MutL homolog 1 |
| HMT | 4'-hydroxymethyl-4,5',8-trimethylpsoralen |
| HN2 | Methchlorethamine |
| HNPCC | Hereditary non-polyposis colorectal cancer |
| HNSCC | Head and neck squamous cell carcinoma |
| HPV-16 E6 | Human papilloma virus-16 E6 protein |
| HR | Homologous recombination |
| HRR | Homologous recombination repair |
| HtrA2/Omi | HtrA-like serine protease/Omi stress-regulated endoprotease |
| HU | Hydroxyurea |
| IA | Intrastrand crosslink |
| IAP | Inhibitor of apoptosis protein |

| | |
|---|---|
| $IC_{50}$ | Inhibitory concentration 50% |
| ICL | Interstrand crosslink |
| ID2/3 | Inhibitor of DNA binding 2/3 |
| IDS | Interval debulking surgery |
| IDL | Insertion deletion loops |
| IL-1α | Interleukin 1 alpha |
| IL-3 | Interleukin 3 |
| ITGB1BP1 | Integrin beta 1 binding protein 1 |
| JNK | c-Jun-N-terminal kinase |
| kD | Kilodaltons |
| LMO4 | LIM-domain only 4 |
| MARCKS | Myristoylated alanine rich protein kinase C substrate |
| MEST | Mesoderm specific transcript homolog (mouse) |
| MDR | Multi-drug resistance associated protein |
| MGMT | O6-methylguanine DNA methyltransferase |
| MLH | MutL homolog |
| MMC | Mitomycin C |
| MMR | Mismatch repair |
| MNNG | N-methyl-N`-nitro-N`nitrosoguanidine |
| mRNA | Messenger RNA |
| MSH2 | MutS homolog 2 |
| MT | Metallothionein |
| MTIIA | Metallothionein II A |
| MTX | Methotrexate |
| MVA | Mean variance pairs |
| $NCC^{FA}$ | Nuclear core complex |
| NCI | National Cancer Institute |
| NEOC | Non-epithelial ovarian carcinoma |
| NER | Nucleotide excision repair |
| NM | Nitrogen mustard |
| NMR | Nuclear magnetic resonance |
| NSCLC | Non-small cell lung cancer |
| nt | Nucleotide |
| -OH | Hydroxyl group |

| | |
|---|---|
| OS | Overall survival rate |
| PBD | Pyrrolobenzodiazepine dimer |
| PBS | Phosphate-buffered saline |
| PCNA | Proliferating cell nuclear antigen |
| PCR | Polymerase chain reaction |
| Pgp | P-glycoprotein |
| PLD | Pegylated liposomal doxorubicin |
| PFGE | Pulse field gel electrophoresis |
| PFI | Platinum-free interval |
| PFKP | Phosphofructokinase |
| PFS | Progression-free survival |
| pol | Polymerase |
| Q-PCR | Quantitative-polymerase chain reaction |
| RFC | Replication factor C |
| RIR | Recombination independent repair |
| RNAi | RNA interference |
| RPA | Replication protein A |
| RPE | Qiagen RNeasy reagent |
| RTL | Qiagen RNeasy reagent |
| RT-PCR | Reverse transcriptase-polymerase chain reaction |
| RWI | Qiagen Rneasy reagent |
| S100A2 | S100 calcium binding protein 2 |
| SAGE | Serial analysis of gene expression profiling |
| SCE | Sister chromatid exchange |
| SCID | Severe combined immunodeficiency |
| SCLC | Small cell lung cancer |
| SDS | Sodium dodecyl sulphate |
| SHO | Senior House Officer |
| siRNA | Small interfering RNA |
| SJG-136 | (A selective PBD) |
| Smac/DIABLO | Second mitochondria-derived activator of caspase/Diablo homolog (*Drosophila*) |
| SNP | Single nucleotide polymorphism |
| SRB | Sulforhodamine B assay |

| | |
|---|---|
| SSA | Single strand annealing |
| SSB | ssDNA binding protein |
| SSC | Sodium chloride sodium citrate |
| ssDNA | Single stranded DNA |
| SU5416 | Z-3-[(2,4-dimethylpyrrol-5-yl)methylidenyl]-2-indolinone |
| TACSTD1 | Tumour associated signal transducer 1 |
| TAE | Tris-acetate EDTA buffer |
| TBS | Tris-buffered saline |
| TC-NER | Transcription coupled-nucleotide excision repair |
| TFIIH | Transcription factor II H |
| UCHL1 | Ubiquitin carboxy-terminal esterase L1 |
| UVC | Ultraviolet C |
| V | Volts |
| VEGF | Vascular endothelial growth factor |
| XP | Xeroderma pigmentosum |
| XRCC | X-ray repair cross complementing defective repair in Chinese hamster cells |

## Chapter 1: Introduction

### 1.1. Background

Ovarian cancer is a difficult disease to come to terms with. It is a silent killer, quietly growing and spreading without any obvious symptoms (Wikborn *et al.* 1996). In most cases by the time a patient is diagnosed, the disease is already established and very difficult to eradicate (Katz *et al.* 1981). At the time of diagnosis two thirds of ovarian tumours have spread outside of the ovaries, forming distant metastases (Pettersson *et al.* 1995).

Another factor complicating the effective treatment of ovarian cancer is the evolution of drug resistance to platinum-based chemotherapy, the first-line treatment for this disease. Despite the fact that the majority of ovarian cancers will exhibit initial sensitivity to platinum, the overall five-year survival rate is only 30% in patients with advanced ovarian cancer (Agarwal *et al.* 2003).

If clinical resistance to chemotherapy could be overcome then automatically the prognosis for ovarian cancer sufferers would greatly improve. If research can pin point why, for instance, a responsive tumour becomes a resistant tumour, then the mechanism of resistance can be targeted, in order to re-sensitise and destroy the cancerous tissue. Research has unveiled many different resistance mechanisms that prevent cytotoxicity from chemotherapeutics. They are complex, and highly dependent on the mechanism of action of the drug itself.

This study focuses on investigating the mechanisms of clinical resistance to platinum-based chemotherapy, namely cisplatin and carboplatin, in ovarian cancer. Both compounds are used to treat a variety of cancer types, but specifically are of interest in reference to ovarian cancer. The overall aim of this work is to improve our understanding of how ovarian cancer responds to conventional chemotherapy, with the hope of using this knowledge to develop improved chemotherapeutics, leading to an improved prognosis for these patients.

## 1.2. Ovarian Cancer

### 1.2.1. Ovarian Cancer: Pathology

Ovarian carcinomas arise from the three cell types constituting the ovary. These are the epithelial cells that cover the surface of the ovary, the stromal or connective tissue that holds the ovary together and the cells that produce the ova (America cancer society: Ovarian cancer detailed guide, 2004). Epithelial ovarian carcinomas (EOC) account for 80-90% of ovarian carcinomas (Kristensen *et al.* 1997). The remaining types of ovarian tumours are classified as non-epithelial ovarian cancers (NEOC), this category of ovarian tumour includes germ cell tumours and stromal tumours (Sanchez-Zamorano *et al.* 2003). Epithelial ovarian carcinomas are further divided histologically, into serous, mucinous, endometrioid, clear cell, transitional, squamous, mixed, undifferentiated, and unclassifiable sub-types (Bell, 2005, Kristensen *et al.* 1997).

A patient's ovarian cancer is then described according to the level of invasion of tumour cells from the ovary to the rest of the body. The level of dissemination is described by the 'stage' of the tumour, following guidelines published by the International Federation of Gynaecology and Obstetrics (FIGO), with Stage 1 indicating that the tumour is restricted to the ovary or ovaries, and Stage 4 indicating that the tumour is within the ovary or ovaries with distant metastasis to organs outside of the peritoneal cavity.

Additionally, an ovarian carcinoma can be described according to the level of dedifferentiation of the tumour cells. This status is indicated by the 'grade' of the tumour, with Grade 1 tumour cells more closely resembling normal tissue, and Grade 3 tumours less closely resembling the normal tissue, being poorly differentiated. The grading system does not apply to non-epithelial tumours (FIGO Guidelines 2004).

Both the grade and the stage of ovarian tumours are important prognostic factors, with low grade, low stage tumours being associated with a favourable prognosis, in comparison with high grade, high stage tumour being associated with decreased survival (Jolles *et al.* 1985). The grade of a tumour is correlated with the stage of the

tumour, in one study involving 571 cases of ovarian cancer in Norway, 78% of patients with Grade 3 tumours, had Stage III or IV disease, 76% of patients with Grade 1 tumours were found to have Stage I or II disease (Tingulstad *et al.* 2003). High grade tumours are thought to be more aggressive and to spread faster than low grade tumours.

As discussed, the prognosis for patients with low stage ovarian cancer is significantly better than for patients with more widespread disease. It is therefore important to detect ovarian cancer as early as possible in its development to provide patients with an increased chance of surviving the disease.

### 1.2.2. Ovarian Cancer: Statistics

Statistically the lifetime risk of women in the UK being diagnosed with ovarian cancer, as calculated in 1997, was 1 in 48 (CancerStats Incidence UK, published by Cancer Research UK, Feb 2004). In the UK in the year 2000, 6734 women were diagnosed with ovarian cancer, equal to 22.3 new cases per 100,000 women. In 2002, 4687 women died of ovarian cancer in the UK, accounting for 6% of all female cancer deaths that year (CancerStats Mortality UK, published by Cancer Research UK, Feb 2004). The American Cancer Society estimates that in America, approximately 25,580 new cases of ovarian cancer will be diagnosed in 2004, and 16,090 deaths will occur from the disease in the same time period (American Cancer Society 2004. Cancer Facts and Figures 2004. Atlanta GA).

### 1.2.3. Ovarian Cancer : Treatment

Surgical resection of ovarian tumours, so that less than 1-2 cm tumour deposits remain, greatly improves a patients chance of survival (Ozols *et al.* 1980, Makar *et al.* 1995, Bristow *et al.* 2002, Tingulstad *et al.* 2003). Interestingly, a significant improvement in patient survival corresponded with treatment by specialist gynaecological oncology surgeons versus general surgeons (Junor *et al.* 1999). Where is it not possible to optimally debulk a tumour, performing interval debulking surgery within a chemotherapeutic regime has been shown to induce a survival advantage of approximately 6 months (van der Burg *et al.* 1995).

Previously, a combination of cyclophosphamide and cisplatin was used as the first line treatment for ovarian cancer patients, until it was shown that a combination of paclitaxel and cisplatin conferred a greater increase in patient survival (McGuire *et al.* 1996). More recently, in a study of 792 ovarian cancer patients, it was shown that a combination of carboplatin and paclitaxel resulted in the same response rates as the combination of cisplatin and paclitaxel, but was significantly less toxic and easier to administer (Ozols *et al.* 2003). The standard treatment for ovarian cancer has been to optimally debulk the tumour, followed by 6 cycles of paclitaxel/carboplatin chemotherapy, administered three weekly (Moss and Kaye, 2002). Interestingly, two randomised controlled trials have shown no survival benefit treating patients with paclitaxel and cisplatin/carboplatin vs. treatment with cisplatin/carboplatin as a single agent (Muggia *et al.* 2000, Colombo *et al.* 2000).

Recently it has been demonstrated that treating stage IIIC ovarian cancer patients with three cycles of platinum and paclitaxel chemotherapy, followed by interval debulking surgery and the completion of the final 3 cycles of chemotherapy resulted in a mean survival time of 42 months, versus a 23 months mean survival time for patients treated with tumour debulking followed by 6 cycles of platinum-taxane chemotherapy (Kuhn *et al.* 2001). This result suggests that neoadjuvant chemotherapy, used to reduce the tumour mass to facilitate surgical removal, in conjunction with interval debulking, to specifically target the remaining chemo-resistant tumour tissue confers a greater chance of survival compared with initially attempting to optimally debulk an ovarian tumour, then to administer drug therapy.

As clinical trails become more sophisticated and more is learnt about tumour and patient responses to differing chemotherapeutic and surgical regimes, standard treatment options will evolve and change, hopefully leading to a significantly improved prognosis for ovarian cancer sufferers. A detailed description of the chemotherapeutics used to treat ovarian cancer can be found in the following section.

## 1.3. Cancer Chemotherapy

The impetus to cure and treat cancer has led to the development and usage of many types of chemotherapeutics. The following section includes a brief summary of the

most widely used anti-cancer drugs, detailing their origins, mechanisms of action and uses.

### 1.3.1. Antimetabolites

The antimetabolite anticancer agents were developed from the 1940's onwards (Pratt *et al.* 1994). They interfere with the synthesis of nucleic acids by inhibiting the production of the immediate precursors of DNA synthesis, deoxyribonucleoside triphosphates, via competition for anabolic enzymes, leading to DNA synthesis inhibition (Galmarini *et al.* 2002). In addition to interfering with the production of precursors, some antimetabolites are so similar in structure to purines or pyrimidines that they become incorporated into, and alter, the newly synthesized RNA and DNA (Galmarini *et al.* 2002). These agents effectively block DNA synthesis and induce apoptotic cell death (Galmarini *et al.* 2002). Antimetabolites include anti-purines and anti-pyrimidines, and as several tetrahydrofolates are essential to the synthesis of purines and pyrimidines, this class of anti-cancer agents includes anti-folates (Priestman, 1989). Antimetabolite agents include the pyrimidine antagonist 5-fluorouracil (5-FU), the purine antagonist, mercaptopurine (6-MP), and the folate antagonist, methotrexate (MTX) (Pratt *et al.* 1994). 5-fluorouracil is used to treat colorectal, breast, head and neck, gastric and pancreatic cancers (Pratt *et al.* 1994), mercaptopurine is used to treat acute leukaemias, methotrexate is used to treat gestational choriocarcinoma, acute lymphocytic leukaemia, osteogenic sarcoma, head and neck cancer and breast cancer (Pratt *et al.* 1994).

Capecitabine is an interesting oral 5-FU-derived prodrug that undergoes tumour-specific conversion into the active drug, leading to increased tolerability and intra-tumour drug concentrations (Walko *et al.* 2005). A phase II trial of capecitabine was recently carried out in recurrent ovarian cancer (Vasey *et al.* 2003). Results indicated that both the efficacy and safety of this agent compared favourably with other monotherapies used to treat platinum-refractory epithelial ovarian cancer, but with the advantage of oral delivery versus intravenous administration (Vasey *et al.* 2003).

2',2'-difluorodeoxycytidine 5'-triphosphate (gemcitabine) is a recently developed antimetabolite with an unusually mild toxicity profile, which predisposes this agent to be used in combination with other chemotherapeutic agents (Tonato *et al.* 1995).

Clinical trials have shown clear anti-cancer activity using gemcitabine against non-small cell lung, pancreatic, breast, bladder and ovarian cancers (Barton-Burke, 1999).

### 1.3.2 Topoisomerase I and II Inhibitors

The topoisomerase enzymes are involved in inducing topological changes in DNA to facilitate essential functions such as replication and transcription (Pommier *et al.* 1998, Burden *et al.* 1998). These proteins cut and reanneal DNA strands, for these processes to take place, in a way that prevents damage to DNA. Type I topoisomerases produce transient breaks in one strand of DNA, while type II enzymes produce transient double strand breaks (Pommier *et al.* 1998, Burden *et al.* 1998). As the topoisomerase enzymes form DNA breaks, they become covalently bound to the DNA strands, this structure is known as the 'cleavable' complex (Pommier *et al.* 1998, Burden *et al.* 1998). Topoisomerase inhibitors that stabilize the cleavable complex, preventing strand reannealing and enzyme dissociation, are called poisons, other inhibitors that function on other steps in the catalytic cycle are called catalytic inhibitors (Garcia-Carbonero and Supko, 2002, Larsen *et al.* 2003). In the case of the topoisomerase I poisons stabilisation of the covalent 'cleavable complex' induces single strand breaks, but it is the collision of replication folks with this complex, and the subsequent formation of double strand breaks that is thought to cause cell death (Tsao *et al.* 1993). Topoisomerase II poisons increase the steady-state concentration of the covalent cleavable complex, creating double strand breaks, leading to mutagenesis and cell death (Burden *et al.* 1998).

Several types of topoisomerase inhibitor are used in the clinic to treat cancer (Pratt *et al.* 1994). These agents include the topoisomerase I poisons; the camptothecins (e.g. topotecan and irinotecan), and the topoisomerase II poisons, the anthracyclines (doxorubicin, daunorubicin, and epirubicin) and etoposide (Pratt *et al.* 1994, Pommier *et al.* 1998). Topotecan has shown significant anti-tumour activity in both platinum-sensitive and platinum-resistant ovarian cancer patients (Herzog, 2003). Irinotecan is used to treat colon cancer (Pommier *et al.* 1998). Etoposide is used to treat small cell lung cancer, as well as leukaemias, lymphomas and germ-line cancers (Burden *et al.* 1998). Clinical trials have shown oral etoposide, both in conjunction with cisplatin

and as a single agent, to exhibit considerable activity with tolerable toxicity treating relapsed ovarian cancer (van de Burg *et al.* 2002, Alici *et al.* 2003).

The anthracyclines are discussed in more detail in a later section.

1.3.3. Antimitotic Agents

The vinca alkaloids are anti-mitotic agents extracted from the Periwinkle plant (*Catharanthus rosea* (Rowinsky and Donehower, 1991). Initial research by Johnson *et al.* (1963) using mouse models showed alkaloid fractions of this plant to have anti-leukaemic properties. These agents (vincristine and vinblastine) disrupt microtubule assembly by binding to free tubulin dimers, interfering with microtubule polymerisation and depolymerisation resulting in dissolution of microtubules, collapse of the mitotic spindle, arrest of cells in metaphase and cell death (Toso *et al.* 1993, Jordan, 2002). Vincristine used in combination with prednisone and L-asparaginase to treat lymphocytic leukemia in children, produced a 80-90% remission rate (Ortega *et al.* 1977). Other Vincristine combination therapy is used to treat both Non-Hodgkin's and Hodgkin's lymphoma, small cell lung cancer, breast cancer, Wilm's tumour, neuroblastoma, rhabdomyosarcoma and Ewing's sarcoma (Pratt *et al.* 1994). Vinblastine is used mainly to treat Hodgkin's Lymphoma and Non-Hodgkin's Lymphoma (Pratt *et al.* 1994).

Taxanes are another subgroup within the antimitotic class of chemotherapeutic agents. Paclitaxel was initially isolated from the Pacific yew, *Taxus brevifolia*, in 1971 (Huizing *et al.* 1995). Docetaxel is a semi-synthetic analogue produced from the European yew, *Taxus baccata* since the 1980's (Wani *et al.* 1971, Gligorov and Lotz, 2004). Unlike the Vinca alkaloids, paclitaxel and docetaxel bind to the β-subunit of tubulin dimers leading to stabilisation of tubulin polymerisation, they inhibit depolymerisation and together this effectively blocks mitosis and leads to cell death (Schiff and Horwitz, 1980, Jordan, 2002, Gligorov and Lotz, 2004). The two agents have different microtubule targets, with paclitaxel damaging the mitotic spindle and docetaxel affecting centrosome organisation (Haldar *et al.* 1997). Paclitaxel is used to treat advanced ovarian cancer and metastatic breast cancer (Miller and Ojima, 2001). The standard treatment of ovarian cancer patients has

been to optimally debulk the tumour, followed by six cycles of combined paclitaxel and carboplatin administered three weekly (Moss and Kaye, 2002). Docetaxel was licensed in 1996 by the American Food and Drug Administration (FDA) for the treatment of advanced breast cancer (Miller and Ojima, 2001). Recent findings have shown that treating ovarian cancer patients with docetaxel and carboplatin compared to paclitaxel and carboplatin, produces similar progression-free survival and clinical response, but with reduced neurotoxicity (Reviewed in Katsumata, 2003).

### 1.3.4. DNA-Damaging Agents

#### 1.3.4.1. Anthracycline Antibiotics

The anthracycline class of antibiotics, are produced from different strains of *Streptomyces* and includes the anti-cancer drugs doxorubicin (trade name adriamycin), daunorubicin and epirubicin (Pratt *et al.* 1994). These agents bind non-covalently to DNA, intercalating between base pairs (Pratt *et al.* 1994). While the exact cause of cytotoxicity is still being debated, these agents induce DNA double strand breaks mediated by the enzyme topoisomerase II (see above) (Cummings *et al.* 1991, Nielsen *et al.* 1996). This link was suggested after CHO cell lines resistant to a topoisomerase II poison (epipodophyllotoxin) were found to be cross-resistant to doxorubicin (Glisson *et al.* 1986). Interestingly, *in-vitro* transcription analysis carried out by Phillips and colleagues (1989) demonstrated that doxorubicin formed covalent adducts with DNA. Purification and characterisation of these adducts by the same group (Zeman *et al.* 1998) revealed that doxorubicin covalently binds to one strand of DNA, forming an uncommonly strong non-covalent bond to the opposite strand. This produces a bridge between the two DNA strands behaving much like a classical covalent interstrand crosslink (Zeman *et al.* 1998). Konopa (1983) reported the formation of interstrand crosslinks by doxorubicin and daunorubicin in HeLa cells. Cell-line research has revealed a strong correlation between the cytotoxicity of anthracyclines and their crosslinking capability (Skladanowski and Konopa, 1994a, 1994b). Daunorubicin is used to treat acute myelogenous leukaemia (Pratt *et al.* 1994). Doxorubicin is used to treat a broad spectrum of cancers, including; breast, bladder, endometrial, lung, ovarian, stomach and thyroid, as well as sarcomas of the bone and soft tissue (Pratt *et al.* 1994).

Pegylated liposomal doxorubicin (PLD) is produced when a polyethylene glycol layer surrounds a doxorubicin containing liposome following the process of pegylation (Thigpen *et al.* 2005, Rose, 2005). Interestingly, due to this surrounding layer of polyethylene glycol these liposomes evade uptake by mononuclear phagocytes, and due to their size they extravasate through the leaky tumour vasculature. Together these factors mean that this agent has an increased plasma half-life, compared to single agent doxorubicin, and has tumour specific delivery (Thigpen *et al.* 2005, Rose, 2005). In clinical trials PLD has shown efficacy in the treatment of relapsed ovarian cancer (Muggia *et al.* 1997, Gordon *et al.* 2000, Gordon *et al.* 2001). The Food and Drug Administration (FDA) in America has approved PLD for the treatment of metastatic ovarian cancer in patients with disease resistant to both paclitaxel and platinum chemotherapy (Doxil: Ortho Biotech Products LP;2001). The National Institute of Clinical Excellence (NICE) in the UK, has recommended the use of PLD for advanced ovarian cancer patients for whom first-line therapy has failed (National Institute for Clinical Excellence, July 2002).

1.3.4.2. Alkylating Agents

Several types of chemotherapeutic agent are capable of alkylating DNA, and so are listed according to this function. In general, simple alkylating agents react most readily with the N7 position of guanine, which is the most negative site of the bases of DNA (Pullman and Pullman, 1981 and Hartley, 1993). This electrostatic potential is increased if the guanine is situated within a run of guanines, resulting in enhanced DNA-binding of mustard and chloroethylnitrosoureas agents at these locations (Pullman and Pullman, 1981, Mattes *et al.* 1986). The O6 and N1 positions of guanine, the N7, N3 and N1 positions of adenine and the N3 position of cytosine and the O4 position of thymine are additional alkylation sites (Damia *et al.* 1998).

Figure 1.1 shows the chemical structure of several commonly used DNA-alkylating agents.

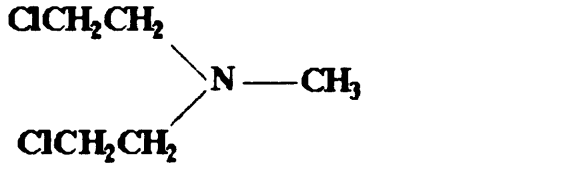

Mechlorethamine
(nitrogen mustard)

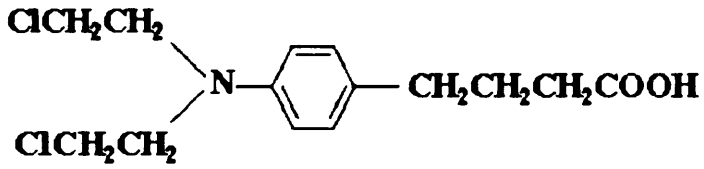

Chlorambucil
(mustard)

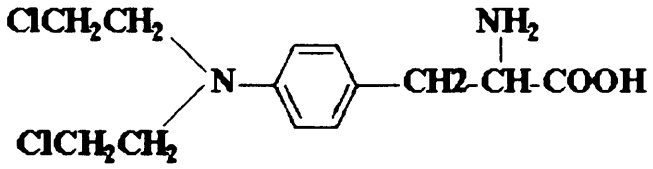

Melphalan
(L-phenylalanine mustard)

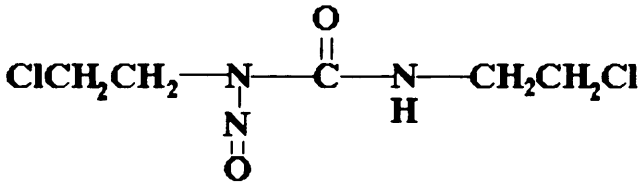

BCNU
(chloroethylnitrosourea)

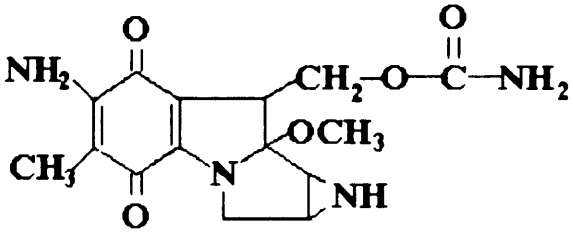

Mitomycin C
(aziridine)

Figure 1.1. The chemical structures of several clinically used alkylating agents, with the class of agent indicated in brackets below the name.

1.3.4.2.1. Mustards

The first clinical trial with nitrogen mustard was reported in 1946 (Gilman and Phillips, 1946). Since then a wide range of mustard chemotherapeutics have been used to treat a variety of cancers.

Bifunctional mustards are considerably more cytotoxic than their monofunctional compounds, due to their ability to crosslink DNA (Lawley and Phillips, 1996). Two chloroethyl (alkylating) groups are required for the anti-tumour activity of these agents (Lown, 1983). In aqueous solution each of the chloroethyl side chains can spontaneously cyclise to form a positively charged aziridinium ion, these ions attack electron rich centers in biological macromolecules (Ludlum, 1967, Lown 1983).

Members of the bifunctional mustard family include mechlorethamine, melphalan, chlorambucil, cyclophosphamide and ifosfamide. Melphalan, mechloethamine and chlorambucil each react directly with DNA. Cyclophosphamide and ifosfamide are activated as alkylating agents *in-vivo*, by the cytochrome P450 enzymes (Montgomery and Struck, 1973, Rooseboom *et al.* 2004)

These agents react with DNA to produce monofunctional N7 guanine adducts, DNA-protein crosslinks and interstrand N7-N7 guanine crosslinks (as mentioned, interstrand crosslinks are covalent bridges between opposing DNA strands) (Figure 1.2) (Povirk *et al.* 1994). Bauer and Povirk (1997) detected intrastrand crosslinks (covalent bridges on the same DNA strand) induced by mechlorethamine and phosphoramide mustard at a G-G-C sequence in double stranded DNA, using a comparison of cleavage patterns of 5'- and 3'- end-labelled DNA. No intrastrand crosslinks were detected in the samples treated with melphalan. Melphalan and chlorambucil both also react with the N3 position of adenine (Povirk *et al.* 1994). Approximately 5% of nitrogen mustard-DNA adducts are interstrand crosslinks formed in the sequence d(GpNpC), causing major distortion of the DNA double helix (Dronkert and Kannar, 2001). The nitrogen mustard ICLs are relatively unstable with a half-life of only approximately 2 hours (Henriques *et al.* 1997).

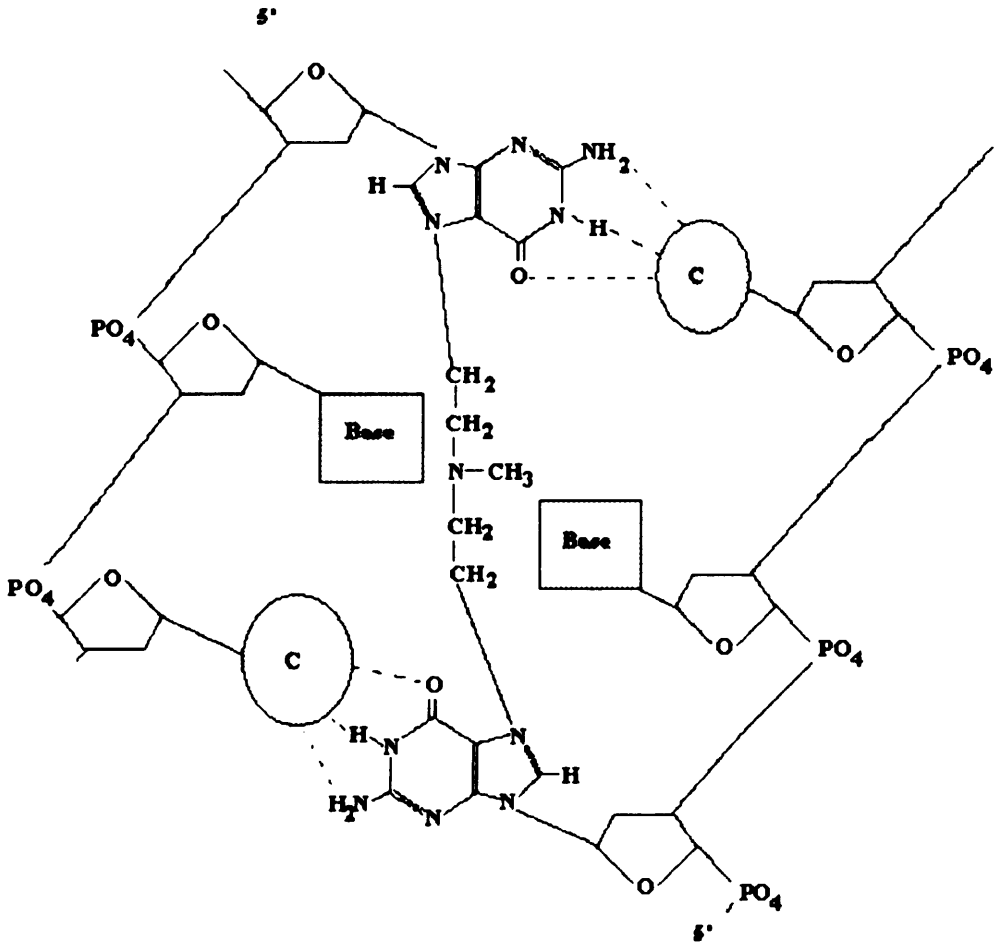


Figure 1.2. A mechlorethamine interstrand crosslink between complementary DNA strands, showing the interaction between two guanines binding at the N7 position.

The interstrand crosslink is postulated to be the cytotoxic lesion induced by mustard drugs. The formation and removal of mechlorethamine ICLs and melphalan ICLs have been closely correlated with loss of colony survival in a human melanoma cell line (Hansson *et al.* 1987). Sunters *et al.* (1992) investigated ICL formation directly in cells and in isolated DNA, using melphalan (L-PAM), chlorambucil (CHL) and 4-[bis(2-chloroethyl)amino] benzoic acid (BAM). Surprisingly, the cytotoxicity of these agents (L-PAM>CHL>BAM) did not correlate with their respective chemical reactivity or rate of hydrolysis (CHL>L-PAM>BAM), but did correlate directly with ICL formation (Sunters *et al.* 1992). The formation and removal of mechlorethamine ICLs was correlated with the loss of colony survival in murine leukaemic cell lines (Ross *et al.* 1978, O'Connor *et al.* 1990). Souliotis *et al.* (2003) examined gene specific melphalan ICL formation and repair in *p53* and *N-ras* following *in-vitro* exposure, using peripheral lymphocytes from multiple myeloma patients. Out of the seven patients samples examined, the three patients whose lymphocytes showed the least ICL damage (represented by the area under the curve, over time) did not respond to treatment with high-dose melphalan. Spanswick *et al.* (2002) investigated ICL repair in clinical samples from patients with multiple myeloma. They reported elevated ICL repair in samples from patients previously exposed to melphalan, and *in-vitro* sensitivity correlated with ICL repair capability (Spanswick *et al.* 2002). Overall this study was able to correlate enhanced melphalan-ICL repair in multiple myeloma with clinical resistance to this drug (Spanswick *et al.* 2002).

1.3.4.2.2. Chloroethylnitrosoureas (CENUs)

This group of agents includes 1,3-bis(2-chloroethyl)-1-nitrosourea (BCNU), 1-(2-chloroethyl)-3-cyclohexyl-1-nitrosourea (CCNU) and methyl-CCNU. The nitrosoureas decompose in aqueous media into alkylating and carbamoylating moieties (Pratt *et al.* 1994). Chloroethylnitrosoureas form cytosine and guanine monoadducts, guanine N7 intrastrand adducts, and guanine N1-cytosine N3 interstrand crosslinks (Dronkert and Kanaar, 2001,Tong and Ludlum, 1981, Tong *et al.* 1982). Interestingly, the formation of the interstrand crosslink is a multi-step process beginning with the chlorethylation of the O6 position of guanine (Tong *et al.* 1982, Kohn 1983). This disrupts the hydrogen bonding between the paired cytosine, and facilitates access to the N1 position of guanine, which the chlorethyl group at the

O6 position reacts with, resulting in the loss of the chloride and the formation of an ethano bridge (Tong *et al.* 1982, Kohn 1983). The N3 of cytosine then reacts with this newly formed cation leading to the formation of the observed N1 guanine- N3 cytosine interstrand crosslink (Tong *et al.* 1982 and Kohn 1983).

These agents are lipid soluble and can pass the blood brain barrier and are therefore used to treat some brain tumours (Edwards *et al.* 1980). This class of agents are also used to treated Hodgkin's lymphoma and melanoma, and are used as secondary treatments against non-Hodgkin's lymphoma, myeloma, lung cancer, and colorectal cancer (Pratt *et al.* 1994).

1.3.4.2.3. Mitomycin C (MMC)

In 1958 an interesting non-anthracycline natural anti-tumour antibiotic called mitomycin C was isolated from cultures of *Streptomyces caespitosus* in Japan (Wakaki *et al.* 1958). *In-vivo* reduction of the quinone groups within the structure of MMC by a variety of enzymes transforms this agent into a highly reactive bifunctional alkylating agent (Hashimoto *et al.* 1985). Reduced MMC reacts with DNA to form monoaducts, intrastrand crosslinks and interstrand crosslinks (Cummings *et al.* 1995). This agent covalently binds to DNA at the O6 guanine, N6 adenine and N2 guanine positions (Hashimoto *et al.* 1985). MMC induced interstrand crosslinks have been identified between the N2 position of guanines, at d(CpG) sequences within the minor groove, causing relatively little DNA distortion (Tomasz *et al.* 1987, 1988, 1995 and Dronkert and Kanaar, 2001). Interstrand crosslinks are thought to constitute approximately 5-13% of all DNA adducts induced by mitomycin C (Dronkert and Kanaar, 2001). Interstrand crosslinks are suggested to be responsible for the toxicity of this compound, causing DNA synthesis inhibition, cell cycle arrest, and apoptosis (Pratt *et al.* 1994). Volpato *et al.* (2005) reported a good correlation between mitomycin C induced ICL formation, measured using the comet assay, and cellular response. This agent is particularly interesting as it is selectively toxic to hypoxic tumours (Sartorelli *et al.* 1994). MMC is used to treat gastrointestinal and head and neck cancers, and is given by direct intravesicular administration to treat papillary bladder cancer (Priestman, 1989, Pratt *et al.* 1994).

#### 1.3.4.3. Platinum Agents

Platinum-agents are not alkylating agents, but do interact with and damage DNA. Platinum-based agents used in the clinic include cisplatin, carboplatin and oxaliplatin (Figure 1.3). The main platinum-based agents are discussed in more detail in the following section.

## 1.4. Platinum Chemotherapy

### 1.4.1. Cisplatin

#### 1.4.1.1. Cisplatin: Discovery and Development

The possible biological usefulness of platinum compounds was discovered by accident, when it was noticed that in the presence of ammonium chloride buffer, products from a platinum electrode blocked cell division in *E.coli* (Rosenberg *et al.* 1965 and 1969). Since then thousands of platinum compounds have undergone preclinical evaluation, with 28 compounds proceeding to full clinical trials (Lebwohl *et al.* 1998).

As well as blocking cell division, it was noted that the platinum exposure induced filamentous growth by the *E.coli*, up to 300 times the length of a normal cell (Rosenberg, 1967). Filamentous growth had also been noted in *E.coli* in response to the DNA damaging agents UV radiation (Witkin, 1967), mitomycin C (Suzuki *et al.* 1967) and hydroxyurea (Rosenkranz *et al.* 1966), suggesting that the platinum was affecting the cellular DNA. Filamentous growth is thought to occur as a result of continued growth of the bacteria, in the absence of DNA synthesis (Eastman, 1999).

Further pre-clinical analysis revealed the anti-tumour affect of these platinum compounds. *Cis*-diamminedichloroplatinum(II), or cisplatin, proved to be one of the best performing agents. Cisplatin was found to inhibit the growth of sarcoma and leukaemia cells in mice, and mammary carcinoma cells in rats (Rosenberg *et al.* 1970, Kociba *et al.* 1970, Welsch, 1971). In 1974, results of early clinical trials with cisplatin in testicular and ovarian cancer were published with objective responses in

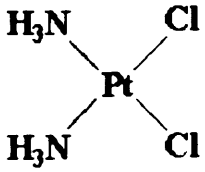


Cisplatin

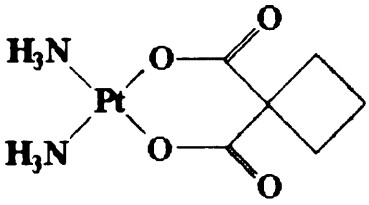


Carboplatin

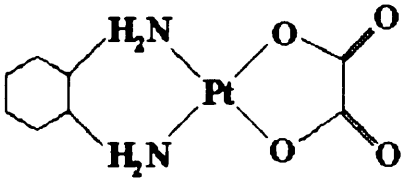


Oxaliplatin

Figure 1.3. Structures of platinum anti-cancer drugs

3/7 testicular cancer patients (Higby *et al.* 1974) and 7/19 ovarian cancer patients (Wiltshaw *et al.* 1974). During these early clinical trials it was also discovered that cisplatin caused serious organ toxicity, specifically affecting the kidneys. In 1976 strategies to overcome cisplatin-induced nephrotoxicity were being developed and used, namely high volume fluid hydration and forced diuresis (Hayes *et al.* 1976 and Merrin *et al.* 1976). In the 1980s carboplatin was discovered, with the same clinical efficacy of cisplatin, but with a much lower organ toxicity (Calvert *et al.* 1982).

1.4.1.2. Cisplatin: Cellular Target

Cisplatin reacts with many cellular components, and produces several different lesions, so how exactly cisplatin kills cells is still being debated. As mentioned *E.coli* exposed to cisplatin stopped dividing, and began filamentous growth, which had been previously identified as a DNA damage response. Cisplatin treatment of *E.coli* cells containing bacteriophage λ caused cell lysis, also indicating that DNA damage was occurring (Reslova, 1971).

Interestingly, when the level of cisplatin binding to the different macromolecules within the cell were measured using HeLa cells treated (at the mean lethal concentration) with $^{195m}$Pt-radiolabeled cisplatin, it was discovered that 1 out of $3x10^4$-$3x10^5$ protein molecules contained a platinum atom, 1 out of 10-1000 RNA molecules contained a platinum atom, and there were 9 platinum atoms bound to each molecule of DNA (Akaboshi *et al.* 1992).

Further evidence of the correlation between cisplatin-DNA damage and cytotoxicity comes from the finding that DNA repair deficient mutants display increased sensitivity to cisplatin in bacteria (Keller *et al.* 2001) and mammalian cells (Hoy *et al.* 1985, Damia *et al.* 1996, De Silva *et al.* 2002b). Cisplatin-resistant human ovarian cancer cell lines exhibited a significant increase in [3H]thymidine incorporation into DNA following cisplatin exposure, compared to the parental sensitive cell line, indicating an elevated level of DNA repair (Behrens *et al.* 1987). In several studies mammalian cells exhibiting enhanced repair of DNA-CDDP lesions are resistant to cisplatin (Lai *et al.* 1988, Ferry *et al.* 2000). A positive correlation was reported in ovarian and testicular cancer patients linking formation of cisplatin-DNA adducts and

response to cisplatin chemotherapy (Reed *et al.* 1986). Agents that inhibit the repair of cisplatin DNA damage, are often seen to increase the cytotoxicity of the compound (Li *et al.* 2000 and 2001, Yunmbam *et al.* 2001, Zhong *et al.* 2003).

Further research investigating the selective uptake and incorporation of radiolabelled precursors of RNA, DNA and protein into human AV3 cells *in-vitro* (Harder *et al.* 1970) and Ehrlich ascites cells *in-vivo* (Howle *et al.* 1970) discovered that cisplatin selectively inhibits DNA synthesis compared to RNA and protein synthesis. When a M13 bacteriophage containing a single cisplatin-DNA adduct was transfected into *E.coli*, survival fell to 10-12%, an affect that was attributed to DNA replication inhibition (Naser *et al.* 1988). Salles *et al.* (1983) investigated inhibition of DNA synthesis by platinum compounds in the leukaemic cell line L1210. DNA replication was reduced to 50% of the control when $1.8 \times 10^{-4}$ and $2.4 \times 10^{-4}$ Pt atoms were bound per nucleotide for cis-, and trans- derivatives, respectively. They concluded that DNA synthesis inhibition was not correlated with anti-tumour activity. In 1988 Sorenson and Eastman produced contradictory results using DNA repair proficient and deficient CHO cells. DNA repair deficient cells died at cisplatin concentrations that did not inhibit DNA synthesis and, DNA repair proficient cells treated with cisplatin survived at concentrations that inhibited DNA synthesis and induced S phase arrest (Sorenson *et al.* 1988, Eastman *et al.* 1988). These data support the hypothesis that inhibition of DNA synthesis is not the critical step in cisplatin-induced cytotoxicity. Indeed replication of DNA can occur past certain cisplatin-DNA lesions, via translesion synthesis (Albertella et al. 2005). However transcription cannot bypass cisplatin lesions. The two most common classes of cisplatin-DNA adduct, accounting for over 90% of cisplatin-DNA adducts, were found to present a strong block to RNA polymerase II progression (Tornaletti *et al.* 2003).

### 1.4.1.3. Cisplatin: Pharmacology

Upon entering the blood stream cisplatin molecules are maintained in their neutral state, whereby hydrolysis is suppressed by the relatively high chloride ion concentration of approximately 100mM. When these molecules enter a cell the reduced chloride ion concentration (2-30mM) of the cytoplasm facilitates the reversible exchange of the two chloride ligands with water molecules (Jaimeson and

Lippard, 1999). The resultant reactive aqua species, *cis*-$[PtCl(NH_3)_2(H_2O)]^+$, *cis*-$[Pt(NH_3)_2(H_2O)_2]^{2+}$ and *cis*-$[Pt(OH)(NH_3)_2(H_2O)]^+$ are highly nucleophilic. Once inside a cell, cisplatin reacts with many cellular targets including membrane phospholipids, cytoskeletal proteins, RNA, protein and DNA (Jaimeson *et al.* 1999).

The first exchange of a chloride ligand for a water molecule has a calculated $t_{1/2}$ of 1.9-2.5 hours, measured using NMR in aqueous solution at pH 6.5 and 37°C (Bancroft *et al.* 1990, Barnham *et al.* 1995). This cationic aquated species is then able to react with nucleophilic sites on macromolecules, forming protein, RNA and DNA adducts (Jaimeson *et al.* 1999). This mono-aquated species is easily substituted by the N7 of guanine or adenine, forming a mono-functional adduct ($t_{1/2}$=0.1-0.14hrs (Bancroft *et al.* 1990, Barnham et al. 1995)). A second reaction can occur, converting the mono-adduct into a bifunctional intra- or interstrand crosslink ($t_{1/2}$ =2.1-2.6hrs (Bancroft *et al.* 1990, Barnham *et al.* 1995)). When cisplatin DNA-platination was measured over time, a 15 minute incubation resulted in 40% monofunctional-N7 guanine adducts, whereas incubations over several hours resulted in no evidence of mono-functional adducts, suggesting the conversion of initially formed monoadducts into bifunctional adducts over time (Eastman, 1999).

Legendre *et al.* (2000) suggest that it is the doubly aquated derivatives of cisplatin that are the actual DNA binding species. By comparing the ability of cisplatin and its three aquated species (*cis*-$[PtCl(NH_3)_2(H_2O)]^+$, *cis*-$[Pt(NH_3)_2(H_2O)_2]^{2+}$ and *cis*-$[Pt(OH)(NH_3)_2(H_2O)]^+$) to react with two DNA sequences containing GG and AG, they discovered that the singly aquated cisplatin molecule ($[PtCl(NH_3)_2(H_2O)]^+$) showed a similar reactivity to both sequences, whereas the doubly aquated species (*cis*-$[Pt(NH_3)_2(H_2O)_2]^{2+}$ and *cis*-$[Pt(OH)(NH_3)_2(H_2O)]^+$) reacted three times faster with the GG sequence than with the AG sequence. They argue that as cisplatin is known to preferentially react with GG sequences *in-vitro* and *in-vivo*, the actual DNA platination species are derived from the double hydrolysis of cisplatin (Legendre *et al.* 2000).

1.4.1.4. Cisplatin: DNA Adducts.

The major DNA adducts induced by cisplatin were identified by Fichtinger-Schepman *et al.* in 1985 through enzymatic digestion of cisplatin treated salmon sperm DNA, chromatographic separation and nuclear magnetic resonance (NMR) analysis. Cisplatin-treated DNA contains approximately 65% 1,2-d(GpG), 25% 1,2-d(ApG) intrastrand crosslinks, and 5-10% 1,3-intrastrand crosslinks (each reacting with the same strand of DNA) and approximately 1% interstrand crosslinks (reacting with both DNA strands) (Fichtinger-Schepman *et al.* 1985). When levels of adducts were quantified using immunochemical detection, in the peripheral leukocytes of patients receiving cisplatin for the first time, the following levels of DNA adducts were discovered; 65% 1,2-d(GpG), 22% 1,2-d(ApG), 13% 1,3-d(GpNpG) and interstrand crosslinks, and approximately 1% monoadducts (Fichtinget-Schepman *et al.* 1987), confirming *in-vivo* their previous *in-vitro* findings. The types of cisplatin-DNA crosslink adducts are represented in Figure 1.4. Figure 1.5 depicts a cisplatin interstrand crosslink formed between guanines at the N7 position.

Early research by Zwelling *et al.* (1979a, 1979b) and Erickson *et al.* (1981) suggested that the cisplatin-interstrand crosslink was the cytotoxic lesion. Zwelling *et al.* (1979b) examined DNA-protein crosslinks and DNA-interstrand crosslinks induced by cisplatin and the less active compound transplatin using alkaline elution, in V79 Chinese hamster lung cells. At an equitoxic dose that reduced cell survival by between 80-90%, the levels of interstrand crosslinks induced by both compounds was comparable. This result was echoed, again using alkaline elution, in a normal and a SV40 transformed human embryo cell strain (Erickson *et al.* 1981). However, other publications have failed to correlate interstrand crosslinking with cisplatin cytotoxicity (Ducore *et al.* 1982).

It has been suggested that the failure of the trans-isomer of cisplatin, trans-DDP to form the 1,2-intrastrand crosslinks, due to its stereochemistry, (Lepre *et al.* 1987) accounts for its relative lack of toxicity. Adducts produced by transplatin are the 1,3-intrastrand crosslink, and the interstrand crosslink (Eastman *et al.* 1987 and 1988). The slower rate of closure of monofunctional adducts into bifunctional adducts could also account for the difference in cytotoxicity, as this time delay can facilitate

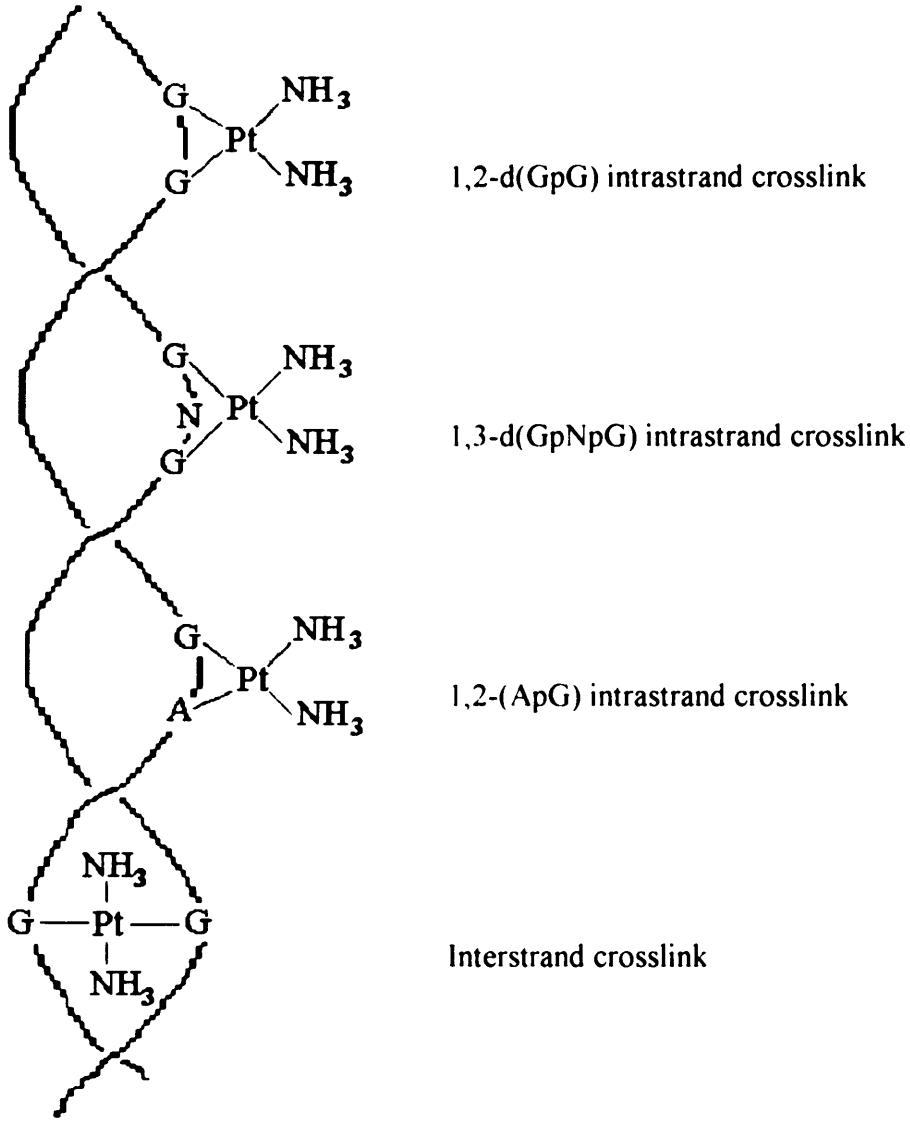


Figure 1.4. Cisplatin-DNA crosslinks. Adapted from Crul *et al.* (2002).

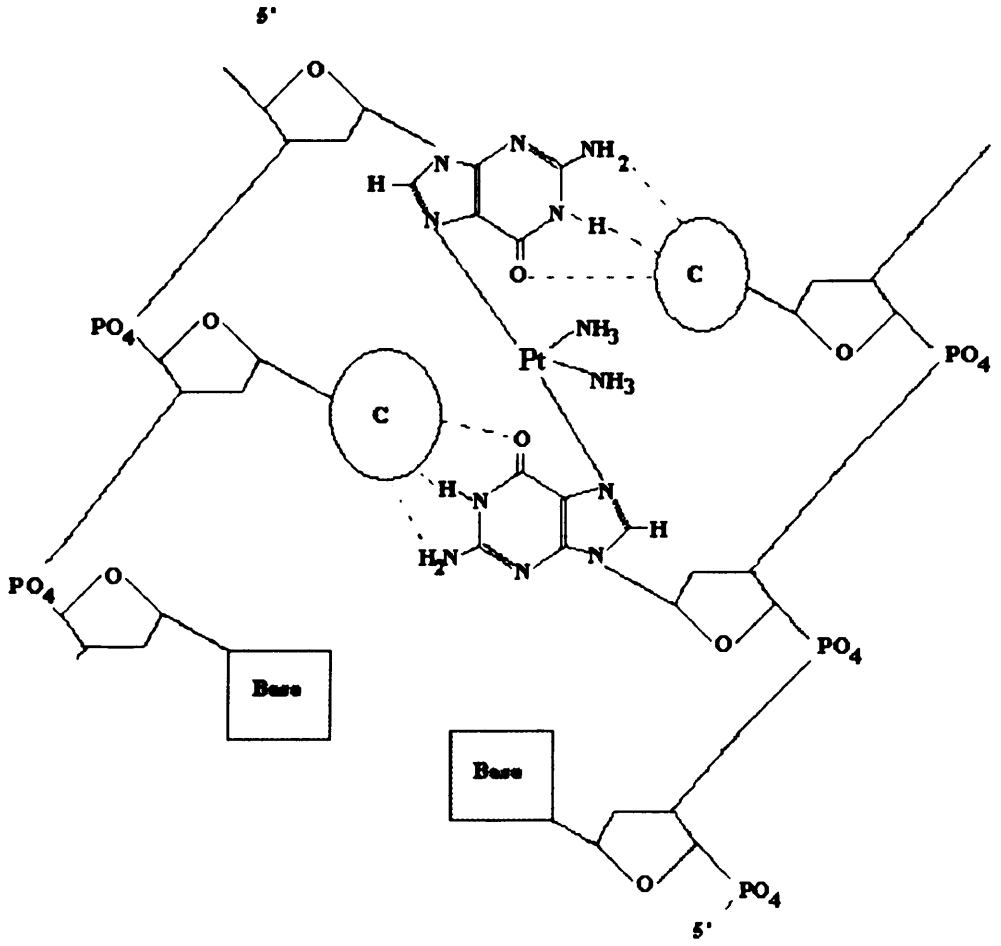


Figure 1.5. A cisplatin interstrand crosslink occurring between complementary DNA strands, interacting between two opposite guanines, at the N7 position. Cytosines are represented by the grey circles. Hydrogen bonds between complementary guanines and cytosines are shown with a broken line. A simplified representation of the sugar phosphate backbone has been used.

glutathione binding to the monoadduct, preventing bifunctionality (Eastman *et al.* 1987). Research using CHO cell lines consistently correlated cisplatin cytotoxicity with the 1,2-d(ApG) lesion (Fichtinger-Schepman *et al.* 1995). The 1,3-intrastrand crosslink is more easily repaired than the 1,2-intrastrand crosslink, providing further evidence that points to the 1,2-intrastrand crosslink as the cytotoxic lesion (Szymkowski *et al.* 1992, Moggs *et al.* 1997, Calsou *et al.* 1992). The reduced 1,2-intrastrand crosslink repair has been linked to the binding and corresponding shielding of the lesion by several proteins, namely the human mismatch repair protein, hMutSα and high mobility group (HMG) proteins (Zamble *et al.* 1996, Duckett *et al.* 1996). The mismatch repair protein, hMutSα binds to, but does not remove the 1,2-d(GpG) lesion (Duckett *et al.*1996). Moggs *et al.* (1997) specifically investigated repair of cisplatin 1,2- intrastrand crosslinks with regard to possible shielding by hMutSα, and concluded that the rate of repair of this lesions was indifferent to any possible protein shielding. They performed fractionation of cell extracts to remove putative shielding proteins, and recorded no difference in 1,2-intrastrand crosslink repair rates (Moggs *et al.* 1997). Moggs *et al.* (1997) also reported that hMutSα mutant cell extracts exhibited the same patterns of intrastrand crosslink repair as wild type cell extracts.

Zamble *et al.* (1996) observed inhibited 1,2-intrastrand crosslink repair in the presence of proteins containing a high mobility group (HMG) domain DNA-binding motif, in particular, rat HMG1, confirming previous findings by Huang *et al.* (1994). High mobility group proteins (HMG1 and 2) bind specifically to the DNA distortion induced by the 1,2-intrastrand crosslink (Pil *et al.* 1992), and these proteins do not bind to transplatin damaged DNA (Toney *et al.* 1989). HMG binding was suggested to underline the cytotoxic importance of the 1,2-intrastrand crosslink, until Kasparkova *et al.* (1995) showed the HMG1 protein to bind to cisplatin induced ICLs, in a similar fashion to 1,2-intrasrand crosslinks. No binding to transplatin ICLs was seen. The fact that transplatin is relatively inactive, and it does not produce the 1,2-intrastrand crosslink justified the argument that this was the cytotoxic lesion. If transplatin produces 1,3-intrastrand crosslinks and ICLs and isn't toxic, then these lesions were assumed to be sublethal. The interstrand crosslinks (ICLs) induced by cisplatin and transplatin are however clearly different, illustrated by the finding that

HMG1 only binds to the cisplatin crosslinks. This difference between the two types of interstrand crosslink might be responsible for the differential cytotoxicity induced by these two compounds. The question of which lesion is most damaging in terms of blocking transcription has been investigated by several groups. The 1,2 intrastrand crosslink and the 1,3 intrastrand crosslinks were found to present a strong block to RNA polymerase II progression (Tornaletti *et al.* 2003). However, analysis by Cullinane *et al.* (1999) found 1,3 intrastrand adducts to block RNA pol II by 80 percent, whereas the 1,2-d(GpG) intrastrand crosslink was bypassed by the polymerase.

Which cisplatin-DNA adduct causes cisplatin cytotoxicity is still being debated (Eastman, 1999). Further research is needed to understand the clinical importance of each type of lesion. With only approximately 1% of intracellular cisplatin reacting to form DNA-adducts (Gonzalez *et al.* 2001), Wang *et al.* (1996) argue that the affects of cisplatin on molecules with in the plasma membrane, (phospholipids and proteins), and platinum binding to the cytoskeleton, especially actin, are partly responsible for the toxicity of this compound.

### 1.4.2. Carboplatin

In order to diminish the extreme nephrotoxicity induced by cisplatin, researchers developed a cisplatin analogue with less labile leaving groups (Rose *et al.* 1985, Calvert *et al.* 1982 and 1993). The leaving group of carboplatin is a cyclobutanedicarboxylate ligand, compared to the chloride leaving group of cisplatin (Knox *et al.* 1986) (Figure 1.3). As the aquation rate of carboplatin ($7.2 \times 10^{-7} s^{-1}$) is much slower than cisplatin ($8 \times 10^{-5} s^{-1}$), the drug is effectively less reactive than cisplatin (Knox *et al.* 1986). Therefore, approximately 20-fold more carboplatin is required to produce the same level of cytotoxicity as cisplatin in CHO cells (Blommaert *et al.* 1995, Fichtinger-Shepman *et al.* 1995). To obtain the same level of platination following a four-hour exposure, 230 times more carboplatin was required (Blommaert *et al.* 1995). When the levels of the different DNA-carboplatin lesions were quantified using atomic absorption spectroscopy (AAS), and enzyme-linked immunosorbent assay (ELISA) *in-vitro* and *in-vivo* experiments produced slightly different results (Blommaert *et al.* 1995). *In-vitro* the most prevalent adduct is the

d(GpG) intrastrand crosslink (58%), *in-vivo* the G-pt-G adducts (including intra and interstrand crosslinks at this sequence) were most prevalent (40%) (Blommaert *et al.* 1995). The levels of adducts measured *in-vivo* using the ELISA technique, were 30% d(GpG), 16% d(ApG), 40% G-pt-G and 14% monoadducts at guanine, 10% of the G-pt-G lesions were estimated to represent interstrand crosslinks, assessed using alkaline elution (ICLs therefore represented 3-4% of total adducts) (Blommaert *et al.* 1995). The levels of adducts formed *in-vitro*, assessed using AAS were, 58% d(GpG), 11% d(ApG), 9% G-pt-G and 22% monoadducts at guanine (Blommaert *et al.* 1995).

Using alkaline sucrose gradient profiles, Knox *et al.* (1986) reported equal formation of interstrand crosslinks by both agents (cisplatin and carboplatin), once bound in equal amounts to DNA *in-vitro*, producing equal cytotoxicity. Conversely, at equitoxic doses, carboplatin was reported to form more interstrand crosslinks than cisplatin (measured using alkaline elution) with the peak occurring approximately 12-hours after a one-hour treatment, compared to the cisplatin ICL peak level, which occurred approximately nine hours after a one-hour treatment (Fichtinger-Schepman *et al.* 1995).

Carboplatin exhibits cross-resistance with cisplatin, which limits its clinical use (Gore *et al.* 1989, Brabec *et al.* 2005). Unlike cisplatin, carboplatin does not induce emesis, ototoxicity or nephrotoxicity, its rate limiting toxicity is myelosuppression (Calvert *et al.* 1982, Von Hoff *et al.* 1979). Meta-analyses of updated individual patient data from 37 randomised controlled trials, involving 5667 patients, indicated that cisplatin and carboplatin were equally effective in the treatment of advanced ovarian cancer (Aabo et al. 1998). Carboplatin is equally as effective, but considerably less toxic than cisplatin, and is therefore used as an alternative to cisplatin. Carboplatin is the key chemotherapeutic used to treat ovarian cancer.

### 1.4.3. Oxaliplatin

More recently a 1,2-diaminocyclohexane (DACH) platinum compound was developed in France, called (trans-R,R)1,2-Diaminocyclohexaneoxalatoplatinum(II), or oxaliplatin (O'Dwyer *et al.* 1998). Oxaliplatin forms the same types of adducts at

the same DNA sequences as cisplatin, namely 60-65% d(GpG) intrastrand crosslinks, 25-30% d(ApG) intrastrand crosslinks, 5-10% d(GpNpG) intrastrand crosslinks and 1-3% interstrand crosslinks (GG) (Jennerwein *et al.* 1989, Chaney *et al.* 2005). However, the hydrolysis reaction that converts oxaliplatin into a reactive species is slower than the hydrolysis reaction of cisplatin (Brabec *et al.* 2005). At the same dose, oxaliplatin formed significantly fewer DNA-adducts than cisplatin, measured using AAS (Woynarowski *et al.* 2000). Using a technique that measure the reactivation of drug-treated plasmids, Woynarowski *et al.* (2000) concluded that oxaliplatin adducts are repaired with similar kinetics as cisplatin adducts. Interestingly, it was reported that despite lower DNA reactivity, oxaliplatin was more cytotoxic that cisplatin, this was in part attributed to the fact that oxaliplatin was more efficient at inhibiting DNA strand elongation (per equal number of DNA adducts), than cisplatin (Woynarowski *et al.* 2000).

This particular platinum analogue is interesting as it often lacks cross-resistance with cisplatin, and can therefore be used to treat cisplatin/carboplatin-resistance tumours (Tashiro *et al.* 1989). Oxaliplatin is used in combination with 5-fluorouracil and folinic acid (leucovorin) to treat colorectal cancer, a disease that shows little response to cisplatin/carboplatin treatment (Andre *et al.* 1999, 2004, O'Dwyer *et al.* 1998). Interestingly, an Italian research group has just published a phase II clinical trial using pegylated liposomal doxorubicin (PLD) and oxaliplatin to treat relapsed advanced ovarian cancer (Nicoletto *et al.* 2005). They reported this combination of drugs to be active and well tolerated in these patients (Nicoletto *et al.* 2005).

## 1.5. Cellular Processing of Crosslinked DNA

As discussed, the majority of cisplatin-DNA adducts are intrastrand crosslinks, where the damage is confined to one strand of DNA. An intrastrand crosslink and a DNA protein crosslink both involve damage on one strand of DNA. The unique coding of a passage of double helix dictates that a portion of one strand can be removed, and repaired using the complementary strand as an accurate template. However other types of damage affect both strands of a region of DNA at the same time, namely double strand breaks (DSB) and interstrand crosslinks. This type of damage needs to be overcome so that the cell can function, replicating its DNA. This presents a

fundamentally different problem to the single stranded damage. The repair mechanisms responsible for the resolution of both single stranded and double stranded DNA damage are discussed in the following sections.

### 1.5.1. Repair of Intrastrand Adducts

#### 1.5.1.1. Nucleotide Excision Repair (NER)

DNA-intrastrand crosslinks are removed via the nucleotide excision repair (NER) pathway (Moggs *et al.* 1996, 1997, Szymkowski *et al.* 1992, Huang *et al.* 1994, Visse *et al.* 1994). This highly conserved repair pathway removes bulky, helix-distorting DNA adducts including UV-induced cyclobutane pyrimidine dimers and (6-4) photoproducts (Batty *et al.* 2000).

Excision repair cross complementing group 1 (*ERCC1*) was the first human nucleotide excision repair (NER) gene to be cloned (Westerveld *et al.* 1984). It was cloned following its ability to correct the excision repair defect in the mitomycin C (MMC) and UV light sensitive Chinese hamster ovarian (CHO) cell line 43-3B. Its name describes it as complementation group 1 of the CHO excision repair mutants. Other NER proteins were identified through manipulation of UV sensitive mutant CHO cells (ERCC1-11). Genes involved in NER (XPA-XPG), were also discovered as proteins mutated in patients suffering from Xeroderma Pigmentosum, a recessively inherited medical condition leaving patients hypersensitive to UV light, leading to a greatly increase risk of sun-induced skin cancers (Magnaldo *et al.* 2004). Genes involved in the NER of adducts on the transcribed strands of active genes (CSA-CSB), were discovered through the analysis of proteins mutated in Cockayne's Syndrome patients, who suffer from developmental defects and a sun-induced rash (Lehmann, 2003).

Researchers were able to reconstitute the complete NER process with purified mammalian proteins to successfully resolve different forms of DNA adduct. The initial incision stage of NER required all of the following proteins, replication protein A (RPA), XPA, transcription factor IIH (TFIIH), XPC, XPG, ERCC1-XPF and a factor known as IF7, for the repair of UV-induced DNA adducts (Aboussekhra *et al.*

1995), cisplatin 1,3-d(GpTpG) intrastrand crosslinks (Moggs *et al.* 1996, Araujo *et al.* 2000) and a cholesterol lesion (Mu *et al.* 1996).

The secondary gap filling repair synthesis stage required the addition proteins RPA, Proliferating cell nuclear antigen (PCNA), replication factor C (RFC), DNA pol ε or pol δ (with flap structure specific endonuclease 1 (FEN1)), and DNA ligase I (Aboussekhra *et al.* 1995, Araujo *et al.* 2000). The fact that the same purified proteins are required to recreate NER *in-vitro* with different types of DNA adduct confirms the concept of a conserved, common repair pathway.

There are two branches of NER, global genomic repair (GG-NER) and transcription coupled repair (TC-NER). TC-NER repairs transcription blocking lesions within the transcribed strand of active genes, GG-NER repairs lesions within the non-transcribed strand of active genes and in all other areas of the genome (Hanawalt, 2001). They differ in the initial damage recognition process. In GG-NER the protein complex XPC/hHR23B recognizes and binds to a site of DNA damage and distortion, leading to the recruitment and binding of TFIIH (Sugasawa *et al.* 1998, Volker *et al.* 2001). In TC-NER damage recognition is thought to be initiated by the stalling of RNA polymerase II, leading to its displacement and the recruitment of NER proteins (Leadon and Lawrence, 1991, Mellon 1987). There is continuing debate as to the possible role of XPA in the initial recognition of bulky DNA damage, as XPA preferentially binds to UV-irradiated DNA over non-irradiated DNA (Jones *et al.* 1993, Batty *et al.* 2000)

Early evidence of TC-NER included the finding that repair of UV induced damage on the transcribed strand of an active metallothionein gene occurred at least 3 times faster than that on its non-transcribed strand (Leadon and Lawrence 1991). Inducing higher levels of transcription using dexamethasone treatment led to increased repair of the transcribed strand of the active gene (Leadon and Lawrence, 1991). The observed strand selective repair was eliminated by treatment with α-amanitin, an inhibitor of RNA polymerase II (Leadon and Lawrence, 1991). It was also reported that cells from Cockayne's Syndrome (CS) patients were unable to recover RNA synthesis following UV irradiation (Mayne and Lehmann 1982). Following the detection of DNA damage by RNA polymerase II, two proteins deficient in

Cockayne's Syndrome patients, CSA and CSB, are believed to activate the common NER pathway (Troelstra *et al.* 1992). CSA is thought to function to recruit repair proteins to the site of damage, and CSB encodes a putative helicase (Troelstra *et al.* 1992). It has been proposed that CSB displaces RNA polymerase II at the site of damage, and unwinds the local DNA, to facilitate the binding of repair proteins mediated by CSA (Leadon *et al.* 1999).

Irrespective of which pathway detects the damage, once detection and recruitment have occurred a common NER pathway becomes active to resolve the damage. This process involves TFIIH, which contains the DNA helicases XPB and XPD, that unwind the DNA into a bubble structure around the bulky adduct (Sancar, 1994). Once the pre-incision complex is formed, recruitment of the structure-specific 5' to 3' endonuclease ERCC1-XPF is dependent on the presence of XPA, however the 3' to 5' endonuclease XPG binding is independent of XPA (Volker *et al.* 2001).

Analysis of the structure-specific endonuclease activity of this protein complex ERCC1-XPF, indicated that the incisions produced 5' to a artificial stem loop structure co-localised precisely with those produced by the yeast homolog protein complex Rad1-Rad10 (Sijbers *et al.* 1996). The heterodimeric complex acts as a structure-specific endonuclease, incising DNA at junctions between a duplex and a single strand, with the strand moving 5' to 3' away from the junction (Sijbers *et al.* 1996). Replication protein A (RPA) bound to the undamaged strand of DNA, is thought to confer strand specificity to the ERCC1-XPF heterodimer, in the presence of XPA (Saijo *et al.* 1996). XPG creates the 3' incision approximately 2 to 8 nucleotides away from the lesion, ERCC1-XPF then creates the 5' incision approximately 15-24 nucleotides away from the lesion (Evans *et al.* 1997). Matsunaga *et al.* (1995) used XPG and ERCC1 antibodies to investigate formation of incisions flanking cisplatin adducts. XPG antibodies inhibited the 3' incision, and ERCC1 antibodies disrupted both the 3' and 5' incisions, implicating a role in the formation of both incisions (Matsunaga *et al.* 1995). Mu *et al.* (1996) investigated the NER of a single thymidine dimer in a 140bp duplex, interestingly they described normal 3' incisions occurring in the absence of the ERCC1-XPF heterodimer.

Following incision, the ERCC1-XPF complex leaves a hydroxyl group at the 3'terminus of the incision product, therefore no further modification is required for the commencement of gap filing DNA synthesis (Sijbers *et al.* 1996). PCNA and RFC facilitate the assembly of DNA polymerases Pol δ and Pol ε, which carry out the DNA synthesis reaction (Shivji *et al.* 1992, Wood *et al.* 1997). The repair process is completed when ligation of the 5' end of the newly synthesized strand to the original sequence is fulfilled by DNA ligase I (Tomkinson *et al.* 1997). RFC has been reported to load PCNA on to the incised repair template, in order to resynthesise the damaged strand using DNA pol δ or pol ε (Podust *et al.* 1994). As mentioned, once the gap has been filled, the nick is resolved by DNA ligase I, and human cells from a patient lacking expression of this protein exhibit enhanced UV sensitivity *in-vitro*, and the patient exhibited sun sensitivity, stunted growth and immunodeficiency (Barnes *et al.* 1992). The process of NER is represented in Figure 1.6.

Interestingly, Furuta *et al.* (2002) investigated cisplatin sensitivity in human GG-NER mutant cells and TC-NER mutant cells. They found that the GG-NER mutant cell lines (lacking XPC) showed similar sensitivity to cisplatin as wild type cells, conversely TC-NER mutants (lacking either CSA or CSB) were hypersensitive to cisplatin compared to wild type cells (Furuta *et al.* 2002). This result implies that it is the repair of cisplatin-induced damage within the transcribing strand of active genes that determines the cytotoxicity of cisplatin.

Moggs and Colleagues (1997) researched the specific mechanisms of NER resolution of cisplatin intrastrand crosslinks. They confirmed previous findings (Szymkowski *et al.* 1992) that the 1,3-d(GpTpG) crosslinks were repaired by NER more effectively than the 1,2 –d(GpG) and 1,2-d(ApG) intrastrand crosslinks. This confirmed findings by Calsou *et al.* (1992) that the 1,2-intrastrand lesion was poorly repaired by human cell extracts *in-vitro*. This difference in repair rate was attributed by Moggs and colleagues, to the difference in helix distortion caused by the binding of the different types of adducts. The 1,3- intrastrand crosslink unwinds DNA by 23° degrees, whereas 1,2–d(GpG) and 1,2-d(ApG) intrastrand crosslinks unwind DNA by 13° degrees, both types of lesion also bends the DNA by 35° and 33°, respectively (Bellon *et al.* 1991). Similar experiments into the repair of UV-induced DNA-adducts discovered that the (6-4) photoproducts were repaired approximately 5-10 fold more

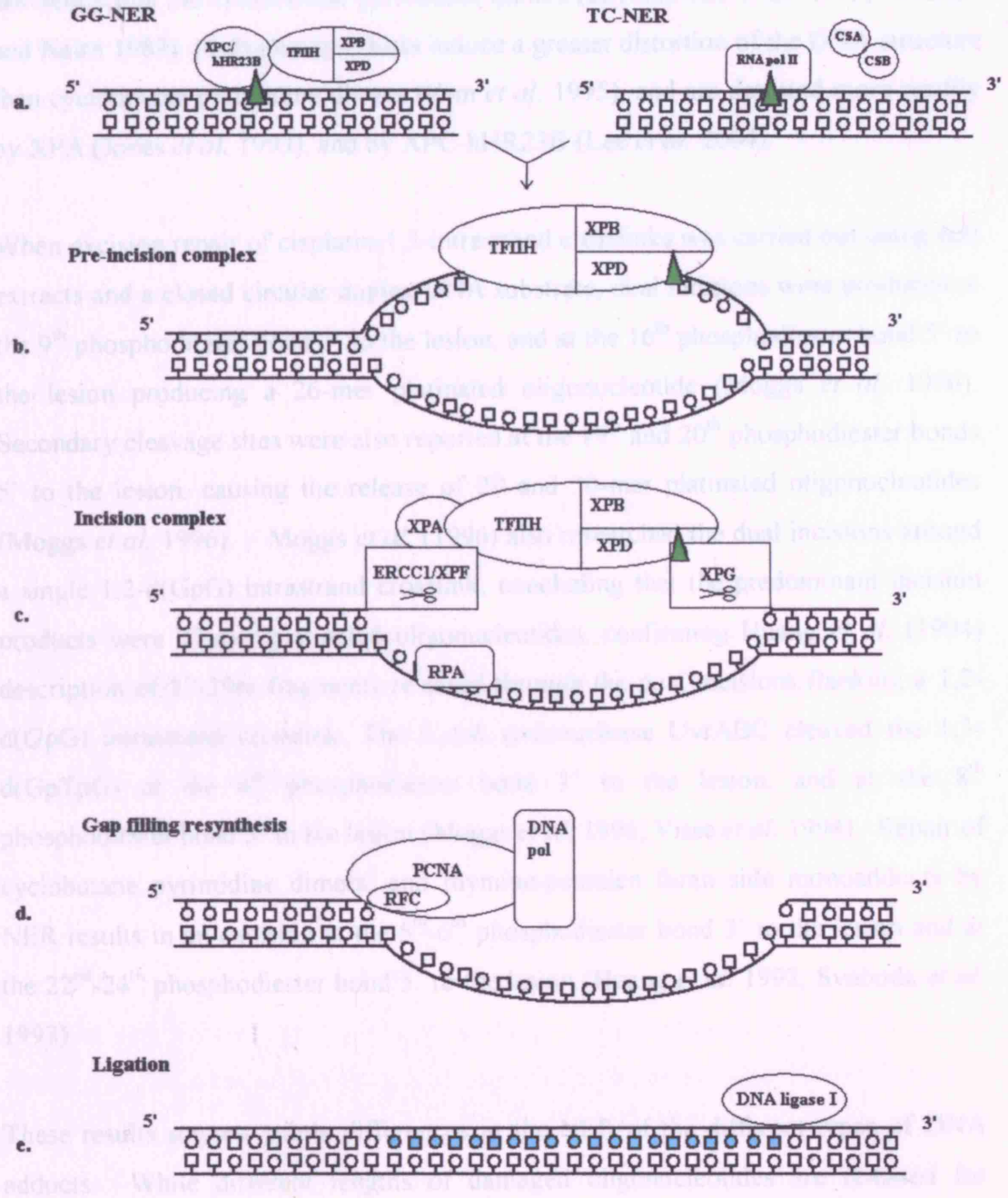


Figure 1.6. Nucleotide excision repair (NER). A bulky intrastrand DNA adduct is represented by a triangle, circles and squares represent nucleotides. a. The two NER pathways global-genomic-repair (GG-NER) and transcription coupled-repair (TC-NER) utilise different proteins to detect bulky DNA damage b. Both pathways merge after initial damage recognition into a common pathway. Whereby the binding of TFIIH results in the XPB and XPD helicases unwinding the DNA strands into a bubble structure. c. the structure specific endonucleases ERCC1/XPF and XPG are recruited to the pre-incision complex with XPA, ERCC1-XPF creates the 5' incision approximately 15-24 nucleotides away from the damage, XPG creates the 3' incision approximately 2-8 nucleotides away from the damage. Following incision ERCC1-XPF leaves a hydroxyl group (-OH) at the 3' terminus of the incision product. d. RFC loads PCNA onto the incised repair template, where the proteins facilitate the assembly of DNA polymerase δ or ε, to carry out the DNA synthesis reaction. Shaded nucleotides are newly synthesized. e. Finally DNA ligase 1 resolves the nick remaining after the resynthesis reaction. (XPA may play a role in the initial recognition of bulky DNA damage).

efficiently that the cyclobutane pyrimidine dimers (Szymkowski *et al.* 1993, Mitchell and Nairn 1989). (6-4) photoproducts induce a greater distortion of the DNA structure than cyclobutane pyrimidine dimers (Kim *et al.* 1995), and are detected more readily by XPA (Jones *et al.* 1993), and by XPC-hHR23B (Lee *et al.* 2004).

When excision repair of cisplatin-1,3-intrastrand crosslinks was carried out using cell extracts and a closed circular duplex DNA substrate, dual incisions were produced at the 9$^{th}$ phosphodiester bond 3' to the lesion, and at the 16$^{th}$ phosphodiester bond 5' to the lesion producing a 26-mer platinated oligonucleotide (Moggs *et al.* 1996). Secondary cleavage sites were also reported at the 19$^{th}$ and 20$^{th}$ phosphodiester bonds 5' to the lesion, causing the release of 29 and 30-mer platinated oligonucleotides (Moggs *et al.* 1996). Moggs *et al.* (1996) also researched the dual incisions around a single 1,2-d(GpG) intrastrand crosslink, concluding that the predominant incision products were 27-mer platinated oligonucleotides, confirming Huang *et al.* (1994) description of 27-29nt fragments released through the dual incisions flanking a 1,2-d(GpG) intrastrand crosslink. The *E.coli* endonuclease UvrABC cleaved the 1,3-d(GpTpG) at the 4$^{th}$ phosphodiester bond 3' to the lesion, and at the 8$^{th}$ phosphodiester bond 5' to the lesion (Moggs *et al.* 1996, Visse *et al.* 1994). Repair of cyclobutane pyrimidine dimers, and thymine-psoralen furan side monoadducts by NER results in an excision at the 5$^{th}$-6$^{th}$ phosphodiester bond 3' to the lesion and at the 22$^{nd}$-24$^{th}$ phosphodiester bond 5' to the lesion (Huang *et al.* 1992, Svoboda *et al.* 1993).

These results suggest subtle differences in the NER of the different types of DNA adducts. While different lengths of damaged oligonucleotides are released for different types of damage, the same type of adduct is always released in the same length of oligonucleotide suggesting that a common pathway is used to repair different adducts. This also suggests that differences in the DNA distortion surrounding the adduct affects the lengths of excised DNA.

### 1.5.2. Repair of Interstrand Adducts

#### 1.5.2.1. *E.coli*

The main route for ICL repair in *E.coli* was suggested by Cole *et al.* (1973), and involves collaboration between NER and homologous recombination repair (HRR), a pathway involved in the repair of DNA double strand breaks (DSB). It begins with dual incisions 5' and 3' to the ICL adduct on one DNA strand. Using psoralen crosslinks these incisions were found to be achieved by the *E.coli*-NER enzymes UvrABC, positioned at the third phosphodiester bond 3' to the lesion, and the ninth phosphodiester bond 5' to the lesion (Van Houten *et al.* 1986). DNA polymerase I, acts as a 5' exonuclease on the nicks to produce a ssDNA gap region, on the 3' side of the lesion (Sladek *et al.* 1989). The ssDNA in the gap is then bound by RecA, which polymerises in the 3' direction, and extends into the double strand region (Sladek *et al.* 1989). This nucleoprotein filament then interacts with intact homologous DNA, causing strand exchange (Sladek *et al.* 1989). Strand exchange results in a heteroduplex DNA including the passage still covalently bound to the 11bp oligonucleotide by the crosslink (Sladek *et al.* 1989). Strand exchange into the homologous dsDNA stimulates DNA synthesis (Sladek *et al.* 1989). The Holliday junctions that occur as a result of the exchange are resolved (Sladek *et al.* 1989, Dronkert and Kanaar, 2001). The final stage involves a conventional NER driven removal of the monoadduct on the damaged complementary strand, with UvrABC dual incisions 5' and 3' to the damage, then the ssDNA gap is filled by DNA polymerase I and ligated (Dronkert and Kanaar, 2001).

In RecA mutants repair of psoralen-induced ICLs is 2% of wild type repair, and repair of nitrogen mustard ICLs is 30% of wild type (Piette *et al.* 1988, Berardini *et al.* 1997). Mutants lacking other recombination proteins (RecB, RecC, RecD, RecF, RecG, RecO and RecR) are also sensitive to cisplatin, compared to wildtype (Zdraveski *et al.* 2000). RecFOR promotes the binding of RecA to single stranded DNA, by overcoming inhibition of RecA by single stranded DNA binding protein (SSB), and facilitates homologous pairing by RecA (Dronkert and Kanaar, 2001). RecO and RecR bind to ssDNA binding protein (SSB) when it is complexed to

ssDNA, and alter the complex to facilitate the addition of RecA (Dronkert and Kanaar, 2001). RecO and RecR remain complexed to RecA, forming presynaptic filaments, functioning in homologous pairing by RecA. (Umezu *et al.* 1994). RecBCD aids in loading RecA on to the ssDNA (Anderson *et al.* 1997). RecG aids in the resolution of recombination intermediates.

Recombination-independent repair of nitrogen mustard ICLs has also been reported in *E.coli* (Berardini *et al.* 1999). In the absence of RecA, repair of ICL's is dependent on a collaboration between NER and DNA polymerase II. This pathway involves the same initial dual incision, unhooking of the crosslink in one strand by UvrABC (Berardini *et al.* 1999). DNA polymerase II then performs low-fidelity translesion synthesis across the gap region (Berardini *et al.* 1999). Having repaired one strand, it only remains for UvrABC to perform a standard NER removal of the damaged strand covalently linked to the oligonucleotide that was initially incised. (Berardini *et al.* 1999). Berardini *et al.* hypothesise that the finding that an *E.coli* NER mutant treated with mitomycin C exhibited reduced mutagenicity could be explained by a reduction in the level of this error-prone NER/polII pathway (Berardini *et al.* 1999, Murayama *et al.* 1973).

1.5.2.2. Yeast and Mammalian.

A model of ICL repair in dividing eukaryotic cells has been produced that is based on the model of ICL repair in bacteria proposed by Cole *et al.* (1973), involving a co-operation between NER factors and homolgous recombination, summarized in McHugh *et al.* (2001) (Figure 1.7). In this model, as a replication fork moves towards the ICL, unwinding the local DNA structure, it stalls, disintegrates and falls off the DNA, leading to a DSB. ERCC1-XPF then produces dual incisions flanking the ICL, effectively unhooking one arm of the crosslink. Strand invasion and homologous recombination occur across the newly formed gap (stimulated by the DSB), and finally NER removes the remaining adduct, and resynthesises across the gap, using the template strand produced by homologous recombination (See Figure 1.7.) (McHugh *et al.* 2001).

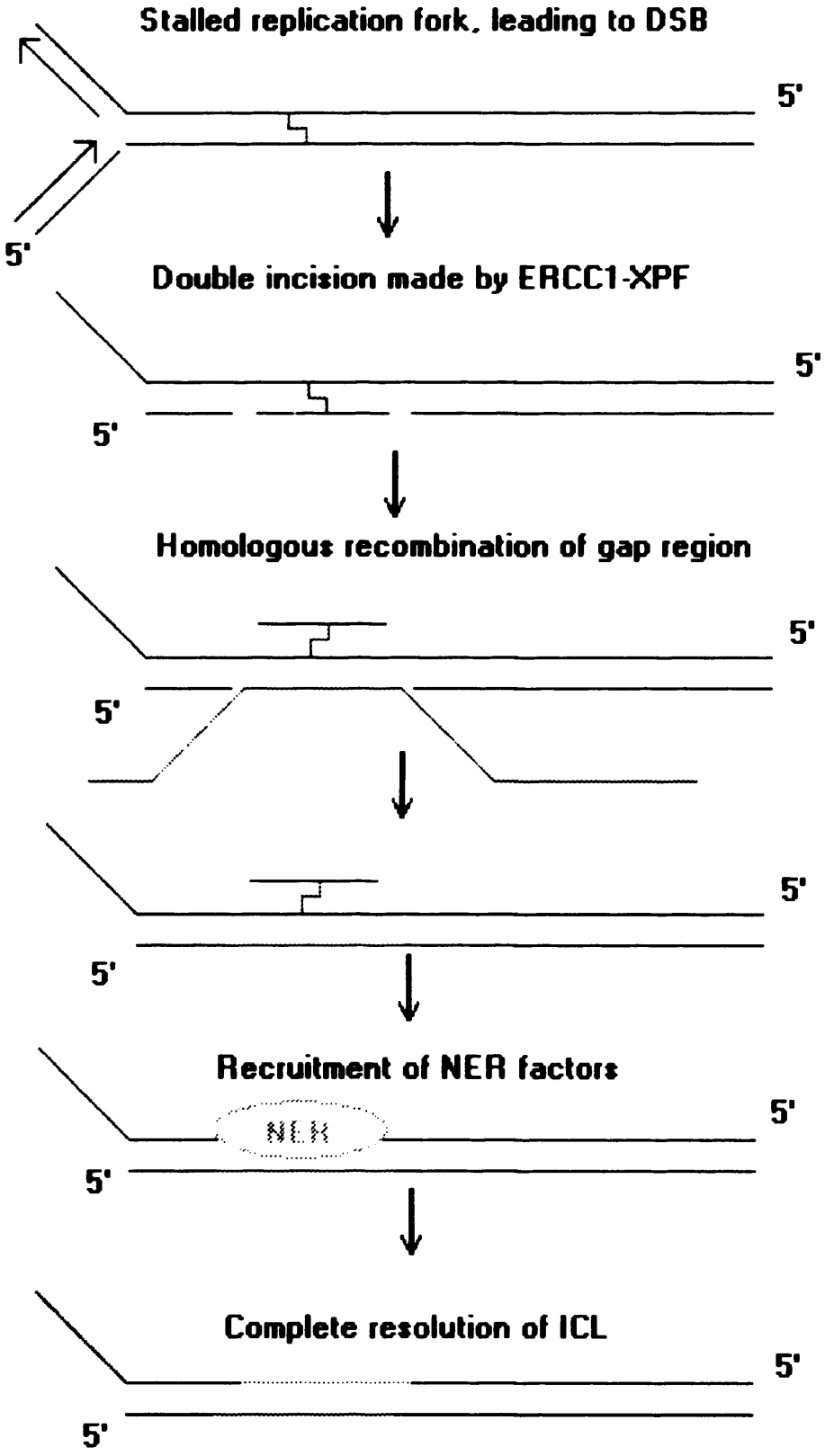


Figure 1.7. Proposed model for ICL repair in dividing mammalian cells, adapted from McHugh *et al.* 2001. A similar model minus the DSB formation was proposed by Kuraoka *et al.* 2000.

Evidence for this model and for a homologous recombination step in the resolution of ICLs is firstly, the hypersensitivity of certain NER and HRR mutants to ICL-inducing agents, secondly, the ability of the ERCC1-XPF heterodimer to incise both 5' and 3' to an interstrand crosslink, thirdly evidence for DSB formation in response to ICLs. The key findings supporting this model are summarized below.

As discussed, mutant Chinese hamster ovarian (CHO) cell lines deficient in separate DNA repair proteins were tested for cytotoxicity to ICL causing agents, compared to the wild type cell line. ERCC1 and XPF mutant CHO cells were found to be hypersensitive to cisplatin (Lee *et al.* 1993, Damia *et al.* 1996, DeSilva *et al.* 2002b), mechlorethamine (DeSilva *et al.* 2000) and melphalan (Damia *et al.* 1996). XRCC2 and XRCC3 (members of the Rad51 family of proteins involved in homologous recombination) mutant CHO cells were found to be hypersensitive to cisplatin (DeSilva *et al.* 2002b) and mechlorethamine (DeSilva *et al.* 2000). When the initial step of ICL unhooking was investigated using mutant cell lines, several mutants were incapable of unhooking cisplatin ICL (ERCC1, XPF, XRCC2, XRCC3), and mechlorethamine ICL (ERCC1, XPF) (DeSilva *et al.* 2000 and 2002b). Interestingly, XRCC2 and XRCC3 mutants were able to unhook mechlorethamine ICL (DeSilva *et al.* 2000).

As discussed, ERCC1 and XPF form a heterodimer that can act as an endonuclease at the junction between single stranded and double stranded DNA (De Laat, 1998). A more complicated role for ERCC1-XPF is implicated by the dual functions of the yeast homologs Rad1-Rad10. The yeast complex Rad1-Rad10 as well as being involved in NER is involved in a recombination pathway called single strand annealing (SSA). SSA is a pathway facilitating double strand break (DSB) repair, where the DSB is flanked by homologous regions of DNA. Single strand annealing is a form of recombination repair that involved homologous sequences on the broken chromosome (in comparison with another form of recombination repair of DSB involving a homologous chromosome), which involves a 5' to 3' resection and strand invasion from the homologous duplex. During SSA the DSB is enzymatically resected in a 5' to 3' direction. The 3' single stand overhangs then anneal at sites of 60 to 90bp homology, and the overhanging ends are resected by the Rad1-Rad10 heterodimer (Sugawara *et al.* 1992, Fishman-Lobell *et al.* 1992, Ivanov *et al.* 1995).

Sargent *et al.* (2000) investigated the high frequency of rearrangements caused by spontaneous recombination between direct repeats and the adenine phosphoribosyltransferase (APRT) locus in ERCC1(-) cells. They discovered that ERCC1-XPF is required for the removal of non-homologous 3' tails, as with Rad1-Rad10, concluding that the high frequency of rearrangements observed in the ERCC1 mutant cell line, were formed by the mis-processing of recombination intermediates (Sargent *et al.* 2000). Therefore, in mammalian cells the non-homologous 3' tails produced through SSA, are removed by the action of the ERCC1-XPF complex (Sargent *et al.* 2000).

Kuraoka *et al.* (2000) found that ERCC1-XPF alone was capable of producing incisions both 5'and 3' to a psoralen ICL located within seven nucleotides of a Y structure, releasing one arm of a psoralen interstrand crosslink. They suggest that the junction between single stranded DNA and duplex near to the ICL could result from a stalled replication fork (Kuraoka *et al.* 2000). Following the release of one arm of the crosslink, strand exchange with a homologous donor could occur to replace the damage strand and the other arm of the crosslink could be removed by a simple NER reaction (Kuraoka *et al.* 2000).

Recent work has shown that in dividing yeast ICLs lead to the development of DSBs (McHugh *et al.* 2000). This event is highly cycle dependent, with no DSBs in stationary phase yeast cells (McHugh *et al.* 2000). It is probable that DSBs are produced when replication forks encounter either ICLs themselves (McHugh *et al.* 2001) or strand break intermediates resulting from attempted repair pathways (McHugh *et al.* 2000). Similar experiments carried out in mammalian cells found that nitrogen mustard treatment of dividing CHO cells resulted in double strand break (DSB) formation, DSBs were not formed in confluent cells (DeSilva *et al.* 2000). This DSB formation was independent of NER proteins, with breaks occurring in NER mutants including XPF and ERCC1 (DeSilva *et al.* 2000). Repair of DSB was severely impaired in the homologous recombination repair CHO mutant cell lines lacking functional XRCC2, and XRCC3 (DeSilva *et al.* 2000). Together these data implicate homologous recombination as an essential element in the resolution of ICL induced DSBs (De Silva *et al.* 2000).

Mitomycin C (MMC)-induced interstrand crosslinks were also associated with the formation of DSB in mammalian cells, a process that was found to be independent of ERCC1, as it occurred in ERCC1 mutants (Niedernhofer *et al.* 2004). While ERCC1 was not involved in the MMC DSB induction, it was necessary for DSB resolution, via homologous recombination, indicated by significantly delayed DSB resolution in ERCC1-/- cells, and a lack of sister chromatid exchange (SCE) (Niedernhofer *et al.* 2004). These findings suggest that the ERCC1-XPF protein complex is required for MMC ICL-induced DSB repair via homologous recombination (Niedernhofer *et al.* 2004). XPA was not necessary for DSB resolution, suggesting that the repair of ICL-induced DSB was independent of NER (Niedernhofer *et al.* 2004). De Silva *et al.* (2000) describe no delay in DSB formation in ERCC1-/- CHO cells treated with nitrogen mustard, compared with wild-type cells, supporting the lack of ERCC1 involvement in ICL-induced DSB formation. Interestingly, delayed DSB formation was observed in ERCC1-/- human cells following treatment with the ICL inducer photoactivated 4'-hydroxymethyl-4,5',8-trimethylpsoralen (HMT), suggesting that an ERCC1/XPF incisional event is a necessary precursor for DSB formation in response to this type of ICL (Rothfuss and Grompe, 2004). In each of these studies DSB formation in response to ICL formation was dependent on entry into S-phase and cell cycle progression (De Silva *et al.* 2000, Niedernhofer *et al.* 2004, Rothfuss and Grompe, 2004). Interestingly, no DSBs were detected following cisplatin treatment of CHO cells (DeSilva *et al.* 2002b).

The possibility that the initial incision events early in ICL repair were independent of replication fork stalling, and therefore cell cycle progression and S phase, was approached by Rothfuss and Grompe (2004). They examined ICL unhooking in human cells using the modified gel electrophoresis comet assay. They found significant ICL unhooking in G1-arrested cells, concluding that this initial incision event was independent of cell cycle progression (Rothfuss and Grompe, 2004). The model of the initial events in ICL repair suggested by Rothfuss and Grompe, (2004) is represented in Figure 1.8.

The model includes the finding that during the repair of psoralen induced ICLs by CHO cell extracts, the NER machinery produces dual incisions 5' to the lesion, leading to the removal of a 22- to 28- nucleotide long damage free strand (Bessho *et*

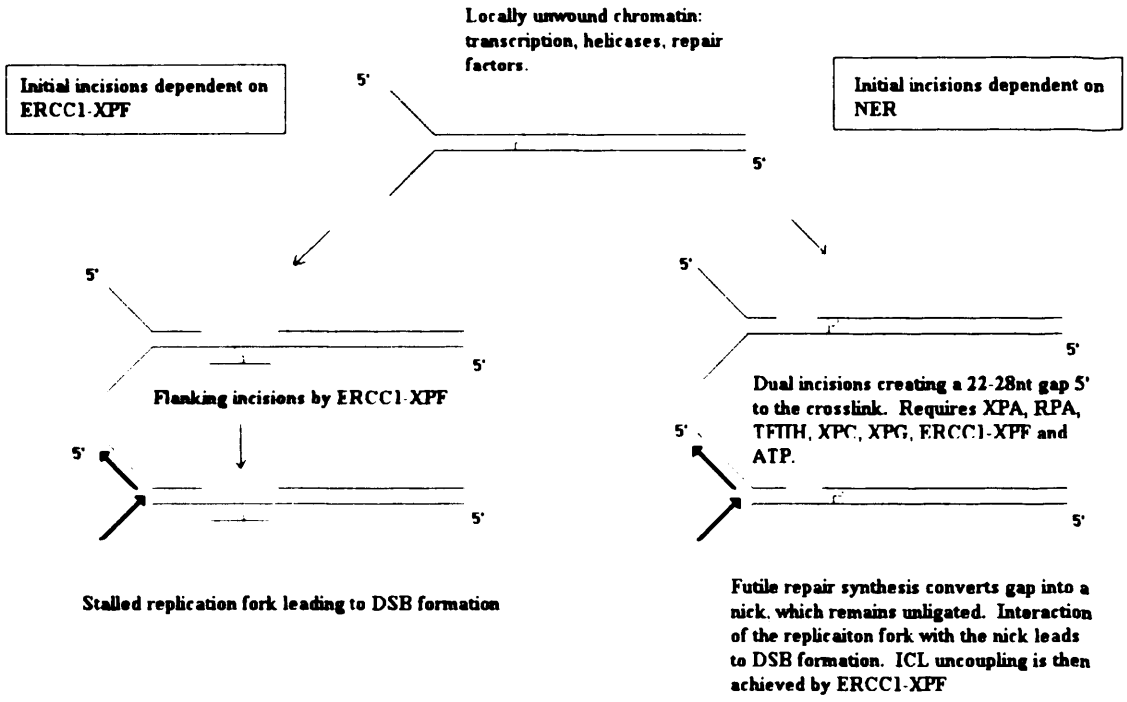


Figure 1.8. Models of the initial incisional events in ICL repair in human cells, proposed by Rothfuss and Grompe (2004). In this model formation of the initial incisions are independent of S-phase, however DSB formation is dependent on S-phase. Based on the findings of Mu *et al.* 2000, Bessho *et al.* 1997 and Kuraoka *et al.* 2000.

*al.* 1997). This gap is subsequently filled by a futile synthesis reaction, that is rarely ligated, leaving the ICL intact with a nick 5' to the lesion (Mu *et al.* 2000). In the suggested model the interaction of a replication fork with the 5' nick leads to DSB formation, leading to ICL uncoupling by the ERCC1-XPF complex (Rothfuss and Grompe, 2004). This pathway would only results in DSBs during S-phase as a replication fork approaches the 5' nick, so would not show as unhooking in G1 arrested cells. In the alternate pathway, ERCC1-XPF produces dual incisions either side of the ICL (in response to chromatin unwinding caused by transcription, chromatin remodelling via the action of a helicase, or in response to replication fork stalling in S phase) (Kuraoka *et al.* 2000), leading to ICL unhooking (Rothfuss and Grompe, 2004). Evidence that XPB, XPG, XPF and ERCC1 CHO mutant cells are unable to unhook cisplatin ICLs, measured using the single cell gel electrophoresis 'comet' assay, support the role of NER in the resolution of cisplatin induced interstrand crosslinks (De Silva *et al.* 2002b).

Interesting research by Aloyz *et al.* (2002) has provided evidence for a link between NER proteins and the resolution of interstrand crosslinks via homologous recombination repair, independent of NER activity. They specifically investigated XPD in cisplatin resistance. By artificially elevating XPD expression in a human glioma cell line they induced a two to four-fold increase in cisplatin resistance, that correlated with an increase in Rad51 foci formation, sister chromatid exchange (SCE) rate, and elevated ICL unhooking. They reported no difference in NER in the cell line, shown by no change in UV sensitivity, and no change in the repair of a cisplatin damaged plasmid (Aloyz *et al.* 2002). This research strongly implicates a role of XPD in the homologous recombination repair phase of cisplatin ICL unhooking.

Zhang *et al.* (2002) implicate the mismatch repair protein hMutSβ in conjunction with ERCC1-XPF and PCNA in the recognition step of psoralen ICL processing. They present an alternative theory to explain DSB formation in ICL repair. In their model incisions on one strand of DNA, occur on either side of an ICL, leading to the unhooking of one side of the lesion, DNA synthesis fills the gapped region, but stalls opposite the adducted thymine in the template strand. A second incision occurring on either side of the remaining adduct on the template strand would then produce a DSB (Zhang *et al.* 2002). This theory of DSB formation does not address the necessity for

S phase progression in the formation of DSB's in response to ICL. While further research is needed to produce a definitive model of ICL resolution, considering that different types of ICLs produced by different agents may be repaired via different pathways, one aspect is certain: the necessity for ERCC1 in efficient ICL removal.

1.5.2.3. Recombination Independent Repair (RIR).

A model of recombination independent repair (RIR) of ICLs has been suggested. Wang *et al.* (2001a) used a gene reactivation assay, utilizing a single psoralen ICL in a reporter plasmid which blocked expression of a reporter gene, expression of the gene was dependent on the resolution of the ICL. They found no significant reporter gene expression in NER mutants (Wang *et al.* 2001a). Homologous recombination mutants XRCC2 and XRCC3 were capable of ICL repair and reporter gene expression similar to the wild-type controls (Wang *et al.* 2001a). Further analysis showed frequent base substitutions at or near the site of the ICL, showing an error prone recombination independent repair pathway (Wang *et al.* 2001a).

Zheng *et al.* (2003), researched MMC ICL repair in the absence of undamaged homologous sequences, in mammalian cell lines. They found all five key molecules of NER essential for RIR of mitomycin C (MMC) ICL (Zheng *et al.* 2003). XRCC2 and XRCC3 mutants exhibited the same MMC ICL repair as parental cell lines (Zheng *et al.* 2003). This is further evidence for repair of ICLs in the absence of functional homologous recombination.

The proposed model of RIR of ICL (as shown in Zheng *et al.* 2003) suggests an initial NER dependent incision step placing two nicks on the same strand flanking the ICL crosslinked base. The incised oligonucleotide results in a gap structure, which is then filled by lesion bypass polymerases (translesion synthesis). This produces the error prone repair of one strand of the DNA, the strand still containing the crosslink undergoes a standard NER reaction, involving incision, synthesis and ligation. If the bypass synthesis of the first strand involves a misincorporation, then this error will be repeated in the second synthesis reaction.

In yeast the pso1/rev3 locus encodes a DNA polymerase (ζ) capable of translesion synthesis (Henriques *et al.* 1980). The pso1 mutants are hypersensitive to psoralen crosslinks (Henriques *et al.* 1980). In yeast rev3 mutant cells are considerably more sensitive to nitrogen mustard in stationary phase than in the exponential growth phase, when sensitivity resembles the parental cell line response (McHugh *et al.* 2000). During S and $G_2$ phases homologous sequences can be used to repair ICL damage, whereas during stationary phase, no homologous regions are present, so repair of damage relies on error prone RIR. As RIR relies on translesion synthesis and thus translesion polymerases, it follows that during stationary phase the loss of rev3 results in enhanced sensitivity of the mutants to nitrogen mustard. No DSBs were seen when stationary phase yeast cells were treated with nitrogen mustard, thought to relate to lack of replication forks colliding with damage causing the DSBs. Together this would imply that the XPF/ERCC1 act before both of these alternative events, because in both the recombination and RIR pathways, XPF and ERCC1 remain vital to the process.

The fact that mammalian NER mutants (XPF and ERCC1) are unable to repair ICLs, compared to wild-type contradicts recent work carried out by Bessho *et al.* (1997) and Mu *et al.* (2000). Their research suggest that in response to an ICL, dual incisions are formed 5' to the ICL, this results in gap formation. Gap formation leads to a synthesis reaction, but inefficient ligation in the majority of cases, leading to an unresolved nick (Bessho *et al.* 1997, Mu *et al.* 2000). The ICL therefore remains in place on the DNA (Bessho *et al.* 1997, Mu *et al.* 2000). In their research the futile synthesis reaction was dependent on functional NER (Bessho *et al.* 1997, Mu *et al.* 2000). Interestingly, no ICL repair was noted in their NER proficient cells (Bessho *et al.* 1997, Mu *et al.* 2000). Mu and colleagues propose that this futile repair synthesis is responsible for the cytotoxicity of ICL-inducing agents, through the mediation of pre-apoptotic signals, rather than as a result of a block to replication.

1.5.2.4. The Role of FANC Proteins, Rad51 and BRCA.

The possible role of Rad51 and Fanconi's Anaemia (FA) proteins in cellular response to interstrand crosslinking agents was implicated by the hypersensitivity to these

agents, of cells lacking these proteins. For example XRCC2 and XRCC3 (members of the Rad51 family of proteins) mutant Chinese hamster ovary (CHO) cell lines are hypersensitive to cisplatin and nitrogen mustard (HN2) (De Silva *et al.* 2000 and 2002b).

In the presence of ATP and replication protein A (RPA), Rad51 functions in double strand break (DSB) repair via homologous recombination, the protein interacts with ssDNA to form a nucleoprotein filament, that leads to homologous pairing and strand exchange (Sung *et al.* 1995). Bishop *et al.* (1998) reported the formation of Rad51 foci in CHO cells in response to ionising radiation and cisplatin. Rad51 foci formation occurs after irradiation during S phase (Gasior *et al.* 2001). A CHO cell line lacking XRCC3 (irsISF) previously shown to be hypersensitive to cisplatin (Caldecott *et al.* 1991, De Silva *et al.* 2002b) showed defective Rad51 foci formation in response to cisplatin (Bishop *et al.* 1998). Transfection of irsISF cells with *XRCC3* cDNA expression constructs partially corrected sensitivity to cisplatin (Tebbs *et al.* 1995). Two independent cell lines derived from irsISF stably transfected with XRCC3, showed normal Rad51 foci formation in response to cisplatin (Bishop *et al.* 1998). This research links reduced XRCC3 with reduced Rad51 foci formation in response to cisplatin treatment, and hypersensitivity to cisplatin (Bishop *et al.* 1998). Interestingly, Liu *et al.* (1998) used a yeast two-hybrid assay and immunoprecipitation in human cell extracts to discover a physical interaction between HsRad51 and XRCC3. Xu *et al.* (2005) transfected *XRCC3* into MCF-7 breast cancer cells. They reported increased Rad51 foci formation in response to cisplatin exposure (Xu *et al.* 2005). Elevated cisplatin and melphalan resistance correlated directly with the elevated XRCC3 protein levels in the transfected cell lines (Xu *et al.* 2005).

In vertebrates the Rad51 paralogs assemble into two complexes consisting of a heterodimer of XRCC3 and Rad51C, and a tetramer of Rad51B, Rad51C, Rad51D and XRCC2 (Masson *et al.* 2001). Chicken DT40 cells lacking either Rad51C, Rad51D, XRCC2 or XRCC3 exhibited severely impaired Rad51 foci formation following exposure to gamma irradiation (Takata *et al.* 2001) Each of these mutants exhibited approximately eight-fold increased sensitivity to cisplatin compared to

wild-type cells, complementation of each cell line with the corresponding human cDNA, restored its cisplatin resistance (Takata *et al.* 2001).

Connell and colleagues investigated a synthetic peptide that corresponds with residues 14-25 of Rad51C, that interferes with this protein's interactions with both XRCC3 and Rad51B. Treatment of CHO cells with this synthetic peptide followed by cisplatin led to reduced Rad51 foci formation and increased sensitivity (Connell *et al.* 2004).

BRCA1 has also been reported as an essential component in the assembly of Rad51 foci following cisplatin exposure and ionising radiation in mouse embryonic stem (ES) cell lines (Bhattacharyya *et al.* 2000). $BRCA1^{-/-}$ ES cells were five times mores sensitive to cisplatin than wild type cells (Bhattacharyya *et al.* 2000). Previously Yuan *et al.* (1999) reported the need for BRCA2, but not BRCA1 for the assembly of Rad51 foci in response to ionising radiation. There is, therefore, direct evidence for the role of BRCA1/2, XRCC3 and Rad51 in the cellular response to interstrand crosslinking agents.

Fanconi's anaemia is an autosomal recessive cancer susceptibility syndrome, characterized by progressive bone marrow failure and congenital anomalies (Bagby 2003). Cellular sensitivity to crosslinking agents is such a prevalent trait in cells from these patients, that exposure to mitomycin C is used in a diagnostic test for the disease, whereby a patient's cells are exposed to the drug, and then examined as metaphase spreads for evidence of chromosome breaks and radial chromosomes (Bagby *et al.* 2003). Interestingly, certain homozygous mutations in BRCA2 can result in Fanconi's anaemia (Howlett *et al.* 2002). FANCA, -B, -C, -E, -F, -G and –L interact to form a complex, sometimes referred to as the nuclear core complex (or $NCC^{FA}$) (Garcia-Higuera *et al.* 2001). Following exposure to DNA damaging agents, during S-phase this complex carries out the monoubiquitination of FANCD2 (Taniguchi *et al.* 2002). Once monoubiquitinated FANCD2 can be translocated to the site of DNA damage foci, containing Rad51 or BRCA1, to contribute towards homologous repair functions (Garcia-Higuera *et al.* 2001, Taniguchi *et al.* 2002). Taniguchi *et al.* (2003) reported disruption of the FANC/BRCA pathway in a subset of cisplatin-sensitive ovarian tumour cell lines. Complementation of these cells with

functional FANCF, led to monoubiquitination of FANCD2 and cisplatin resistance (Taniguchi *et al.* 2003). Within the studied cell lines FANCF was found to be epigenetically silenced through methylation of its CpG island, and demethylation led to acquired cisplatin resistance (Taniguchi *et al.* 2003).

Interestingly, Ohashi *et al.* (2005) reported normal BRCA2-dependent Rad51 focus formation in the absence of FANCD2.

## 1.6. Resistance to Chemotherapy

### 1.6.1. Overview

Whether a patient is intrinsically resistant to a chemotherapeutic, or goes on to develop a resistant phenotype, this will seriously complicate their treatment. Loss of response or lack of response to a drug, reduces the chemical arsenal a clinician can deploy to attack the developing cancer. Several cancer types are intrinsically drug resistant, including, melanomas, non-small cell lung and pancreatic cancers (Pommier *et al.* 2004). Ovarian and breast cancers and leukaemia frequently develop acquired drug resistance during treatment, presenting with resistant relapsing disease (Pommier *et al.* 2004).

Hope lies in understanding the basic mechanisms of cancer drug resistance. Once a cancer drug is administered to a patient a huge array of factors influence how effectively the drug can reach and kill tumour cells. A sufficient dose of the drug has to travel to and enter the cancer cells. Once within the cell the agent has to overcome inherent 'protection' mechanisms, which work towards rendering the drug damage sublethal. These intracellular mechanisms range from detoxification enzymes and membrane pumps, to sophisticated DNA repair pathways. The exact mechanism of cell kill of an agent provides a selection pressure, leading to the survival and repopulation by cells able to withstand this mechanism. The intracellular target of the agent is an important consideration when examining cancer drug resistance mechanisms.

The pharmacokinetics of an agent, or the processes involved in the distribution and metabolism of the drug in the body, affect the total drug exposure of tumour cells *in-vivo*. Total drug exposure is calculated by the following equation; drug concentration x time of exposure = area under the curve (AUC), and the cytotoxicity of a chemotherapeutic is relative to the total drug exposure (Iyer *et al.* 1998, Agarwal and Kaye, 2003). Pharmacokinetic factors include renal clearance of an agent, tumour vasculature, as well as interpatient variation in drug detoxifying enzymes (Iyer *et al.* 1998). Pharmacokinetics also influence cytotoxicity where pro-drugs are administered to become activated *in-vivo*. Interpatient variation in activating enzyme systems can lead to varying patient response (Iyer *et al.* 1998, Agarwal and Kaye, 2003). The interpatient differences in the pharmacokinetics of an agent could therefore significantly affect total drug exposure and thus patient responses to that agent, accounting for some cases of clinical resistance (Iyer *et al.* 1998).

The localized tumour microenvironment is another important factor affecting tumour cell sensitivity to chemotherapeutics. Solid tumours have areas lacking sufficient blood supply, and these stressed areas exhibit low pH, glucose starvation and hypoxia (Tomida *et al.* 1999). Stressed tumour tissue generally exhibits enhanced resistance to chemotherapeutics, including etoposide, doxorubicin, camptothecin and vincristine, thought to be mediated via G1 arrest (Tomida *et al.* 1999). This resistance is generally reversible upon the reduction in the stressed conditions (Tomida *et al.* 1999). Interestingly, stressed cells become hypersensitive to cisplatin (Tomida *et al.* 1999). Enhanced cisplatin sensitivity was observed in a human epidermoid carcinoma cell line treated with glucose starved stress (Mese *et al.* 2001). As mentioned, the bioreduction and activation of MMC as an alkylating agent are enhanced in hypoxic tumours, leading this agent to be selectively toxic to this type of tumour tissue (Sartorelli *et al.* 1994).

Assuming that the drug reaches and enters the cell, many mechanisms exist within cancer cells to overcome the action of the drug. These mechanisms depend on the target within the cell. Upstream resistance mechanisms that take effect before the chemotherapeutic has reacted with its target include; increased efflux, or decreased influx of an agent. Altered drug metabolism through the action of detoxification

enzymes is also an upstream mechanism, achieved by conjugation with molecules such as glutathione or metallothionein leading to a reduction in the active agent.

Altered target gene expression, both at the level of gene expression and the isotype of the target protein can also lead to enhanced survival and resistance. For example, paclitaxel-resistant epithelial ovarian tumour cells from patients were found to express altered patterns of beta-tubulin isotypes, compared to untreated primary ovarian tumours (Kavallaris *et al.* 1997). Human lung cancer cell lines made resistant to paclitaxel *in-vitro*, also exhibited an altered ratio of beta-tubulin subunits (Kavallaris *et al.* 1997).
Inhibition of drug-induced apoptosis can also lead to chemo-resistance. The Bcl-2 family of proteins contribute towards the control of the mitochondrial apoptotic pathway (Mignotte *et al.* 1998). Elevated levels of the anti-apoptotic protein Bcl-2 have been measured in drug resistant tumour cells compared to sensitive tumour cells (DiPaola *et al.* 1999).

In the following sections, specific mechanisms of drug resistance are discussed and categorised according to whether they occur upstream or downstream of the drug reaching and binding to its intracellular target. Platinum-resistance mechanisms are dealt with separately.

### 1.6.2. Upstream Resistance Mechanisms

#### 1.6.2.1. ABC Transporters

ATP-binding cassette (ABC) transporters are efflux pumps that use ATP to actively transport substrates across the plasma membrane (Leslie *et al.* 2005). These proteins carry out a protective role in cells preventing xenobiotic accumulation and toxicity (Leslie *et al.* 2005). Overexpression of these efflux pumps is often linked to multi-drug resistance (MDR) whereby cells treated in the laboratory with one agent, become cross-resistant to other anticancer agents that are structurally and functionally different from the original agent (Choi, 2005). An example of an ABC transporter protein associated with anti-cancer drug resistance is P-glycoprotein (MDR1), a 170kD glycoprotein, which confers resistance to many natural products, including,

anthracyclines, actinomycin D, etoposide, mitomycin C, taxanes and vinca alkaloids (Choi, 2005). P-glycoprotein mediated multi-drug resistance is often referred to as 'classical' drug resistance.

The ABC transporters multidrug resistance protein 1 and 2 (MRP1 and MRP2) (MRP2 is also known as canalicular multispecific organic anion transporter, or cMOAT) are capable of transporting the metabolites of alkylating agents including cyclophosphamide and chlorambucil, they also transport vincristine and daunorubicin in conjunction with reduced glutathione (Leslie *et al.* 2005). The ABC transporter, breast cancer resistance protein (BCRP) is associated with multi-drug resistance to anthracyclines, mitoxantrone, camptothecin and methotrexate. It does not confer cross-resistance to vinca alkaloids, paclitaxel, epipodophyllotoxins or cisplatin (Allen and Schinkel, 2002, Leslie *et al.* 2005).

1.6.2.2 Glutathione (GSH)

Glutathione is an intracellular antioxidant thiol that binds to and detoxifies a wide range of electrophiles (O'Brien and Tew, 1996). Conjugation can be spontaneous or mediated by members of the glutathione S-transferase superfamily of dimeric phase II metabolic enzymes (O'Brien and Tew, 1996). Glutathione S-transferases react with intracellular glutathione producing a glutathione thiolate anion (GS-) which acts as a nucleophile to attract electrophiles (Spurdle *et al.* 2001). Mammalian soluble GSTs can be subdivided into 7 groups, alpha (α), mu (μ), pi (π), theta (θ), kappa (κ,) sigma (σ) and omega (ω) (Landi *et al.* 2000). GSH conjugation results in the compound becoming less toxic, and more hydrophilic, so that it is more readily excreted (O'Brien and Tew, 1996). A common approach used to investigate the role of glutathione in drug resistance is to reduce intracellular GSH and observe the effect on cytotoxicity. GSH depletion is achieved by treating cells with buthionine sulfoximine (BSO), which inhibits the enzyme γ-glutamyl cysteine synthetase (γGCS), effectively blocking GSH synthesis (Meijer *et al.* 1992, Fojo *et al.* 2003).

With regards to many alkylating agents, the aziridinium ions formed just prior to DNA alkylation are thought to be the GST substrates for GSH conjugation (Bolton *et al.* 1993, Yuan *et al.* 1991). Binding of glutathione to a bifunctional DNA alkylating

agent abrogates bifunctionality and prevents crosslinks formation, reducing the cytotoxicity of the compound (O'Brien and Tew, 1996).

Artificially elevated GSTα and GSTπ expression in *Saccharomyces cerevisiae* resulted in up to an eight-fold increase in chlorambucil resistance (Black *et al.* 1990). A ten-fold chlorambucil resistant NIH3T3 murine fibroblast cell line called N50-4, had a seven to ten-fold increase in intracellular GSH, a three-fold increase in GST activity and increase in steady state GSTα mRNA, compared to the parental sensitive cell line (Yang *et al.* 1992). Simultaneous depletion of intracellular GSH with BSO, and inhibition of GST activity with ethacrynic acid in N50-4 cells led to chlorambucil resistance being almost completely abolished (Yang *et al.* 1992). Transfection of GSTA2 into NIH3T3 cells conferred a five-fold increase in chlorambucil resistance and a ten-fold increase in mechlorethamine resistance (Greenbaum *et al.* 1994).

An investigation into four human melanoma cell lines resistant to alkylating agents revealed an overall three to five-fold increase in GST activity, three to five-fold increase in GSTπ protein levels, and eight to 15-fold increase in GSTπ mRNA levels (Wang *et al.* 1989). Horton *et al.* (1999) produced a chlorambucil resistant human ovarian cancer cell line, derived from A2780, via repeated exposure to increasing concentration of the drug. Their 10-fold resistant cell line A2780(100), expressed 11-fold more GSTμ, and produced six-fold more GSH-CBL conjugates, than the parental cell line. Transfection of COS monkey cells with GSTα conferred an increase in resistance to chlorambucil and melphalan (1.3 and 2.9-fold, respectively) (Puchalski and Fahl, 1990). Reversion of transient GSTα expression resulted in a total loss of chlorambucil resistance (Puchalski and Fahl, 1990).

A melphalan resistant rat mammary carcinoma cell line, that was cross-resistant to both chlorambucil and mechlorethamine, has been described with a two-fold increase in intracellular GSH concentration and a five-fold increase in GST activity, compared to wild-type sensitive cells (Alaoui-Jamali *et al.* 1992). Examination of crosslink formation in wild type cells, following melphalan or chlorambucil revealed that crosslink formation continued up to 8 hours after drug exposure, decreasing over a 24 hour period. No significant crosslink formation was observed 0-24 hours after melphalan or chlorambucil exposure, in the melphalan resistant cell line (Alaoui-

Jamali *et al.* 1992). Treatment of both cell lines with mechlorethamine resulted in immediate crosslink formation, followed by a subsequent decrease during the 24 hour drug free incubation, however significantly lower levels of crosslinking were observed in the melphalan-resistant cell line (Alaoui-Jamali *et al.* 1992). Both suppression of intracellular glutathione with BSO and inhibition of GST with ethacrynic acid resulted in increased sensitivity to melphalan and increased crosslink formation (Alaoui-Jamali *et al.* 1992).

Interestingly, two publications failed to report any change in chlorambucil or melphalan resistance following GSTα transfection (Leyland-Jones *et al.* 1991) or melphalan resistance following GSTπ transfection (Moscow *et al.* 1989) into MCF-7 human breast cancer cells.

1.6.2.3. Metallothionein

There are four main isoforms within the metallothionein (MT) family of low molecular weight, cysteine-rich proteins, which exhibit a high affinity for metal ions (Theocharis *et al.* 2003). These proteins are thought to play a major regulatory role in zinc uptake, storage and release (Vasak *et al.* 2000).

Cells with acquired resistance to chlorambucil, displayed elevated metallothionein expression and activity (Ebadi *et al.* 1994). Embryonic fibroblast cells from transgenic mice with targeted disruptions of the *MTI* and *MTII* genes, showed enhanced sensitivity to melphalan exposure, compared to wildtype cells (Kondo *et al.* 1995). Cells transfected with metallothionein IIA (MTIIA) using bovine papilloma virus expression vectors were resistant to melphalan and chlorambucil (Kelley *et al.* 1988) and to N-methyl-N'-nitro-N' nitrosoguanidine (MNNG) and mitomycin C (MMC) (Lohrer *et al.* 1989).

1.6.2.4. Aldehyde Dehydrogenase (ALDH)

ALDH enzymes catalyse the oxidation of an active intermediate of cyclophosphamide (aldophosphamide) into an inactive compound, carboxyphosphamide (Hilton *et al.* 1984). A cyclophosphamide resistant L1210 cell

line was found to have unusually high aldehyde dehydrogenase activity (Hilton *et al.* 1984). Transfection of rat class 3 ALDH isozyme into a human breast cancer cell line MCF-7, led to a cyclophosphamide (CPA) analog mafosfamide resistance (Bunting *et al.* 1994).

1.6.2.5. Topoisomerase.

Tan *et al.* (1987b) investigated mechlorethamine resistance in human Burkitts lymphoma cell lines. They reported reduced ICL formation in the resistant cell line, but no difference in ICL repair. The resistant cell line contained higher GSH levels, but treatment of the resistant cells with BSO, did not affect mechlorethamine sensitivity. The resistant cell line also exhibited elevated topoisomerase II expression and activity (Tan *et al.* 1987b). Tan and colleagues proposed that topoisomerase II was facilitating an enhanced repair of HN2 monoadducts, before they became bifunctional interstrand adducts. They postulated that topoisomerase II was altering the chromatin structure to facilitate efficient monoadduct repair, citing previous research (Tan *et al.* 1987a) proving that chromatin from the resistant cell line was more easily digested by DNase I than the parental sensitive cell line (Tan *et al.* 1987b). Removal of the weekly treatment of the resistant cells with HN2, resulted in increased HN2 sensitivity, the loss of the resistant phenotype was also accompanied by a decrease in topoII expression, and an increased susceptibility to HN2 interstrand crosslink formation (Tan *et al.* 1987b)

Pu *et al.* (1999, 2000) reported elevated topoisomerase II protein expression and activity in a melphalan resistant human B-lymphoid cell line, and human leukaemic cell line, compared to the parental sensitive cell lines. Pre-incubation of the cells with doxorubicin, a topoisomerase II inhibitor, resulted in significantly increased melphalan induced ICL formation and cytotoxicity in the resistant cells, as compared to the sensitive cells (Pu *et al.* 1999, 2000).

1.6.3. Downstream Resistance Mechanisms

This section deals with the resistance mechanisms that occur after the anti-cancer agent has reacted with its cellular target.

1.6.3.1. Altered DNA Repair

Torres-Garcia *et al.* (1989) were able to correlate resistance to mustards in chronic lymphocytic leukaemia with enhanced removal of melphalan-induced crosslinks. Bramson *et al.* (1995a) investigated mechanisms of mustard drug resistance using B lymphocytes from patients with mustard resistant chronic lymphocytic leukaemia, screening cells for cross-resistance to other compounds. Cells showed no increased resistance to methyl methanesulfonate or UV, suggesting that neither base excision repair (BER) or NER were upregulated in resistant cells (Bramson *et al.* 1995a). Lymphocytes from resistant patients were cross resistant to the other mustards, chlorambucil and melphalan, and to other crosslinking agents cisplatin and mitomycin C (Bramson *et al.* 1995a). Together these results suggest that clinical resistance to mustard in these patients is caused by elevated ICL repair (Bramson *et al.* 1995a). More recently, clinical research into ICL repair as a mechanism of acquired resistance found repair of interstrand crosslinks to be linked to melphalan resistance in patients with multiple myeloma (Spanswick *et al.* 2002).

1.6.3.1.1. Nucleotide Excision Repair (NER)

ERCC2 (XPD) expression was correlated with chloroethylnitrosourea (CENU) resistance using quantitative competitive polymerase chain reaction (PCR) in six human tumour cell lines (Chen *et al.* 1996). ERCC2 (XPD) protein levels also correlated with 1,3-bis-(2-chloroethyl)-1-nitrosourea (BCNU) cytotoxicity in 14 chloroethylnitrosourea (CENU) resistant human cancer cell lines (Chen *et al.* 1997). ERCC1 expression was elevated in lymphocytes from NM-resistant chronic lymphocytic leukaemia patients, compared to cells from untreated patients (Geleziunas *et al.* 1991). However Bramson *et al.* (1995b) failed to correlate ERCC1, or ERCC2 (XPD) with nitrogen mustard resistance in cells from chronic lymphocytic leukaemia patients. Western blot analysis of the National Cancer Institute (NCI) panel of 60 human tumour cell lines, revealed a strong correlation between XPD protein levels and resistance to alkylating agents (Chen *et al.* 2002).

1.6.3.1.2 Homologous Recombination Repair (HRR)

Homologous Recombination has been implicated to play a role in melphalan resistance (Wang *et al.* 2001b) where elevated XRCC3 protein levels and increased density of Rad51 foci correlated with melphalan resistance.

Hazelhurst *et al.* (2003) investigated gene expression profiles of melphalan resistant-melanoma cell lines with parental sensitive cell lines using affymetrix oligonucleotide microarrays. The melphalan-resistant myeloma cell line 8226/LR5 was found to have elevated FANCF and RAD51C expression, and lower levels of ICL. These findings led Chen *et al.* (2005) to specifically investigate the expression of 11 FANC/BRCA genes in melphalan-resistant myeloma cell lines using custom designed real-time PCR microfluid cards. They report over a two-fold increased expression of FANCA, FANCC, FANCF and FANCL in a melphalan-resistant cell line that shows elevated melphalan ICL unhooking, compared to the parental sensitive cell line (Chen *et al.* 2005). The differential expression of FANCF was found not to be as a result of CpG methylation (Chen *et al.* 2005). Following exposure to melphalan, this resistant cell line showed over a two-fold higher levels of FANCD2-L, the monoubiquitinated form of FANCD2, compared to the parental line, despite having lower levels of melphalan ICL (Chen *et al.* 2005). Only monoubiquitinated D2 can be transported to DNA damage foci, to perform its repair function (Garcia-Higuera *et al.* 2001, Taniguchi *et al.* 2002). siRNA knock-down expression experiments found that reduced FANCF expression in the resistant cell line led to reduced ICL unhooking capability (Chen *et al.* 2005). Chen *et al.* (2005) also reported that overexpression of FANCF in melphalan sensitive cell lines enhanced cell survival following melphalan treatment.

1.6.3.1.3. $O^6$-Methylguanine DNA Methyltransferase (MGMT)

$O^6$-methylguanine-DNA-methyltransferase (MGMT) is also known as $O^6$-alkylguanine DNA alkyltransferase. $O^6$-alkylguanine adducts can be repaired by the 'suicide' protein $O^6$-alkylguanine DNA alkyltransferase, which acts as an acceptor protein for the alkyl group, effectively inactivating itself in the process (Gerson 2002). Nitrosoureas alkylate the O6 position in guanine, which eventually produces an interstrand crosslink between the N3 position of guanine and the N1 position of

cytosine (Damia *et al.* 1998). Interestingly research by Yarosh *et al.* (1986) correlated chloroethylnitrosourea (CENU) resistance with increased $O^6$-alkylguanine DNA alkyltransferase activity and reduced ICL formation. Beith *et al.* (1997) investigated $O^6$-alkylguanine DNA alkyltransferase levels in human glioma cell lines, they reported a strong correlation between increasing enzyme level and increasing resistance to 1,3-bis(chloroethyl)-nitrosourea (BCNU). Esteller *et al.* (2000) researched *MGMT* expression and clinical response to gliomas to BCNU/cisplatin combination chemotherapy. Patients that had evidence of *MGMT* promoter methylation and loss of $O^6$-alkylguanine DNA alkyltransferase activity showed improved disease free survival (Esteller *et al.* 2000).

1.6.3.2. Altered Apoptosis

Apoptosis is a form of cell suicide that facilitates the death of cells, in a way that leads to the controlled absorption of the cellular components without inducing an inflammatory response, as it the case with the other form of cell death, necrosis (Lowe and Lin, 2000). Apoptosis regulates the cell number of an organism, exactly balancing cell loss with gain, and is essential during development, for instance for the formation of separated fingers on a hand (Raff, 1998). Examples of uncontrolled apoptosis, for instance in neurones, manifest in diseases like Alzheimer's and Parkinson's (Ashkenazi and Dixit, 1998). Cells undergoing apoptosis exhibit cell shrinkage, membrane blebbing, chromosome condensation, and nuclear fragmentation (Lowe and Lin, 2000).

In response to the cellular damage induced by cytotoxics, cells firstly detect the damage, and then initiate either a stalling of the cell cycle to repair the damage, or cell suicide (Pommier *et al.* 2004). P53 is a tumour suppressor gene that functions as a check-point protein, regulating cell cycle arrest in order to maintain genomic integrity following DNA damage (Lowe and Lin, 2000). The most prevalent genetic change, at the gene level in cancer is the p53 mutation, with approximately 50% of cancers showing a missense mutation of one allele, and the deletion of the second allele (Harris *et al.* 1993, Nigro *et al.* 1989, Takahashi *et al.* 1989, Vogelstein, 1990, Hollstein *et al.* 1991, Cho *et al.* 1994).

The majority of chemotherapeutic drugs induce the mitochondrial pathway of programmed cell death, as opposed to the death-receptor mediated pathway (Kostanova-Poliakova and Sabova, 2005). This response is mediated by the Bcl-2 family of proteins, which includes over 30 proteins capable of binding to form homo- and heterodimers (Pommier *et al.* 2004). Pro-apoptotic Bcl-2 family members include; Bad, Bak, Bcl-$X_S$ and Bax, anti-apoptotic proteins include; Bcl-2 and Bcl-$X_L$ (Hickman, 1996). A positive ratio of pro- and anti-apoptotic Bcl-2 proteins leads to the initiation of apoptosis, via the permeabilisation of the mitochondrial membrane. For example, Bax:Bax homodimers promote apoptosis, but it is the level of Bcl-2, and therefore the level of Bcl-2:Bax heterodimers, that determines apoptosis by limiting Bax homodimerisation (Hickman, 1996).

Permeabilisation of the outer mitochondrial membrane leads to the leakage of apoptotic factors, including cytochrome C, Smac/DIABLO, HtrA2/Omi, endonuclease G and AIF (Kostanova-Poliakova and Sabova, 2005). Smac/DIABLO and HtrA2/Omi function to prevent inhibitor of apoptosis proteins (IAPs) from blocking caspases and preventing cell death (Suzuki *et al.* 2001, Verhagen *et al.* 2000, Kostanova-Poliakova and Sabova, 2005). Cytochrome C functions as the key mediator of apoptosis, as once released into the cytoplasm it complexes with Apaf-1 and pro-caspase 9 to form an apoptosome (Li *et al.* 1997, Zou *et al.* 1999, Kostanova-Poliakova and Sabova, 2005). Complex formation causes the activation of caspase-9, which subsequently activates caspase-3, leading to apoptosis (Li *et al.* 1997, Zou *et al.* 1999, Kostanova-Poliakova and Sabova, 2005).

By altering the processes of apoptosis cells can become resistant to the damage induced by chemotherapeutics. Interestingly, Miyashita *et al.* (1994) identified a p53-dependent negative response element in the *Bcl-2* gene, suggesting the active suppression of expression of this protein via p53. As a large percentage of tumours have defective p53, this block to Bcl-2 expression would be effectively removed. These tumours would therefore inherently express elevated Bcl-2, which could lead to a resistant response to drug therapy. Fan *et al.* (1994) correlated mutant p53 with decreased sensitivity of human lymphoma cells to DNA damaging agents, namely $\gamma$–rays, mechlorethamine and etoposide.

The role of altered apoptosis in cancer drug resistance has been investigated using cell line models, by artificially manipulating the stable expression of key apoptosis mediators. For example Miyashita *et al.* (1992) infected two murine lymphoid cell lines with a recombinant retrovirus encoding the human Bcl-2 protein. These cell lines exhibited increased resistant to methotrexate, 1-beta-D-arabinofuranosylcytosine and vincristine. Ohmori *et al.* (1993) transfected Bcl-2 into a human small cell lung cancer cell line, and reported resistance to doxorubicin, irinotecan and mitomycin C. No difference in sensitivity was noted in response to etoposide, ACNU, methotrexate or paclitaxel (Ohmori *et al.* 1993). Kondo *et al.* (1994) increased Bcl-2 expression in bone marrow cells using retroviral gene transfer, and reported increased resistance to apoptosis induced by camptothecin, etoposide and doxorubicin. Erythroleukaemic cells transfected with Bax, showed higher fractions of apoptotic cells in response to Ara-C, and doxorubicin exposure than control cells (Kobayashi *et al.* 1998). Their Bcl-2 transfectants had fewer apoptotic cells in response to Ara-C, doxorubicin and etoposide expression than the control cell population (Kobayashi *et al.* 1998).

The drug resistance mediated by elevated levels of anti-apoptotic molecules occurs downstream of DNA damage, as several research groups have reported no change in DNA damage formation and repair between control cells and resistant transfected cell lines. Walton *et al.* (1993) reported elevated mechlorethamine drug resistance in a murine, IL-3 dependent cell line transfected with Bcl-2 compared to control cells. Equimolar doses of mechlorethamine produced similar rates of ICL formation and repair in both the sensitive and resistant cell lines (Walton *et al.* 1993). Hashimoto *et al.* (1995) and Kamesaki *et al.* (1994) investigated the effect of Bcl-2 expression on etoposide mediated cytotoxicity in Chinese hamster cells, and mouse B-cells, respectively. Both model systems showed elevated etoposide resistance in the Bcl-2 transfected cells compared to their relative controls. Hashimoto *et al.* (1995) reported similar levels of single strand breaks in the control and Bcl-2 cell lines. Kamesaki *et al.* (1994) reported little or no difference in the formation and repair of DNA-protein crosslinks, single strand breaks, or double strand breaks in the Bcl-2 transfected cells or the control cells. Schmitt *et al.* (1998) reported camptothecin resistance in human leukaemic cell lines transfected with Bcl-XL, compared to control cells. The level of DNA strand break formation, and synthesis inhibition in response to camptothecin exposure was similar in control and transfected cells.

Interestingly, Sawa *et al.* (2000) transfected human gastric cancer cells with Bax, and also with Bcl-2. The Bax cells were more sensitive to treatment with paclitaxel, 5-fluorouracil and doxorubicin, and Bcl-2 were more resistant, compared in both cases to the control cells. Western blot analysis revealed that the Bax cells contained higher cytosolic levels of cytochrome C than control cells. Following drug exposure the cytosolic levels of cytochrome C rose significantly within the Bax cells, and at each time point assessed were higher than those of the control cells (Sawa *et al.* 2000). Marked activation of caspase 3 was also noted in the Bax cells 48 and 72 hours after drug exposure, compared to the control cells.

Walton *et al.* (1993) investigated the affect of Bcl-2 overexpression using a murine, IL-3 dependent cell line. Mechlorethamine exposure resulted in two-fold less cell death and DNA degradation in cells overexpressing Bcl-2, compared to control cells transfected with an empty vector. Other research groups have correlated Bcl-2 or Bcl-XL induced cancer drug resistance with a reduced rate of DNA degradation, following drug exposure. A Bcl-2 negative human neuroblastoma cell line was transfected with Bcl-2 (Dole *et al.* 1994). Following etoposide exposure, analysis using flow cytometry of propidium iodide stained nuclei, and pulse-field gel electrophoresis (PFGE), revealed significantly reduced DNA degradation in Bcl-2 transfected cells compared to vector-transfected controls (Dole *et al.* 1994). The same pattern of significantly reduced DNA degradation was observed using the same technique in a human neuroblastoma cell line transfected with Bcl-XL, and exposed to 4-hydroperoxy-cyclophosphamide(4-HC) (Dole *et al.* 1995).

Interestingly, Gibson *et al.* (1999) have postulated that the synergistic elevation in Bax expression, and reduction in Bcl-2 expression following the combined treatment of human breast cancer cell lines with etoposide and cyclophosphamide, could explain the clinical efficacy of this regime in advanced breast cancer.

Clinical research into the significance of the expression of various apoptotic mediators in relation to response to chemotherapy have provide interesting results. For instance, immunoblot analysis of 58 peripheral blood B-cell chronic lymphocytic leukaemia (B-CLL) specimens indicated that high levels of the anti-apoptotic protein

Mcl-1 were strongly correlated with failure to achieve complete remission in B-CLL (there were 42 patients in this study) (Kitada *et al.* 1998). Analysis of lymph nodes from 327 Hodgkin's lymphoma patients, using immunohistochemistry, correlated high Bcl-2 expression with poor response to treatment and/or short time of survival, where treatment consisted of COPP (cyclophosphamide, vincristine, procarbazine, prednisone), MOPP (nitrogranulogen, vincristine, procarbazine, prednisone) or ABVD (adriamycin (doxorubicin), bleomycin, vinblastine, dacarbazine) Smolewski *et al.* 2000).

Analysis of Bcl-2 protein expression was undertaken in 82 samples of newly diagnosed acute myeloid leukaemia (Campos *et al.* 1993). High expression of Bcl-2 was associated with low complete remission rate after intensive chemotherapy (an anthracycline drug or mitoxantrone and cytosine arabinosine (Ara-C)) (Campos *et al.* 1993). Western blot analysis of 19 cases of AML indicated that high expression of Bcl-2 and of Bax were associated with bad clinical prognosis and a poor clinical outcome to intensive chemotherapy in AML (Zhou *et al.* 1998). In a separate study, involving real-time quantitative PCR using 232 samples of AML patients at diagnosis, both high Bax and a high Bcl-2/Bax ratio were independent predictors of unfavourable outcome in AML (Kohler *et al.* 2002).

High Bcl-2 expression in breast cancer has been related to positive and negative response to chemotherapy. For instance, Pusztai *et al.* (2004) investigated Bcl-2 level in 29 paired pre- and postchemotherapy (doxorubicin-based) breast tissue samples of locally advanced breast cancer. In this study lack of Bcl-2 was correlated with a higher probability of complete pathological response to doxorubicin-based chemotherapy (Pusztai *et al.* 2004). Similar research has been published by Van Slooten *et al.* (1996) and Lipponen *et al.* (1995) involving 441 node-negative breast cancer patient samples, and 202 breast cancer patient samples, respectively. High Bcl-2 expression was correlated with favourable outcome, with better disease free and overall survival following chemotherapy (5-fluorouracil, doxorubicin, cyclophosphamide) (Van Slooten *et al.* 1996, Lipponen *et al.* 1995). Diadone *et al.* (1999) reviewed independent studies involving approximately 5000 breast cancer patients. They concluded that Bcl-2 expression is strongly correlated with biologic features of a differentiated phenotype, namely, slow proliferation, high steroid

receptor levels, absence of p53 and c-erB-2 expression, also with favourable outcome to chemotherapy. The relationship between Bcl-2 expression in breast cancer and response to chemotherapy is therefore complicated by these associated characteristics, and deserves further research.

Miyazaki *et al.* (2005) failed to relate Bcl-2 or Bax expression with response to therapy, involving radiation and chemotherapy (cisplatin, nedaplatin and 5-fluorouracil) in oesophageal squamous cell carcinoma.

1.7. Resistance to Cisplatin

Elucidating the exact processes involved in cisplatin resistance is complicated because the drug acts in several ways. Studies have linked resistance to increased drug efflux (Parker *et al.* 1991a), decreased influx (Safaei and Howell 2005), enhanced replicative bypass (translesion synthesis) (Bergoglio *et al.* 2001), altered DNA repair (Reed, 1998a), and intracellular detoxification (GSH) (Godwin *et al.* 1992). Each of these mechanisms effectively prevents or overcomes cisplatin damage, in such a way to render it sublethal. Mechanisms of resistance to cisplatin are discussed in the following sections.

Altered cisplatin-DNA adduct processing has been reported in many cases of cisplatin resistance. Using atomic absorption spectrometry (AAS) to measure platinum-DNA binding in leukocytes from 49 patients with 23 histological types of malignancy (Reed *et al.* 1993) and from other solid tumour patients (Schellens *et al.* 1996 and Parker *et al.* 1991b) high platinum adduct formation was linked to a positive response to platinum based chemotherapy. However, Fisch *et al.* (1996) failed to correlate high platinum adduct level, measured using AAS, and favourable outcome in patients with advanced germ cell cancer.

Testing intrastrand crosslinking in leukocytes from ovarian and testicular cancer patients (Reed *et al.* 1986, 1987 and 1988) and from ovarian, testicular, colon and breast cancer patients (Poirier *et al.* 1993) researchers correlated high intrastrand crosslinking with consistently improved clinical responses to platinum chemotherapy.

Reduced interstrand crosslink formation has been reported in cisplatin-resistant human cell lines, including; small cell lung cancer (Hospers *et al.* 1988), non-small cell lung cancer (Bungo *et al.* 1990), head and neck squamous carcinoma (Teicher *et al.* 1987), bladder carcinoma (Bedford *et al.* 1987), colon cancer (Fram *et al*, 1990), osteosarcoma (Perego *et al.* 1999) squamous carcinoma (Esaki *et al.* 1996) and ovarian cancer (Johnson *et al.* 1994a and Zhen *et al.* 1992). These studies provide evidence of resistance mechanisms functioning upstream of cisplatin-adduct formation.

Enhanced ICL repair has been reported in cisplatin-resistant human squamous carcinoma cell lines (Esaki *et al.* 1996), and in human ovarian cancer cell lines (Behrens *et al.* 1987, Masuda *et al.* 1988 and 1990, Lai *et al.* 1988, Parker *et al.* 1991a, Zhen *et al.* 1992, Sargent *et al.* 1996, Johnson *et al.* 1994a and 1994b). These studies provide evidence of enhanced repair as a downstream resistance mechanism.

In the following sections cisplatin resistance mechanisms have been classified as functioning either upstream or downstream of cisplatin-DNA adduct formation.

### 1.7.1. Upstream Cisplatin Resistance Mechanisms

#### 1.7.1.1. ABC Transporters

Low levels of P-glycoprotein (Pgp) have been detected in ovarian cancer tissue (Leonard *et al.* 2003). Ozalp *et al.* (2002) measured Pgp expression in ovarian tumour tissue using immunohistochemistry, they reported no correlation between Pgp expression and overall patient survival. Chen *et al.* (2000) failed to establish a link between Pgp or MRP expression and cisplatin resistance in human ovarian cancer cell lines, following expression analysis using flow cytometry. In a study of 33 human ovarian cancer patients, Codegoni *et al.* (1997) reported no correlation between Pgp expression and response to chemotherapy (mainly platinum-based with or without doxorubicin and cyclophosphamide). Conversely, Cheng *et* al. (2001) reported elevated Pgp expression, measured using western blotting and RT-PCR, in a cisplatin-resistant human ovarian cancer cell line. Baekelandt *et al.* (2000) investigated Pgp expression in a cohort of 73 human patients with advanced ovarian

cancer. They correlated negative Pgp expression with a significantly better response to chemotherapy (cisplatin and epirubicin), and using a multivariate survival analysis, they reported that Pgp was an independent predictor of both overall and progression free survival (Baekelandt *et al.* 2000).

cMOAT is also known as MRP2 and according to the Human Gene Nomenclature Committee, ABCC2 (Materna *et al.* 2005). Four to six-fold higher levels of cMOAT expression were detected in three cisplatin-resistant cell lines that exhibited decreased drug accumulation, compared to the parental sensitive cell lines (Taniguchi *et al.* 1996). Kool *et al.* (1997) reported that cMOAT mRNA levels correlated with cisplatin resistance in several cell lines. Overexpression of cMOAT was associated with cisplatin resistance, and reduced cisplatin-intrastrand crosslink formation, measured using an immunocytologic assay, in a human melanoma cell line (Liedert *et al.* 2003). Enhanced expression of cMOAT, but not MRP1 in the human liver cancer cell line HepG2 was reported in response to cisplatin exposure (Schrenk *et al.* 2001). Cisplatin-resistant HepG2 cells expressing cMOAT, were made cisplatin-sensitive using antisense cDNA (Koike *et al.* 1997). Recently anti-MRP2 hammerhead ribozymes were used to inhibit the expression of MRP2 specific mRNA in a cisplatin-resistant ovarian cancer cell line (Materna et al. 2005), exposure led to a 50% reduction in cisplatin resistance, and an increased level of cisplatin-d(GpG) intrastrand crosslink formation (measured using an immunocytological assay), compared to the cisplatin-resistant cell line (Materna *et al.* 2005).

1.7.1.2. Copper Transporters

Recent findings have implicated two efflux transporters and an influx transporter with cisplatin resistance. The role of the copper influx transporter CTR1, and the efflux transporters ATP7A and ATP7b in platinum resistance has recently been reviewed by Safaei and Howell (2005). *Saccharomyces cerevisiae* that did not express the yCTR1 transporter were found to be relatively resistant to cisplatin, and so show reduced drug accumulation (Ishida *et al.* 2002). A cisplatin resistant prostate cancer cell line was found to express higher levels of ATP7B than its parental sensitive cell line (Komatsu *et al.* 2000). The cisplatin-resistant ovarian cancer cell lines A2780/CP and 2008/C13*5.25 were found to express higher levels of ATP7A, and IGROV-1/CP

was found to express higher levels of ATP7B, than their respective parental sensitive cell lines (Katano *et al.* 2002). Transfection of hCTR1 into A2780 human ovarian cancer cells resulted in increased cisplatin accumulation and sensitivity (Samimi *et al.* 2003). Transfection of ATP7B into an epidermoid cancer cell line, resulted in a 8.9-fold increase in cisplatin resistance, and a two-fold increase in copper resistance (Komatsu *et al.* 2000). Recently Samimi *et al.* (2003) reported a correlation between increased expression of ATP7A and poor survival in ovarian cancer. Therefore, increased expression of the influx pump correlates with increase sensitivity, as more drug enters the cell, and increased expression of the efflux pump correlates with increased resistance, as the cell can rapidly export the cytotoxic from the cell before it can reach and bind its target.

1.7.1.3. Glutathione (GSH)

Cisplatin resistance has been positively correlated with glutathione content in human cells, including; small cell lung cancer cells (Hospers *et al.* 1988, Meijer *et al.* 1992), human fibroblasts (Hansson *et al.* 1996), human osteosarcoma cells (Komiya *et al.* 1998), and human liver cancer cells (Zhang *et al.* 2001). Cisplatin resistance specifically in ovarian tumour cancer cell lines has also been closely correlated with glutathione content (Hamilton *et al.* 1985, Godwin *et al.* 1992, Hamaguchi *et al.* 1993, Kudoh *et al.* 1994, Shellard *et al.* 1991).

Interestingly, Shellard *et al.* (1991), reported elevated glutathione in the cisplatin-resistant human ovarian cancer cell line, SKOV-3, compared to the three-fold more sensitive human ovarian cancer cell line TR175 (both cell lines were produced from patients treated with alkylating agents, but not cisplatin). Within the resistant SKOV-3 cells, this difference in glutathione content correlated with a 16% reduction in total DNA platination, but conversely, with a higher level of ICL formation, compared to the sensitive TR175 cells (Shellard *et al.* 1991).

Researchers have reported a correlation between BSO incubation and enhanced cisplatin cytotoxicity in human ovarian cancer cell lines (Lee *et al.* 1992, Hamilton *et al.* 1985, Andrews *et al.* 1988, Kudoh *et al.* 1994, Oguchi *et al.* 1994, Perez *et al.* 2001, Jansen *et al.* 2002), and in a human stomach cancer cell line (Lee *et al.* 1992), a

human colon cancer cell line (Robichaud *et al.* 1990), a human small cell lung cancer (Meijer *et al.* 1990), and human liver cancer cell lines (Zhang *et al.* 2001). As expected, several of these groups also reported elevated intracellular platinum levels, and cisplatin interstrand crosslinking as a result of BSO treatment, in human cancer cell lines (Robichaud *et al.* 1990, Meijer *et al.* 1990, Zhang *et al.* 2001) and in a rat xenograph model (Chen and Zeller, 1991).

Godwin and co-workers (1992) exposed human ovarian cancer cell lines to cisplatin, resulting in increasing degrees of stable-cisplatin resistance, which closely correlated with an increase in intracellular glutathione. This group reported that the mRNA of two key enzymes involved in glutathione synthesis were elevated in cases of very high cisplatin resistance (Godwin *et al.* 1992). The enzymes reported were γ-glutamyl transpeptidase (GGT) and γ-glutamyl cysteine synthetase (γGCS). GGT is a membrane bound protein that cleaves extracellular glutathione into its component amino acids, which are subsequently transported into the cell and used as the building blocks for further glutathione synthesis (Hochwald *et al.* 1996, Hanigan *et al.* 1993). Oguchi *et al.* (1994) also reported increased GGT activity and mRNA expression in human ovarian cancer cell lines in response to cisplatin exposure. However, they failed to correlate GGT activity or cisplatin-induced GGT mRNA expression with their cisplatin resistant phenotype. Hanigan *et al.* (1999) and Nishimura *et al.* (1998) researched GGT expression in clinical samples from human germ cell cancer patients and human head and neck cancer patients. Both groups reported that clinical response to platinum was independent of GGT levels.

γGCS is composed of a light and a heavy subunit (Huang *et al.* 1993). The heavy subunit is believed to house the catalytic activity of the enzyme and the light subunit is thought to play a regulatory role (Huang *et al.* 1993). Yao *et al.* (1995) reported a correlation between the relative steady state mRNA levels of the heavy subunit of γGCS and cisplatin cytotoxicity in cisplatin-resistant human ovarian cancer cell lines derived from A2780. This difference was due to a proportional increase in transcription rate, and was found not to be because of an increase in mRNA stability (Yao *et al.* 1995). Further research revealed a link between nuclear extract binding activity of the AP-1 response element (upstream of the transcription initiation site of the gene encoding the heavy subunit of γGCS), and γGCS gene expression (Yao *et al.*

1995). A supershift assay showed that the AP-1 binding complexes were predominantly formed by dimers of the Jun family of proteins (Yao *et al.* 1995) . The group also reported elevated expression of c-JUN in cisplatin-resistant cells, in comparison with sensitive tumour cells (Yao *et al.* 1995). This research therefore links elevated GSH production with altered expression of γGCS and of related transcription factors. Interestingly, this group also described a C-200 ovarian cancer cell subclone that is a partial revertant (by removal of selection pressure). This cell line confirmed their previous findings as it shows lower GSH levels, and increase in cisplatin sensitivity, decreased γGCS expression and deceased AP-1 binding activity (Yao *et al.* 1995). Treatment of the cisplatin resistant human ovarian cancer cell line with antisense DNA directed against c-jun resulted in reduced γGCS mRNA expression, and decreased cellular GSH (Pan *et al.* 2002). Transfection of A2780 with c-jun, resulting in a nine-fold increase in c-jun protein level, led to a ten-fold increase in GSH content, and a two-fold increase in cisplatin resistance (Pan *et al.* 2002)

As discussed, glutathione S-transferases react with intracellular glutathione resulting in the formation of a glutathione thiolate anion (GS-), this can then react with cisplatin, producing a conjugate bis-(glutathionato)-platinum, which is then effluxed through ATP-binding cassette transporters (ABCs) such as multispecific organic anion transporter (cMOAT) (also known as MRP2) and multidrug resistance-associates protein 1 (MRP1).

Research has linked elevated GST with increased numbers of GSH-DDP conjugates (Goto *et al.* 1999). A cisplatin-resistant human colonic cancer cell line, with elevated GSTπ, compared to the parental sensitive cell line, showed elevated GSH-DDP adduct formation (Goto *et al.* 1999). Treatment of cells with ethacrynic acid, a GSTπ inhibitor, led to a complete loss of GSH-DDP adduct formation (Goto *et al.* 1999). Artificially elevating GSTπ levels in the parental sensitive cell line (HCT8) using transfection, resulted in a parallel increase in GSH-DDP adduct formation (Goto *et al.* 1999).

Pulchalski and Fahl (1990) transfected monkey COS cells with GSTα, μ, and π, each resulting in an increase in cisplatin resistance. The greatest increase in resistance

resulted from transfection with the μ isoform (Pulchalski and Fahl, 1990). Oguchi *et al.* (1994) reported elevated GSTπ mRNA expression and activity in a cisplatin resistant human ovarian cancer cell line NOS2CR compared to the parental sensitive cell line NOS2. Both the GSTπ activity and mRNA expression levels remained the same in both cell lines following cisplatin exposure (Oguchi *et al.* 1994).

Cisplatin resistant CHO cells (C/CDP1 and C/CDP2) were found to contain higher levels of GSTπ mRNA (five-fold) and four to six-fold higher enzyme activity compared to the parental CHO cell line (Saburi *et al.* 1989, Okuyama *et al.* 1994). A cisplatin sensitive revertant R1 produced from C/CDP2, following five months cisplatin free growth, displayed GSTπ activity and mRNA levels similar to the parental cell line (Saburi *et al.* 1989).

Interestingly, Goto *et al.* (2002) reported nuclear accumulation of GSTπ in response to cisplatin exposure in three human cancer cell lines. Blocking nuclear accumulation of this protein using edible mushroom lectin (*Agaricus bisporus* lectin (ABL)) resulted in increased cisplatin sensitivity (Goto *et al.* 2002).

Several research groups have investigated GST expression in clinical samples. Nishimura *et al.* (1996) and Shiga *et al.* (1999) researching GST levels in head and neck carcinomas found that elevated GSTπ, measured using immunohistochemistry, was associated with poor response to platinum-based chemotherapy, and that GSTπ overexpression was especially common in relapsed tumours. Gastric tumours defined as being GSTπ negative were more sensitive to *in-vitro* cisplatin exposure than those tumours defined as being GSTπ positive (Okuyama *et al.* 1994). Immunohistochemical analysis of paraffin embedded material from 213 ovarian tumours produced a strong correlation between high GSTπ expression and clinical response to chemotherapy (Mayr *et al.* 2000). Measuring GSTπ levels in ovarian cyst fluid, Boss *et al.* (2001) found that significantly higher GSTπ concentrations were present in malignant ovarian tumours compared to benign tumours. Higher GSTπ levels correlated with the worse prognostic factors (Boss *et al.* 2001). In the sub-group of patients that received platinum-based chemotherapy, significantly higher GSTπ concentrations occurred in patients with recurrence, compared to patients without recurrence (Boss *et al.* 2001).

Castagna *et al.* (2004) researched cisplatin resistance using a proteomic approach on paired cisplatin sensitive and resistant human cervix squamous cell carcinoma cell lines. Following a one-hour cisplatin incubation, the cisplatin-sensitive cell line A431 showed a two-fold increase in GSTπ protein levels compared to the cisplatin treated A431/Pt cell line. Cullen *et al.* (2003) used fluorescence *in situ* hybridisation (FISH) and immunohistochemistry to perform a comparative genomic hybridisation of ten head and neck cancer cell lines, increased GSTπ copy number was found in 90 % of the cell lines, GSTπ amplification (11q13) was detected in 70% of cell lines. They concluded that a GSTπ amplification was a common occurrence in head and neck squamous cell carcinomas, which could account for the development of resistance and poor clinical outcome amongst these patients

Conversely, Moscow *et al.* (1989) failed to induce cisplatin resistance in MCF-7 human breast cancer cells through transfection with GSTπ. Transfection of GSTμ and GSTα2 into the same cell line also failed to alter cisplatin cytotoxicity (Townsend *et al.* 1992).

1.7.1.4. Metallothionein

Early research by Endresen *et al.* (1984) involved injecting 24 nude mice with a cisplatin-resistant murine fibroblast, metallothionein-rich variant cell line, and another 24 animals with the parental sensitive cell line. Following three intravenous doses of 4mg/kg cisplatin on days 12, 26 and 33 days, tumour volume was reduced by approximately 80% in the tumours from the parental/sensitive line, whereas the tumours from the MT-rich cells were almost completely resistant (Endresen *et al.* 1984). In a study using C3H mice injected with MBT-2 murine bladder tumour cells, cisplatin sensitivity, measured as a decrease in tumour volume, was significantly increased through the suppression in metallothionein production, mediated by propargylglycine (Saga *et al.* 2004). Propargylglycine is an irreversible inhibitor of γ-cystathionase, leading to a decrease in the intracellular pool of free cysteine (Abeles *et al.* 1973), therefore decreasing metallothionein and glutathione synthesis. Interestingly, Satoh *et al.* (1993) reported that propargylglycine treatment of MBT-2 cells does not result in a decrease in glutathione content.

Many publications report an increase in metallothionein expression in response to exposure to chemotherapeutics including cisplatin. Cisplatin-resistant cell lines, created by repeated exposure to escalating doses of cisplatin, displayed elevated metallothionein (MT) expression compared to the levels in the corresponding parental cell lines, including a head and neck carcinoma (SCC-25/CP), a small cell carcinoma (SW2/CP) a large cell carcinoma (SL6/CP) and a melanoma (G3361/CP) (Kelley *et al.* 1988). Elevated MTIIa has been reported in two cisplatin-resistant, human ovarian cancer cell lines IGROV-1/pt0.5 and IGROV-1/pt1, compared to the parental sensitive line (Perego *et al.* 1998). Kikuchi *et al.* (1997) also reported elevated metallothionein expression, approximately three-fold, in a cisplatin-resistant human ovarian cancer cell line TYK/R, in comparison to the parental sensitive line TYK. Cisplatin-resistant human small cell lung cancer cell lines H69/CP and SW2/CP, express two-fold and 3.6-fold more hMTIIa respectively, than their cisplatin sensitive parental cell lines (Yang *et al.* 1994). A cisplatin-resistant human oral squamous carcinoma cell line SCC25/CP showed a nine-fold increase in hMTIIa basal steady state mRNA, and a three-fold increase in transcription rate, as well as a five-fold increase in hMTIe mRNA (Yang *et al.* 1994).

Clinical research using 97 surgical specimens from lung cancer patients indicated that metallothionein expression increased after the patients were exposed to chemotherapy including cisplatin, in non-small-cell lung cancer tissue, and in small-cell lung cancer tissue (Matsumoto *et al.* 1997). Other clinical research into metallothionein has linked high metallothionein expression in tumours to reduced patient survival compared to patients whose tumours registered lower metallothionein expression, in urothelial transitional cell carcinoma (Siu *et al.* 1998), and oesophageal carcinoma (Hishikawa *et al.* 1997).

Transfection of the gene encoding metallothionein (IIA) into murine C127 cells using a bovine papilloma virus construct led to a 4.4-fold increase in cisplatin resistance compared to cells transfected with vector alone (Kelley *et al.* 1988). However, similar experiments carried out, again using mouse C127 cells, and a bovine papilloma virus-metallothionein gene construct, led to no change in cisplatin cytotoxicity (Schilder *et al.* 1990). Stable transfection of MTIIA into the human ovarian cancer cell line A2780 led to a 3.8-fold resistance to cadmium chloride and a

seven-fold resistance to cisplatin (Holford *et al.* 2000). The fold difference in MTIIA following the transfection was not quoted in the original paper.

Transgenic mice with targeted disruptions of MTI and MTII genes displayed enhanced sensitivity to cisplatin (Kondo *et al.* 1995). However, extensive research by Schilder *et al.* (1990) failed to connect cisplatin resistance in ovarian cancer cell lines to metallothionein exposure. Specifically they tested for metallothionein expression in OVCAR-5 and OVCAR-7 cell lines derived from untreated patients, and the highly cisplatin resistant OVCAR-8 and OVCAR-10, developed from patients previously exposed to intensive chemotherapy. OVCAR-5 and OVCAR-7 were found to express metallothionein, whereas OVCAR-8 and OVCAR-10 were not (Schilder *et al.* 1990).

1.7.1.5. Topoisomerase

A cisplatin-resistant murine leukaemia cell line was found to exhibit a three-fold increase in topoisomerase II activity compared to the parental sensitive cell line (Barret *et al.* 1994). Analysis revealed that this was not explained by differences in the level of protein expressed. Sequential exposure of both cell lines to cisplatin and a specific topo II inhibitor (4`-(9-acridylamino)methane-sulfon-m-anisidide), led to an additive cytotoxic effect on the sensitive cell line, and a supra-additive effect in the resistant cell line, suggesting a significant role of topo II in the cisplatin-resistant phenotype of this cell line (Barret *et al.* 1994). Mestdagh *et al.* (1994) reported elevated topoisomerase II activity in two cisplatin-resistant murine leukaemia cell lines, compared to the parental sensitive cell line. Li *et al.* (2004) correlated elevated topo I, topo IIβ with cisplatin and carboplatin resistance in human ovarian cancer cell lines.

1.7.2. Downstream Cisplatin Resistance Mechanisms

1.7.2.1. Altered DNA Repair

Repair of cisplatin-induced damage can be measured using many techniques, including examining unscheduled DNA synthesis rates, atomic absorbance

spectroscopy (AAS), the comet assay, quantitative polymerase chain reaction (Q-PCR) and host reactivation assays (whereby plasmids containing easily detectable genes are silenced with platinum binding, and expressed according to the removal of the damage). When understanding repair results it is important to understand which type of platinum induced DNA damage is being removed. Enhanced repair has been clearly linked to cisplatin resistance, but it is necessary to establish what is being measured.

Behrens *et al.* (1987) and Masuda *et al.* (1990) quantitated cisplatin-DNA repair by analysing unscheduled DNA synthesis. In both studies cisplatin-resistant ovarian cancer cell lines exhibited elevated DNA repair rates, compared to the parental sensitive cells. Masuda and colleagues (1990) used aphidicolin, a specific inhibitor of DNA polymerase α, to produce a dose dependent inhibition of DNA repair, increasing cytotoxicity in the resistant but not the parental cell line. Sargent *et al.* (1996) evaluated cisplatin-DNA repair in samples from 25 ovarian cancer patients. They reported an increase in sensitivity to cisplatin upon co-incubation with aphidicolin. The larger the relative resistance to cisplatin, the more significant affect from aphidicolin. This paper concluded that aphidicolin overcame platinum resistance in fresh cells from primary ovarian tumours, clearly identifying Pt-DNA repair as the factor responsible for platinum resistance in clinical samples (Sargent *et al.* 1996).

Interestingly, research has shown increased cisplatin cytotoxicity in human ovarian cancer cell lines exposed to compounds that suppress DNA repair and inhibit cisplatin induced expression of a gene important in removing each type of Pt-DNA lesions, ERCC1. These compounds include the proteasome inhibitors Lactacystin and ALLnL (Li *et al.* 2000 and 2001, Yunmbam *et al.* 2001), vascular endothelial growth factor (VEGF) inhibitor SU5416 (Zhong *et al.* 2003) and IL-1α (Benchekroun *et al.* 1993 and 1995, Li *et al.* 1998a).

Johnson *et al.* (1994a and 1994b) using renaturing agarose gel electrophoresis reported enhanced ICL repair in specific DNA sequences, both coding and non-coding, in cisplatin resistant human ovarian cancer cell lines, compared to the

parental sensitive lines. Working with two sets of cisplatin-sensitive and -resistant human ovarian cancer cell lines, Zhen *et al.* (1992) described lower ICL formation in the overall genome of the two resistant cell lines. They also reported no difference in total genomic repair, but enhanced gene specific repair of ICLs by both resistant cell lines.

Cisplatin-resistant cell lines, produced from primary testicular teratoma from untreated patients, where resistance was not associated with uptake or GSH and related enzymes, were analysed for processing of each of the major cisplatin induced adducts. SUSA/CP+ cells were more efficient in removing the intrastrand adducts Pt-AG and Pt-(GMP)2, as well as ICLs. H12.1/DDP cells were specifically proficient in removing the major Pt-GG intrastrand crosslink (Hill *et al.* 1994a).

Gene specific repair of the cisplatin ICL in the housekeeping gene dihydrofolate reductase (DHFR) has been observed in cisplatin-resistant human ovarian cancer cell lines, compared with the parental sensitive, but no difference was seen in intrastrand crosslink (IA) repair between the cell lines (Zhen *et al.* 1992). No difference was observed in total genomic repair of either the IA or the ICL. (Zhen *et al.* 1992). Similar results were published by Petersen *et al.* (1996), using a mouse leukaemia cell lines. Again enhanced removal of the cisplatin ICL was observed in the constitutively active dihydrofolate reductase (DHFR) gene in the resistant cell line compared to the parental sensitive line, and again there was no observable difference in overall genomic repair of the cisplatin ICL. Jones *et al.* (1991) found intrastrand crosslinks to be repaired more rapidly in transcribed genes than in regions of no transcription, or the overall genome. This study found no difference in the ICL repair of the cisplatin interstrand crosslinks in transcriptionally active and silent genes. A later study by the same group attributed this apparent lack of difference in repair rates to the high dose of cisplatin used. When the experiments were repeated with a lower dose of cisplatin, there was preferential repair of the cisplatin ICL in active genes compared to an inactive region (Larminat *et al.* 1993). In cells taken from 6 human gliomas, ICL rates were measured using an ethidium bromide assay, and ICL repair capability was linked to the level of cisplatin resistance (Ali-Osman *et al.* 1995).

1.7.2.1.1. Nucleotide Excision Repair (NER)

Enhanced expression of NER proteins has been correlated with cisplatin resistance, both *in-vitro* and *in-vivo*. Ferry *et al.* (2000) analysed ERCC1 expression in cisplatin-resistant human ovarian cancer cell lines derived from the parental A2780 line. They discovered a consistent increase in the steady state levels of ERCC1 within the cisplatin resistant lines (Ferry *et al.* 2000). Selvakumaran *et al.* (2003) used antisense RNA methodologies to disrupt NER through the reduction of ERCC1. Using this technique they were able to sensitise the relatively platinum sensitive ovarian cancer cell line A2780 (from a platinum naïve patient), and a relatively cisplatin resistant ovarian cancer cell line, OVCAR-10 (from a patient after platinum therapy and relapse) to cisplatin. Their host cell reactivation assay also indicated reduced DNA-damage repair capacity by the OVCAR-10 antisense-ERCC1 cell lines (Selvakumaran *et al.* 2003) Interestingly, SCID mice injected intraperitoneal (i.p) with the OVCAR-10 antisense-ERCC1 cell lines showed significantly enhanced survival following cisplatin treatment compared with the OVCAR-10 xenographs (Selvakumaran *et al.* 2003).

Cisplatin exposure has also been shown to induce the expression of ERCC1 mRNA in human ovarian cancer cell lines, by over two-fold as early as 6 hours after treatment, leading to a peak level of four to six-fold 24 to 48 hours after exposure (Li *et al.* 1998c, Li *et al.* 1999). Treatment of A2780 and the cisplatin-resistant sub-line CP70 with cisplatin led to a six-fold increase in steady state ERCC1 mRNA (Li *et al.* 1998b). This increase was produced by both an increase in transcription and a 60% increase in the half life of ERCC1 mRNA (Li *et al.* 1998b).

Clinical studies have correlated elevated ERCC1 expression with poor response to platinum-based chemotherapy in non-small cell lung cancer (NSCLC) (Rosell *et al.* 2001) and ovarian cancer (Dabholkar *et al.* 1992, 1994). Clear cell ovarian carcinomas, which are inherently resistant to cisplatin, were found to express elevated ERCC1 and XPB compared with the other forms of ovarian cancer (Reed *et al.* 2003).

Advanced testicular germ cell cancers are cured in approximately 80% of patients, using cisplatin-based chemotherapy (Bosl *et al.* 1997). Investigations to understand the positive response of these tumours to cisplatin were carried out. Koberle *et al.* (1997) using both atomic absorption spectroscopy and quantitative PCR to measure the repair of platinated DNA in the whole genome, and in specific genes, revealed that 3 bladder cancer cell lines removed cisplatin damage and were therefore repair proficient, whereas 2 testicular cancer cell lines showed no repair and a third testicular cancer cell line showed only moderate levels of repair. Further analysis using human testis tumour cell lines revealed that they had a reduced ability to carry out the incision steps of NER (Koberle *et al.* 1999). Immunobloting experiments discovered that these cell lines expressed low levels of XPA and ERCC1-XPF (Koberle et al. 1999). Addition of XPA to testis cell line extracts restored dual incision activity, enabling them to excise a cisplatin 1,3-d(GpTpG) intrastrand crosslink (Koberle *et al.* 1999). Hill et al (1994b) reported that four testicular teratoma cell lines were unable to repair the 1,2-d(GpG) intrastrand crosslink, and 2 of the 4 lines tested showed deficient removal of the 1,2-d(ApG) intrastrand crosslink. Interestingly, they reported no difference in expression of ERCC1 or XPB (Hill *et al.* 1994b).

1.7.2.1.2. Homologous Recombination Repair (HRR)

As discussed, Bishop *et al.* (1998) reported the formation of Rad51 foci in CHO cells in response to ionizing radiation and cisplatin. Brca1-/- murine embryonic cells showed defective Rad51 foci formation following exposure to X-rays or cisplatin. These cells are five times more sensitive to cisplatin than parental cell lines (Bhattacharyya *et al.* 2000). The Brca1-/-cells show proficient NER (Bhattacharyya *et al.* 2000). Brca1 is therefore thought to promote the assembly of Rad51 at sites of cisplatin damage (Bhattacharyya *et al.* 2000). As mentioned previously, Aloyz *et al.* (2002) investigated the specific role of XPD in cisplatin resistance. They artificially elevated XPD expression in a human glioma cell line and recorded a two to four-fold increase in cisplatin resistance, that correlated with an increase in Rad51 foci formation, sister chromatid exchange (SCE) rate, and elevated ICL unhooking (Aloyz *et al.* 2002). They reported no difference in NER in the cell line, shown by no change in UV sensitivity, and no change in the repair of a cisplatin damaged plasmid (Aloyz

*et al.* 2002). This research strongly implicates a role of XPD in the homologous recombination repair phase of cisplatin ICL unhooking.

Disruption of two complexes involved in HRR, XRCC3-Rad51C and Rad51B-Rad51C interactions using a peptide corresponding to the amino acids 14-25 of Rad51C sensitizes hamster cells to cisplatin and reduced cisplatin-induced Rad51 foci (Connell *et al.* 2004). As discussed, Taniguchi *et al.* (2003) reported disruption of the FANC/BRCA pathway in cisplatin sensitive tumour cell lines. The addition of functional FANCF, led to monoubiquitination of FANCD2 and cisplatin resistance (Taniguchi *et al.* 2003). FANCF was found to be epigenetically silenced through methylation of its CpG island, and demethylation led to acquired cisplatin resistance (Taniguchi *et al* 2003).

1.7.2.1.3. Loss of Mismatch Repair

Mismatch repair (MMR) is a DNA repair pathway responsible for correcting single base mispairs (for example G:T) and insertion deletion loops (IDLs), which mainly occur as replication errors (Jiricny, 2000). The loss of functional mismatch repair can therefore result in the accumulation of point mutations and frame shift mutations which can be detected as high microsatelite instability (Fishel, 1999).

Key mismatch repair recognition proteins have been shown to detect and bind to cisplatin-DNA adducts. The human mismatch recognition complex MutSα has been shown to recognize the cisplatin 1,2-d(GpG) intrastrand crosslink (Duckett *et al.* 1996). Yamada *et al.* (1997) investigated MMR detection of cisplatin lesions that had undergone post-mutagenic replication (through replicative bypass). They concluded that mismatch repair appears to be triggered preferentially by 1,2 guanine intrastrand crosslinks that have undergone replicative bypass (Yamada *et al.* 1997).

The importance of this pathway in cancer has been illuminated by its role in hereditary non-polyposis colorectal cancer (HNPCC). Germline mutations of two mismatch proteins hMLH1 and hMSH2 are thought to be involved in over half of all cases of HNPCC (Fishel *et al.* 1999). HNPCC constitutes approximately 10% of all colorectal cancers (Fishel *et al.* 1999). A loss of MMR function corresponding with

poor disease free survival has also been linked to reduced hMLH1 expression following chemotherapy (combinations of cyclophosphamide, doxorubicin and cisplatin) in breast cancer (MacKay *et al.* 2000).

Aebi *et al.* (1996) correlated the loss of hMLH1 with cisplatin resistance in a human ovarian cancer cell line, and a human colon cancer cell line, and the loss of hMSH2 with cisplatin resistance in a human endometrial cancer cell line. Complementation experiments where the missing gene was replaced in the colon and endometrial cancer cell lines, through the addition of the appropriate chromosome, led to increased cisplatin sensitivity in both cases (Aebi *et al.* 1996). Two cisplatin-resistant cell lines produced from the human ovarian cancer cell line A2780, were shown to lack the hMLH1 polypeptide and to express low levels of PMS2 (Drummond *et al.* 1996).

Expression of the *hMLH1* gene has been reported to be silenced by hypermethylation in the promoter region (Strathdee *et al.* 1999). Other genes known to be hypermethylated and therefore silenced in tumour cells included two tumour suppressor genes RB1 and p16 (Jones *et al.* 1999). The majority of cisplatin resistant sublines of A2780 have shown methylation of the promoter region of hMLH1 correlating with lack of expression (Strathdee *et al.* 1999). The study also examined hMLH1 expression in clinical samples pre- and post- chemotherapy, they found a high frequency of hMLH1 promoter methylation following exposure to cisplatin (9% compared to 50%). Samimi et al (2000) found decreased staining of hMLH1 and hMSH2 in ovarian cancer samples following platinum therapy. Low expression of hMLH1 has been associated with poor survival in ovarian cancer through immunohistochemical studies (MacKean *et al.* 1999). There is an increase in the percentage of ovarian tumour samples that are negative for hMLH1 expression following second look laparotomy after chemotherapy, compared to untreated tumours (36% compared to 10%) (Brown *et al.* 1997). These findings suggest a selection of cells without hMLH1.

Gifford *et al.* (2004) measured *hMLH1* methylation using plasma DNA from ovarian cancer patients, before carboplatin/taxoid chemotherapy, and at relapse. They reported that methylation of *hMLH1* was increased at relapse. Interestingly, 25% of

the relapse samples that showed methylation of *hMLH1*, showed no methylation in the preceding pre-chemotherapy samples. This acquisition of *hMLH1* methylation at relapse predicted poor overall survival of ovarian cancer patients (Gifford et al. 2004).

Initially loss of mismatch repair was correlated with resistance, as it was believed that binding of mismatch proteins to cisplatin lesions led to those lesions being shielded from the cells repair machinery. Fishel (1999) proposes a 'sliding clamp signaling model' for mismatch repair, where mismatch proteins directly stimulate apoptosis, therefore loss of these factors causes a degree of resistance.
Interestingly, Zhang *et al.* (2002) reported that the mismatch repair protein hMutSβ (hMSH2-hMSH3) is required for the recognition and unhooking of psoralen interstrand crosslinks. There is evidence that a mismatch repair protein is involved in ERCC1-mediated cisplatin resistance. Lan *et al.* (2004) used RNA interference (RNAi) to investigate the relationship between MSH2 and ERCC1. Suppression of ERCC1, using RNAi in XPA(-) human and mouse cells resulted in an increase in cisplatin sensitivity, implicating an XPA-independent, ERCC1-mediated mechanism of cisplatin resistance (Lan *et al.* 2004). Suppression of ERCC1, again using RNAi, in mouse cells lacking both XPA and MSH2 had no effect on cisplatin sensitivity, suggesting that the ERCC1 mediated cisplatin resistance is dependent on the presence of MSH2 (Lan *et al.* 2004).

1.7.2.2. Altered Apoptosis

The stable transfection of A2780 cells with HPV-16 E6 led to a cell line that was functionally null for p53. These cells were three to four fold more sensitive to cisplatin than the parental cells, or the empty-vector control cells (Pestell *et al.* 2000). The removal of DNA-platinum adducts, measured using atomic absorption spectroscopy (AAS) was reduced in the E6 transfected cells, providing a clear correlation between reduced p53 and reduced cisplatin-DNA adduct repair (Pestell *et al.* 2000).

When the stabilisation of p53 following cisplatin exposure was investigated in a paired cisplatin-sensitive (A2780) and resistant cell line (CP70), the half-life of p53

in the resistant cell line was increased 31-fold, compared to a six-fold increase in half-life in the sensitive cell line (Yazlovitskaya *et al.* 2001). Yazlovitskaya *et al.* 2001 concluded that the prolonged p53 stabilisation and accumulation observed in the CP70 cells in response to cisplatin could explain the resistant phenotype of this cell line.

Perego *et al.* (1996) investigated p53 and Bax expression in two cisplatin-resistant human ovarian cancer cell lines and their sensitive parental cell line. They reported mutated p53 in each of the resistant cell line compared to the parental cell line. One of the cell lines also expressed reduced Bax mRNA level, suggested to be caused by inability of the dysfunctional p53 to transactivate Bax. Perego *et al.* concluded that resistance in the two cell lines was attributable to altered apoptosis in response to cisplatin exposure.

Four independent clinical studies involving over 500 ovarian cancer patients have provided evidence for a strong correlation between elevated p53 in tumour tissue and poor survival and clinical outcome following platinum-based chemotherapy (Herod *et al.* 1996, Levesque *et al.* 2000, Reles *et al.* 2001, Nakayama *et al.* 2003). Interesting research by Rubbi and Milner (2003) has shown that following UV irradiation p53 functions as an accessibility factor, altering the chromatin structure over the whole nucleus to facilitate NER of the UV-induced DNA damage. Brabec and Kasparkova (2005) have suggested a model whereby cisplatin-DNA adducts are recognised by NER factors, which mediate a signal to activate p53 and induce cell cycle arrest to facilitate the efficient repair of the induced damage. Co-operation between p53 and NER could explain the observed correlation between elevated p53 and reduced survival following platinum-treatment in ovarian cancer.

P73 is a structural homolog of p53, and like p53 is thought to function as a tumour suppressor (Agami *et al.* 1999). P73 is capable of mediating apoptosis in association with the non-tyrosine kinase c-Abl (Agami *et al.* 1999). The expression and half-life of a p53-related protein, p73, was found to be elevated following cisplatin exposure of human colon cancer cell lines (Gong *et al.* 1999). This affect was not seen in cells unable to carry out mismatch repair (MMR) or unable to activate c-Abl following cisplatin (Gong *et al.* 1999). These results suggest that p73 and c-Abl function as part

of a mismatch repair mediated apoptotic pathway (Gong *et al.* 1999). The stable transfection of p73 into a human ovarian cancer cell line resulted two clones exhibiting UV and cisplatin-resistance, two to three-fold and three to four-fold, respectively (Vikhanskaya *et al.* 2001). Microarray, RT-PCR and northern blot analysis revealed that the two resistant cell lines showed a marked increase in the expression of DNA repair genes, including XPA, XPG and XPD, indicating that the relationship between elevated p73 and cisplatin resistance involves complex molecular interactions which deserve further investigation (Vikhanskaya *et al.* 2001).

Yang *et al.* (2004) used RT-PCR and western blots to analysed the expression of Bcl-2 and Bcl-XL in two paired sensitive and resistance human ovarian cancer cell lines. Both resistant cell lines expressed elevated Bcl-2 and Bcl-XL compared to the parental sensitive lines. Following cisplatin treatment the resistant cell lines exhibited reduced caspase 3 activity and apoptosis, compared to the sensitive cells (Yang *et al.* 2004). Miyake *et al.* (1998) induced cisplatin-resistance in human bladder cancer cell lines through transfection with Bcl-2. Transfection of Bcl-2 in to human neuroblastoma cell lines resulted in cisplatin resistance and reduced DNA degradation, measured using pulse-field gel electrophoresis (PFGE) and flow cytometry of propidium iodide stained nuclei (Dole *et al.* 1994 and 1995). Simonian *et al.* (1997) transfected lymphoid cells with Bcl-2, and with Bcl-XL. Both transfectant cell lines showed cisplatin resistance, although Bcl-XL provided better protection against cisplatin exposure (Simonian *et al.* 1997). Conversely, Ohmori *et al.* (1993) failed to induce cisplatin-resistance in a Bcl-2 transfected human small cell lung cancer cell line, observing no difference in the level of DNA degradation following cisplatin in the Bcl-2 transfected cells or the empty-vector control cells. Two cisplatin-resistant bladder cancer cell lines were analysed for Bcl-2 expression using RT-PCR and western blot assay (Hong *et al.* 2002). Both cell lines expressed elevated Bcl-2 compared to the parental sensitive cell line (Hong *et al.* 2002). Cisplatin exposure induced Bcl-2 expression in a dose dependent manner in the parental cell line, with no change in expression in the two resistant cell lines (Hong *et al.* 2002). Treatment with antisense Bcl-2 oligonucleotides caused significantly enhanced cisplatin sensitivity in the two cisplatin resistance cell lines (Hong *et al.* 2002).

In xenograph studies using A2780 cells transfected with an empty vector and with Bcl-2, the Bcl-2 expressing tumours continued to grow following cisplatin exposure, compared to the tumours transfected with the empty vector, which disappeared after drug treatment (Williams *et al.* 2005). This same publication reported a correlation between expression of Bcl-XL and a reduced disease-free survival in ovarian cancer patients that have been treated with platinum-based chemotherapy (Williams *et al.* 2005).

Rudin *et al.* (2003) recently reported a novel correlation between Bcl-2 expression, glutathione and cisplatin resistance in a human breast cancer cell line, and a lymphocytic precursor cell line. Transfection of both cell lines with Bcl-2 led to elevated GSH expression and cisplatin resistance. Treatment of the transfected cells with buthionine sulfoximine (BSO) resulted in reduced GSH level and completely abrogated Bcl-2 mediated cisplatin resistance, without affecting Bcl-2 expression (Rudin *et al.* 2003). They postulate that glutathione mediates apoptotic regulatory pathways via its function as an antioxidant (Rudin *et al.* 2003).

Yang *et al.* (2005) investigated the role of HtrA2/Omi, XIAP and caspase 3 in paired cisplatin-sensitive and resistant human ovarian cancer cell lines. Cisplatin exposure induced reduced XIAP expression and elevated cytosolic HtrA2/Omi and caspase 3 activity in the two cisplatin sensitive cells lines, but did not affect these factors in the cisplatin-resistant cell lines (Yang *et al.* 2005). Down-regulation of XIAP using anti-sense oligonucleotides resulted in elevated caspase 3 activity, cytosolic HtrA2/Omi, and cisplatin sensitivity in the resistant cell line (Yang *et al.* 2005).

### 1.7.3. Cisplatin Resistance Mechanism with Unknown Function: Collagen

Collagen VI alpha 3 was one of many extracellular matrix proteins found to be highly upregulated in cisplatin resistant human ovarian cancer cells (Sherman-Baust *et al.* 2003). When cisplatin sensitive cells were grown in the presence of collagen VI protein they became resistant (Sherman-Baust *et al.* 2003). Growing sensitive cells on plates pre-coated with collagen type I also induced a refractory response but to a lesser extent (Sherman-Baust *et al.* 2003). The same publication was able to correlate an increase in collagen VI expression with increasing tumour grade (Sherman-Baust

*et al.* 2003). Low grade (highly or moderately differentiated) tumours expressed lower levels of COL6A3 than higher grade (poorly differentiated) tumours. Patients with lower grade ovarian tumours, (and therefore lower COL6A3 expression), have higher survival rates, than patients with higher grade tumours (Ozols *et al.* 1980, Sherman-Baust *et al.* 2003).

1.8 Aims of the Study.

As discussed, research suggests that platinum-drug resistance is often linked to the altered cellular processing of interstrand crosslinks. However it is unclear how relevant cell line studies are to the situation that occurs in the clinic.

The recent development of the comet assay to facilitate the measurement of interstrand crosslinks, using a low cell number, has enabled us to design a novel study to measure platinum interstrand crosslink processing *ex-vivo*, in tumour cells from clinical samples from human ovarian cancer patients. These data are of direct clinical relevance because ovarian cancer patients classically exhibit resistance to platinum drugs, which forms part of the first-line treatment for this disease.

Samples were available from platinum-naïve ovarian cancer patients, and from patients previously treated with platinum. We were therefore able to ask the question; Are there any differences in the formation and/or unhooking of cisplatin-interstrand crosslinks within these two categories of ovarian cancer patients? These data are reported in Chapter 2.

A cisplatin sensitive human ovarian cancer cell line produced from a platinum-naïve patient was exposed to increasing doses of cisplatin overtime, to produce a stably cisplatin-resistant cell line (Behrens *et al.* 1987). These resistant cells were shown to exhibit unscheduled DNA synthesis following cisplatin exposure (Behrens *et al.* 1987). These cell lines were analysed using the comet assay, to examine any difference in cisplatin-ICL processing over time. These data are reported in Chapter 3. Follow-up experiments with the two cell lines were carried out using nylon microarrays and RT-PCR, and are reported in Chapter 4.

Overall the aim of this study was to investigate cisplatin-ICL processing using the two human ovarian cancer models outlined above, and where possible to relate these data to cisplatin sensitivity, previous exposure and clinical outcome. It was hoped that this information would contribute towards our knowledge of platinum-drug resistance, to be used to improve future treatment strategies and patient prognosis.

## Chapter 2: DNA Interstrand Crosslink (ICL) Formation and Unhooking in Clinical Samples from Ovarian Cancer Patients Treated with Cisplatin *Ex-vivo*.

### 2.1. Introduction

As discussed earlier, the pre-existence or the development of drug resistance to platinum chemotherapy (cisplatin and carboplatin) greatly reduces the number of ovarian cancer patients still alive five years after diagnosis (Moss *et al.* 2002). If the mechanisms of resistance could be understood and overcome, then strategies could be developed to improve the treatment and prognosis for patients with this disease.

Many research strategies have been devised to address this problem. Much insight has been gained from research using human ovarian cancer cell lines. These models of platinum resistance are produced through the continuous and prolonged exposure of cell lines to platinum drugs over a period of time, to induce a stable resistant phenotype. Paired parental sensitive and resistant sub-lines have then been extensively analysed, although the relevance of many of these studies to the clinical situation is unclear.

Previous clinical research into cisplatin-DNA interactions and clinical outcome have focused on measuring total platinum-DNA binding, using atomic absorption spectroscopy (AAS) and measurement of cisplatin intrastrand crosslinking, using a competitive enzyme linked immunosorbent assay (ELISA) (Reed *et al.* 1986, 1987, 1988, 1993, Schellens *et al.* 1996, Fisch *et al.* 1996, Poirier *et al.* 1993). Using AAS to measure platinum-DNA binding in leukocytes from 49 patients with 23 histological types of malignancy (Reed *et al.* 1993) and from other solid tumour patients (Schellens *et al.* 1996 and Parker *et al.* 1991b) high platinum adduct formation was linked to a positive response to platinum based chemotherapy. Testing intrastrand crosslinking in leukocytes from ovarian and testicular cancer patients (Reed *et al.* 1986, 1987 and 1988) and from ovarian, testicular, colon and breast cancer patients (Poirier *et al.* 1993) researchers again correlated high intrastrand crosslinking with consistently improved clinical responses to platinum chemotherapy. This body of work has revealed a strong correlation between platinum-adduct formation following *in-vivo* exposure and clinical response to platinum therapy. Fisch

*et al.* (1996) however failed to correlate high platinum adduct level, measured using AAS, and favourable outcome in patients with advanced germ cell cancer.

Research into cisplatin ICL formation in clinical material has been hindered by an inability to measure this lesion sensitively using a low sample cell number. Previous research into ICL processing at pharmacologically relevant doses was carried out using fluorometric alkaline elution. For example, Rudd et al. (1995) measured cisplatin ICL formation and repair using fluorometric alkaline elution in peripheral blood mononuclear cells treated *ex-vivo*, from healthy volunteers under 25 years of age, and over 70. They reported reduced ICL unhooking over time by the cells from the older patients. However this technique was not suitable for research using tumour material, as the cell number required per experiment was relatively large. This problem was overcome when a technique used to quantify single strand breaks in a single cell population, the single cell gel electrophoresis 'comet' assay (Ostling *et al.* 1984, Fairbairn *et al.* 1995), was modified in order to facilitate the efficient measurement of ICL at a single cell level, using a comparatively low total cell number (Spanswick et al 1999). A comparison of the ability of alkaline elution and the comet assay to examine chloroambucil-induced ICL revealed that the comet assay could measure interstrand crosslinks with a ten-fold increased sensitivity and required a much smaller sample size. In addition it gave information on individual cells (Kohn *et al.* 1981, Hartley *et al.* 1999).

The comet assay was successfully used to analyse ICL levels in lymphocytes harvested from Ewings Sarcoma patients, following their treatment with the crosslinking agent ifosfamide (Hartley *et al.* 1999). The comet assay was therefore shown to be a highly sensitive method for assessing ICL formation and repair at a single cell level, and has subsequently been used in a number of clinical settings (Spanswick *et al.* 2002, Webley *et al.* 2001). To date, there has been no published research into ICL formation and unhooking in ovarian cancer using the comet assay. In the present study tumour cells were obtained from ascitic and primary tumour samples. Samples were obtained from two patient populations; those that were platinum-naïve and those who had previously received platinum based chemotherapy. Where possible mesothelial cell samples were also harvested, to facilitate the comparison of tumour and non-tumour cells from the same patient. Cisplatin-induced

ICL formation and repair was measured using the comet assay following treatment of cells *ex-vivo* with cisplatin.

## 2.2. Methods

### 2.2.1. Patient Recruitment

Ethics approval for this project was gained from the Joint UCL/UCLH Committee on the Ethics of Human Research, and from the Royal Free Hospital Ethics Committee. Ethics Study Number: 00/0254

Between February 2001 and April 2003 ovarian cancer patients receiving treatment from UCL Hospitals (the Middlesex Hospital and University College Hospital) and the Royal Free Hospital were recruited to participate in this study. The research project was explained to each patient, and an information sheet was provided (see Appendix A1). Informed consent was gained from the patient and witnessed by their doctor (see Appendix A2). Clinical information for each patient was gathered by requesting and reviewing all notes at a later date.

### 2.2.2. Processing of Clinical Material

#### 2.2.2.1. Separation of Tumour and Mesothelial Cells from Ascitic Fluid.

Ascitic fluid was collected from patients by medical staff either in the operating theatre or on the ward. In theatre it was collected during the laparotomy, into sterile 2L cylindrical bags. On the wards it was collected during a sterile paracentesis, directly into a sterile 2L catheter bag. Once the catheter bag was full, a sterile bag change was carried out. The full catheter bag was clamped to prevent loss of content. The 2L sample was taken to the lab for processing.

In a category II tissue culture hood using aseptic technique, the tap at the bottom of the catheter bag was thoroughly and carefully cleaned with alcohol. Fluid was then drained directly from the tap into 175cm$^2$ plastic tissue culture flasks (VWR International). The large cylindrical bags used to collect ascites in theatre had only

one tube leading into the bag at the top. These had to be very carefully cleaned with alcohol, and then inverted over open 175cm$^2$ tissue culture flasks. As no antibiotics were used in the culturing of clinical material, careful sterile technique was used to minimize the chance of infection, which would result in the sample being discarded.

Ascitic samples were aliquoted into conical 50ml plastic tubes (VWR International) and centrifuged at 200xg for 5 minutes. The tubes were carefully replaced in the tissue culture hood, and the supernatant was removed and discarded using a sterile 25ml pipette (Co-star). The cellular pellet was resuspended in Dulbecco's Modified Eagle's Medium (DMEM) tissue culture media containing 10% fetal calf serum (FCS) and 2mM glutamine (all of which were purchased from Autogen Bioclear UK Ltd. Wiltshire, UK). There was a large variation in the quantity of cells produced. When cellular pellets were visually judged to be less than 0.5ml, 4 to 6 samples were combined, by resuspending all of the pellets in a total volume of 25mls of DMEM (at 37°C, with 10%FCS and 2mM glutamine). This volume was pipetted directly into a 175cm$^2$ tissue culture flask. When the pellet from a single 50ml tube was thought to be over 0.5ml, the single pellet was resuspended in 25mls of warmed DMEM (with 10% FCS and 2mM glutamine) and seeded into one 175cm$^2$ tissue culture flask. Flasks were immediately placed horizontally in a humidified incubator, to encourage adherence. All cells were grown at 37°C in a 5% $CO_2$ incubator.

The cell density in suspension did not relate with the proportion of cells that became attached to the plastic surface of the tissue culture flask. Each patient sample behaved differently.

After one hour at 37°C, the flasks were observed under a light microscope (Nikon), to check that a significant number of cells had adhered to the plastic surface. The flasks were returned to the category II tissue culture hood, and the total volume of tissue culture media containing unattached cells was transferred to a fresh 175cm$^2$ tissue culture flask, using 25ml sterile pipettes. The attached cells in the first flask were supplied with 25mls of warmed DMEM (with FCS and glutamine). Both the primary and secondary flasks were incubated at 37°C. Mesothelial cells attach to the surface of tissue culture flasks more rapidly than tumour cells (Personal

communication with Prof. Mike O'Hare, Department of Surgery, University College London). Therefore, the first flask would predominantly contain mesothelial cells and the second flask would contain tumour cells.

Flasks were left overnight in the humidified incubator at 37°C, 5% $CO_2$ to allow the cells to attach and flatten. Flasks were then observed at regular interval using a light microscope, until the characteristic phenotypes became obvious. Tumour cells generally appeared more rounded with a curved edge and no projections. Mesothelial cells grew rapidly and extended into their surroundings, appearing stretched (see Figure 2.1 in the Results section).

After approximately 48 hours contaminant mesothelial cells were removed from the tumour cell flasks, by exploiting a difference in trypsin sensitivity between the two cell types. To carry out the trypsin selection, flasks containing the richest source of tumour cells, i.e., those that required longer than one hour to adhere to a plastic surface, were returned to the tissue culture hood, and the tissue culture media was removed and discarded using a sterile 25ml pipette. 10mls of warmed trypsin (Autogen Bioclear UK, Wiltshire, UK) was pipetted against the growing surface of the flask, using a 10ml sterile pipette, and the lid was replaced. The flask was placed horizontally and gently tipped to ensure contact between the trypsin and the entire surface. The flask was observed under a light microscope. Mesothelial cells were the first to show any effect. In response to the trypsin they would round up and detach from the plastic surface and float after approximately five minutes. At the same time, the tumour cells would show little effect.

When the mesothelial cells appeared to be detached, the flask was returned to the tissue culture hood and 10ml of warmed DMEM (with 10%FCS and 2mM glutamine) was added to the trypsin using a 25ml sterile pipette. The same pipette was used to pipette the entire volume out of the flask into a sterile 50ml plastic tube. 10mls of warmed DMEM (with FCS and glutamine) was pipetted into the flask, which was placed horizontally to wash the growing surface of cells. This volume of media was pipetted from the flask with a sterile 10ml pipette and discarded. 25mls of DMEM (with 10% FCS and 2mM glutamine) was pipetted into the flask, using a sterile

pipette, and the flask was replaced horizontally into the incubator. This flask now contained a purified tumour cell primary culture. The trypsin/DMEM mixture was centrifuged at 200xg for five minutes. The tube was returned to the category II hood, and the supernatant was carefully removed using a sterile 25ml pipette. The cell pellet was resuspended in 20mls of warmed DMEM with 2mM glutamine and 10% FCS, and pipetted using a sterile 25ml pipette into a 175cm$^2$ tissue culture flask. This flask was placed horizontally in the incubator (37°C, 5% $CO_2$). These cells when cultured would provide an additional source of mesothelial cells, and the original flask would now contain a purified source of tumour cells.

2.2.2.2. Processing of Solid Primary Ovarian Tumour Tissue to Yield Primary Cultures or Single Cell Suspensions.

Under sterile conditions, a pathologist dissected tumour tissue from primary ovarian tumours. These samples were transferred to a category II tissue culture hood for processing. Tumour samples were finely dissected in a sterile petri-dish, using sterile individually wrapped disposable scalpels (Swann Morton, Sheffield UK). A single cell suspension was produced by adding 10mls of cold DMEM (containing 2mM glutamine). The suspension was pipetted up and down in a low aperture 2.5ml sterile pipette, then transferred into a 10ml plastic tube. This tube was centrifuged at room temperature for 5 minutes at 200xg. The sample was returned to the category II hood, and the supernatant was removed and discarded using a sterile 10ml pipette. 10ml of cold DMEM (with 2mM glutamine and 10% FCS) was added to the tube, and mixed with the pellet by gently pipetting up and down. The cell suspension was added to a 175cm$^2$ tissue culture flask, which already contained 10mls of cold DMEM (with glutamine and FCS). Care was taken to pipette the suspension at an angle against the growing surface of the flask. The flask was placed horizontally in a tissue culture incubator at 37°C with 5% $CO_2$. After 24 hours the cell cultures were examined using a light microscope. Occasionally a primary adherent culture would develop, which would then be maintained as a monolayer culture prior to the comet assay. Where cells did not attach, they were processed as a single cell suspension. The success rate for producing an adherent primary culture from primary tissue was not as high as for tumour cells in ascitic samples. Of the three primary tumour samples

which were able to be used, within this study, one was successfully grown as an adherent primary culture (the sample from Patient 12), the other two were maintained as single cell suspensions (the samples from Patients 3(ii) and 16). A number of the primary tumour tissue samples that were dissected by the pathologists were lost due to infection. Infection was caused by a combination of inter-personal differences in the handling technique between pathologists, and a lack of appropriate category II tissue culture facilities/hood within that department.

2.2.2.3. Photography of Primary Cultures

Phase-contrast images of live cells were recorded photographically on Kodak Technical Pan 35mm film, using a Zeiss Axiovert inverted phase-contrast microscope fitted with x10 NA 0.25 and x20 NA 0.40 flat-field phase objectives.

2.2.3. Measurement of DNA Interstrand Crosslinking using the Comet Assay

This technique involved cisplatin, propidium iodide and X-rays, each requiring special safety precautions in accordance with University's Health and Safety policy.

2.2.3.1. Preparation of Monolayer cells for Drug Treatment

Large tissue culture flasks ($175cm^2$) of monolayer cells were placed in a category II tissue culture hood, and the tissue culture media was removed and discarded by tipping the flask and pipetting off the entire volume with a sterile 25ml pipette. 10mls of warmed trypsin were added to the flask and brought in contact with the cells by leveling the flask, and gently swirling the volume over the monolayer. The flask was viewed using a light microscope, in order to observe the rounding up and detachment of the cells from the plastic growing surface. When all of the cells had detached, the flask was returned to the hood, and 10mls of warmed DMEM (with 10% FCS and 2mM glutamine) were added to the trypsin. The DMEM was washed against the growing surface using a sterile 25ml pipette. The mixture was pipetted up and down to encourage a single cell suspension, then transferred into a 50ml sterile plastic tube and centrifuged at 200xg for five minutes. The tube was returned to the sterile conditions and the supernatant was discarded using a sterile 25ml pipette. The pellet

was resuspended in 10mls of warmed DMEM (without FCS or glutamine) and mixed by pipetting up and down in a 10ml pipette. A small quantity of the suspension was pipetted into a sterile 7ml tube and removed from the tissue culture hood to the microscope. A glass Pasteur pipette (Volac) was used to mix the suspension in the tube by pipetting up and down, and a small quantity of the suspension was pipetted gently against the side of a coverslip over a haemocytometer. When the suspension filled the area under the coverslip the haemocytometer was observed under a light microscope, and the cell density was measured by counting the cells in all nine squares of the visible grid, and then dividing by nine. This figure was calculated as the cell number x $10^4$cells/ml.

Once the cell density was known, the stock 10ml cell suspension was centrifuged for 5 minutes at 200xg. The tube was transferred back into sterile conditions, and the supernatant was discarded using a 10ml sterile pipette. The correct volume of warm DMEM containing 10% FCS and 2mM glutamine was pipetted on to the pellet, to produce a cell density of $5x10^4$cells/ml, the DMEM was mixed with the pellet by pipetting up and down with a sterile 25ml pipette. At least 1ml of this cell suspension was pipetted into a 10ml conical plastic tube, using a 10ml sterile pipette, and centrifuged at 200xg for 5 minutes, to be stored in a -80°C freezer. The $5x10^4$ cells/ml suspension was seeded into two wells of a six-well plate (VWR International), using five six-well plates per experiment. Cells were left to adhere overnight and drug treated the next day. The centrifuged sample was returned to the tissue culture hood, and the supernatant was removed and discarded using a sterile 10ml pipette. The cellular pellet was resuspended using 1ml of a freezing mix, containing fetal calf serum (FCS) with 10 % dimethylsulphoxide (DMSO) at 4°C. The suspension was transferred into a labelled eppendorf using a sterile 2.5ml pipette. The sample was placed on ice and transferred to a lidded polystyrene box within the -80°C freezer. Frozen samples could then be thawed at a later date for immunocytochemical analysis.

For a single comet assay experiment five six-well plates were required. Conditions for a single experiment were optimised after initial results using tumour and mesothelial cells from patient 1. The sample from patient 1 was processed to produce

data from time points 0, 4.5, 9, 24 and 48 hours after a 1 hour drug treatment, each requiring a six-well plate. Future experiments did not include the 4.5 hour time point. Ideally experiments were repeated in triplicate, with the volume of cells in the clinical samples determining the number of possible repeats.

2.2.3.2. Drug Treatment of Monolayer Cells

Each single experiment required monolayer cells grown in six-well plates. As stated, each experiment required five six-well plates, two wells of each plate containing cells grown at a density of $5x10^4$ cells/ml. Cells were drug treated in sterile conditions by pipetting off the tissue culture medium from the wells of each six-well plate, using a 10ml pipette and tipping the plate slightly. 2.5ml of 100μM cisplatin (100mg/100ml injectable aqueous stock solution containing 900mg/100ml sodium chloride and 100mg/100ml mannitol from David Bull Laboratories (Australia)) in warm DMEM (without FCS or glutamine) was pipetted into 1 well per plate. 2.5mls of DMEM (minus Glutamine or FCS) without cisplatin was pipetted into the remaining five wells (the remaining one per plate). The lids were replaced on the six-well plates and they were placed in the tissue culture incubators at 37°C in a humidified atmosphere with 5% $CO_2$. After 1 hour, the plates were placed back in the category II hood, and separate 10ml pipettes were used to aspirate and remove the drug solution and FCS free DMEM from each well, again tilting the plates at an angle to facilitate efficient removal of the highest volume possible. Immediately one plate was taken aside and 2.5ml of warmed trypsin was pipetted into each of the two wells, one that had contained drug, and a non-drugged control well. While the trypsin incubation was being carried out, fresh DMEM (containing 2mM glutamine and 10% FCS, warmed to 37°C) was added to each of the remaining 4 plates (8 wells), which were replaced in the incubator. Following the successful trypsinisation of the cells that were growing in the plate that was taken aside, 2.5mls of DMEM containing 10% FCS and 2mM glutamine, at 37°C, was added per well. The total volume of 5mls (from each well) was pipetted into a separate labelled 10ml plastic tube. Both tubes were then placed into the centrifuge and spun at 200xg for five minutes, at room temperature. The tubes were replaced into the tissue culture hood, and the supernatant was removed and discarded using a sterile 10ml pipette. 1.5mls of a freezing mix of FCS

and 10% dimethylsulphoxide (DMSO) at 4°C, was used to resuspend the cell pellets. This mixture was transferred into a labelled eppendorf, on ice. When both samples were prepared they were quickly placed into a lidded polystyrene box within the -80°C freezer. These two sample constituted the 0-hour time point cisplatin treated and non-drug treated control cells. Four and a half hours after drug treatment a further two cell samples were frozen using the above protocol, again with a drug treated and a non-drug treated control sample from a single plate. This procedure was repeated 9, 24 and 48 hours after the drug treatment. The usage of a separate plate for each time point, facilitated minimal disruption of each time point's sample at the time of trypsinisation and subsequent freezing.

2.2.3.3. Drug Treatment of Single Cell Suspensions

Cells were grown in a single cell suspension at a concentration of $5x10^4$cells per ml in DMEM containing 2mM glutamine and 10% FCS, at 37°C. In a category II hood, per experiment, 2ml of cell suspension was transferred into ten 10ml tubes, using a sterile 10ml pipette. The ten 10ml tubes were spun at 200xg for 5 minutes. In the tissue culture hood the supernatant was aspirated off each cell pellet using a sterile 10ml pipette, carefully avoiding damaging the pellet. 2ml of 100μM cisplatin solution in DMEM (without 10% FCS or 2mM glutamine at 37°C) was added separately to five tubes, using a separate 10ml pipette each time, carefully pipetting the suspension up and down to ensure proper mixing. 2mls of DMEM (without 10% FCS or 2mM glutamine) at 37°C was added to each of the remaining five tubes, using separate sterile 10ml pipettes, pipetting up and down gently to mix. All ten of the tubes were placed into a tissue culture incubator at 37°C in a humidified atmosphere with 5% $CO_2$, with the lids on but not tightened, to allow some gaseous exchange. After 1 hour the lids were tightened and the tubes were spun in the centrifuge at 200xg for 5 minutes. In the tissue culture hood the supernatant was removed separately from each tube, using separate 10ml pipettes being careful not to disturb the cell pellets at the bottom of the tubes. 2mls of DMEM (containing 10% FCS and 2mM glutamine at 37°C) was added separately to eight of the tubes (four drug treated, and four non-drug treated controls), resuspending each pellet. These tubes were replaced in the incubator, with the lids on but not tightened. The remaining two

samples (one drug treated, and one control) were resuspended separately using 1.5ml of a freezing mix (FCS with 10% DMSO at 4°C). These samples were pipette up and down using a 2.5ml pipette to ensure proper contact between the cells and the DMSO. These samples were then pipetted into labelled eppendorfs on ice. These samples were then quickly placed into a lidded polystyrene freezing box in the -80°C freezer. Four and a half hours after drug treatment a further two cell samples were frozen using the above protocol, again with a drug treated and a non-drug treated control sample. This procedure was repeated 9, 24 and 48 hours after the drug treatment.

2.2.3.4. Slide Preparation

Frosted glass microscope slides were labelled and arranged in rows on a flat surface. 1ml of 1% Type 1-A agarose in $dH_20$ was needed per slide. The agarose solution was prepared by adding 1g of agarose powder to 100ml of $dH_2O$, and microwaving until all of the agarose had dissolved (approximately 1 minute on high in a 750 watt microwave oven). When the agarose had cooled from boiling, a test slide was prepared by pipetting 1ml of solution on to the centre of the lower half of the slide, using a p1000 Gilson pipette. At the correct temperature the agarose spreads to the edges of the slide, without migrating to the top labelled section. It is important that the agarose covers a larger area of the slide than a large coverslip. Slides were left to dry overnight at room temperature. Slides could be prepared in advance and stored at room temperature wrapped in Clingfilm.

2.2.3.5. The Comet Assay

On the day of use, pre-coated slides were arranged side-by-side, flat and face up, in a plastic tray. This tray was placed in the fridge at 4°C, to help keep the samples cold during the assay. This was essential to prevent the repair of the ICLs and the DNA strand breaks induced by the X-ray exposure step of the assay. 1% Type VII agarose in $dH_20$ was prepared in a 500ml glass conical flask by dissolving 1g of agarose powder per 100ml of $dH_2O$ in a microwave set on high. The conical flask was placed into a medium sized beaker of warm water, so that the water made a 'jacket' around

the conical flask. This then was placed in a 40°C water bath until use (approximately 1 hour later). This allowed the jacket of water in the beaker, and the agarose to equilibrate to 40°C.

Frozen comet assay samples were removed from the -80°C freezer and placed on ice to thaw. Samples were frozen at a density of $1x10^5$cells in 1.5mls of freezing mix. Upon thawing each sample was diluted into 2.5mls of cold DMEM (without FCS and glutamine), to produce a final assay density of $2.5x10^4$cells/ml. Samples were kept on ice at all times. Each 4ml sample was divided between two 10ml plastic tubes, this stage was carried out on the bench using non-sterile 10ml pipettes. One 2ml sample was a non-irradiated control, and the other 2ml sample was irradiated on ice with 12.5Gy (2.35Gy/minute), by an X-ray machine (General Electric). Therefore for each experimental time point (0, 4.5, 9, 24 and 48hrs) there was a drug treated and a non-drug treated sample, both of which was divided into an irradiated and a non-irradiated sample. Two slides were prepared for each sample.

The type VII agarose was removed from the 40°C water bath, and used on the bench. To prepare the slides 0.5mls of chilled sample, was added to a well in a 24 well plate (VWR International) also on ice, using a Gilson p1000 pipette. Quickly 1ml of molten Type VII agarose was added to the sample, using a Gilson p1000 pipette, and pipetting up and down once. The same p1000 pipette and tip were then used to transfer the entire 1.5ml mix on to a slide in two actions, and a cover slip was carefully placed over the sample. This step had to be done rapidly but efficiently as each of the slides had to be of the same thickness, with each section of the slide having a similar depth of agarose. If the agarose was allowed to become too cool it would not spread over a slide, and would bubble as it left the pipette tip. Slides were then placed on to ice in a tray. When all of the slides were made the cover slips were carefully removed, and the slides were placed side-by-side, in order and face up in a separate plastic tray on ice. 500ml of ice-cold lysis buffer (100mM disodium EDTA, 2.5M NaCl, 10mM Tris-HCL (all purchased from Sigma) pH 10.5) was prepared by adding 5mls TritonX-100 just before use. The detergent was thoroughly mixed with the buffer and the lysis mixture was carefully poured over the slides until they were all submerged. Slides were left for an hour in the dark, on ice, in the fridge.

After 1 hour the lysis buffer was carefully poured off and discarded, by carefully tilting the tray. Approximately 250mls of ice-cold $dH_20$ was gently poured over the slides, and left in the dark for 15 minutes. After this time the $dH_20$ was poured off the slides and a further 250mls was added. This step was repeated a further two times, so that 1L of ice-cold $dH_20$ had been used in an hour. Slides were transferred lengthwise into a flat-bed electrophoresis tank, and the tank was filled with 1L of ice-cold alkali solution (50mM NaOH, 1mM disodium EDTA, in $dH_2O$, pH12.5) and left for 45 minutes in the dark. The slides were electrophoresed in the dark for 25 minutes at 18V (0.6V/cm), 250mA. Slides were carefully removed from the tank and placed in a slide rack. Approximately 1ml of neutralising buffer (0.5M Tris HCL, pH 7.5) was gently poured over each slide and left for 10 minutes. The neutralising buffer was tipped off each slide and approximately 1ml of PBS solution was added to each slide, and left for 10 minutes. Slides were placed side by side on a shelf in an oven at 45°C, gel side up and left overnight to dry. Before the slides could be stained the gel had to be completely dry. Once completely dry, slides could be stored in a slide box, and then stained at a later date. Providing that the slides were kept in dry conditions they could be stored for several months before use.

2.2.3.6. Staining

To visualise, slides were stained with propidium iodide. First the slides were carefully placed on a tray rack. The gel section of the slides were re-hydrated by liberally pouring $dH_20$ on to each slide, ensuring a reservoir of water sat on each slide. Slides were left for 10 minutes, during which time they were checked, and extra $dH_20$ was added where necessary to ensure constant contact between the $dH_20$ and the gel portion of the glass slide for the full time period. After ten minutes, the water was drained off the slides by placing the side of a plastic Pasteur pipette against the side of the slide, in contact with the bottom of the slide tray, this gently and effectively pulled off the water without disrupting the slides. Removing the water facilitated enhanced contact between the stain and the gel on each slide, preventing further dilution of the stain, leading to efficient staining and subsequent imaging. Just prior to use, the staining mix was prepared by adding 125µl of 1mg/ml propidium iodide stock (Sigma) (stored at 4°C in a dark container, as it is light sensitive) to 50ml

$dH_2O$ in a 50ml plastic tube. 50ml of this 2.5µg/ml propidium iodide in $dH_2O$ was used per experiment, which was sufficient to stain up to 48 slides. 1-2ml of stain was quickly applied to the gel section of each slide using a plastic Pasteur pipette, ensuring that a reservoir sat on each slide. The entire slide tray was covered on the bench, at room temperature with aluminium foil to keep the slides dark during the 15 minute staining period. After staining $dH_2O$ was gently and liberally added to each slide, from a squeezy bottle using over 250ml per set of slides. Care was taken not to damage the fragile re-hydrated gels. The slide tray was again covered with foil and left for 10 minutes. The slides were then carefully lifted from the tray and placed gel side up on a shelf in the oven (45°C) for at least 1 hour to completely dry. When dry the slides were removed from the oven and placed into an opaque light tight slide box, which could be used for long term storage. Propidium iodide was carefully collected into a sealed container after use and disposed of via the university, in accordance with the Departmental Health and Safety protocol.

2.2.3.7. Image Analysis

Analysis was carried out using a NIKON inverted epifluorescent microscope (consisting of a high power mercury vapor light source, a 580nm dichromic mirror, 510 to 560nm excitation filter and 590nm barrier filter) at x20 magnification. For each duplicate slide 25 images were analysed using Komet analysis software (Kinetic Imaging, Liverpool, UK). The Tail Moment for each cell was defined as the product of the percentage of fragmented DNA in the comet tail, and the distance between the means of the head and the tail distributions, as described by Olive *et al.* (1990). Crosslinking was calculated as the percentage decrease in tail moment using the formula:

$$\% \text{ decrease in tail moment} = \left( 1 - \frac{(TMdi - TMcu)}{(TMci - TMcu)} \right) X100$$

where;

TMdi = tail moment of drug treated irradiated sample.

TMcu = tail moment of untreated, unirradiated control.

TMci = tail moment of untreated, irradiated control.

## 2.2.4. Immunocytochemistry

### 2.2.4.1. Slide Preparation

Frozen single cell suspensions of clinical samples were thawed on ice from –80°C, and in non-sterile conditions were diluted in 1ml of cold phosphate buffer saline (PBS-137mM NaCl, 2.7mM KCL and 10mM phosphate buffer solution) (Sigma). The cell number of each sample was measured using a haemocytometer. Cell number was adjusted to a minimum $5x10^4$ cells per ml, using cold PBS.

75mm x 25mm glass single cytospin slides (pre-coated with 3–amino-propyltriethoxysilone (APES)), containing a single white 12mm diameter circle, with frosted tops (Shandon Inc. 171 Industry Drive, Pittsburgh, PA 15275) were labeled with pencil before use. Each slide was paired with a cytofunnel (Shandon single cytofunnels, centrifuge tubes with white filter card, with a deposit area of 6mm (Shandon Inc.) and secured within a cytoclip, a stainless steel slide clip that holds the aperture of the funnel against the circled area of the slide. Cytoclips were then loaded into the cytocentrifuge (Shandon Cytospin 3) in the upright stationary position.

Three drops of single cell suspension (approximately 100µl) were loaded into one cytofunnel per slide. Samples were spun at 500xg for 5 minutes. The slides were carefully removed from the cytoclips, and the cytofunnels were discarded as clinical waste. Slides were placed on a bench and allowed to air dry, before being stored in a plastic slide box, and placed in a –80°C freezer.

### 2.2.4.2. Antibody Staining

Cytospin slides were thawed from –80°C, on the bench to room temperature. Upon thawing cytospin samples were circled using a hydrophobic pen (DakoCytomation). Before staining the slides were submerged and fixed in acetone for 10 minutes, and then left to air dry.

Slides were placed in a metallic tray and washed with Tris buffered saline (TBS)/Tween pH of 7.4 (137mM NaCl, 5mM Tris (tris hydroxymethylamine),

4.4mM HCl, 0.05% Tween 20 (polyethylene glycol sorbitan monolaurate)). Excess liquid was removed from the slides by tipping them forward in the tray. Several drops of the peroxidase blocking solution (200µl hydrogen peroxide in 12mls methanol) (DakoCytomation) were added immediately to the circled sample on each slide, using a plastic pipette. After 10 minutes the slides were thoroughly rinsed with the TBS/Tween buffer using approximately 5ml per slide, added using a squeezable plastic bottle with a fine aperture applicator. Excess fluid was removed by gently tapping the slide on tissue paper and peroxidase blocking solution was added as before, for a further 10 minutes. This solution was washed off using the TBS/Tween buffer, which was left on for two minutes, before a repeat wash using TBS/Tween buffer.

100µl of either of the three primary antibodies Ca125 (Novocastra NCL-CA125), AUA1 (monoclonal antibody, product code M86024 Skybio, Bedfordshire, MK44 3AT) and Calretinin (rabbit polyclonal anti-calretinin, Zymed, product code 18-0211), diluted according to the manufacturer's instructions, was added to the separate slides using a p200 Gilson pipette. The slides were covered and left in the dark for one hour. After the incubation time, the antibody was washed off with TBS/Tween buffer, which was left on the slides for 2 minutes, before a repeat wash. Excess fluid was removed by carefully tilting the slide, and touching tissue paper to the edge of the droplet of liquid within the circled region (called the 'bulb'). Slides were replaced horizontally into the tray, and approximately 3 drops of biotinylated secondary antibody (AB2 biotinylated goat anti-mouse and anti-rabbit immunoglobulins, DakoCytomation, ChemMate Detection kit, catalog # K5001) was added to the circled sample on each slide using a plastic pipette. Slides were left in the dark for 30 minutes. Two further washes were performed using the TBS/Tween buffer, with a 2-minute gap. Excess fluid was removed from the slides, again by tilting the slide and draining the 'bulb' of liquid from the circled region using an absorbent tissue. Slides were replaced in the tray and three drops of streptavidin peroxidase (- streptavidin conjugated to horseradish peroxidase, DakoCytomation, ChemMate Detection kit, catalog # K5001) were added to each slide and left for 30 minutes. Streptavidin was washed off with TBS/Tween. Several drops of 3,3'diaminobenzidine tetrahydrochloride (DAB) (DakoCytomation, ChemMate Detection kit, catalog # K5001) were added to the slides and left for seven minutes.

DAB was washed off using the TBS/Tween buffer, and the slides were washed in running tap water. Slides were stained with Mayer's Haematoxylin for two minutes, then 'blued' in running tap water, differentiated in 1% acid alcohol and blued again in running tap water. Slides were taken through graded alcohols (70% and 100%), cleared in xylene and mounted in a synthetic mountant Leica CVUltra (Leica coverslipper). DAB was handled and disposed of in line with the University Health and Safety protocol.

2.2.4.3. Microscopy.

Slides were visualized using an Axiophot microscope (Zeiss, Jena, Germany), the computer ran as a TWAIN 32 plug-in with all of the following: Adobe Photoshop (v 4.0, Adobe Systems Inc., California, USA), Microsoft Photo Editor (v.3.0 Microsoft Corporation Inc. Washington, USA), Corel Photopaint (v7.37, Corel Corporation, Ontario, Canada). All photographs were taken at X5 magnification. Correction of spatial shading was performed by dividing each pixel value in the region of interest by the equivalent pixel value in the empty field of view and multiplying the product by 250, for each of the three channels (red, green and blue), using Image-Pro Plus (v 3.0, Media Cybernetics, Maryland, USA).

2.2.5. Statistical Analysis

Student T-tests (heteroscedastic) were performed using Excel 2000 (v5.0.2195 Microsoft Corporation Inc. Washington, USA). P values $< 0.05$ were considered to represent a significant difference in results between two sample populations.

2.3. Results

2.3.1. Patient Data

Table 2.1. summarises patient data for the patients analysed in the present study, including the tumour stage, grade and histological type, the patient's age at the time of sample collection, and any previous exposure to platinum based chemotherapy (cisplatin or carboplatin). Where patients were previously treated with platinum their clinical sensitivity to platinum has been defined according to the length of time from the completion of platinum to relapse. If this interval was less than six months the

| Patient Number | FIGO Stage | Grade | Type | Age at sample collection (Years) | Prior Platinum Based-Chemotherapy | Platinum sensitivity status based on PFI | Relapse |
|---|---|---|---|---|---|---|---|
| 1 | IV | | | 53 | Carboplatin | Sensitive | 1st |
| 2 | IIIC | 3 | | 56 | None | - | - |
| 3 (i) | III | 3 | Serous | 48 | None | - | - |
| 3 (ii) | III | 3 | Serous | 48 | Carboplatin | § | § |
| 4 | IV | 3 | Endometroid | 59 | Carboplatin | Sensitive | 1st |
| 5 | IV | | Endometroid | 50 | None | - | - |
| 6 | IV | | Serous | 57 | None* | - | - |
| 7 | IIIC | | Serous | 68 | Carboplatin | Resistant | 7th |
| 8 | IIIC | 3 | | 60 | None | - | - |
| 9 | IIIC | 0 | Borderline | 69 | None | - | - |
| 10 | IIIC | 3 | Serous | 78 | None | - | - |
| 11 | IIIC | | | 71 | Carboplatin | Resistant** | 5th |
| 12 | IIIC | 3 | Serous | 56 | Carboplatin/cisplatin | Resistant | 2nd |
| 13 | IIIC/IV | | | 58 | None | - | - |
| 14 | IV | | | 75 | Carboplatin | Refractory*** | During 1st line - Ascites |
| 15 | IIIC | 3 | Serous | 57 | Carboplatin | | 2nd |
| 16 | IV | 3 | Clear cell | 51 | Carboplatin | § | § |
| 17 | N/A | | | 80 | Carboplatin | Refractory *** | During 1st line - Ascites |
| 18 | III | 2 | | 64 | None | - | - |

Table 2.1. Summary of Patient Data. Blanks indicate that the relevant data is not known. – indicates not applicable. PFI- platinum free interval. * Patient 6 received 1 dose of carboplatin and paclitaxel 5 days before sample collection, her data has been processed as an 'untreated' patient. The relapse column indicates the number of times the patient had relapsed following chemotherapy, prior to collection of the sample. During first line chemotherapy, samples were either collected as the patient produced ascites, or through interval debulking surgery (ID). ** PFI based on previous treatment involving carboplatin, which was discontinued as the patient became allergic, patient 11 was treated with 2 doses of carboplatin/paclitaxel followed by 4 doses of single agent paclitaxel. § samples collected during first-line exposure at interval debulking surgery, so patients defined as 'treated' but have no history about their previous clinical response to platinum.***patients with platinum refractory tumours with accumulation of ascites and increasing Ca125 levels during chemotherapy.

patient was defined as platinum-resistant, over six months meant that the patient was clinically sensitive to platinum (Markman *et al.* 1991). The number of times that a patient had relapsed before sample collection was also recorded in the last column of Table 2.1.

The average age of patients was 61.7 years. The average age for the platinum-treated patients was 60 years, and the average age for the chemotherapy-naïve patients was 61.8 years. Samples were taken from the chemo-naïve patients around the time of diagnosis, before chemotherapy had commenced. The patients from the 'platinum treated' group, most of whom had been treated for ovarian cancer for a number of years were therefore on average younger at diagnosis. Samples were collected from several patients with a suspected diagnosis of ovarian cancer who subsequently were found not to have the disease. Many 'suspected' samples were partially processed and subsequently dropped from the study, upon a negative diagnosis. As clinical samples were grown without antibiotics, several samples had to be discarded following infection. Therefore, while 19 samples were completely processed, from appropriate clinical subjects, 30 samples were collected in total, of which 6 were lost due to infection and 5 turned out not to be ovarian cancer samples.

### 2.3.2. Clinical Sample Purification and Immunocytochemistry

Figure 2.1. shows phase contrast photographs of the separated tumour, and mesothelial primary cultures, from the ascitic sample from patient 1. Gross phenotypic differences can be observed. The tumour cells appear rounded with few projections. The mesothelial cells appear stretched, long and thin, with many projections. The primary cultures from patient 1 (shown in Figure 2.1), and primary cultures from patients 9 and 10 were analysed using immunocytochemistry, to assess the purity of the samples. Several antibodies were tested to find the best system for clearly distinguishing between epithelial tumour cells and mesothelial cells.

Ca125 and AUA1 antibodies were selected to detect epithelial/ovarian cancer cells (Epenetos *et al.* 1982, Kocjan *et al.* 1992) and calretinin antibodies to detect mesothelial cells (Nagel *et al.* 1998). Calretinin is a calcium binding protein containing six helix-loop-helix structures, known as EF-hand

a.

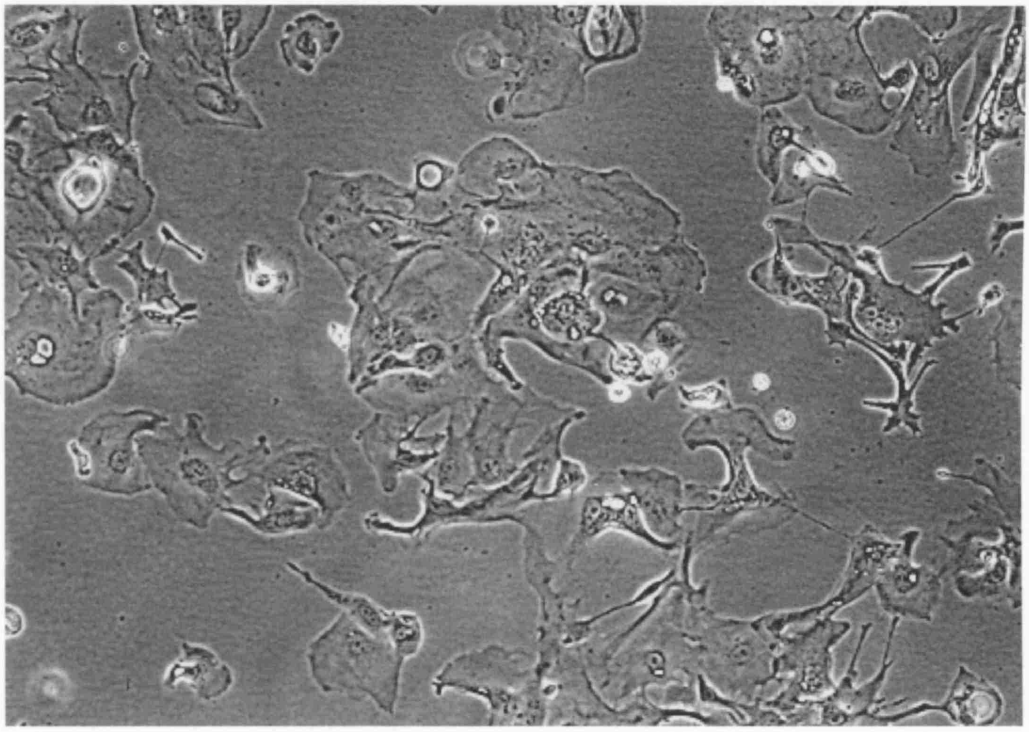

b.

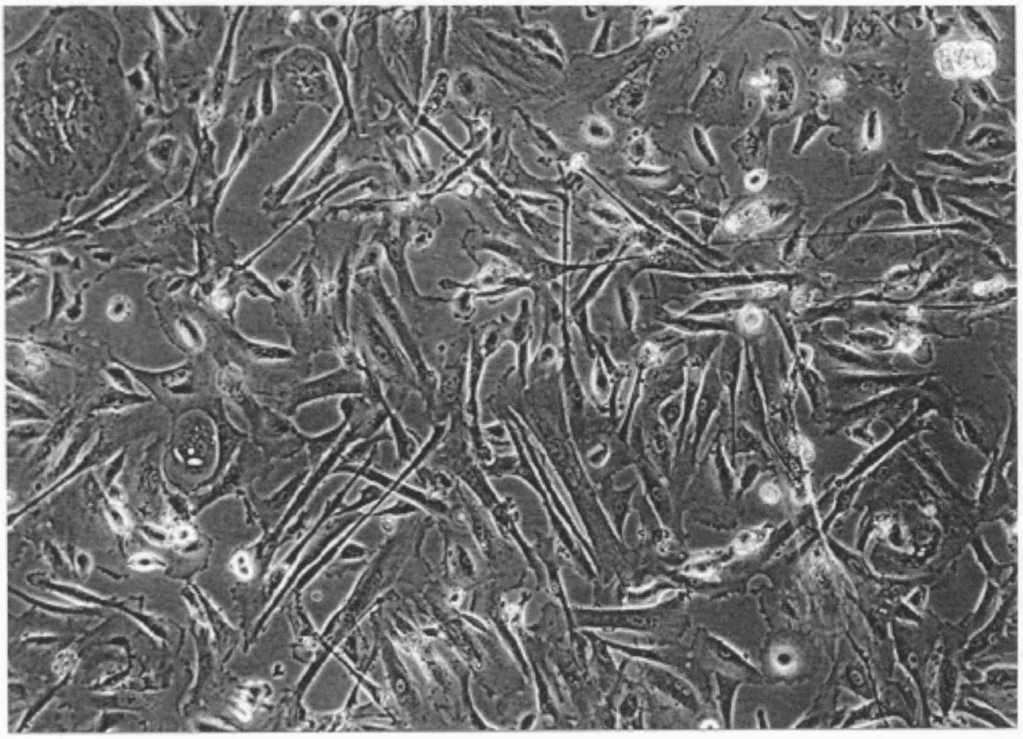

Figure 2.1.
Phase contrast images of primary cultures of cells isolated from an ascitic sample from patient 1. a. Primary culture of tumour cells. b. Primary culture of mesothelial cells.

stretches, and is found expressed within the nervous system (Stryer *et al.* 1995, Rogers *et al.* 1990). Anti-calretinin polyclonal antibodies have been found to stain mesothelial cells (Nagel *et al.* 1998) and mesothelioma (Doglioni *et al.* 1996). Ca125 is a tumour antigen, first detected by a mouse monoclonal antibody (OC125) in 1981 (Bast *et al.* 1981). Ca125 forms the basis of the serum assay used to measure ovarian cancer progression (Rapkiewicz *et al.* 2004). This protein is thought to be a high molecular weight mucin (Yin *et al.* 2002). AUA1 is a monoclonal antibody which is specific for epithelial cells (Epenetos *et al.* 1982, Kocjan *et al.* 1992), binding to a 35kDa cell surface molecule called tumour associated signal transducer-1 (TACSTD1) (also known as epithelial cell adhesion molecule or Ep-CAM) only expressed on cells of epithelial origin.

While the anti-calretinin antibody failed to stain positive control slides containing malignant mesothelioma, Ca125 and AUA1 antibodies both produced positive staining for ovarian cancer cells. Figure 2.2 depicts AUA1 and Ca125 antibody staining of the tumour sample from ascites collected from patient 1. While both antibodies show positive staining of the cells, AUA1 showed a deeper more consistent level of staining. For this reason the AUA1 antibody was selected to stain and identify epithelial tumour cells. Figures 2.3, 2.4 and 2.5 show the immunocytochemical analysis using AUA1 to estimate the purity of primary cultures of tumour cells and of mesothelial cells produced from ascitic samples taken from Patients 1, 9 and 10.

Immunocytochemical analysis using the clinical samples from patient 1, reveals a significant amount of AUA1 antibody binding within the suspected tumour cell primary culture (Figure 2.3a). This result confirms that the cells in the primary culture believed to be epithelial tumour cells, are in fact of epithelial origin. As the sample was ascites, this could only be accounted for by the large number of tumour cells present. The tumour sample without AUA1 (2.3b), shows haematoxylin staining with low level brown staining, representing back-ground staining using the enzyme system. This indicates that the brown colouration seen in Fig. 2.3a is a result of the antibody AUA1 binding to its antigen on the cells, and not as a result of non-specific antibody binding, or enzyme activity associated with the immunocytochemistry protocol.

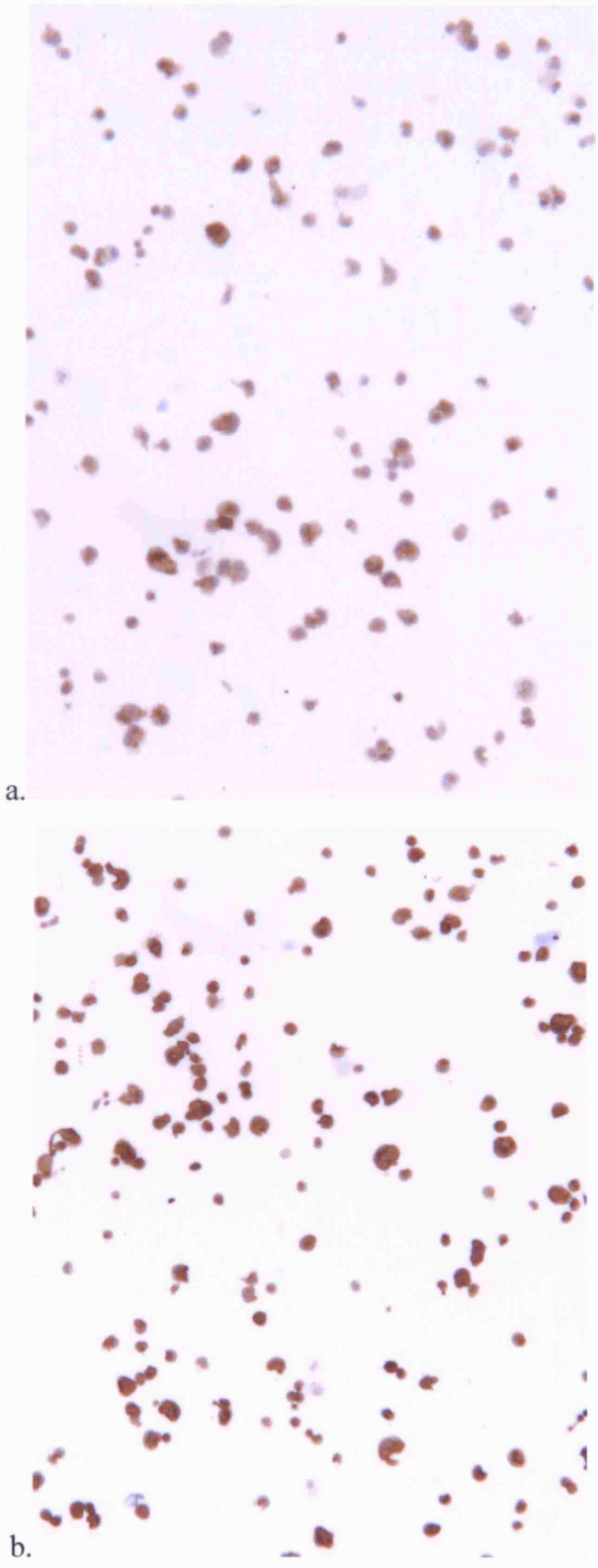


Figure 2.2. Comparison of Ca125 and AUA1 antibody staining of an ovarian tumour cell sample, from a primary culture produced from ascites from patient 1. a. Tumour cells + Ca125, b. Tumour cells +AUA1 (X5 magnification). Haematoxylin staining of nucleic acids highlights the nuclei of the cells.

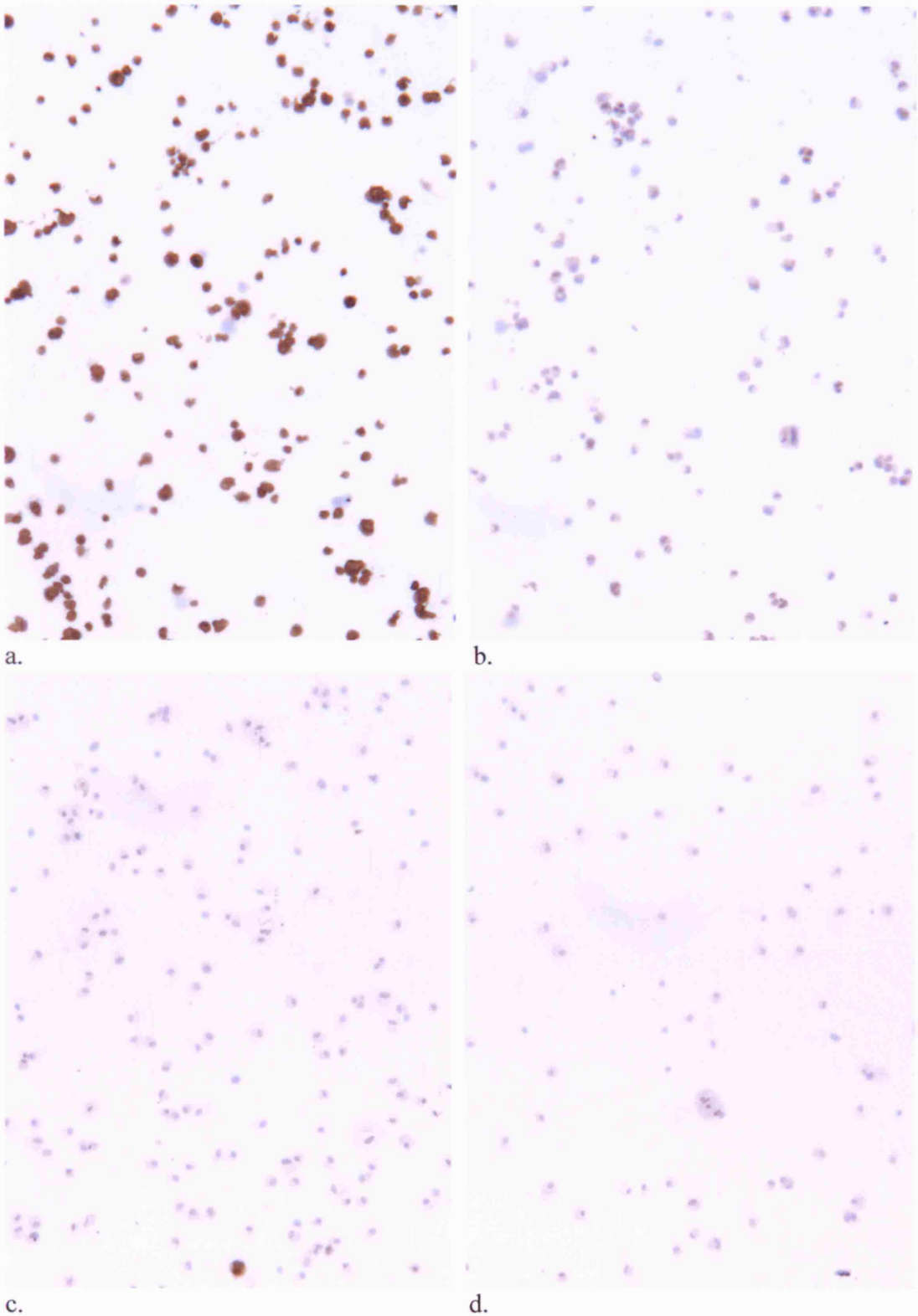


Figure 2.3. Immunocytochemical analysis using AUA1 and haematoxylin to estimate the purity of primary cultures of mesothelial and tumour cells produced from an ascitic sample from patient 1.a. Primary culture of tumour cells, stained with the AUA1 antibody. b. Primary culture of tumour cells, -AUA1. c. Primary cultures of mesothelial cells, stained with the antibody AUA1.d. Primary cultures of mesothelial cells –AUA1. X5 magnification

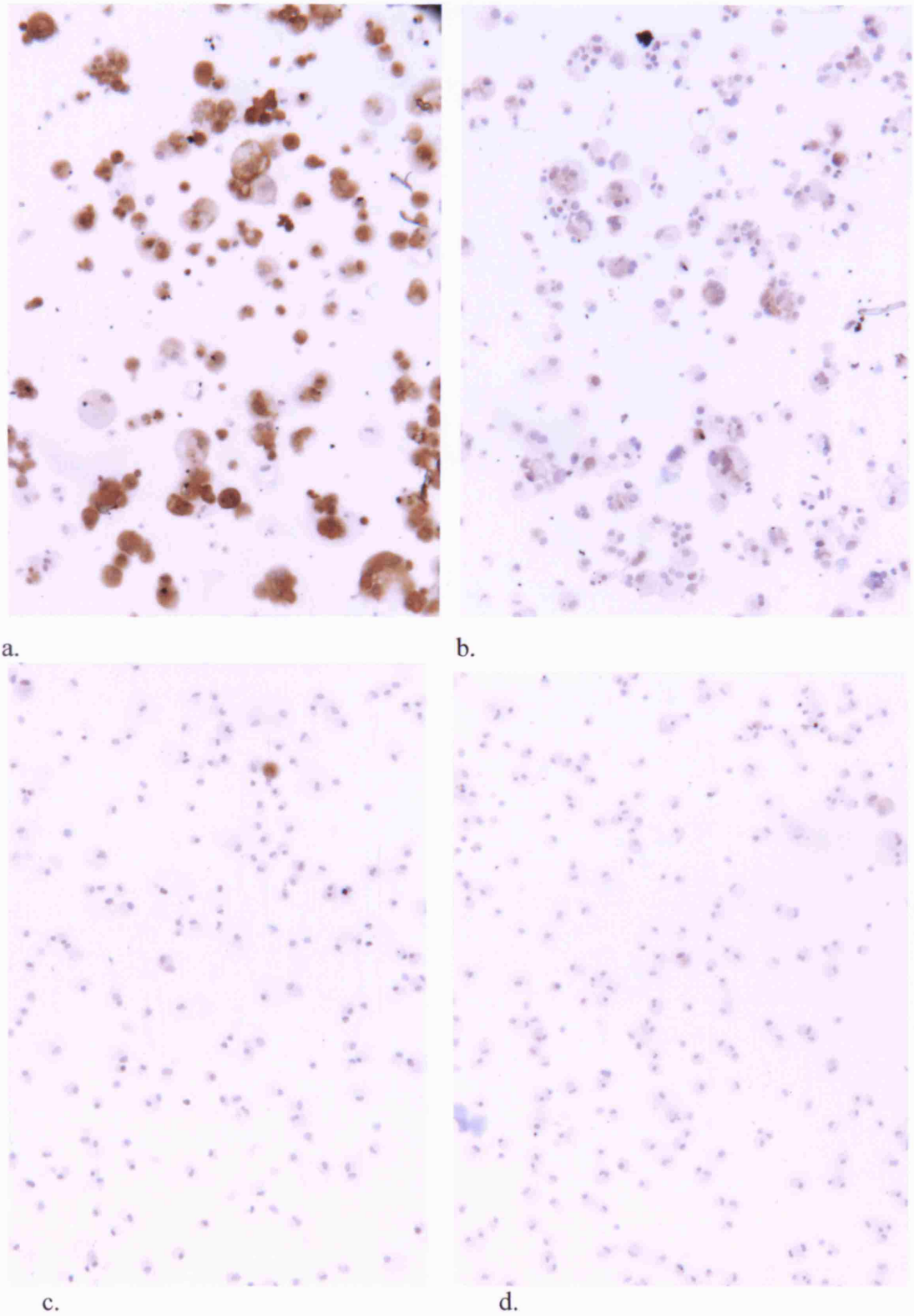


Figure 2.4. Immunocytochemical analysis using AUA1 and haematoxylin to estimate the purity of primary cultures of mesothelial and tumour cells produced from an ascitic sample from patient 10. a. Primary culture of tumour cells, stained with the AUA1 antibody. b. Primary culture of tumour cells, -AUA1. c. Primary cultures of mesothelial cells, stained with the antibody AUA1.d. Primary cultures of mesothelial cells –AUA1. X5 magnification

a.

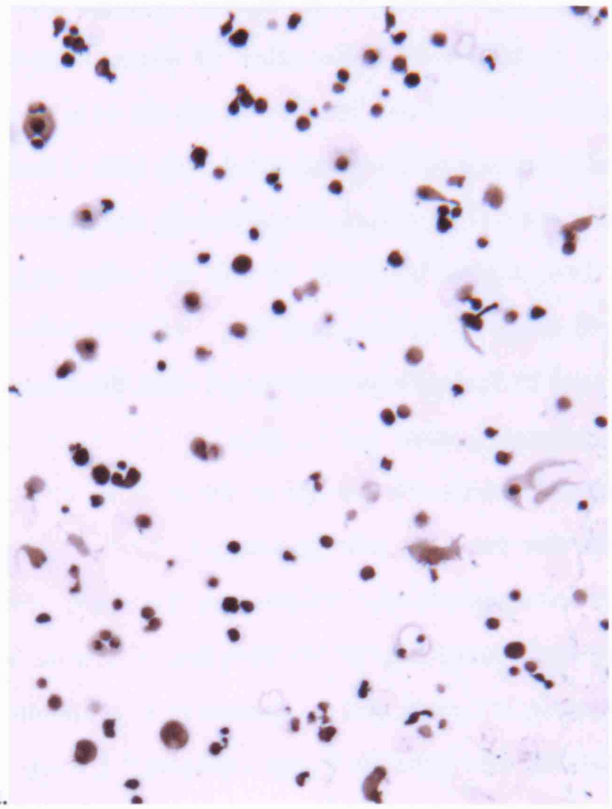

b.

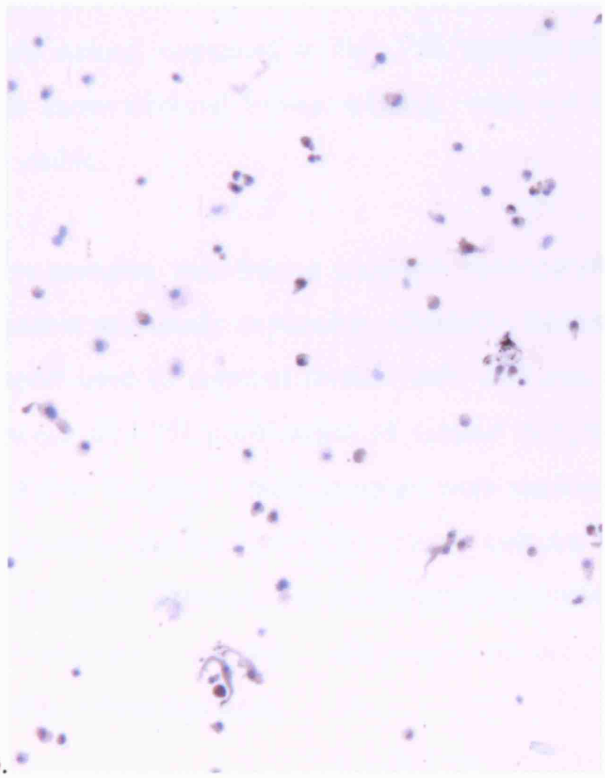

Figure 2.5. Immunocytochemical analysis using AUA1 and haematoxylin to estimate the purity of a primary culture of ovarian tumour cells produced from an ascitic sample from patient 9. (There was no mesothelial sample from this patient) a. Primary culture of tumour cells, stained with the AUA1 antibody. b. Primary culture of tumour cells, -AUA1. X5 magnification

Fig. 2.3c shows primary cultures thought to be mesothelial cells, reacted with the AUA1 antibody. Approximately 15 cells within this field of view are positively stained (altogether there is in excess of 500 cells in this view in total). This would indicate a small fraction (~3%) of tumour cells within the mesothelial culture. The majority of cells are clearly not stained by the antibody. This would confirm that the large majority of these cells are not of epithelial origin, and therefore can be concluded to be mesothelial cells. Fig. 2.3d shows the same mesothelial primary culture in the absence of antibody. Again this shows a lack of false positive staining. Figure 2.4a presents the AUA1 staining of the tumour samples from patient 10. Approximately 20% of the cells in this image are not stained brown indicating a lack of anti-AUA1 antibody binding, suggesting that they are not epithelial in origin. These cells most likely represent mesothelial contaminants in the tumour sample. When the mesothelial sample is analysed for the presence of epithelial cells (2.4c) a lower level of contamination is revealed, of less than 1% tumour cells within the mesothelial sample. Figure 2.5 presents AUA1 staining of a tumour cell sample from patient 9. Fig. 2.5a shows the tumour sample with AUA1, and every cell in view appears to be positively stained, compared to Fig. 2.5b, tumour cells without AUA1, where all of the cells show minimal brown staining, with the blue haematoxylin stained nuclei clearly visible.

Analysis of these three samples, two from a platinum-naïve patient (patients 9 and 10) and one from a patient previously exposed to platinum chemotherapy (patient 1) suggest that the protocol used to selected tumour cells and mesothelial cells from ascites produced between 80-97% purification of tumour samples, and over 95% purification of mesothelial samples. These samples were randomly selected to be representative of the levels of purification of the primary cultures produced from the clinical samples. As the same technique for separation was applied to each sample, this immunocytochemical analysis was felt to adequately indicate the levels of sample purification achieved throughout this study.

2.3.3. Measurement of Cisplatin-Induced DNA Interstrand Crosslinks in Clinical Samples using the Comet Assay

Cells were drug treated for 1 hour with 100μM cisplatin in warm DMEM (without glutamine or FCS). This dose was chosen to produce approximately 50% decrease in tail moment at the peak of crosslinking, based on previous results using human ovarian cancer cell lines A2780 and A2780cisR, reported in Chapter 3. After 1 hour the drug was removed and drug-free medium containing 10% FCS was added to the cells and incubated at 37°C. Samples were processed immediately after a 1-hour treatment (time 0) and 4.5, 9, 24 and 48 hours after exposure.

Interstrand crosslinking was assessed using the comet assay, whereby interstrand crosslinking induces a reduction in the tail-moment of the comets produced as a direct result of random single-strand DNA breakage induced by X-ray exposure. Figure 2.6, shows typical comet images of human ovarian tumour cells processed using the comet assay, nine-hours after cisplatin-exposure. Ovarian tumour cells that were not exposed to cisplatin or X-rays show minimal tail formation (2.6a). Ovarian tumour cells with no cisplatin exposure, but with X-ray exposure, display significant comet tails as the electrophoresis has caused the migration of the fragmented DNA through the gel with the current (2.6b). Ovarian tumour cells that were exposed to cisplatin, but not to X-rays show no comet tail formation (2.6c). Finally, ovarian tumour cells treated with cisplatin and X-rays, show significantly retarded comet formation, as a result of the ICLs inhibiting the migration of DNA fragments during electrophoresis (2.6d).

Figure 2.7 is the comet assay time course data using the tumour and mesothelial primary cultures from patient 1. Data is expressed as the % decrease in tail moment compared to an irradiated non-drug treated control. Very few crosslinks are seen immediately after a 1 hour treatment, represented by the 0 hours time point. The level of crosslinking increases until a peak of crosslinking is reached approximately 9 hours post treatment. The tumour cells show a rapid reduction in interstrand crosslinking by 24 hours. The mesothelial cells show only a slight reduction in crosslinking at 24 hours, and a significant level of crosslinking persists at 48 hours. The mean values of two independent experiments are represented by the line graph.

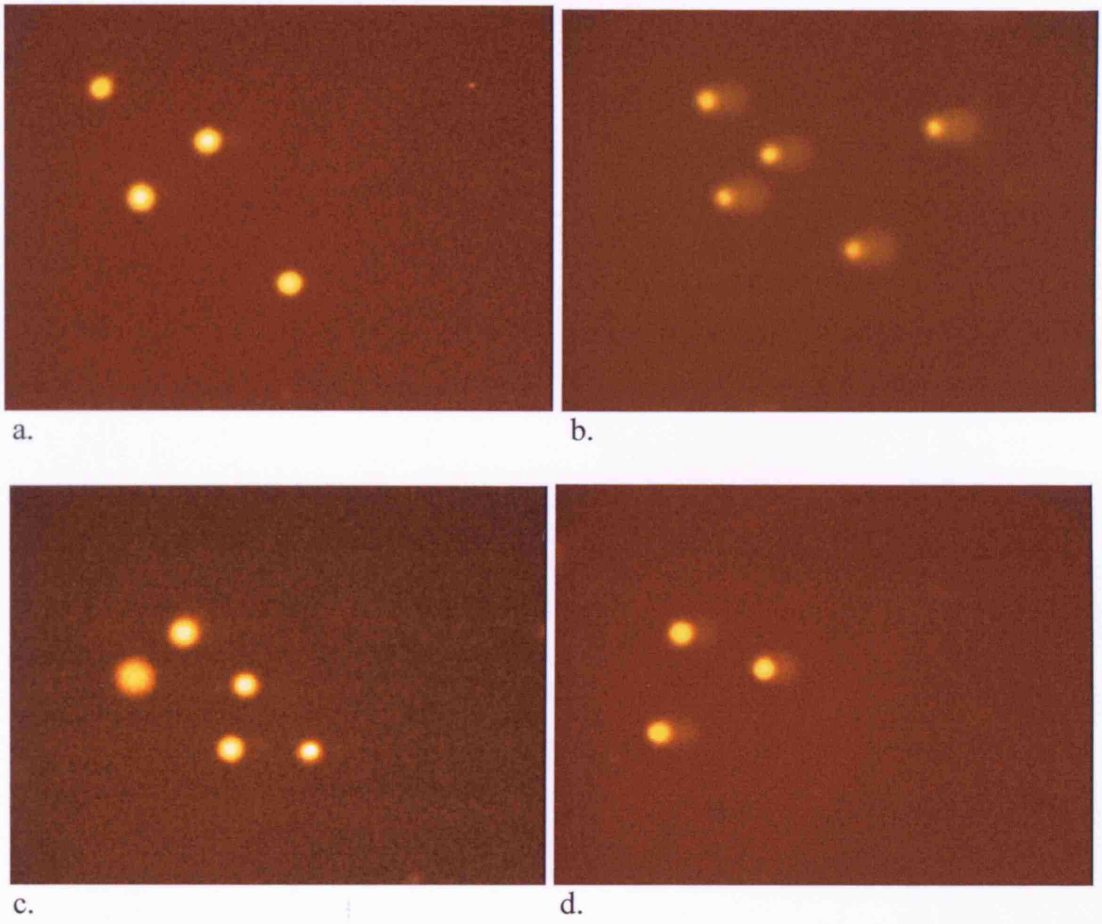


Figure 2.6. Typical comet images showing cisplatin-interstrand crosslinking in human ovarian cancer cells, at the peak of crosslinking nine-hours after a one-hour drug exposure using 100μM cisplatin. a. non-irradiated non-drug treated cells. b. irradiated, non-drug treated cells. c. non-irradiated, drug treated cells. d. Irradiated drug treated cells.

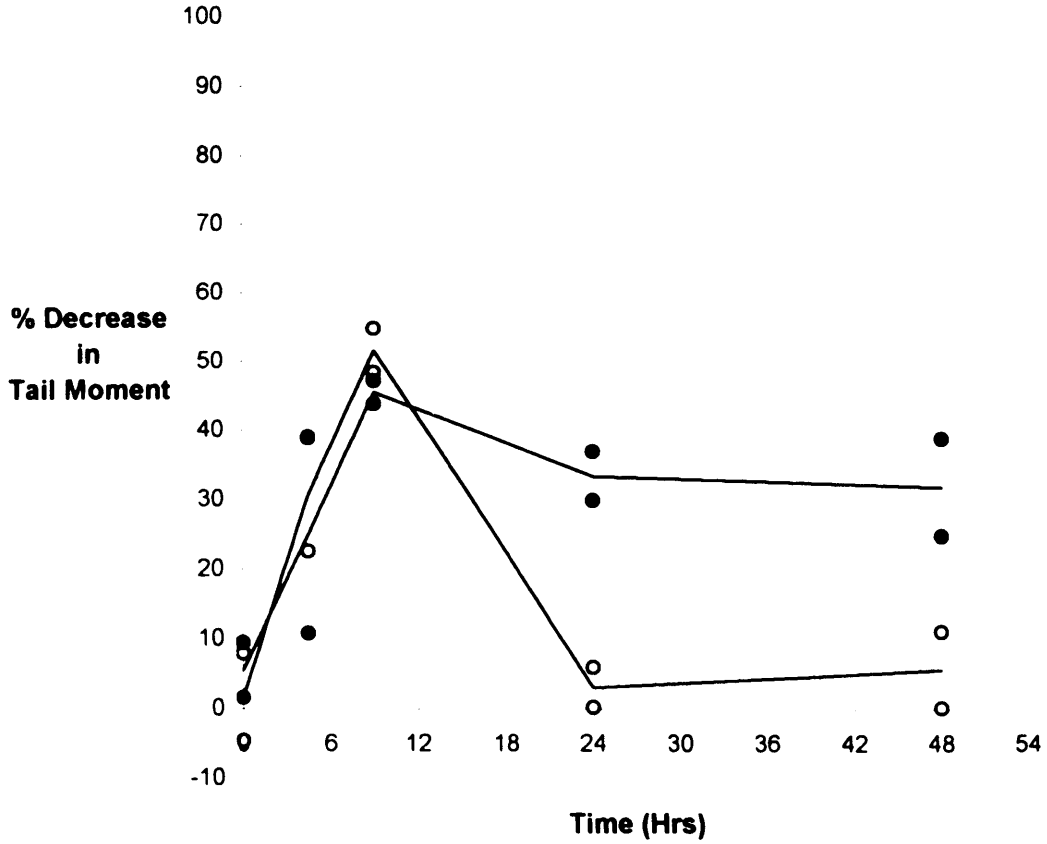


Figure 2.7. Cisplatin-induced interstrand crosslinking measured using the comet assay, using primary cultures of ovarian tumour cells and mesothelial cells from an ascitic sample from patient 1, represented as % decrease in tail moment against time, following a 1 hour drug treatment with 100μM cisplatin. Lines represent the mean data of two independent experiments with each individual data point represented by a single data point. Open circles represent tumour cell data, and closed circles represent mesothelial cell data.

Each data point represents the mean values for 50 cells, counted from two duplicate slides. In subsequent patient samples the 4.5 hour time point was not performed. This time point was not necessary to establish the peak level of crosslinking and subsequent repair (unhooking). The drug treated non-irradiated slides were not performed after initial experiments determined that drug treatment with cisplatin was not inducing a significant level of single strand breaks (data not shown). A reduced number of time points was necessary in some clinical samples due to a limited sample cell number

In total 19 patient samples were successfully analysed, two of which came from one patient (3) at different stages of treatment. Where it was possible to only carry out single experiments, data are represented by single line graphs. Where experiments were carried out in duplicate, each data point represents data from a single experiment, the mean of the data is represented by a line graph. Where experiments were carried out in triplicate mean data is represented by a line graph with standard error bars at each data point. On each graph the source of the clinical material (eg. ascites) is indicated beside the patient number. The crosslinking data from all of the patient samples are shown in Figure 2.8.

All of the treated cell samples showed clear crosslinking following a 1-hour cisplatin exposure. The peak of crosslinking occurred around the 9 hour time point, with the exception of four tumour samples that showed slightly higher crosslinking 24 hours after drug exposure. Where more than one experiment was carried with the same starting sample, good reproducibility was observed between independent experiments. Most of the samples tested showed clear evidence of ICL unhooking over a 48 hour period. The degree of ICL unhooking observed varied between samples.

### 2.3.4. Comparison of Crosslink Formation at the Peak of Crosslinking in Clinical Samples

The % decrease in tail moment value nine hours after cisplatin exposure represents the peak of ICL formation. Figure 2.9. represents the peak level of crosslinking for all of

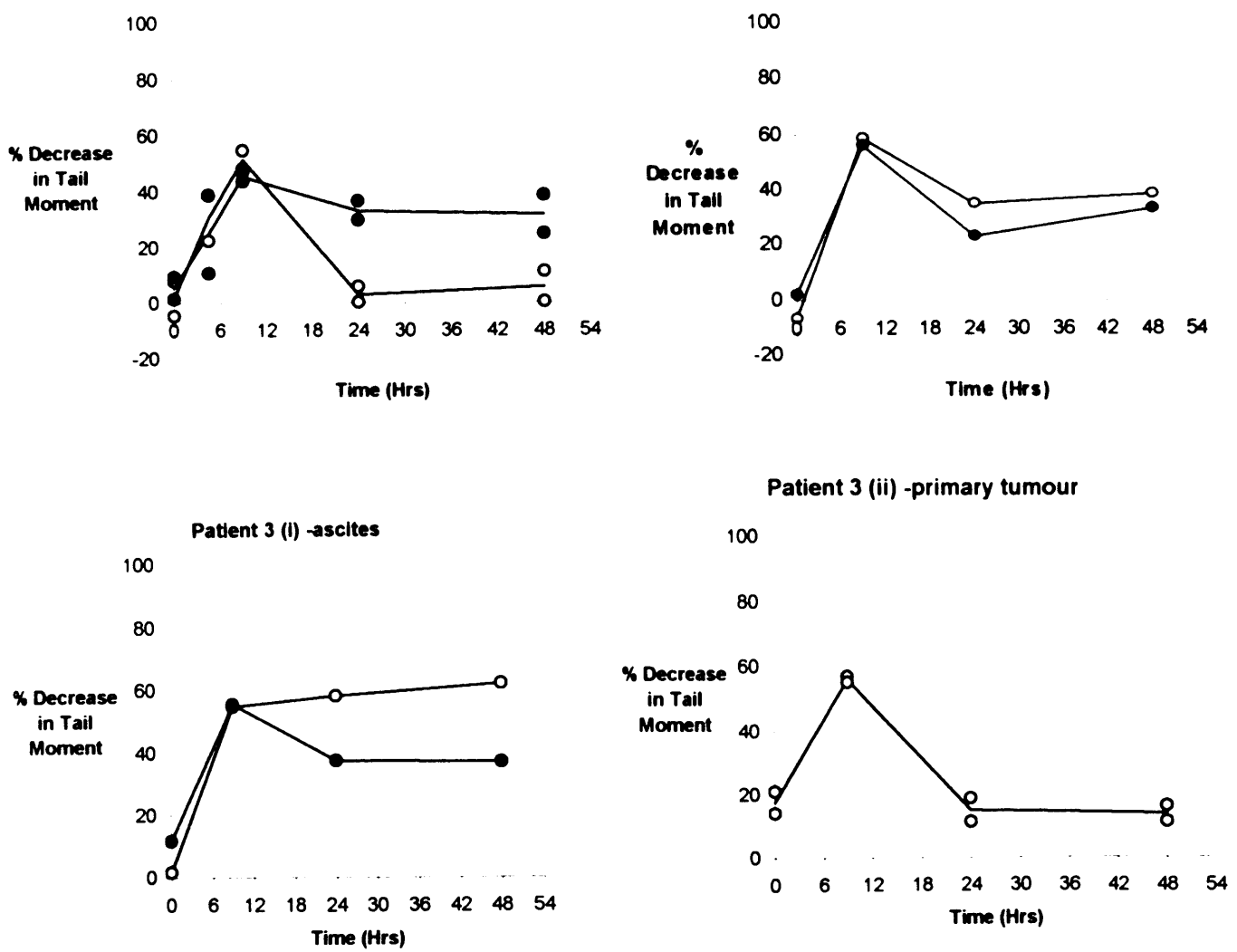


Figure 2.8. Cisplatin induced DNA interstrand crosslinking measured using the comet assay in cells from the 18 ovarian cancer patients, represented by % decrease in tail moment against time, following a 1-hour drug treatment with 100μM CDDP. Single experiments are represented by single line graphs. Where experiments were carried out in duplicate, each data point is represented and a line graph represents the mean result. Where experiments were carried out in triplicate the mean of the three experiments is represented by a line graph. Y-error bars represent the standard error values from the three data sets. Open circles represent tumour cell data, and closed circles represent mesothelial cell data.

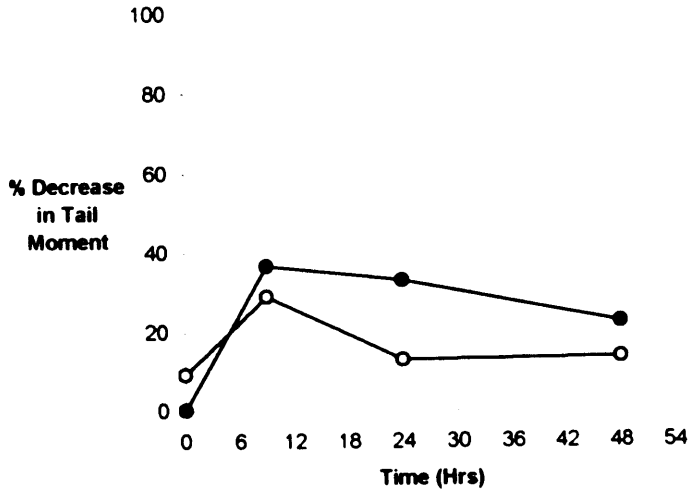


Patient 6 -ascites

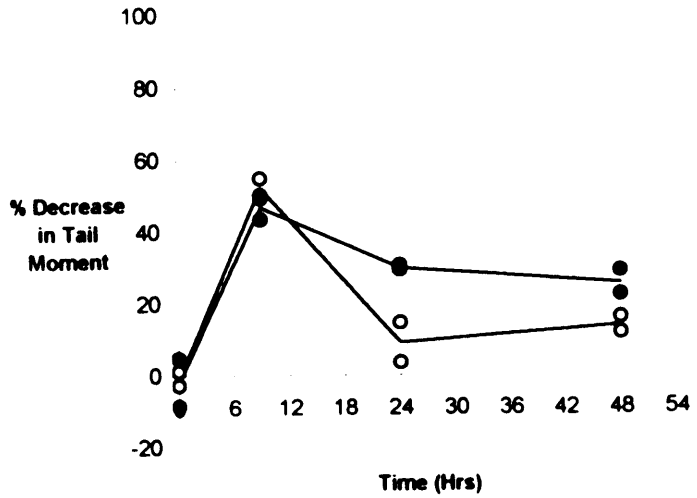


Patient 7 -ascites

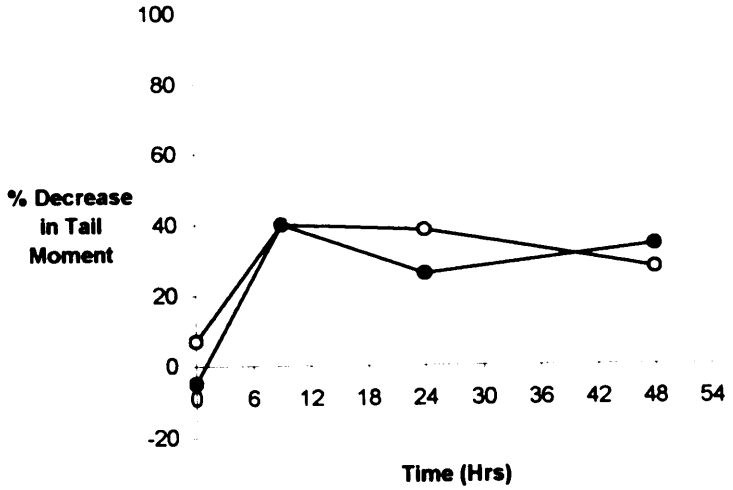


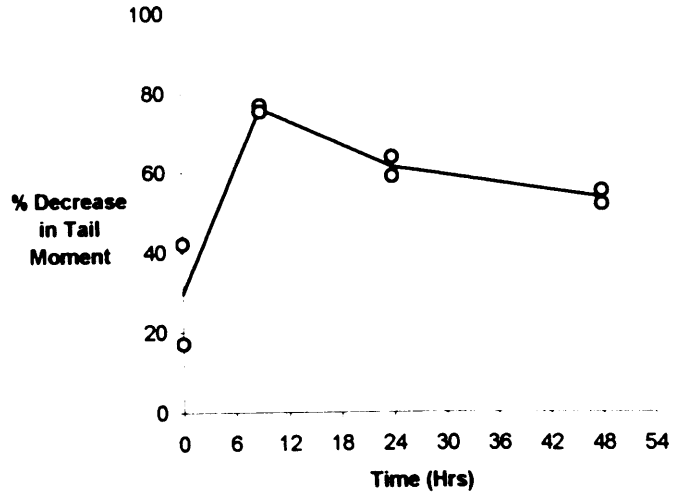


Figure 2.8 continued.

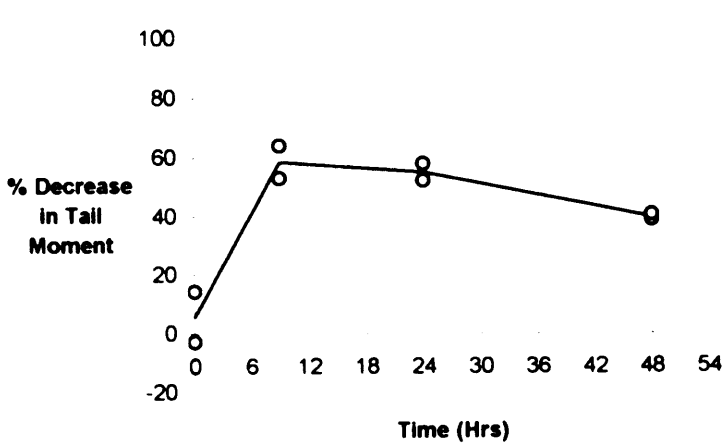


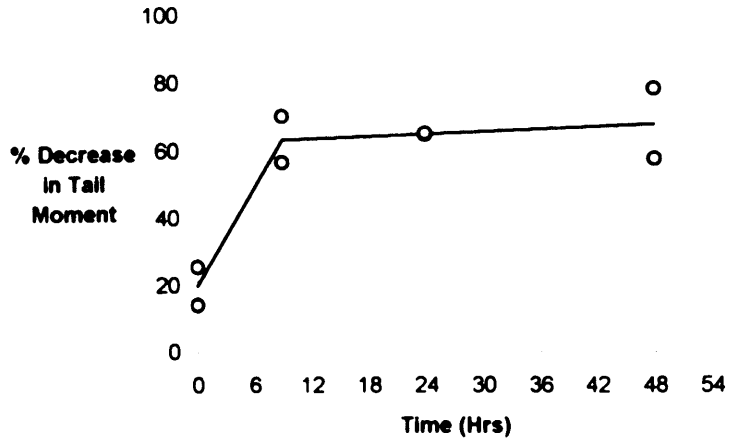


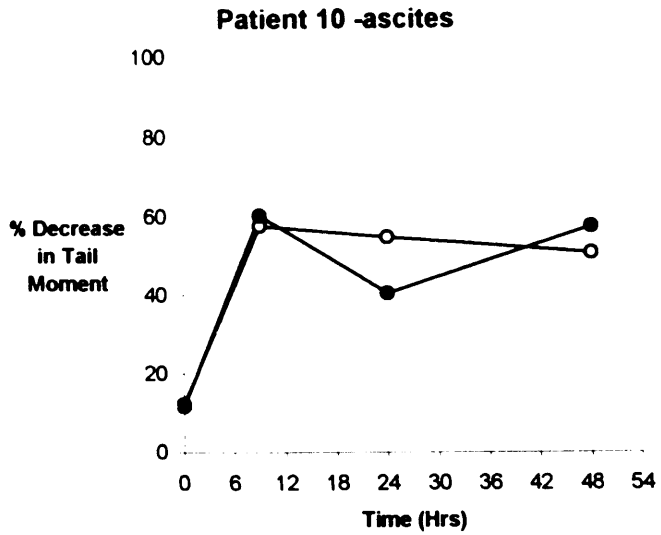


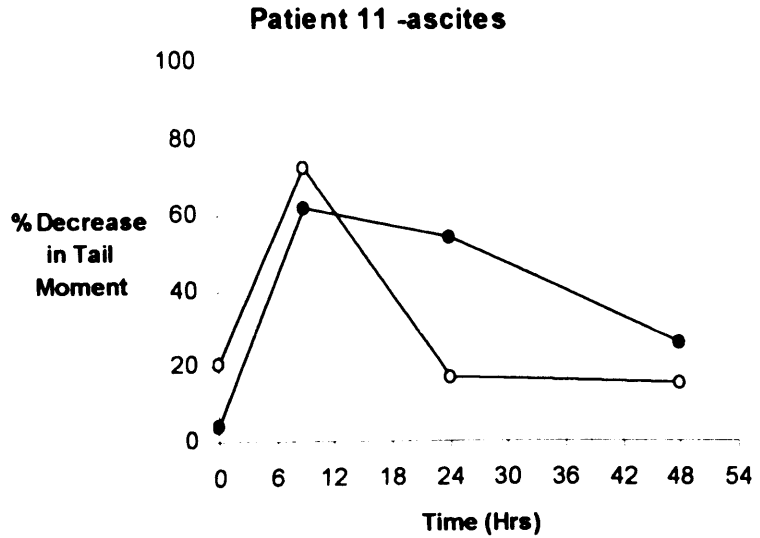


Figure 2.8 continued.

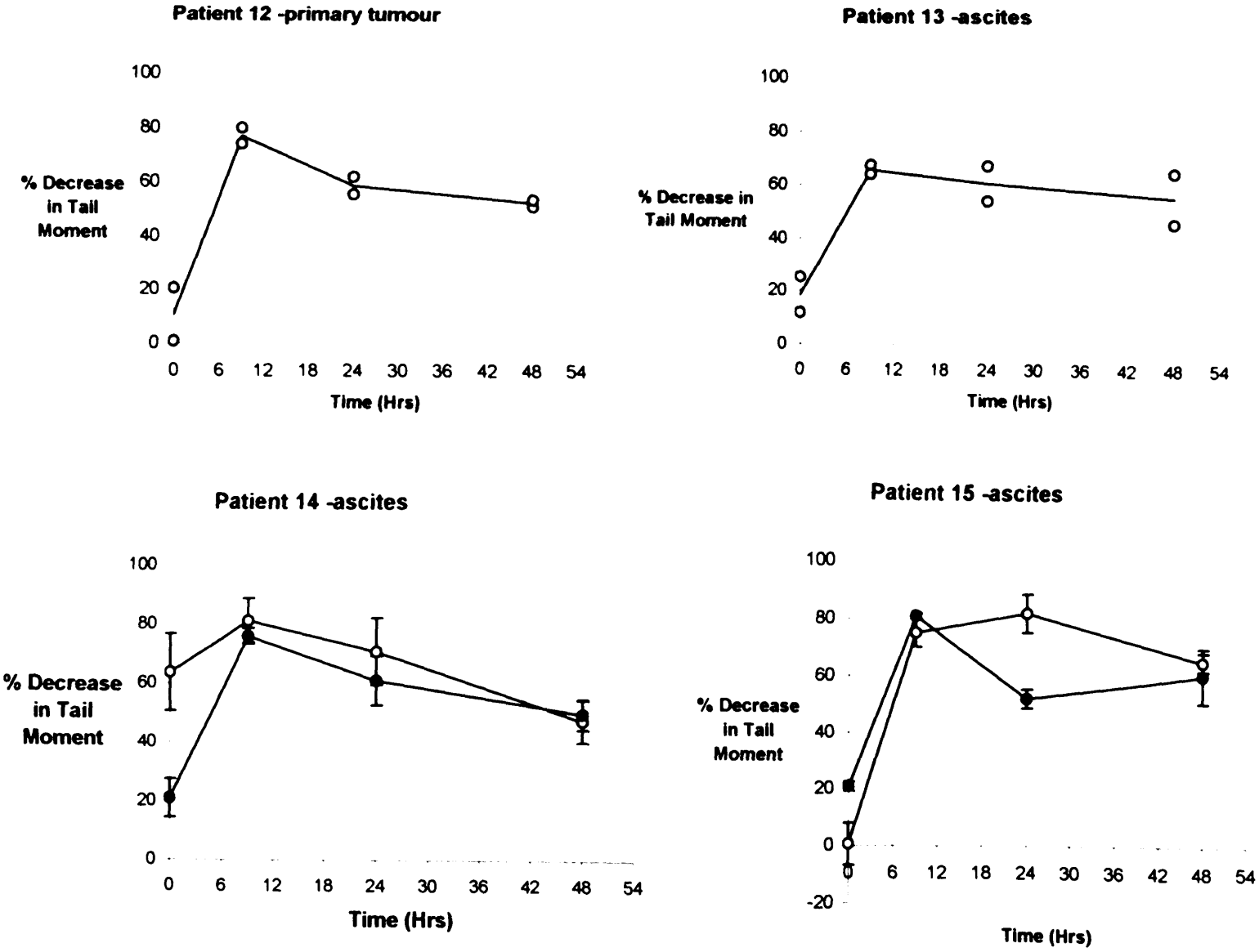


Figure 2.8 continued.

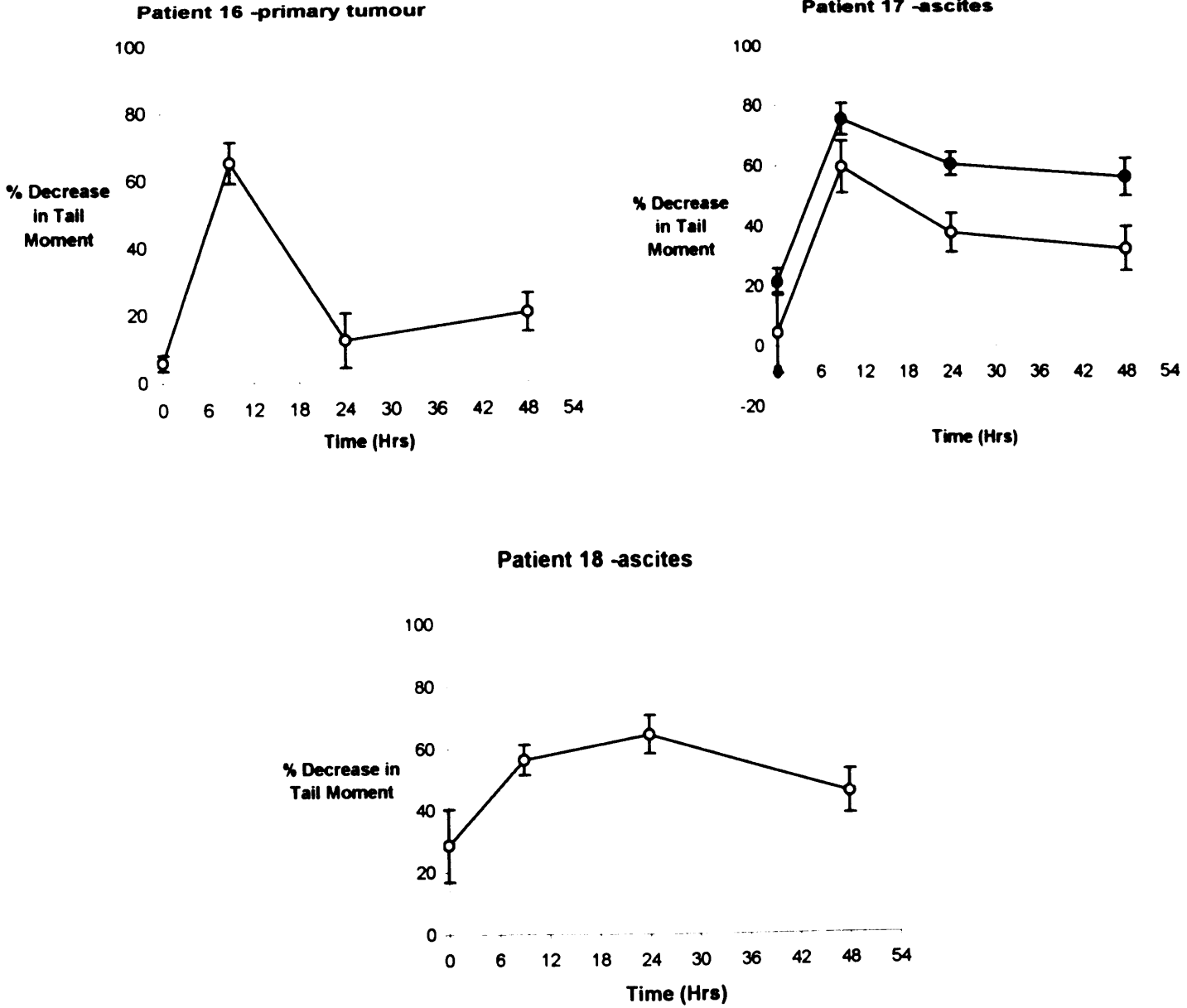


Figure 2.8 continued.

the ovarian cancer cell samples from the 19 patient samples, separated according to whether or not the patient was previously exposed to platinum-based chemotherapy.

The data represented in Figure 2.9a and summarized in 2.9b suggest that ICL formation was similar in all of the clinical ovarian tumour samples. No significant difference was observed in ICL formation between the tumour cells from the platinum naïve and platinum exposed patients ($p=0.256$). Similarly, ICL formation, measured as a % decrease in tail moment at the nine-hour peak of crosslinking, was compared in the samples from patients that yielded both tumour and mesothelial cells. Figure 2.10 summarises the ICL levels at the peak of crosslinking in the five paired tumour and mesothelial samples from platinum-naïve patients, and six paired mesothelial and tumour samples from patients previously treated with platinum. The data presented in Figure 2.10, indicates similar levels of ICL formation in both cell types from each individual patient. Statistical analysis using the t-test indicated that there was no significant difference in ICL formation from paired samples, between tumour and mesothelial cells from untreated and treated patients (all p values over 0.24). When all of the treated samples were compared to all of the untreated samples (mesothelial and tumour) the p value was 0.11. Statistical significance was inferred in this study to a p-value below 0.05.

### 2.3.5. Comparison of Persistence of Cisplatin ICL in Clinical Samples

Clear differences were observed in the persistence of crosslinks between different patient samples. In order to compare the data numerically, the % removal (unhooking) of the crosslinks formed at nine hours was calculated at 24 hours. Figure 2.11 presents % ICL unhooking data for all of the patient tumour cell samples.

There is a large variation in the % ICL unhooking in the tumour samples in both the untreated and treated patient groups. Negative values indicate that the ICL level increased between the nine and 24-hour time points following a one-hour cisplatin treatment. These values were used for the statistical analysis, however negative values are later quoted as '0'% ICL unhooking. The majority of the nine untreated patient tumour cell samples showed low levels of ICL unhooking, with seven showing <10% unhooking.

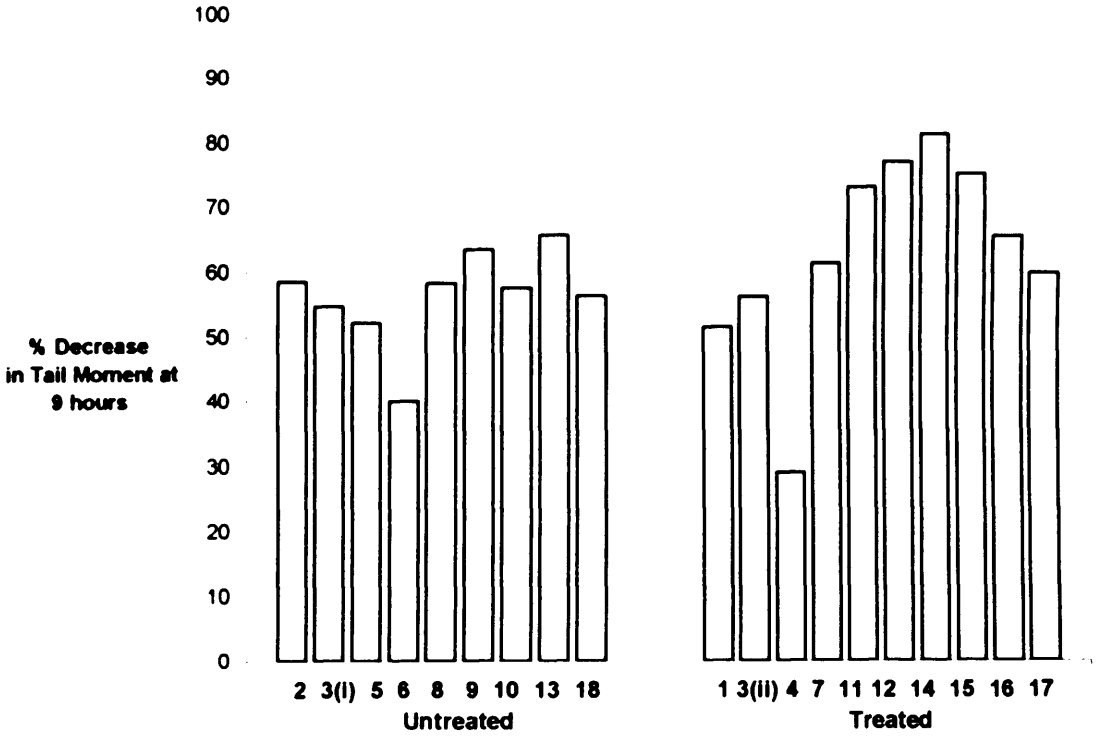


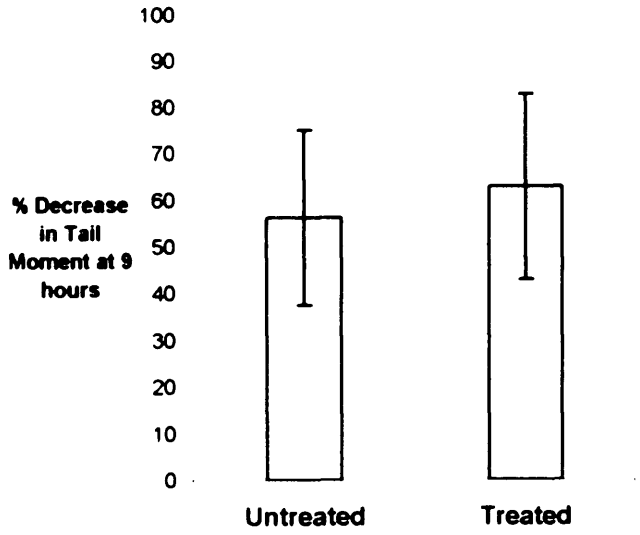


b.

Figure 2.9. The % decrease in tail moment at the peak of crosslinking, nine hours after drug exposure, in 19 ovarian tumour cell samples, divided according to the patient's previous exposure to platinum chemotherapy. a. data for all patient tumour samples, b. mean data for the two patient populations. Y-error bars represent the standard deviation from the mean.

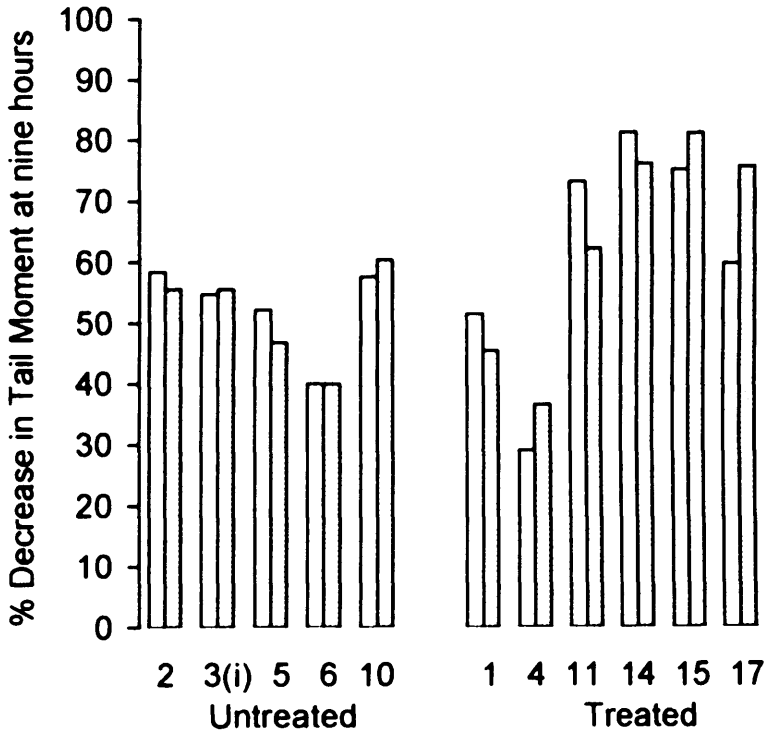


a.

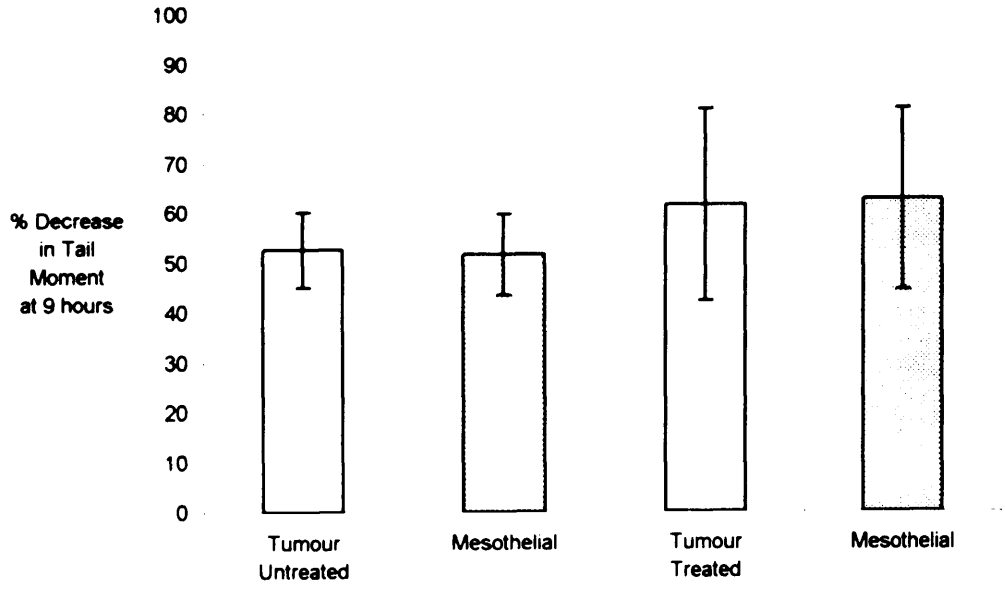


b.

Figure 2.10. % decrease in tail moment at the peak of crosslinking nine hours after drug exposure, in primary cultures from the eleven patient samples that yielded both tumour and mesothelial cells. a. individual patient peak of crosslinking data. White bars represent tumour samples, and grey bars represent mesothelial samples. b. Mean patient peak of crosslinking data. Y-error bars represent the standard deviation from the mean

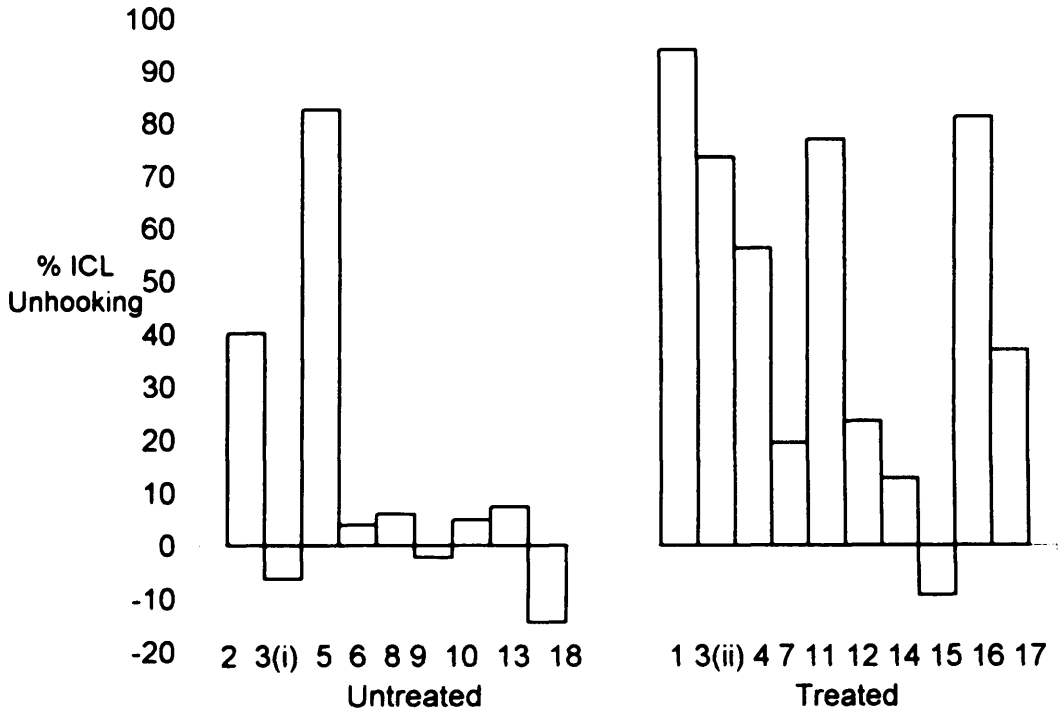


b.

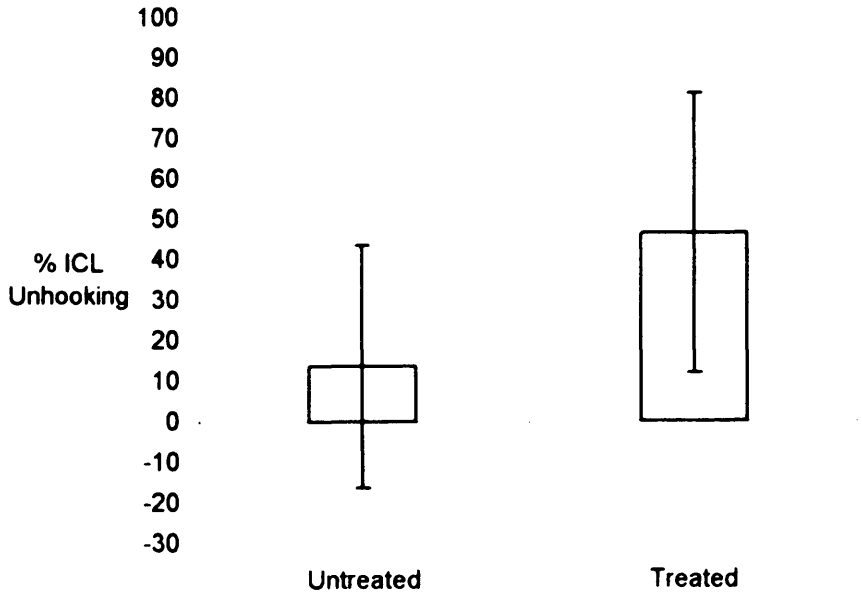


Figure 2.11. % ICL unhooking at 24 hours by tumour cells in 19 ovarian tumour cell samples, divided according to the patient's previous exposure to platinum chemotherapy. a. data for individual patient samples (patient number on the X-axis) b. mean data for the two patient populations. Y-error bars represent the standard deviation from the mean.

The exceptions showed 40% (patient 2) and 83% (patient 5) ICL unhooking, respectively. In contrast, the majority of the ten previously treated patient tumour cell samples showed significant ICL unhooking, with nine samples showing >10% unhooking, and four showing >70% ICL unhooking (Figure 2.11). The average % ICL unhooking for the untreated and treated patient samples are summarised in Figure 2.11b.

The average % ICL unhooking between 9 and 24 hours following a 1-hour drug treatment for the tumour samples from untreated patients was 13.6%. The average value for the tumour samples from treated patients was 46.5%. When the two data sets were analysed using a t-test, the p value of 0.04 suggests that the observed difference was significant. Therefore elevated ICL unhooking was observed by the tumour cells from patients previously treated with platinum chemotherapy, compared with low levels of ICL unhooking by the tumour samples from platinum-naïve patients.

Figure 2.12. presents the ICL unhooking data for the eleven patient samples that yielded both tumour and mesothelial cells. Whereas the ICL formation data (Figure 2.10) for the paired samples revealed similar ICL formation by mesothelial and tumour samples from the same patient, no similarity in ICL unhooking data can be seen when comparing the two cell types from the same patient (Figure 2.12).

Overall the mean % ICL unhooking for mesothelial cells was 29.4%. This population of normal cells gave a much more homogenous response than tumour cells (Figure 2.12b). Interestingly % ICL unhooking appears to be elevated in the mesothelial samples from untreated patients (39%), compared with those from treated patients (21.5%). When the two data sets were compared using a t-test, the p value of 0.01 suggests that the observed difference was significant. As a small number of samples were used to produce this data, (untreated mesothelial samples (n=5), treated mesothelial samples (n=6)), further research would clarify the observed effect. If normal cells from patients previously exposed to platinum show a reduced capacity to unhook the interstrand crosslink, a second treatment with these compounds could prove more toxic to the patient then the initial exposure. As tumour cells from patients previously exposed to platinum show an enhanced capacity to unhook the

a.

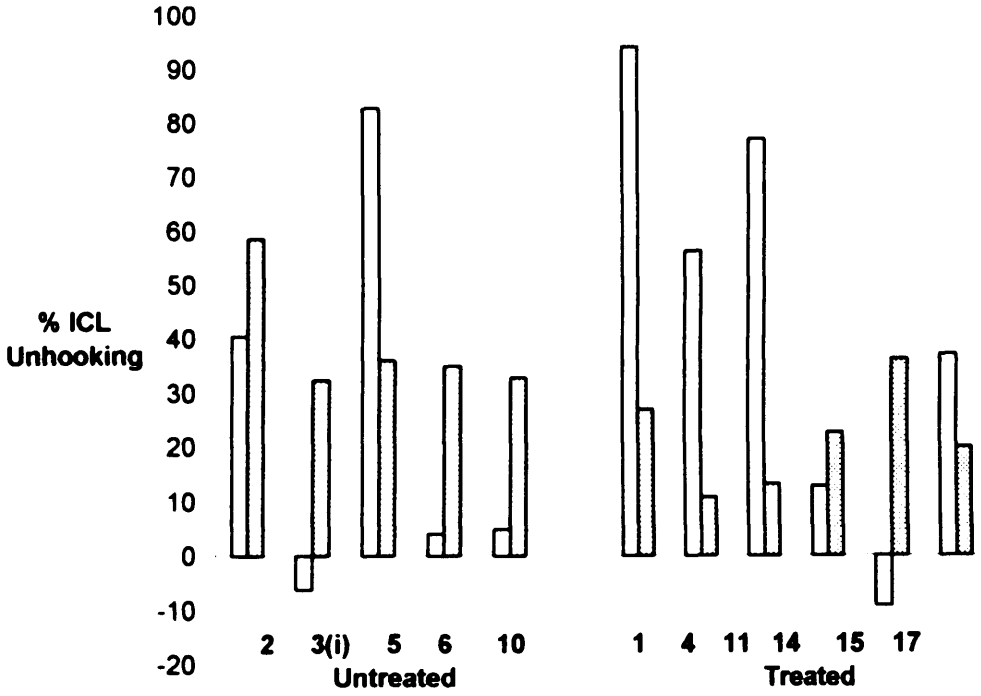


b.

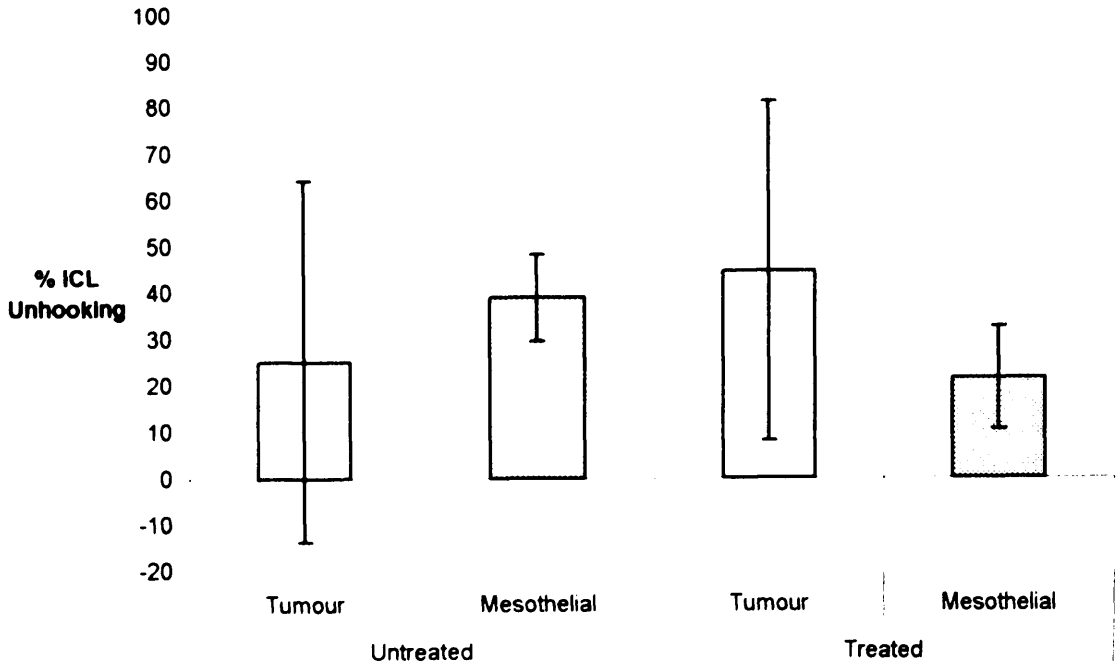


Figure 2.12. % ICL unhooking in primary cultures from the eleven patient samples that yielded both tumour and mesothelial cells. White bars represent tumour samples, and grey bars represent mesothelial samples. a. Individual patient ICL unhooking data. b. Mean patient ICL unhooking data.

ICL, a second treatment with platinum could prove more damaging to normal cells and less damaging to tumour tissue, than the initial exposure. Interestingly, the mean % ICL unhooking for tumour cells from platinum-naïve patients was 13.6%, compared to 39% for normal cells, indicating that normal cells performed a higher level of ICL unhooking than the tumour cells from platinum-naïve patients. This would suggest that the first time a patient is treated with platinum the tumour cells will be less able to remove the interstrand crosslinks than the surrounding tissue, and should therefore be more sensitive to platinum killing than normal cells. Theoretically this data would suggest that ovarian tumour cells are most sensitive to platinum treatment the first time that they are exposed to platinum, and that the normal tissue within the patient would tolerate a higher dose of platinum than the naïve-tumour tissue. This would present an ideal clinical scenario where the tumour tissue is inherently more sensitive to the chemotherapeutic than the non-tumour tissue. The major conclusion of the comparison of ICL unhooking between paired mesothelial and tumour cells from the same patient is that the two cell types (tumour and mesothelial) process cisplatin ICL very differently. Three of the untreated tumour samples show significantly lower cisplatin ICL unhooking compared with their paired mesothelial samples (3(i), 6, 10) (Figure 2.12).

### 2.3.6. Comparison of Samples from the Same Patient both Pre- and Post-Chemotherapy

One patient provided samples both before she was exposed to platinum chemotherapy, and after interval debulking surgery mid-way through the course of chemotherapy (Figure 2.13). The untreated sample was a primary culture from ascites, and the treated sample was primary tumour removed at the patient's interval debulking surgery after three cycles of carboplatin/paclitaxel combined chemotherapy. This tumour tissue was processed as a single cell suspension. Figure 2.13 shows the crosslinking data from the two tumour samples. The peak of crosslinking following drug exposure is very similar between the two tumour samples (Figure 2.13b). However, both samples differ in ICL unhooking at 24 hours (Figure 2.13c). The tumour sample that was collected after the patient had been exposed to platinum chemotherapy shows clearly enhanced ICL repair between the 9 and 24-hour time points, compared to the complete lack of ICL repair observed by the

a.

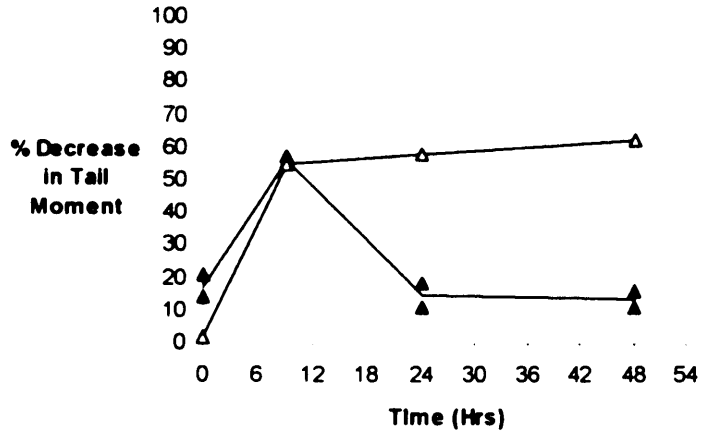


b.

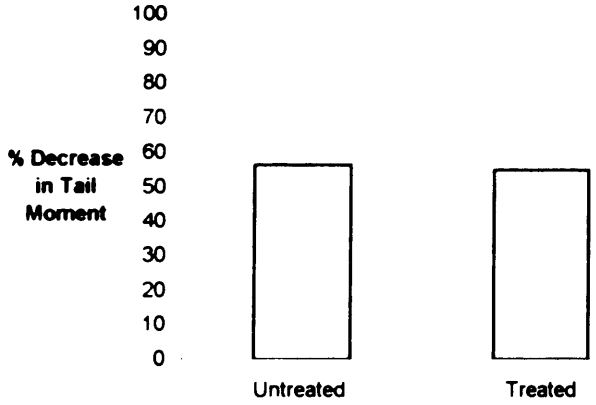


c.

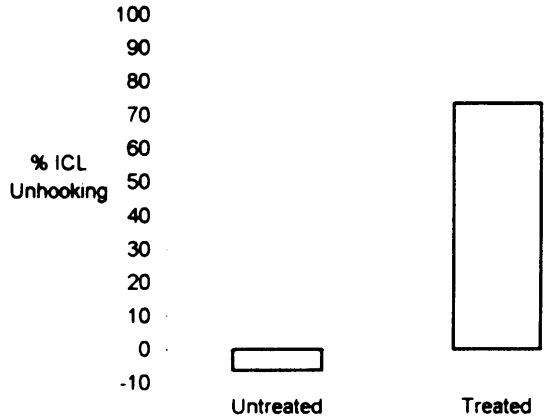


Figure 2.13. Comparison of *in-vitro* response to a one hour treatment with 100μM cisplatin in tumour cells samples from patient 3, collected both before and after the patient had been treated with carboplatin chemotherapy. (Untreated data represents a single experiment. Treated data represents two experiments, in 12b. and 12c. the mean data is used) a. cisplatin-induced ICL measured using the comet assay, % decrease in tail moment in untreated tumour samples (open triangles) and treated tumour samples (closed triangles). b. % decrease in tail moment at the peak of crosslinking 9 hours after drug exposure. c. % ICL unhooking between the 9 and 24 hour time points.

tumour cells collected while the patient was platinum-naïve.

## 4. Discussion

The results from the immunocytochemical analysis of primary culture samples suggest a consistently high level of sample purity. Results using this technique estimated 80% and greater purity in tumour cell cultures, and over 95% purity in mesothelial cell cultures.

The results show that the formation of cisplatin ICL is similar in all of the clinical samples, both tumour cells and normal cells (mesothelial). The peak of crosslinking occurred approximately 9 hours after cisplatin exposure. Figures 2.9 and 2.10 indicate that a direct comparison of cisplatin ICL formation by all of the tumour cells (from 'untreated' and 'treated' patients), and a comparison of the 11 patients samples which yielded both mesothelial and tumour samples, indicate similar ICL formation. The similarity in ICL formation provides evidence against a functioning upstream resistance mechanism in any of the tumour samples. This is with the possible exception of patient 17, whose tumour cells showed 59.7% ± 14.98 ICL at 9 hours, compared to 75.5% ± 8.95 in the mesothelial sample (Figure 2.8). Upstream resistance mechanisms, including glutathione conjugation and detoxification or reduced uptake of drug, therefore did not occur either as an inherent characteristic, which would have been implicated by a significant reduction in ICL formation in platinum-naïve tumour cells, especially in comparison to mesothelial cells, or as an acquired characteristic, following a patients exposure to platinum-based chemotherapy. This is significant as many cell line based studies have recorded reduced ICL formation following cisplatin exposure in cancer cell lines that have been made resistant through continuous cisplatin exposure over time (Hospers *et al.* 1988, Bungo *et al.* 1990, Bedford *et al.* 1987, Fram *et al.* 1990, Esaki *et al.* 1996, Perego *et al.* 1999, Johnson *et al.* 1994a, Zhen *et al.* 1992). These model systems often correlate resistance with elevated glutathione, and/or glutathione S-transferase and metallothionein (Hamilton *et al.* 1985, Godwin *et al.* 1992, Hamaguchi *et al.* 1993, Kudoh *et al.* 1994, Shellard *et al.* 1991, Saburi *et al.* 1989, Okuyama *et al.* 1994, Perego *et al.* 1998).

Using clinical samples, Nishimura *et al.* (1996) and Shiga *et al.* (1999) correlated elevated GSTπ expression with poor response to platinum based chemotherapy in head and neck carcinomas, and expression of this isotype was particularly prevalent in relapsed tumours. Mayr *et al.* (2000) correlated high GSTπ expression and clinical response to chemotherapy using 213 paraffin-embedded samples of ovarian cancer. Measuring GSTπ levels in ovarian cyst fluid, Boss *et al.* (2001) correlated higher GSTπ levels with the worse prognostic factors. In the sub-group of patients that received platinum-based chemotherapy, significantly higher GSTπ concentrations occurred in patients with recurrence, compared to patients without recurrence (Boss *et al.* 2001). The relationship between elevated GSTπ expression in ovarian tumour samples and poor response to platinum-chemotherapy has been confirmed by several other research groups (Kigawa *et al.* 1998, Hirazono *et al.* 1995 and Cheng *et al.* 1997). Investigations into GSH expression in clinical samples from ovarian cancer patients, has revealed a correlation between previous platinum exposure and elevated GSH expression (Lewandowicz *et al.* 2002, Cheng *et al.* 1997). However, Murphy *et al.* (1992), Wrigley *et al.* (1996) and van der Zee *et al.* (1992) all failed to correlate GST expression with the response of ovarian cancer patients to platinum-containing chemotherapy. The evidence provided in this chapter argues against any upstream resistance mechanisms functioning in the clinical samples.

The resolution of ICL involves a multi-step repair process, including the detection of the damage, the unhooking of one arm of the crosslink, followed by the removal of the second arm, and synthesis and re-ligation (Cole *et al.* 1973, Dronkert *et al.* 2001, McHugh *et al.* 2001). The decrease in ICL detected using the comet assay represents the initial unhooking of one arm of the crosslink, whether or not the lesion is then effectively processed beyond this point is not indicated using this technique.

The most striking observation produced by this work was the fact that most of the tumour samples from patients previously exposed to platinum-based chemotherapy (cisplatin/carboplatin) exhibited an enhanced ability to unhook cisplatin interstrand crosslinks, when compared to tumour cells from platinum-naive patients ($p=0.04$) (Figures 2.11 and 2.13), and to mesothelial cells from both patient groups (Figure 2.12).

A comparison of the 11 patients samples which yielded both mesothelial and tumour samples, echoed this result, with 'treated' tumour cells unhooking 44.6% of ICLs, and untreated tumour cells unhooking 25.2% of ICLs by the 24 hour time point (Figure 2.12). However, statistical analysis (t-test) suggested that this was not a significant result (p=0.42). The large variation in results, in both data sets, ranging from <-5% and >80% ICL unhooking could explain the relatively high p value. The low sample number involved in the comparison of paired samples (5 untreated patient samples, compared with 6 treated samples) might explain the difference in ICL processing observed between the untreated and treated mesothelial samples. Further research with a larger sample number would be needed to support or contradict this result.

In one case, patient 3, tumour samples were obtained before exposure to platinum chemotherapy; and after three cycles of treatment at the time of interval debulking surgery. The untreated tumour sample was obtained from ascites, and the treated tumour sample from a single cell suspension following dissection of primary tumour collected at laparotomy. The purpose of the combination of chemotherapy and interval debulking is to first eliminate the platinum sensitive tumour, then to surgically remove any refractory tissue that remains. This would suggest that any viable tumour cells harvested during the interval debulking surgery would be less sensitive to platinum therapy. This patient provides a unique opportunity within this study to measure the response of ovarian tumour cells to platinum treatment *in-vivo*. No difference was seen in ICL formation by the tumour cells from the two samples (Figure 2.13). A major difference was, however, observed in ICL unhooking after the 9-hour time point, with an 80% difference in ICL repair capability between the two samples. Results examining ICL formation and repair in patient 3 mirror the overall results for all of the 19 patient samples, i.e. a greater tendency towards enhanced ICL repair following a patient's previous platinum treatment.

It is possible that there is an active selection of tumour cells with the enhanced ability to unhook platinum-ICLs following cisplatin/carboplatin exposure. In this model the process of selection would occur at the time of platinum exposure, which is prolonged for approximately four and a half months, while a patient undergoes six cycles of carboplatin at three weekly intervals. As the selection pressure was

removed the tumour cells that had survived the chemical exposure, either through adapted or inherent characteristics, would then slowly repopulate to the point of clinically recognized relapse/progression. This model would explain why cells with these characteristics occur more frequently in relapse tumour tissue.

Romanet *et al.* (1999) investigated platinum ICL unhooking using the comet assay. They reported a relationship between platinum-ICL repair in lymphocytes from patients with head and neck squamous cell carcinoma (HNSCC) undergoing combination chemotherapy, and tumour response. They concluded that clinical resistance to platinum drugs was attributable to enhanced DNA repair. Ali-Osman *et al.* (1995) investigated cells taken from 6 human gliomas, they correlated enhanced repair of cisplatin-induced ICL, measured using the ethidium bromide assay, with platinum resistance. Similar work was carried out examining melphalan ICL repair in multiple myeloma, using the same modified comet assay used in this study (Spanswick *et al.* 2002). They reported similar levels of ICL formation, and clearly enhanced ICL repair by the plasma cells of patients previously exposed to melphalan, compared to the cells from melphalan-naïve patients. Souliotis *et al.* (2003) examined gene specific melphalan ICL formation and repair in p53 and N-ras following *in-vitro* exposure, again using peripheral lymphocytes from multiple myeloma patients. Out of the seven patients samples examined, the three patients whose lymphocytes showed the least ICL damage (represented by the area under the curve, over time) did not respond to treatment with high-dose melphalan.

In order to examine the relationship between the cellular processing of the cisplatin ICL by ovarian tumour cells *ex-vivo*, and a patient's clinical response to platinum based chemotherapy it was essential to attempt to classify patient responses to platinum. This task was complicated by the variety of starting points of each patient, i.e. what stage in their cancer progression the sample was collected. The difference in treatment regimes also complicated analysis. For example, it was difficult to assess the impact of one treatment strategy on a patient, when several have been deployed, for example interval debulking surgery and combination chemotherapy. Each complicating factor made it harder to ascertain the impact of the platinum alone on the progression of the cancer. Markman *et al.* (1991) stated that if a patient had been treated with platinum-based chemotherapy (cisplatin or carboplatin) and relapsed

within six months of completion, they could be categorized as being clinically platinum resistant. If relapse occurred after six months then the patient at that time would be defined as platinum sensitive (Markman *et al.* 1991). Within this study, the criteria for defining a patient's relapse included, symptomatic evidence of disease progression, a doubling of Ca125 level or evidence from comparative CT scans.

In order to analyse the clinical response of patients to platinum several parameters were applied to their clinical histories. Two categories were used, the platinum-free interval (PFI), and the progression- free survival (PFS) interval. Where patients had been previously treated with platinum, the length of their platinum-free interval following the completion of therapy, before relapse, was measured. The progression-free survival from the time of progression and sample collection, to relapse for each of the patients was also measured. These data are presented, alongside the % cisplatin-ICL unhooking data, and information of any previous patient exposure to platinum chemotherapy, in Table 2.2.

Patients 7, 11 and 12 had each previously been treated with platinum. Following the completion of their platinum chemotherapy these patients each progressed within 6 months. According to the Markman definition, these patients were described as being clinically platinum-resistant. When % ICL unhooking was analysed in the tumour samples from these patients the results were 19.5%, 76.9% and 23.5% for patients 7,11 and 12, respectively. There appears to be a lack of correlation between the ICL unhooking capability of tumour samples and the fact that these patients were defined as being clinically resistant to platinum.

Patient 14 received carboplatin in combination with paclitaxel and patient 17 was treated with carboplatin monotherapy. Both patients' tumours showed clinical progression during early platinum treatment, in the form of the accumulation of ascites and increasing Ca125 levels. The % ICL unhooking data for these patients were 12.7% and 37%, for 14 and 17, respectively. These patient's tumours appeared to be intrinsically refractory to platinum treatment, and their ICL unhooking capabilities were relatively low. Interestingly, Patient 14 eventually died two years after diagnosis, despite exhibiting primary platinum resistance. Again there appears to be a lack of correlation between clinical resistance to platinum and ICL unhooking

| Patient Number | History of previous treatment with platinum | % Cisplatin ICL unhooking | Category | Platinum Free Interval (PFI) (months) | Progression Free Survival (PFS) (months) |
|---|---|---|---|---|---|
| 2 | Untreated | 40.3 | New | - | >55 |
| 5 | Untreated | 82.7 | New | - | 9 |
| 6 | Untreated | 4 | New | - | 20 |
| 8 | Untreated | 6 | New | - | Died |
| 9 | Untreated | 0 | New | - | >54 |
| 10 | Untreated | 4.9 | New | - | 12 |
| 13 | Untreated | 7.4 | New | - | 17 |
| 18 | Untreated | 0 | New | - | 10 |
| | | | | | |
| 3 | | 0 and 73.6 | IDS | - | 15 |
| 16 | | 81.2 | IDS | - | >36 |
| | | | | | |
| 1 | Treated | 94.1 | >6 months | 24 | 5 |
| 4 | Treated | 56.2 | >6 months | 27 | 9 |
| 15 | Treated | 0 | >6 months | 10 | - |
| | | | | | |
| 7 | Treated | 19.5 | <6 months | 6 | 11 |
| 11 | Treated | 76.9 | <6 months | 4 | 4 |
| 12 | Treated | 23.5 | <6 months | 2 | 0 |
| 14 | Treated | 12.7 | <6 months | 0 | - |
| 17 | Treated | 37 | <6 months | 0 | Died |

Table 2.2. Clinical Information Regarding Patients' Clinical Response to Platinum Therapy.

Within Table 2.2 platinum-free interval (PFI) (if previously exposed) describes the time in months from the completion of previous platinum treatment to relapse. Progression-free survival (PFS) describes the time interval in months from progression and sample collection to relapse. Within the 'Category' column, 'New' indicates untreated patients, IDS indicates that the patients were undergoing IDS during their first treatment with platinum chemotherapy, >6 indicates a PFI of more than 6 months, and <6 indicates a PFI of less than 6 months. For patient 3, tumour samples were collected before platinum exposure, and during IDS. - indicates not applicable. Patient 8 died a few days after her first cycle of platinum therapy, so PFS not assessable. Patient 17 never responded to her last chemotherapeutic regime (single agent carboplatin) dying soon after completion, so PFS not assessable.

capability. Patients 1 and 4 were each previously treated with platinum chemotherapy, their platinum-free intervals were 24 and 27 months, respectively. Their tumour samples unhooked 94.1% and 56.2% of cisplatin-induced ICLs, respectively. Their progression-free survival intervals were 5 and 9 months, respectively.

Interestingly, one of the patients in the study was diagnosed with clear cell carcinoma of the ovary, patient 16. The % ICL unhooking for the tumour sample from this patient was very high at 81.2% unhooking. Clear cell ovarian tumours are clinically resistant to platinum, and respond poorly to platinum-containing chemotherapeutic regimes (Sugiyama *et al.* 2000). However, the PFS for this patient was >36 months as the patient remains in remission following carboplatin and paclitaxel combination chemotherapy and interval debulking surgery. Interestingly, the tumour sample from this patient was removed at interval debulking surgery. As discussed, it could be argued that viable tumour tissue remaining following several doses of platinum-chemotherapy, is actually relatively resistant, and that therefore by collecting a sample during interval debulking surgery we are actually selecting the platinum-resistant sub-population of cells.

When the % ICL unhooking of the other tumour sample collected at interval debulking surgery is considered, it was approximately 73.6% by tumour cells from patient 3. Interestingly the ICL unhooking capability of tumour cells from this patient collected before platinum-exposure was 0. It could therefore be that collecting tumour samples at interval debulking surgery (IDS) is providing intrinsically resistant tissue, the ICL unhooking data from which is not representative of the general ICL unhooking capability of the heterogeneous tumour population from that patient overall. In spite of the high ICL unhooking capability of the tumour cells from patient 3 collected at IDS, the PFS for this patient was 15 months.

Two tumour samples from previously untreated patients showed relatively high ICL unhooking capabilities. Tumour samples from patients 2 and 5 unhooked approximately 40.3% and 82.7% of cisplatin induced ICLs, respectively. When the progression free survival for these patients were considered, i.e. the length of time from diagnosis to relapse, the PFS for patient 2 was >55 months, as the patient

remained in remission, and the PFS for patient 5 was nine months. Interestingly, patient 5 died two months after relapse, with brain metastases, indicating that this patient was suffering from very aggressive disease.

Interestingly, six untreated patients tumour samples showed ICL unhooking values of between 0 and 7.5%, and correspondingly had PFS ranging from 10 months to >54 months. These patients were 3, 6, 9, 10, 13 and 18. Therefore, in this case, patients with tumours that were generally poor at unhooking platinum-ICLs had long PFS intervals. However, it should be noted that Patient 9 had a borderline tumour;- this type of ovarian tumour is less aggressive then other types of ovarian tumour, with a better prognosis. The survival rate 5 years after diagnosis for serous and mucinous borderline ovarian tumours is approximately 97% (Cadron *et al.* 2006).

Of the remaining patients, patient 8 died shortly after her first dose of platinum-chemotherapy, therefore this patient's response to platinum therapy could not be assessed. Patient 15 provided a sample having already been treated with platinum-based chemotherapy. Interestingly, the tumour sample from this patient was the only sample from 'treated' patients to show no cisplatin ICL unhooking between the 9 and 24-hour time-points. There was in fact, an increase in interstrand crosslinking between these two time-points, which is reflected in the negative value in Figure 11 for this patient's sample. Patient 15 was treated with carboplatin and paclitaxel, and suffered a relapse 18 months later, she was treated with three doses of carboplatin, but developed an allergic reaction, she was subsequently treated with 6 doses of topotecan and then tamoxifen, her platinum-free interval (PFI) was 10 months. Our sample was collected following this second relapse. As this patient was suffering from very poor renal function she was not retreated with platinum. Her platinum was stopped not because of resistance, but due to allergy, so her clinical response to platinum cannot be classified. This patient could have been platinum sensitive at the time that our sample was collected.

Attempting to examine the possible relationship between cisplatin-ICL unhooking *ex-vivo* and a patient's clinical response to platinum has been complicated. Each patient has been treated with a variety of additional chemotherapeutic agents, and the level of surgical intervention also varied between patients. There was a significant level of

heterogeneity between % ICL repair and a patient's PFI/PFS.

While the research presented within this chapter does not allow us to identify a relationship between tumour cisplatin-ICL unhooking capability and clinical response to platinum, we did identify a direct correlation between a patient's previous exposure to platinum-chemotherapy and enhanced cisplatin-ICL unhooking. Further research using a strict entrance-criteria that would eliminate some of the many inter-patient variables would be necessary to further examine the relationship between ICL unhooking and patient survival.

## Chapter 3: DNA Interstrand Crosslink Formation and Unhooking in Human Ovarian Cancer Cell Lines.

### 3.1. Introduction

Human cancer cell lines, produced from cancer patients, provide an essential research resource. These lines are valuable for several reasons. Firstly they provide an almost limitless cell number, facilitating repetition of experiments using the same starting material. Cell lines also provide a uniformity whereby research groups around the world can investigate the same cell lines, and therefore build up a comprehensive understanding of the characteristics and behaviour of a single cell type. Cell lines have been used extensively to study mechanisms of resistance to cancer chemotherapeutics. Acquired resistant cell lines are produced by treating cells with increasing concentrations of drug *in-vitro*. Resistant cell lines are described as having stable or transient resistance, according to whether or not the drug of interest has to be present in the tissue culture media of the cells to maintain the resistant phenotype. Paired parental sensitive and resistant cancer cell lines have been extensively investigated to learn more about the cellular pathways involved in acquired cancer drug resistance.

The aim of the research contained in this thesis was to investigate the mechanism of clinical platinum resistance in ovarian cancer. Two paired human ovarian cancer cell lines were chosen as a relevant *in-vitro* model; A2780, a cell line produced from a chemo-naïve patient, and A2780cisR, a stably resistant sub-line derived from A2780 following stepwise increased exposure to cisplatin (Behrens *et al.* 1987). A2780 and A2780cisR have been investigated by several different research groups. When A2780cisR was originally described (as $2780^{CP8}$), elevated glutathione was recorded in A2780cisR in comparison with A2780 (Behrens *et al.* 1987). Pretreatment of A2780cisR cells with L-Buthionine sulfoximine (BSO) resulted in reduced cisplatin resistance, while it had little affect on A2780 cells (Perez *et al.* 2001 and Jansen *et al.* 2002). Approximately 2.4-fold reduced intracellular cisplatin accumulation has also been reported in cisplatin treated A2780cisR cells compared to A2780 cells (Holford *et al.* 1998).

Interestingly, Masuda *et al.* (1988) used a [$^3$H] thymidine incorporation assay to detect a two-fold increased overall repair ability in A2780cisR compared to A2780, following cisplatin exposure. Using the same technique Behrens *et al.* (1987) described A2780 cells as having 'essentailly no repair capacity' to repair cisplatin induced damage. Treatment of A2780cisR (known as 2780CP) with aphidicolin, a specific inhibitor of DNA polymerase α, resulted in a three-fold increase in cisplatin sensitivity in A2780cisR, with no effect on A2780 sensitivity (Masuda *et al.* 1988). Colella *et al.* (2001) used these cell lines to assess the level of DNA damage in the N-*ras* gene immediately following a five-hour exposure to the cisplatin $IC_{50}$ dose, and 6, 24 and 48 hours later. Using a quantitative PCR method this group reported similar levels of adduct accumulation and repair in both A2780 and A2780cisR (known as A2780cp8), with both types of cell capable of repairing over half of the lesions. As intrastrand lesions constitute approximately 90% of cisplatin induced DNA adducts (Fichtinger-Schepman *et al.* 1985 and 1987) this technique would have predominantly assessed the ability of these cell lines to repair intrastrand crosslinks. Interestingly this group also reported no difference in ERCC1 mRNA expression, or protein level between the two cell lines. Colella *et al.* (2001) also reported that A2780cisR cells lacked the mismatch repair (MMR) proteins hMLH1 and hPMS2, compared to A2780 cells which expressed both proteins.

Overall, these findings suggest that reduced intracellular platinum accumulation, reduced mismatch repair (MMR), elevated GSH and increased platinum-DNA adduct repair could all contribute towards the cisplatin resistant phenotype of A2780cisR, compared to the parental A2780 cells.

To date there has been no systematic investigation into ICL formation and repair using both A2780 and A2780cisR. Holford *et al.* (1998) used alkaline elution to measure cisplatin ICL over time in A2780 following a two-hour drug treatment with five times the $IC_{50}$ (28.5μM). The peak of crosslinking was found to occur five hours after exposure. Interestingly, most of the crosslinks were rapidly repaired by the 24-hour time point. Alkaline elution was also used to measure cisplatin ICL formation at increasing dose in A2780cisR (Perez *et al.* 2001), but repair of ICLs was not examined, and no comparison with A2780 was published.

In this chapter DNA ICL formation and unhooking are studied in the A2780 and A2780cisR cell lines following cisplatin treatment using the comet assay. Mechlorethamine sensitivity and ICL formation and unhooking over time, and UVC sensitivity are also investigated using the same paired cell lines.

Interstrand crosslinks account for up to 5% of mechlorethamine-induced DNA adducts, and are thought to be the cytotoxic lesion (Dronkert and Kanaar, 2001, Hansson *et al.* 1987). Although the details of the repair of this lesion are still to be fully elucidated, the mechanism is known to involve the action of the ERCC1-XPF heterodimer, and homologous recombination (DeSilva *et al.* 2000). UVC exposure leads to the formation of bulky DNA-adducts, namely cyclobutane pyrimidine dimers and (6-4) photoproducts (Thoma, 1999). These lesions are repaired by the nucleotide excision repair (NER) pathway (Aboussekhra *et al.* 1995, Batty *et al.* 2000) which is involved in the recognition and repair of cisplatin-induced intrastrand crosslinks (Huang *et al.* 1994, Moggs *et al.* 1996 and 1997, Araujo *et al.* 2000). By analysing the responses of A2780 and A2780cisR cells to both of these agents, the relative role of specific repair pathways in the resistance mechanism observed in the A2780cisR cells can be evaluated.

## 3.2. Methods

Unless otherwise stated all reagents were purchased from Sigma (St Louis, MO, USA), and all tissue culture plastics were purchased from VWR International (Poole, UK).

### 3.2.1. Cell Lines

The human ovarian cancer cell lines A2780 and A2780cisR were kindly provided by Professor Lloyd Kelland, Institute of Cancer Research, London, UK. The A2780 human ovarian cancer cell line was initially developed from tissue collected from an untreated patient (Louie *et al.* 1985). A2780cisR was developed by exposure of A2780 cells to stepwise-increasing concentrations of cisplatin. Initially, A2780 cells were exposed to 3nM cisplatin three times for three-day periods during a three to six week period. The dose was then doubled and the procedure was repeated until the

cells survived exposure to 8μM cisplatin. This process was reported in Behrens *et al.* (1987) and the cell line was initially called $2780^{CP8}$, later being referred to as A2780cisR by Professor Lloyd Kelland (Confirmed through personal communication with Professor Kelland, Antisoma, London, UK) (Kelland *et al.* 1993).

A2780 and A2780cisR were grown in Dulbecco's Modified Eagle's Medium (DMEM) tissue culture media containing 10% fetal calf serum (FCS) and 2mM glutamine (all of which were purchased from Autogen Bioclear UK Ltd. (Wiltshire, UK)). All cells were grown at 37°C in a 5% $CO_2$ incubator.

Cells were routinely check for mycoplasma contamination. Only mycoplasma-free cells were used. Cells were discarded after twenty doubling times, and fresh stocks were thawed from liquid nitrogen storage and grown. Frozen stocks were maintained in liquid nitrogen, frozen in fetal calf serum containing 10% dimethylsulfoxide (DMSO).

3.2.2. Calculation of Doubling Times of the A2780 and A2780cisR Cell Lines.

Exponentially growing A2780 and A2780cisR cells in 80cm$^2$ tissue culture flasks were trypsinised using the following protocol. Tissue culture flasks of monolayer cells were placed in a category II tissue culture hood, and the tissue culture media was removed and discarded by tipping the flask and pipetting off the entire volume with a sterile 25ml pipette. 10mls of warmed trypsin were added to the flask and brought in contact with the cells by levelling the flask, and gently swirling the volume over the monolayer. The flask was viewed using a light microscope (Nikon), in order to observe the rounding up and detachment of the cells from the plastic growing surface. When all of the cells had detached, the flask was returned to the hood, and 10mls of warmed DMEM (with 10% FCS and 2mM glutamine) were added to the trypsin. The DMEM was washed against the growing surface using a sterile 25ml pipette. The mixture was pipetted up and down to encourage a single cell suspension, then transferred into a 50ml sterile plastic tube and centrifuged at 200xg for 5 minutes. The tube was returned to the sterile conditions and the supernatant was discarded using a sterile 25ml pipette. The pellet was resuspended in 10mls of warmed DMEM (with 10% FCS and 2mM glutamine) and mixed by

pipetting up and down in a 10ml pipette. A small quantity of the suspension was pipetted into a sterile 7ml tube and removed from the tissue culture hood to the microscope. A glass Pasteur pipette (Volac) was used to mix the suspension in the tube by pipetting up and down, and a small quantity of the suspension was pipetted gently against the side of a coverslip on a haemocytometer. When the suspension filled the area under the coverslip the haemocytometer was observed under a light microscope, and the cell density was measured by counting the cells in all nine squares of the visible grid, and then dividing by nine. This figure was used to estimate the cell number (by $10^4$cells/ml). A cell density of $2x10^4$ cells/ml was produced by diluting the appropriate volume of the cell stock with warmed DMEM (containing FCS and glutamine), in a 80cm$^2$ tissue culture flask. 10mls of the $2x10^4$ cells/ml mixture was pipetted into ten 25cm$^2$ tissue culture flasks. These were then placed in to the 37°C, 5% $CO_2$ incubator. At the same time for ten consecutive days a single flask for each cell line was removed from the incubator and trypsinised, and the cell number was counted, using the above protocol. After 10 days the cell number for each cell line was plotted against time (in hours) on a log scale.

### 3.2.3. The SRB Growth Inhibition Assay

#### 3.2.3.1. Preparation of Monolayer Cells

Cytotoxicity was assessed using the sulforhodamine B assay (SRB) that measures the cellular protein content (Skehan *et al.* 1990). Monolayers of exponentially growing A2780 and A2780cisR cells were placed in a tissue culture hood, and tissue culture media was removed from each 80cm$^2$ flask, using a 25ml sterile pipette. 10mls of warmed trypsin was added to each flask, using a separate 10ml pipette. Flasks were replaced horizontally into the incubator for 5 minutes, or until all of the cells had become detached (assessed using a light microscope). Flasks were placed into the tissue culture hood, and 10mls of DMEM (with 10% FCS and 2mM glutamine) was added to the trypsin/cell suspension. Each suspension was pipetted up and down using a sterile 25ml pipette to ensure a single cell suspension. The total volume of 20mls for each cell type was added to a separate 50ml conical plastic tube and centrifuged at 200xg for 5 minutes. After this time, the tubes were replaced in the tissue culture hood, and the supernatant was removed and discarded using separate

25ml pipettes. Each cell pellet was separately resuspended using 10ml of DMEM (with 10% FCS and 2mM glutamine), and pipetted up and down using a sterile pipette to produce a single cell suspension. Cell density was estimated using a haemocytometer, as described previously (Section 3.2.2). Once the cell density was known for each cell line, a density of $3x10^4$cells/ml was produced in DMEM (with 10% FCS and 2mM glutamine). Cell suspensions at a density of $3x10^4$ cells/ml were plated into 96-well plates. 100µl of suspension was added to a row of 6 wells per dose, with a minimum of 12 control (treatment free) wells. A multi-pipette was used to pipette the cell suspension into 6 wells at a time, using sterile 200µl pipette tips.

Once the lids were replaced on the 96-well plates, and they were labelled, they were put into a plastic box, which contained two reservoirs of $dH_2O$ to prevent drying out. These were then replaced in the incubator (37°C, 5% $CO_2$) and left overnight to attach.

3.2.3.2. Treatment of Cell Lines with Cytotoxic Agents.

3.2.3.2.1. Cisplatin and Mechlorethamine

Drug dilutions were prepared just prior to use. Cisplatin was purchased from David Bull Laboratories (Australia) (100mg/100ml injectable aqueous stock solution containing 900mg/100ml sodium chloride and 100mg/100ml mannitol) at a dose of 3.33mM. For each experiment into cisplatin cytotoxicity the following doses of drug were tested; 0.03, 0.1, 0.3, 1, 3, 10, 30, 100µM. These were produced by making 4 stock solutions of cisplatin; 3.33mM, 333µM, 33.3µM and 3.33µM, by simply diluting the original stock solution 1 in 10 sequentially three times. All dilutions were carried out using DMEM (free of FCS and glutamine). Once the stocks were produced, 18µl and 60µl of each stock was added to 2ml of DMEM (minus 18 and 60µl where appropriate). This produced the listed concentrations. Six wells were treated with each dose for each experiment.

Mechlorethamine (HN2) was purchased from Sigma. For each experiment into mechlorethamine cytotoxicity the following doses were used; 0.001, 0.01, 0.1, 1, 10, 100µM. The mechlorethamine powder was carefully transferred and weighed using a

fume hood and a designated cytotoxics balance. Powder was dissolved with DMEM (without FCS or glutamine) to produce a stock solution of 1mM, which was sequentially diluted to produce the correct doses.

For cisplatin and mechlorethamine drug treatments, 96-well plates that had been seeded with cells the night before, were removed from the incubator. The plates were placed into a tissue culture hood and the supernatant was carefully removed from each well using a multi-channel pipette. 200µl of drug solution was added to each of the designated 6 wells using a p1000 Gilson pipette and sterile tips. 200µl of DMEM (without FCS or glutamine) was added to each of the control wells in the same way. Lids were replaced onto each plate, and plates were placed in the 37°C incubator for one hour. After the one-hour drug treatment, plates were replaced in the tissue culture hood, and drug solution was removed by hand, using a p1000 Gilson pipette and a separate sterile tip for each drug dilution. Once this was complete, 200µl of warm DMEM (with 10% FCS and 2mM glutamine) was added to each well using a multi-channel pipette. Lids were replaced on each plate, and plates were returned to the incubator.

Cisplatin and mechlorethamine were handled and disposed of in strict accordance with University Health and Safety protocol.

3.2.3.2.2. UVC

Care was taken to use the appropriate safety goggles when using UVC light sources.

For treatment with UVC, cells were illuminated from above using a UV 254nm lamp, model UVG-11, (UV products, Inc. San Gabriel CA, USA) which was fixed 23cm above the samples, thereby administering a dose of 0.5 $w/m^2$. A two second exposure corresponded to a dose of $1Jm^{-2}$. The following exposure times were used: 0, 2, 6, 18, 36, 60 seconds, delivering the following doses, 0, 1, 3, 9, 18 and 30 $Jm^{-2}$, respectively. 96-well plates that had been seeded the day before, were placed into a tissue culture hood, and the DMEM was removed from each well using a multi-channel pipette. 200µl of sterile phosphate buffered saline (PBS) was added to each well, using a multi-channel pipette. Lids were replaced onto each plate, and the

plates were transferred to the hood with the UVC light source. Each set of 6 wells was exposed to UVC for different time periods, to induce varying UVC doses. Non-treated control wells were constantly covered over to prevent UVC exposure. When each plate had been exposed to varying doses of UVC, the lids were replaced and plates were transferred to a tissue culture hood, where PBS was removed from each well, and replaced with 200µl DMEM (with 10% FCS and 2mM glutamine), using a multi-channel pipette. Lids were replaced on to each plate and they were returned to the incubator.

3.2.3.3. Post-Treatment Incubation and Analysis

Following a 72-hour post-treatment incubation (approximately three doubling times) the final stage of the assay was completed. This involved replacing the tissue culture media in each well with 100µl of ice-cold 10% (wt/vol) trichloroacetic acid, using a multi-channel pipette, on the bench (non-sterile conditions). Lids were replaced and plates were placed at 4°C for 20 minutes. Plates were then washed gently with tap water, four times per plate. 100µl of staining solution (0.4% wt/vol) SRB in 1% acetic acid) was added to each well using a multi-channel pipette. Plates were left to stain for 20 minutes at room temperature. Unbound stain was removed by thoroughly washing each plate six times with 1% acetic acid (in $dH_20$). Plates were left to dry overnight on the bench, with their lids off. For analysis the stain was solubilised by adding 100µl of 10mM Tris base to each well using a multi-channel pipette. After twenty minutes the solution in each well was mixed using a multi-channel pipette and p200 tips. The optical density (O.D) at 540nm was measured per well using a Titertek multiscan (MCC/340) microtitre plate reader. The percentage growth inhibition was calculated by dividing the mean O.D. of the treated wells by the mean O.D. of the non-treated control wells. Experiments were carried out a minimum of three times per cytotoxic agent.

3.2.4. The Comet Assay

The single cell gel electrophoresis 'comet'assay was used to measure DNA interstrand crosslinking. This technique involved mechlorethamine, cisplatin,

propidium iodide and X-rays, each requiring special safety precautions in accordance with University's Health and Safety policy.

3.2.4.1. Preparation of Monolayer Cells

Exponentially growing monolayer cells were trysinised and counted using the protocol described in Section 3.2.2. A cell density of $5x10^4$cells/ml was produced for each cell line. Cells were drug treated in six-well plates. Therefore 2.5mls of the $5x10^4$ cells/ml suspension were seeded into the appropriate number of wells per six-well plate, according to the specific experiment, with different experiments requiring a different number of wells to be used per plate. Cells were left to adhere overnight and drug treated the next day.

3.2.4.2. Drug Treatment of Monolayer Cells

Drug dilutions were prepared just prior to use. For the observation of cisplatin ICL at increasing doses, cells were drug treated for one hour using the following doses; 0, 25, 50, 75, 100 and 200μM. Cells were incubated for six-hours after exposure. For the observation of cisplatin ICL over time following a one-hour drug treatment with 100μM, samples were collected at the following time points; 0, 3, 6, 9, 12, 18, 24 and 48 hours. For the observation of mechlorethamine ICL at increasing doses, cells were drug-treated for one hour using the following doses; 0, 1, 5, 10μM, and collected immediately after treatment. For the observation of mechlorethamine ICL over time following a one-hour drug treatment with 1.5μM, samples were collected at the following time points; 0, 4, 8, 24 and 48 hours.

Cells were drug treated in 6-well plates in sterile conditions by pipetting off the tissue culture medium from the wells of each 6-well plate, using a 10ml pipette and tipping the plate slightly. 2.5ml of the appropriate drug dilution (in warm DMEM without FCS or glutamine) was pipetted into the appropriate wells on each plate. 2.5mls of DMEM (minus Glutamine and FCS) without drug was pipetted into the non-drug treated control well. The lids were replaced on the 6-well plates and they were placed in the tissue culture incubators at 37°C in a humidified atmosphere with 5% $CO_2$.

After one hour, the plates were placed back in the tissue culture hood, and separate 10ml pipettes were used to aspirate and remove the drug solution from each well, again tilting the plates at an angle to facilitate efficient removal of the highest volume possible.

Fresh DMEM (containing 2mM glutamine and 10% FCS, warmed to 37°C) was added to each of the wells containing cells, and the plates were replaced in the incubator. At the appropriate time, DMEM was replaced with 2.5ml of warmed trypsin pipetted into each of the wells, and left to detach the cells. After successful trypsinisation (assessed using a light microscope), 2.5mls of DMEM containing 10% FCS and 2mM glutamine, at 37°C, were added per well. The total volume of 5mls (from each well) was pipetted into a separate labelled 10ml plastic tube. Tubes were placed into the centrifuge and spun at 200xg for five minutes, at room temperature. The tubes were replaced into the tissue culture hood, and the supernatant was removed and discarded using separate sterile 10ml pipettes. 1.5mls of a freezing mix of FCS and 10% dimethylsulphoxide (DMSO) at 4°C, was used to resuspend the cell pellets. This mixture was transferred into a labelled eppendorfs, on ice. When all of the samples were prepared they were quickly placed into a lidded polystyrene box within the -80°C freezer.

3.2.4.3. The Comet Assay

As described in the methods section of Chapter 2.

## 3.3. Results

### 3.3.1. Doubling Times of A2780 and A2780cisR Cells

As stated, A2780 and A2780cisR cells were seeded and grown at a density of $2x10^4$cells/ml, and cell number was measured at the same time each day, for 10 days. Figure 3.1 represents the growth rates of each cell line. A2780 cells had an approximate doubling time of 16.1 hours and A2780cisR cells had an approximate doubling time of 15.1 hours, during the exponential growth phase.

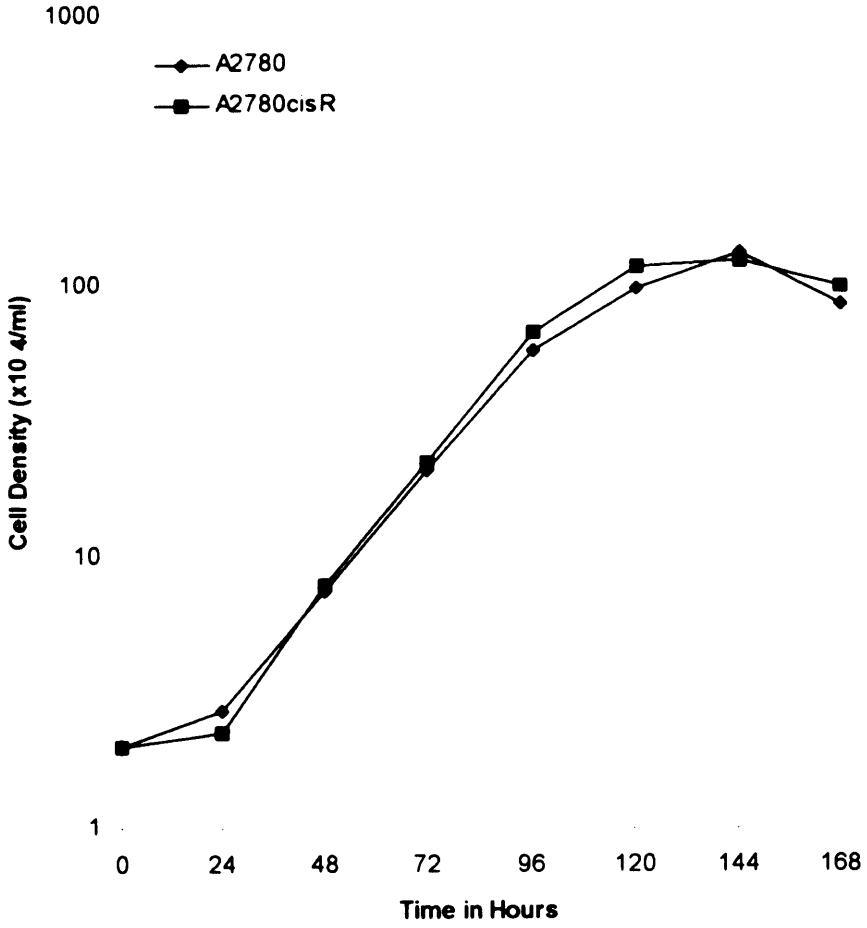


Figure 3.1. Growth curves for A2780 and A2780cisR cells.

### 3.3.2. Cisplatin

#### 3.3.2.1. Cytotoxicity

Cisplatin sensitivity was measured in each cell line using the SRB assay. Figure 3.2 presents the % growth inhibition induced by increasing doses of cisplatin, from 0.1-100μM.

The $IC_{50}$ values for A2780 and A2780cisR were 6.1μM ± 0.89 and 22.6μM ± 3.27, respectively. Clearly A2780cisR is more resistant to cisplatin exposure than the parental cell line A2780, with a 3.7-fold resistance under the conditions employed.

#### 3.3.2.2. Measurement of ICL at Increasing Dose

Cisplatin-induced ICL were measured at increasing doses from 0-200μM using the comet assay. Cells were incubated with cisplatin for one hour, and crosslinks measured six hours later. The % decrease in tail moment values at increasing doses of cisplatin are represented in Figure 3.3.

The level of interstrand crosslinking increased with cisplatin dose in both cell lines. At the 25μM dose both cell lines showed similar crosslink formation. Between 25μM and 100μM doses, crosslink formation by the cell lines appears to differ with a lower number of crosslinks forming in the A2780 cell line, however, at the 100 and 200μM doses the level of crosslinking in response to cisplatin in both cell lines was very similar. A dose of 100μM cisplatin produced approximately 50% decrease in tail moment six hours after cisplatin exposure, in both cell lines. This dose was chosen to measure cisplatin ICL over time in subsequent experiments.

#### 3.3.2.3. Measurement of ICL Over Time

A2780 and A2780cisR cells were treated with 100μM cisplatin for one hour and ICLs were measured 0, 3, 6, 9, 12, 18, 24 and 48 hours after exposure. Figure 3.4 represents the % decrease in tail moment over time in both cell lines following drug treatment.

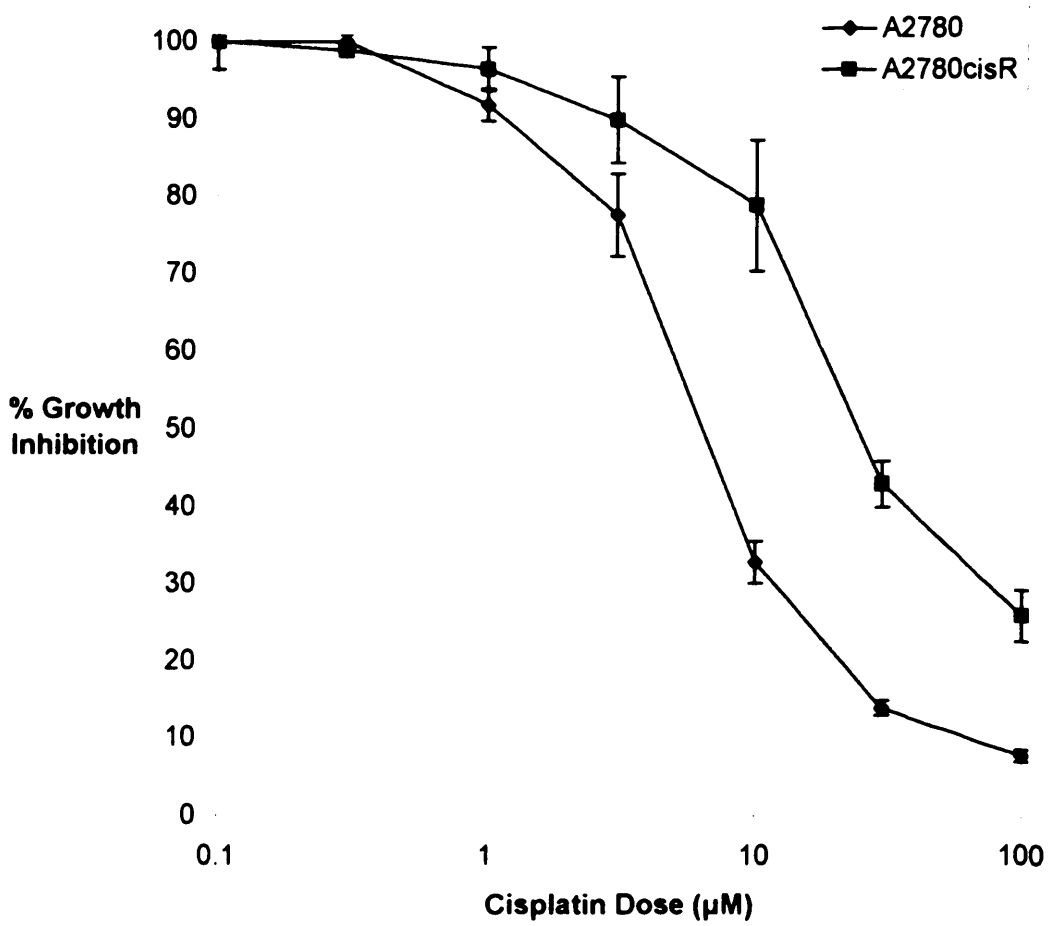


Figure 3.2. Cisplatin-induced cytotoxicity measured in A2780 and A2780cisR, using the SRB assay following a one-hour drug treatment. Each point represents the mean of three independent experiments, with error bars representing standard error values.

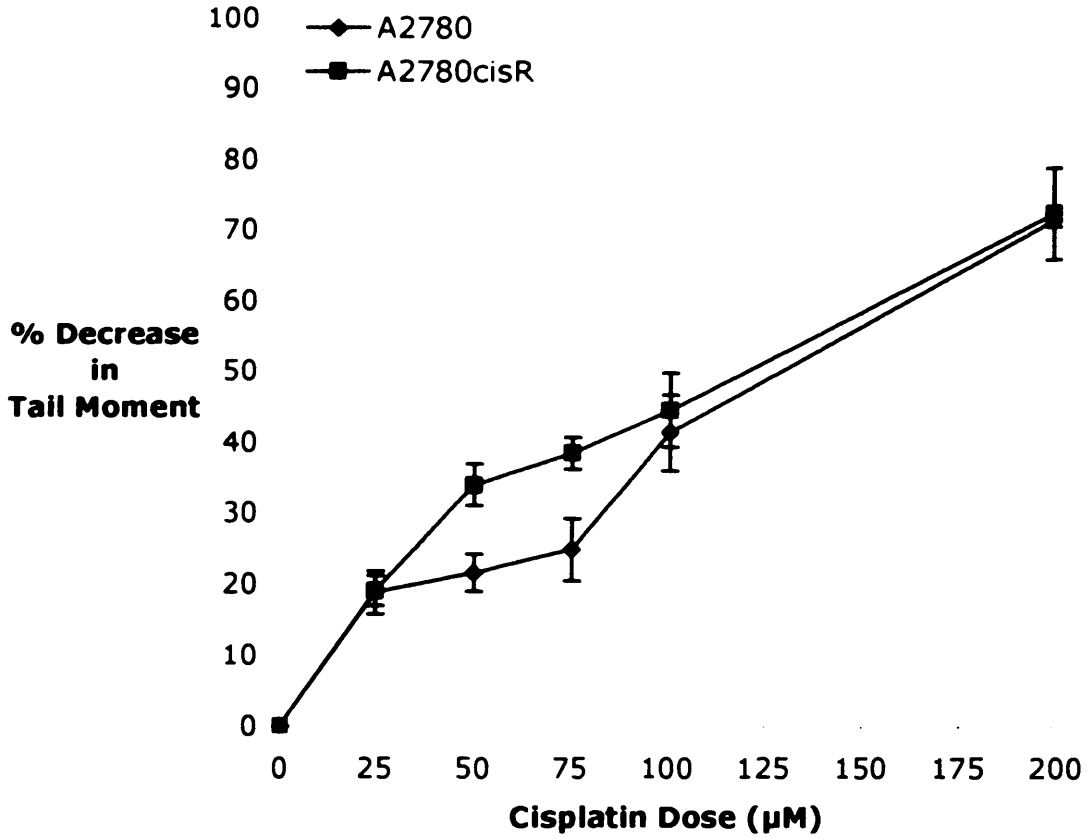


Figure 3.3. Interstrand crosslinking in A2780 and A2780cisR measured using the comet assay, following a one-hour drug treatment with increasing dose of cisplatin, and a six-hour post treatment incubation. Each point represents the mean of three independent experiments, with error bars representing standard error values.

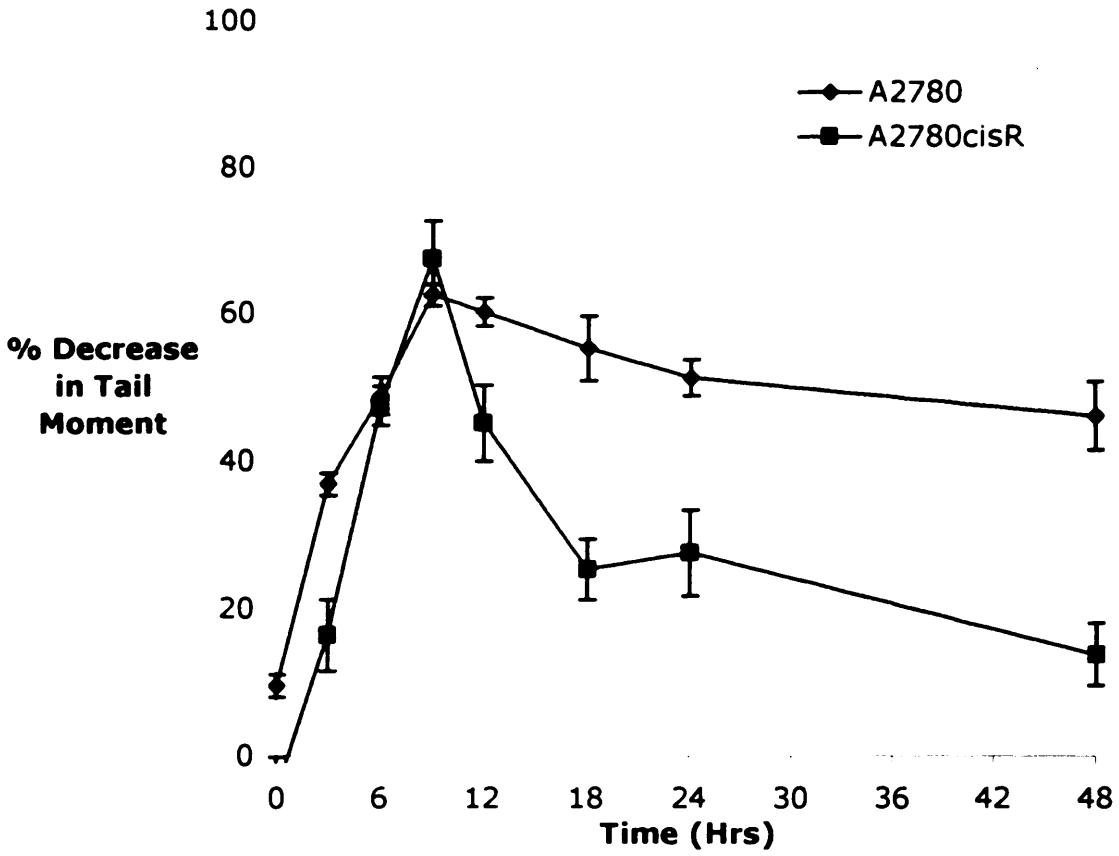


Figure 3.4. Interstrand crosslinking over time in A2780 and A2780cisR, measured using the comet assay, following a one-hour drug treatment using cisplatin (100μM). Each point represents the mean of three independent experiments, with error bars representing standard error values.

Both cell lines showed a similar trend in ICL formation leading to a peak of crosslinking nine hours after the one-hour drug exposure. After the nine-hour time point crosslinks persist in the parental A2780 cells, however rapid ICL unhooking is seen between the nine and 18- hour time points in the A2780cisR cells. The percentages of the ICLs formed at the nine-hour time point unhooked by the 18 hour time point were 11.6% and 62.3% in A2780 and A2780cisR, respectively. By the 48-hour time point the A2780 and A2780cisR cells had unhooked approximately 26.1% and 79.4%, of cisplatin-induced ICL, respectively.

### 3.3.3. Mechlorethamine

#### 3.3.3.1. Cytotoxicity

Mechlorethamine sensitivity was measured in both cell lines, using the SRB assay. Figure 3.5 represents the % growth inhibition at increasing doses of mechlorethamine.

The mechlorethamine $IC_{50}$ for A2780 was 0.44Mm ± 0.14 and for A2780cisR was 0.67μM ± 0.15. A2780cisR cells were therefore approximately 1.5-fold resistant to mechlorethamine than the parental sensitive cell line A2780, following a one-hour drug treatment. Mechlorethamine was toxic at lower doses than cisplatin, requiring 13- and 33-times less drug to kill A2780 and A2780cisR cells, respectively. This agent was therefore a more potent cytotoxic within the paired cell lines than cisplatin.

#### 3.3.3.2. Measurement of ICL at Increasing Dose

Mechlorethamine-induced ICLs were measured in A2780 and A2780cisR cells at increasing doses from 0-10μM using the comet assay. The % decrease in tail moment at increasing doses of mechlorethamine are represented in Figure 3.6.

Crosslinks were clearly detected in both cell lines using a dose of 1μM mechlorethamine. Both cell lines showed similar levels of ICL in response to increasing doses of mechlorethamine, following a one-hour drug exposure. A dose of 5μM mechloethamine caused approximately 100% crosslinking in both cell lines. As

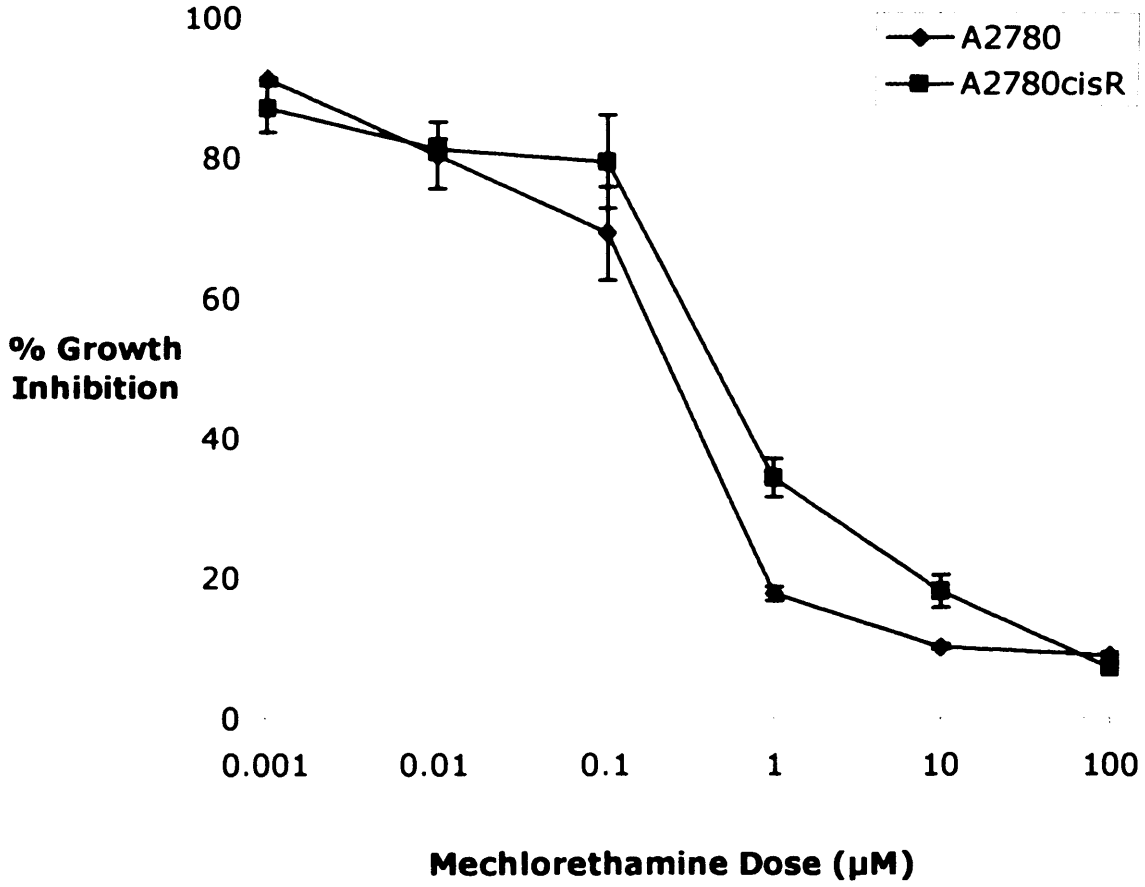


Figure 3.5. Mechlorethamine-induced cytotoxicity measured in A2780 and A2780cisR, using the SRB assay, following a one-hour drug treatment. Each point represents the mean of three indepdendent experiments, with error bars representing the standard error values.

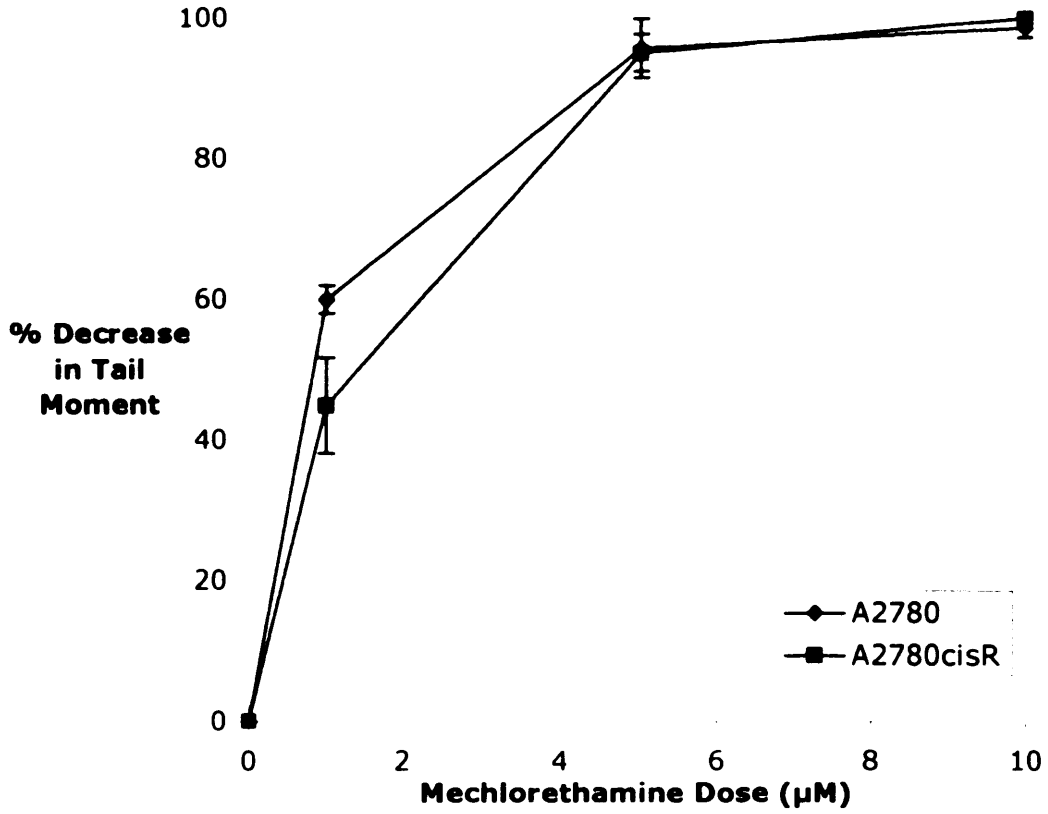


Figure 3.6. Interstrand crosslinking measured in A2780 and A2780cisR using the comet assay, following a one-hour drug treatment with increasing doses of mechlorethamine. Each point represents the mean of three independent experiments, with error bars representing standard error values.

a result of the dose response data represented in Figure 3.6, the dose of 1.5μM was chosen to measure mechlorethamine-induced ICLs over time.

3.3.3.3. Measurement of ICL Over Time

Mechlorethamine ICL processing was measured over time using the comet assay, following a one-hour drug treatment with 1.5μM. Figure 3.7 represents the % decrease in tail moment for both cell lines following drug treatment.

The maximum level of mechlorethamine crosslinking in both cell lines was observed at the 0-hour time point, immediately following drug exposure. Between the 0 and eight-hour time points both cell lines show similar and proficient mechlorethamine-ICL unhooking. By the eight-hour time point both cell lines had removed approximately 60% of induced crosslinks. After this time point, A2780cisR cells unhooked a higher percentage of the remaining crosslinks than A2780 cells. By the 48-hour time point the A2780 cells had unhooked approximately 76% of induced crosslinks, and the A2780cisR cells had unhooked 88%.

3.3.4. UVC Cytotoxicity

UVC sensitivity was measured in both cell lines, using the SRB assay. Figure 3.8 represents the % growth inhibition at increasing doses of UVC. The UVC $IC_{50}$ for A2780 was 4.25 $Jm^{-2}$ ± 1.03 and 4.95 $Jm^{-2}$ ± 0.27 for A2780cisR. Both cell lines therefore showed a similar level of cytotoxicity to UVC exposure.

3.4. Discussion

The doubling times for the A2780 and A2780cisR cells were 16.1 and 15.1 hours, respectively. Therefore the A2780cisR cells grow slightly faster, and double in number in a shorter period of time than their parental cell line A2780. This result is compared to the original doubling times for these cell lines, quoted by Behrens *et al.* (1987) of 25.3±1.0 hours for A2780 and 22.1± 0.7 hours for A2780cisR (mean±SE).

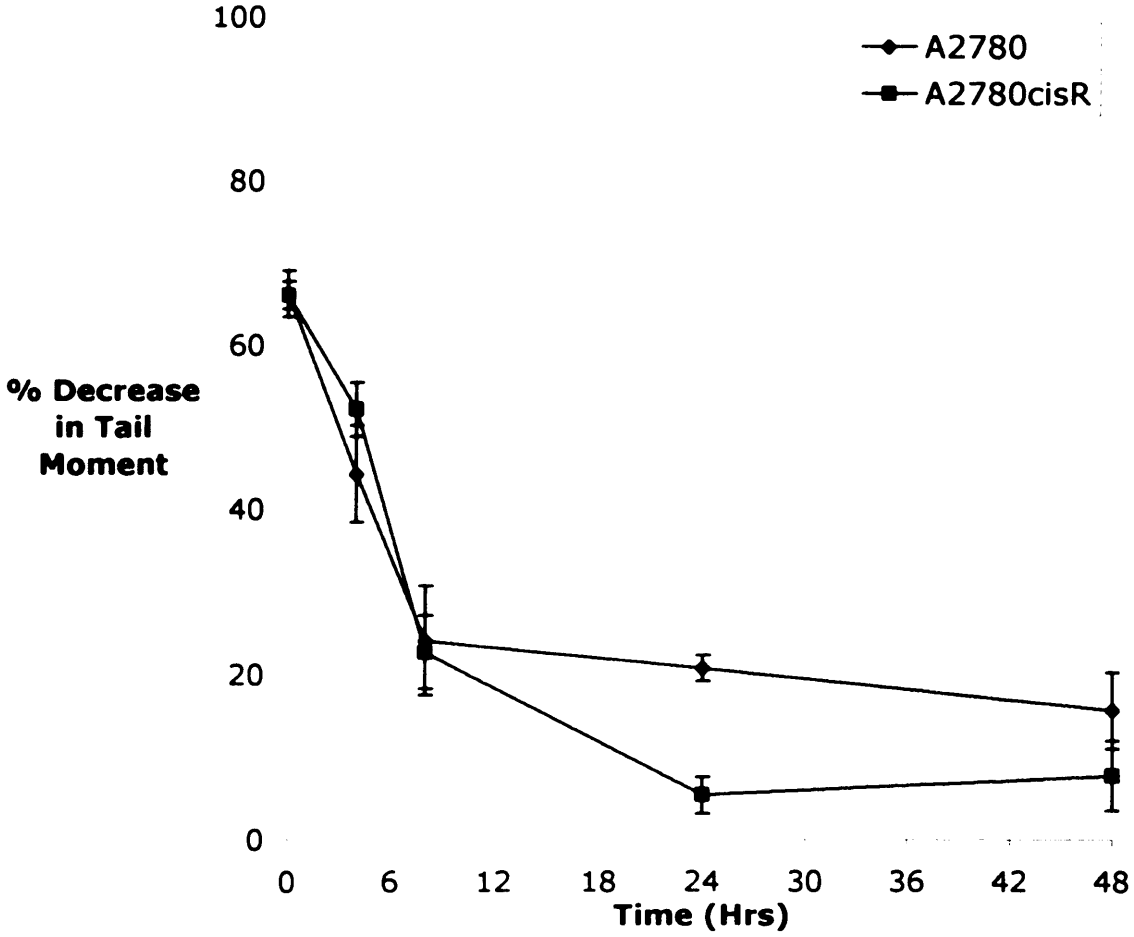


Figure 3.7. Interstrand crosslinking over time in A2780 and A2780cisR measured using the comet assay, following a one-hour drug treatment with mechlorethamine (1.5μM). Each point represents the mean of three independent experiments, with error bars representing the standard error values.

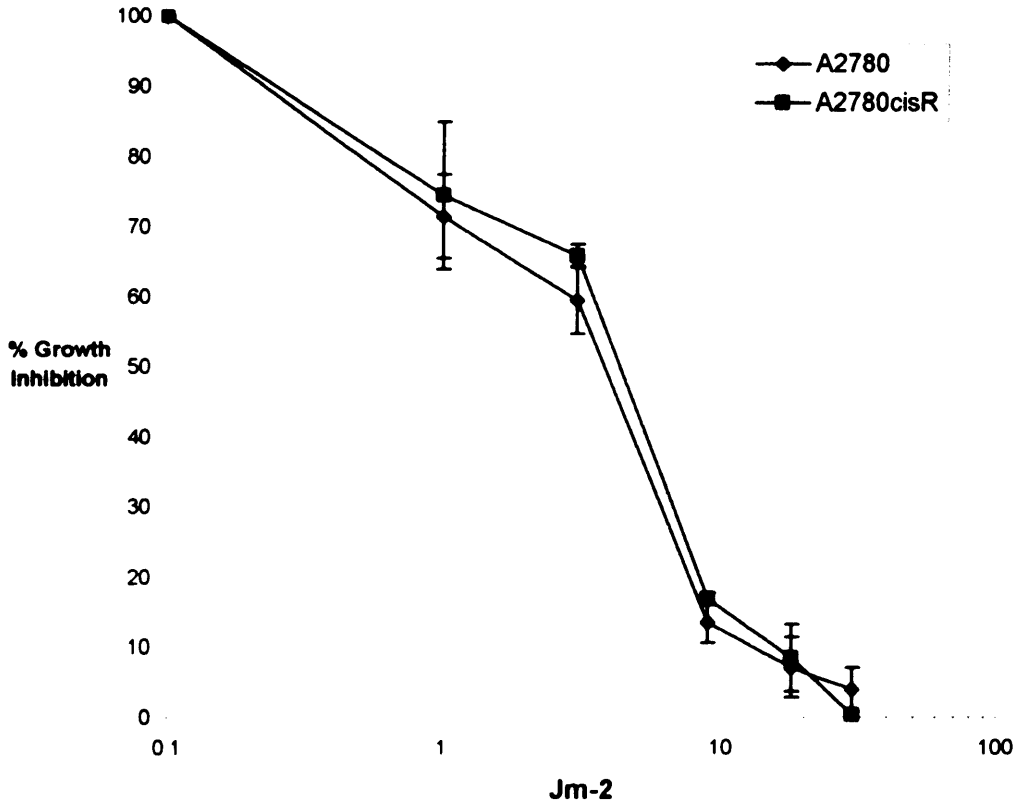


Figure 3.8. UVC-induced cytotoxicity in A2780 and A2780cisR measured using the SRB assay. Each point represents the mean of three experiments, with error bars representing the standard error values.

The level of cisplatin resistance in A2780cisR compared to A2780 was approximately 3.7-fold, measured using the SRB assay. This is comparable with a 3.8-fold cisplatin resistance quoted for these cell lines by Antonini *et al.* (1999), following 96-hours of continuous drug exposure, using the SRB assay. Behrens *et al.* (1987) quoted a 7.3-fold resistance to cisplatin in the A2780cisR cells compared to the parental cell line, using a clonogenic survival assay.

When cisplatin interstrand crosslinking was measured using the comet assay, both cell lines showed a dose-dependent increase in ICL formation. Both cell lines showed similar levels of crosslinking at the 25, 100 and 200μM doses, however A2780cisR cells showed lower levels of ICL at the 50 and 75μM doses. An increased number of repeats of these experiments would help to identify how significant this difference in adduct level was. Both cell lines showed a similar peak level of cisplatin-ICL formation at nine hours after a 100μM, one-hour drug exposure. Interstrand crosslinking has been investigated by several groups using the alkaline elution technique, and the peak of cisplatin-induced ICL has been reported to occur five hours after a two hour exposure (Holford *et al.* 1998), and 12 hours after a one-hour drug exposure (Zwelling *et al.* 1978, Zwelling *et al.* 1979a, Strandberg *et al.* 1982). Using the comet assay and CHO cells, De Silva *et al.* (2002b) reported the peak of cisplatin-ICL formation to occur nine hours after a one-hour exposure.

A2780cisR was previously reported to have a higher intracellular glutathione (GSH) content than A2780 cells (Behrens *et al.* 1987). However, both cell lines showed similar ICL formation up to the peak-level at nine-hours, with mean % decrease in tail moment values of 62.5% for A2780 cells and 67.5% for A2780cisR cells. There was therefore no evidence for any upstream mechanism (e.g. uptake or detoxification) preventing crosslink formation in the resistant cell line. This is interesting because pretreatment of A2780cisR cells with BSO has previously been shown to result in increased sensitivity to cisplatin (Perez *et al.* 2001, Jansen *et al.* 2002), although it was not possible to restore parental sensitivity to A2780cisR using BSO, suggesting that GSH is not the only resistance mechanism at work in this cell line (Perez *et al.* 2001, Jansen *et al.* 2002). If GSH is not preventing cisplatin from forming DNA adducts but its loss sensitises A2780cisR to cisplatin, then it is possible that glutathione is contributing to the resistance of A2780cisR without conjugating

and detoxifying cisplatin molecules. Lai *et al.* (1989) reported a role for GSH in DNA repair of cisplatin damage. Exposure of A2780 and a cisplatin-resistant sub-line $2780^{CP}$ (2780CP70 from Behrens *et al.* 1987) to varying combinations of BSO, glutathione ester, and aphidicolin revealed the involvement of glutathione in the repair capability of cisplatin-resistant ovarian cancer cells, measured as unscheduled DNA synthesis (Lai *et al.* 1989).

Meijer *et al.* (1990) used atomic absorption spectroscopy (AAS) to measure total bound platinum 0 and 22 hours after a four hour cisplatin exposure. They also reported a reduction in the repair of platinum bound to DNA in both a cisplatin-sensitive and a cisplatin-resistant human small cell lung cancer cell line, following a reduction in intracellular GSH caused by pre-treatment with BSO. In addition, the modulatory effect of two DNA repair enzyme inhibitors, arabinofuranosylcytosine (Ara-C) and hydroxyurea (HU) on cisplatin and melphalan, in rat mammary carcinoma cells was more effective when intracellular glutathione was depleted with BSO (Alaoui-Jamali *et al.* 1994). These findings suggest a more complicated role for glutathione in resistance to crosslinking agents, than simple conjugation and detoxification.

Interestingly, despite both cell lines sharing a similar peak in crosslinking at the nine-hour time point, between the nine and 48 hour time points the A2780cisR cells showed significantly enhanced cisplatin-ICL unhooking (~80%) compared to the A2780 cells (~26%).

The relationship between interstrand crosslinks and cytotoxicity is better established for the mustard compounds, than for cisplatin. DNA-interstrand crosslinking induced by melphalan, chlorambucil and 4-[bis(2-chloroethyl)amino]benzoic acid measured using alkaline elution, correlated with the biological activity of the compounds (Sunters *et al.* 1992). Mechlorethamine-ICL formation and removal measured using the alkaline elution technique, have been closely correlated with loss of colony survival in a human melanoma cell line (Hansson *et al.* 1987) and a murine leukemic cell line (Ross *et al.* 1978, O'Connor *et al.* 1990).

Experiments using mechlorethamine and our paired cell lines indicated that A2780cisR was 1.5-fold resistant to this drug, compared to A2780, following a one-hour drug treatment. There has been no comparative study published into the sensitivity of these paired human ovarian cancer cell lines to mechlorethamine. However, Behrens *et al.* (1987) reported the A2780cisR cell line to be 2.1-fold cross-resistant to the mustard melphalan, measured using a clonogenic survival assay. When mechlorethamine interstrand crosslinking was assessed using the comet assay, both cell lines showed increasing ICL formation with increasing dose. Examining mechlorethamine interstrand crosslinking over time both cell lines showed the highest level of crosslinking immediately following a one-hour 1.5μM drug exposure. This results confirmed findings by Ewig *et al.* (1977), Ross *et al.* (1978) and Hansson *et al.* (1987) who all used alkaline elution to measure interstrand crosslinking, and who all reported the peak of mechlorethamine-induced ICL to occur directly after a short drug exposure (30 minutes or one hour). DeSilva and colleagues (2000) measured mechlorethamine ICL in CHO cell lines using the comet assay, they also reported the highest levels of ICLs to occur immediately after a one-hour exposure.

After the observed peak of crosslinking both cell lines proficiently removed approximately 60% of induced ICLs by the eight-hour time point. Between the eight and 48 hour time points, the A2780cisR cells were slightly more efficient at removing the remaining ICLs than the parental cell line A2780, so that by the 48-hour time point, A2780 cells had unhooked approximately 76% of all induced crosslinks, and A2780cisR cells had unhooked approximately 88%. These data suggest very similar cellular processing of the mechlorethamine-induced interstrand crosslinks, by the two cell lines. As the cisplatin-resistant cell line differs significantly from the sensitive cell line in its ability to unhook the cisplatin-induced ICL, it can be concluded that the enhanced unhooking mechanism involved is specific to cisplatin induced lesions, and not a generalised improvement in the cells ability to unhook any type of ICL. As Behrens *et al.* (1987) reported A2780cisR cells to be 2.1-fold resistant to melphalan, melphalan ICL formation and repair could be investigated using the comet assay, in an attempt to investigate the ability of this cell line to repair this specific type of ICL, however, this group used clonogenic survival to assess cytotoxicity, and produced a higher cisplatin-resistance for A2780cisR than our own SRB data, so an additional assessment of the cross-resistance of this cell line to melphalan, measured using the

SRB protocol, would first be necessary to compare directly to the mechlorethamine and cisplatin data.

The interstrand crosslinks formed by mechlorethamine and cisplatin differ significantly, with the cisplatin ICL forming between the guanines in the sequence d(GpC), with a half-life of approximately 29 hours, and mechlorethamine ICLs forming primarily at the sequence d(GpNpC), with a half-life of approximately 2 hours (Dronkert and Kanaar, 2001). While the mechanisms involved in the repair of interstrand crosslinks are still being investigated, several models have been suggested, these have been highlighted in the introduction. Interesting differences in the processing of both type of ICL have also been reported. For example only ERCC1 and XPF are essential for the initial unhooking of mechlorethamine ICL, whereas ERCC1, XPB, XPG, XPF and XRCC3 are all required for the initial unhooking of cisplatin-induced ICL (De Silva *et al.* 2000, and 2002b). DNA double strand breaks have been detected as an intermediate in the repair of mechlorethamine ICL in exponentially growing yeast cells (McHugh *et al.* 2000), and in CHO cells (De Silva *et al.* 2000), but not in the processing of cisplatin ICL in CHO cells (De Silva *et al.* 2002b).

There are two classes of DNA adduct induced by UVC (200-280nm), cyclobutane-pyrimidine dimers (CPD) and pyrimidine (6-4) photoproducts (6-4PPs) (Thoma, 1999). Both types of lesion are repaired by nucleotide excision repair (Aboussekhra *et al.* 1995, Batty *et al.* 2000). Measuring UVC sensitivity therefore gives an indication of any difference in NER efficiency between the two cell lines. There is only an approximate 1.16-fold difference in UVC sensitivity between the cisplatin-sensitive and resistant cell lines. This suggests little difference in the NER processing of DNA-damage on a single strand of DNA between the cisplatin sensitive and resistant cell lines. This has implications for the repair of cisplatin intrastrand crosslinks by A2780 and A2780cisR, as this class of lesion is repaired by NER (Moggs *et al.* 1996, Araujo *et al.* 2000, Huang *et al.* 1994) and would therefore suggest no difference in cisplatin-intrastrand crosslink repair between the two cell lines, although this has not been formally demonstrated in this study. Colella *et al.* (2001) investigated the repair of cisplatin adducts in A2780 and A2780cisR cells in the N-*ras* gene over-time, following a five-hour exposure to the cisplatin $IC_{50}$ dose

using a quantitative PCR. They reported similar kinetics of accumulation and repair of cisplatin-induced DNA lesions in A2780 and A2780cisR cells. This technique would mainly quantify the repair of intrastrand crosslinks, and this type of lesions accounts for approximately 90% of cisplatin-induced DNA adducts (Fichtinger-Schpeman *et al.* 1985).

Research by Aloyz *et al.* (2002) involved artificially elevating XPD expression in a human glioma cell lines. Elevated XPD led to no difference in NER, assessed using a cisplatin damaged plasmid and by measuring UV sensitivity. They reported a two to four-fold increase in cisplatin resistance and a two-fold increase in melphalan resistance. Elevated XPD was also responsible for increased Rad51 foci, and elevated sister chromatid exchange (SCE) and, therefore, homologous recombination. They also reported elevated ICL unhooking, measured using an ethidium bromide assay, in response to cisplatin exposure (Aloyz *et al.* 2002). XPD co-immunoprecipitates with Rad51, providing evidence of a crossover between the NER and HRR pathways (Aloyz *et al.* 2002). This report therefore provided evidence for an enhanced ICL repair pathway involving elevated HRR and Rad51 activity, leading to increased resistance to cisplatin in the absence of increased NER.

Importantly, these paired cell lines (A2780 and A2780cisR) reflect the same trend of enhanced cisplatin-induced ICL unhooking seen in ovarian tumour cells from patients previously exposed to platinum, versus platinum-naïve patients (presented in Chapter 2). They therefore provide a suitable *in-vitro* model representing the pattern observed in the clinical material. Therefore, a detailed gene expression analysis of both cell lines is presented in Chapter 4, using microarrays and RT-PCR, in an attempt to understand the potential genetic elements contributing towards this phenotype.

## Chapter 4: Gene Expression Analysis of Paired Cisplatin-Sensitive and Resistant Human Ovarian Cancer Cell Lines.

### 4.1. Introduction

As described, A2780 is a human ovarian cancer cell line derived from a chemonaïve patient (Louie *et al.* 1985). This cell line was exposed to increasing concentrations of cisplatin over time to produce a stable cisplatin resistant human ovarian cancer cell line A2780cisR (Behrens *et al.* 1987). Results in Chapter 3 of this thesis confirmed the difference in cisplatin sensitivity reported for these cell lines (Antonini *et al.* 1999). Use of the single cell gel electrophoresis 'comet' assay revealed that the formation of cisplatin interstrand crosslinks was very similar for both cell lines over time, leading to a peak in formation nine hours after treatment. However, after the peak in crosslinking the resistant cell line efficiently unhooked the cisplatin ICL, whereas little unhooking occurred in the sensitive cell line.

Similar findings were observed in clinical tumour cell samples from human ovarian cancer patients (Chapter 2). In most cases samples from patients previously treated with platinum chemotherapy exhibited enhanced ICL unhooking following the peak of crosslinking, compared to samples from patients never previously exposed to platinum. The behaviour of the pair of cell lines was therefore mirroring the behaviour of ovarian cancer cells from patients, and it is therefore a relevant cell model to study the mechanism of clinical resistance to platinum drugs. Microarray analysis was chosen to further study the genetic differences between A2780 and A2780cisR.

A DNA microarray is simply a small solid support, which carries sequences from thousands of different genes, immobilized at fixed locations. These supports can be glass microscope slides, silicon chips or nylon membranes. The sequence spots can be genomic DNA, cDNA or oligonucleotides. The basic technique relies on hybridisation, using a labeled nucleic acid mobile probe, which is applied to the microarray containing the immobilized sequences. When the probe comes into appropriate contact with the complementary immobilized sequence they can hybridize and remain attached, providing a signal at the fixed location for the

complementary sequence. Image capture and analysis is therefore a key stage in the efficient management of microarray technology.

The different types of microarray are manufactured using different techniques. For cDNA microarrays, probes are immboilised on to a solid surface using robotic-mediated spotting. In oligonucleotide microarrays, probes are either synthesised and then immobilised, or synthesised directly onto the solid platform (Choudhuri *et al.* 2004). The later group includes the Affymetrix class of array, which is constructed using photolithography and photolabile protecting groups in order to perform on-chip synthesis (Hardiman *et al.* 2004). For cDNA microarrays the immobilised DNA can be PCR fragments or library clones. The length of these sequences can vary from approximately 500 to 5000 bases (Choudhuri *et al.* 2004). For oligonucleotide arrays, the immobilised sequences are approximately 20 to 80 base pairs long (Choudhuri *et al.* 2004).

There are three main applications of microarrays. The first type of microarray is the gene expression chip. Here the immobilized DNA can be cDNA derived from the mRNA of known genes, or specifically designed oligonucleotides. Generally the sample DNA that is hybridized to the microarray is cDNA derived from mRNA. This type of array is used to measure changes in gene expression levels between samples (Kurian *et al.* 1999).

The second type of microarray is used to measure changes in the copy number of a particular gene involved in a disease, looking for genomic gains and losses. Comparative genomic hybridisation (CGH) microarrays use either large sections of genomic DNA or cDNA as immbolised sequences, each spot representing a known chromosomal location (Pollack *et al.* 1999). Here fluorescently labeled genomic DNA from normal and disease tissue make up the hybridisation mixture (Mantripragada *et al.* 2004).

The third type of microarray is used to investigate mutations or polymorphisms in a single gene. The target DNA is that of a single gene. Variations can occur within a gene nucleotide sequence, called a single nucleotide polymorphism (SNP). The hybridisation mixture needs only to contain the genomic DNA derived from a normal

sample to screen for a particular mutation. If a particular SNP pattern is associated with a particular disease state, than SNP microarrays can be used to screen for that particular mutation in patient samples, determining the likelihood of the patient developing that disease (Khan *et al.* 2004). SNP microarrays can be mRNA or oligonucleotide arrays.

In order to compare the gene expression profiles of these two cell lines in the present study the first type of microarray was most applicable. Nylon filters produced by the Research Genetics (ResGen) branch of Invitrogen were chosen. The 'known gene' filter GF211 containing sequences representing thousands of known genes was selected to produce a comparison of gene expression profiles.

The nylon filter GF211 is 5cm by 7cm containing 4324 spots of immobilized DNA representing human genes and control sequences, attached using a robotic device. The cDNA probe was produced by the reverse transcription of an mRNA sample in the presence of a radiolabelled $^{33}P$ nucleotide. The probe was hybridized to the membrane under fixed conditions and the signal was then detected using a phosphor imaging system.

## 4.2. Methods

### 4.2.1. Cell Lines and Cell Culture

Conditions for cell culture and cell storage are as described previously (Chapter 3, Section 3.2.1)

### 4.2.2. RNA Extraction

#### 4.2.2.1. RNA Extraction Protocol

The Qiagen RNeasy Mini kit (Qiagen,West Sussex RH10 9AX, UK) was used for the isolation of total RNA from cells. The kit contained RNeasy mini columns and the buffers RPE, RWI and RTL (Qiagen refuse to disclose the specific content of each buffer, as this information is proprietary).

Ten passages after thawing from liquid nitrogen storage exponentially growing monolayer cells were trypsinized, counted and collected as a cell pellet by centrifuging at 270xg for 5 minutes. The supernatant was poured off with the final volume carefully removed using a p1000 Gilson pipette. The pellet was loosened by flicking the tube by hand. The appropriate volume of buffer RTL was added, ($<5x10^6$ cells/ml 350µl, $5x10^6$ - $1x10^7$ cells/ml 600µl) to the pellet. The sample was then homogenized by passing the lysate at least five times through a 20-guage needle (0.9mm diameter) (Microlance 3, Becton Dickinson) and a 5ml sterile syringe (Becton Dickinson). One volume of 70% ethanol was added to the homogenized lysate and mixed thoroughly by pipetting. 700µl of the sample was pipetted into a RNeasy mini column placed in a 2ml collection tube (provided in the Qiagen kit), which was centrifuged for 15 seconds at 8000xg in a bench microcentrifuge. The solution that had passed through the column was discarded and collection tube reused. Where the volume exceeded 700µl, the excess was loaded in 700µl aliquots to the same column and centrifuged, each time discarding the solution that passed through the column. As a wash 700µl of Buffer RW1 was added to the RNeasy column. The column was centrifuged for 15 seconds at 8000xg. The solution that had passed through the column was then discarded. A fresh 2ml collection tube was connected to the column. 500µl of the RPE buffer was pipetted on to the column. Ethanol was added to the concentrate RPE before use as instructed. The column was centrifuged for 15 seconds at 8000xg, again to wash the column. The solution that had passed through the column was discarded. Another 500µl buffer RPE was added to the column, which was then centrifuged for 2 minutes at 8000xg, to dry the RNeasy silica-gel membrane. To ensure that there was minimal RPE carry over the RNeasy column was placed onto a new 2ml collection tube (provided in the Qiagen kit) and centrifuged at full speed in a microcentrifuge for 1 minute. The RNA was then eluted by transferring the column onto a new 1.5ml collection tube (provided in the Qiagen kit), and pipetting 50µl RNase-free water directly on to the membrane. The column and tube were then centrifuged for 1 minute at 8000g. The elute was snap frozen as 10µl aliquots in 1.5ml eppendorf tubes, on dry ice, and stored in the –80°C freezer.

To calculate the concentration of the RNA, single 10µl samples were placed on ice to thaw. Samples were diluted 300x using DEPC $H_20$, 10µl of sample was added to

2990µl of DEPC, to fill the 3ml volume of the spectrophotomer cuvettes. The diluted RNA was mixed in the cuvette by pipetting up and down using a p1000 gilson pipette. Absorbance was measured using a spectrophotometer (BioRad, Hercules, Ca, USA). The following data was recorded for each sample, absorbance at 260nm ($A_{260}$) and 280nm ($A_{280}$). Pure RNA has a $A_{260}/A_{280}$ ratio of between 1.9 and 2.1. RNA concentration was calculated using the following equation :

RNA concentration (µg/µl) = 40 x $A_{260}$ value x DF, where DF is the dilution factor.

After use, the sample was tipped out of the cuvette and discarded, 1ml of 0.1M NaOH was pipetted into the cuvette, then discarded. 2mls of DEPC $H_20$ was pipetted into the cuvette to complete the rinsing process, the DEPC $H_20$ was discarded, the cuvette was gently inverted and tapped on to a tissue to remove any excess moisture before the next diluted RNA sample was tested.

4.2.2.2. Agarose Gel Electrophoresis Analysis of RNA Extraction Products

A 1% agarose gel was produced using 1g of electrophoresis grade agarose (Sigma) melted in 100ml of 1x Tris-acetate-EDTA (TAE) buffer. (TAE buffer prepared at 50x in 500ml: 0.1M (18.6g) $EDTA(Na)_2$, 2M (121g) Tris-Base, 28.55ml glacial acetic acid). When the agarose had cooled to approximately 50°C 3µl of ethidium bromide (10mg/ml) was added. The gel was poured and allowed to solidify before being placed in to the electrophoresis tank. 1xTAE buffer was poured over the gel, the gel comb was then gently removed before the samples were loaded.

On ice, RNA samples were prepared in PCR tubes. 1µg of RNA was loaded per lane. 2µl of 6x loading dye (Promega) was added to the RNA, to a total volume of 10µl, made up using DEPC $H_20$. 10µl of sample was loaded per well. The gel was run at 80 volts until the loading buffer dyes, xylene cyanol and bromophenol blue had migrated over half of the gel. Bands were visualized using a dual intensity ultraviolet transilluminator (Jencons) in a dark room. Images were captured using an image analysis system, Scion Imager version 1.62 (Scion Corportaion, Maryland, USA).

An RNA ladder (Invitrogen) was used to verify the size of the RNA fragments visualized on the gel. Pure RNA had a $A_{260}/A_{280}$ ratio between 1.9 and 2.1, and showed two distinct bands at 1.9Kb and 5.0Kb corresponding with the human ribosomal RNA subunits 18S and 28S, respectively. Running the gel also functioned as a quality control measure for the spectrophotometer, as 1μg of RNA was loaded per lane according to its measurements, if the same quantity of RNA was loaded per lane, then the lanes should show the same intensity bands.

4.2.3. Microarray Protocol

4.2.3.1. Probe Preparation

The same amount of RNA (5.8μg) was used for each experiment

4.2.3.1.1. Labeling RNA

Frozen RNA samples in eppendorf tubes were gently thawed on ice, just prior to use. On ice 2μl Oligo(dT) (0.5μg/μl) (Invitrogen), and the appropriate volume of RNA were added to an eppendorf, with the volume being made up to 10μl using DEPC $H_2O$. The eppendorf was placed in a 70°C heating block for ten minutes, then placed on ice for two minutes.

4.2.3.1.2. Elongation (cDNA Synthesis Reaction)

The following reagents were thawed on ice, and added on ice to the eppendorf tube containing the RNA mixture. 6.0μl 5x first strand buffer (250mM Tris-HCL, 375mM KCL and 15mM MgCl provided with Superscript II from Invitrogen), 1.0μl Dithiothreitol (DTT) (0.1M supplied with Superscript II from Invitrogen), 1.5μl 20mM, dNTP mix (dGAT), 10μl [$\alpha$-$^{33}$P] dCTP (Amersham Biosciences), 1.5μl Superscript II (RT)(200U/μl). The tube was incubated at 37°C for 90 minutes. After the first 60 minutes of this incubation, a biospin column was prepared. 1ml of chilled Biogel-6 was pipetted on to a biospin disposable chromatography column (Bio-Rad, Hercules, CA 94547) connected to an eppendorf, within a universal tube. The

column was centrifuged at 270xg for five minutes. The eluted material was emptied from the eppendorf. 250µl DEPC water was pipetted onto the column and spun at 270xg for five minutes, the flow through was discarded, and this wash phase was repeated a further three times. After the final wash the eluted material and eppendorf were discarded, and a fresh eppendorf was connected to the biospin column.

Following the 90 minute 37°C incubation, the cDNA synthesis reaction was made up to 100µl using DEPC $H_2O$, this mixture was loaded onto the prepared biospin column, and was centrifuged at 270xg for five minutes. Unincorporated radioactive nucleotides remain in the column. The labeled cDNA, now in the eppendorf, was then measured in a liquid scintillation counter (Wallac 1409, Milton Keynes). Samples measured at over 20,000cpm, were then hybridized to the nylon membranes (ResGen GF211) using the following protocols.

4.2.3.2. Nylon Gene Filter Protocol

4.2.3.2.1. Prehybridisation

New filters were stored at -20°C. To use, new membranes or membranes previously stripped of radioactivity, were washed by boiling 500ml of 0.5% SDS, and adding the filter to the solution in a plastic box with lid, the box was then agitated for five minutes. The filter was then carefully placed in a hybridisation roller tube, with the DNA side facing inside. All bubbles between the glass and the filter were removed to ensure even contact, being careful not to touch the hybridisation dots. 5ml of MicroHyb (ResGen) (warmed to 42°C) was added to the side of the tube, avoiding direct contact with the filter.

5µl (5µg) of human Cot-1 DNA (Invitrogen) was denatured in a 100°C heating block for at least three minutes, and added directly after the MicroHyb. The denatured Cot-1 was carefully dribbled down the side of the roller tube, with care taken to prevent direct contact with the membrane.

5µl of thawed Poly dA (1µg/µl) (ResGen) (on ice) was then added to the tube in the same way. The tube was carefully agitated to thoroughly mix the ingredients,

without dislodging the membrane from the inside of the tube. The roller tube was then placed horizontally into the hybridizer roller oven and incubated at 8-10rpm, at 42°C for two hours.

Before the cDNA was added to the prepared membrane, the eppendorf was placed in a 100°C block for three minutes (temporarily sealed with tape to avoid loss of contents when the tube warmed). After three minutes, the sample was placed on ice for two minutes, before it was carefully pipetted into the roller bottle, avoiding the membrane, and thoroughly mixing with the solution used for the prehybridisation. The roller tube was then placed back, horizontally in the roller oven at 8-10rpm and 42°C for a further 18 hours.

4.2.3.2.2. Post Hybridisation

After 18 hours the radioactive hybridisation solution was carefully poured away, via the appropriate route in the radioactive lab. The membrane was washed in the roller tube using two volumes of 30ml of 2xSSC,1% SDS heated to 50°C, 20 minutes per wash. The roller oven was also set to 50°C. The final wash was 300ml of 0.5x SSC,1% SDS, heated to 55°C. This solution was placed into a plastic box, and the membrane was removed from the hybridisation tube and added to the box, the lid was replaced and the membrane was washed with the solution on a rocker for 30 minutes.

After this time the membrane was carefully removed and placed on a double layer of 3mm Whatmann filter paper, moistened with $dH_2O$, then wrapped in Saran wrap, being careful to avoid any bubbles or creases, which would potentially impede imaging, but also damage the filter when pressure was applied and permanent creases are formed. Saran wrapped radioactive filters were placed against phosphor screens in film cassettes and exposed overnight.

Once the phosphor image was captured, the filter was removed from the saran wrap and placed in a plastic container with 500ml of boiling 0.5% SDS (heated in the microwave). The filter was agitated in this solution for one hour, before being placed on a double thickness of 3mm Whatmann filter paper, and re-wrapped in Saran wrap. The filter was stored at 4°C. Before re-use, the efficiency of the stripping was

checked by re-exposure of a phosphor screen, which was left overnight and analysed the following day. Analysis of the intensity of the stripped images revealed whether the filter was adequately stripped for re-use. Only thoroughly stripped filters were re-used. If radioactive probe was still attached to the filter, providing intensity data for gene spots, then the filter was re-stripped. If this second procedure was not successful then the filter was not re-used.

4.2.3.3. Image Capturing

Images were scanned from the Phosphor screen in a Packard Cyclone Scanner (Packard Instruments Company, Meriden CT 06450, USA, model A4314), and imported into the Optiquant software package (version 3.00, Packard) and saved in the TIF format. These were then opened in the Pathways 2.01 software (Research Genetics, Huntsville, Al 35801, USA) using the 'Import Genefilter' function. The filters were aligned using the known positions of the 'control' total genomic DNA spots in the filter, a grid was overlaid with the centre of each spot crossed in the grid. This alignment allowed the measurement of the raw intensity data for each spot. These data were exported into Excel, by following the 'Analyse Genefilter' function, the intensity distribution bar graph was then produced. A report was generated containing a complete list of genes, filter information and raw intensitiy data. These data were rearranged to leave only the Gene Name, Gene Accession number and Raw Intensity data.

4.2.3.4. Statistical Analysis of Microarray Data

(This was performed and described by Dr Stephen Henderson, Department of Viral Oncology, Wolfson Institute for Biomedical Research, University College London, UK).

All microarrays were quantile-quantile normalised to the array with the median average signal (see mean variance pairs (MVA-pairs) Figure A5 in the Appendix section). Differential expression was analysed using the limma package, part of the Bioconductor suite of bioinformatic packages (http://www.bioconductor.org/), for the R statistical programming language (http://cran.r-project.org/). Briefly the limma

package is a variant of simple linear models but using a moderated empirical Bayesian estimate of the standard deviation to calculate p-values. The empirical estimate comes from the strong mean variance relationship of microarrays, each observed variance being adjusted towards the population variance of genes with a similar mean expression. This is appropriate for studies with relatively few replicates in which the standard deviation of a population of similar genes may be a better estimate than the observed standard deviation of a single gene (Smyth *et al.* 2004).

The significance of contrasts is further moderated by the use of a "false discovery rate" (FDR) algorithm that compensates for the massive multiple testing error inherent in microarray experiments, adjusting p-values upwards (Benjamini *et al.* 1995).

### 4.2.4. Reverese Transcriptase- Polymerase Chain Reaction (RT-PCR) Protocol

#### 4.2.4.1. Reverse Transcription

Using 1µg of RNA. The following ingredients were added to an eppendorf: 1µl oligo (dT) (500µg/ml), 1µg of RNA, 1µl dNTP mix (10mM each of dATP, dGTP, dCTP, and dTTP), made up to 12µl using DEPC $H_2O$. The eppendorf was placed in a 65°C heating block for five minutes, then placed on ice. The mixture was briefly centrifuged, to collect the tube contents. The following reagents were added to the eppendorf: 4µl 5X first strand buffer (provided with Superscript II RT from Invitrogen), 2µl 0.1M Dithiothreitol (DTT) (provided with Superscript II from Invitrogen), 1µl RNase OUT (recombinant ribonuclease inhibitor (40units/µl), Invitrogen). The contents of the tube were mixed briefly by pipetting up and down with a p20 Gilson pipette. The mix was then incubated at 42°C for two minutes. 1µl (200 units) of Superscript II Reverse Transcriptase (Invitrogen) was added to the tube, and was mixed gently by pipetting up and down. Care was taken not to denature the enzyme, by allowing it to become warm, and it was quickly replaced in the –4°C freezer after use. The 20µl mixture was placed in to a heating black set at at 42°C for 50 minutes, after this time the reaction was inactivated by heating to 70°C (in a heating block) for 15 minutes.

The cDNA could then be snap frozen using dry ice, and placed in to a –80°C freezer, or could proceed directly into the PCR reaction. For each PCR experiment only 2µl (10%) of this reaction mixture was used.

4.2.4.2. Primer Selection

Primers were obtained from MWG-Biotech AG (Milton Keynes, UK).

The gene mesoderm specific transcript homolog mouse (*MEST* or *Peg1*, accession number AA598610) is located on chromosome 7q32. The primers used were from Kobayashi *et al.* (1997).

MEST (sense) 5'-CAC TGA TGC AGA AAG ACG TTC-3'

MEST (anti-sense) 5'-CAG CAC CAT TTG CTC ATA GG-3'

To produce a PCR product of 794bp.

The gene S100 calcium binding protein 2 (*S100A2*, accession number AA458884) is located on chromosome 1q 21. The primers used were from Hough *et al.* (2001).

S100A2 (sense) 5'-CTG GTC TGC CAC AGA TCC AT-3'

S100A2 (antisense) 5'-GGT AGT GAC CAG CAC AGC CA-3'

To produce a PCR product of 66bp.

The gene excision repair cross complementing 1 (*ERCC1*, accession number T95289) is located on chromosome 19q13.2. The primers used were from Chang *et al.* (1999).

ERCC1 (sense) 5'-GGA GCT GGC TAA GAT GTG TAT CCT G-3'

ERCC1 (anti-sense) 5'-AGT CCT GCT CTA GCT TCT CCA TCA G-3'

To produce a PCR product of 143bp.

The gene β-actin (accession number R44290) is located on chromosome 7p22. The primers used were from Kotecha *et al.* (2003).

β-actin (sense) 5'-GAG CAC AGA GCC TCG CCT TTG C-3'

β-actin (anti-sense) 5'-GGA TCT TCA TGA GGT AGT CAG TCA GG-3'

To produce a PCR product of 636 bp.

The BLAST programme (http://www.ncbi.nlm.nih.gov/blast/) was used to verify the specificity of the primers, and size of the anticipated PCR fragments.

4.2.4.3. PCR Protocols

Two PCR protocols were used. The first involved Taq polymerase from Promega, the second involved Super Taq from HT Biotechnology, Cambridge, UK. S100A2 was amplified using a 'hot start' and Promega Taq, where the Taq is added only after the sample is heated to above 85°C in the PCR machine, ERCC1 was amplified using SuperTaq and MEST was amplified using Promega Taq. The manufacturers recommended protocols were followed.

A PTC-100™ (programmable thermal controller, MJ Research Inc. Mass. 02171, USA) PCR machine was used for all of the PCR reactions.

4.2.4.3.1. The Promega Taq Protocol

The following reagents were added together in a PCR tube on ice. 4.5µl of 10x PCR buffer (Promega), 2µl of 2mM dNTPs, 2µl of 25mM $MgCl_2$, 5µl of MEST or S100A2 sense primer, 5µl of MEST or S100A2 antisense primer, 5µl of β-actin sense primer and 5µl of β-actin antisense primer, 2µl of cDNA and 0.5µl Promega Taq polymerase (0.5 units). The cycling conditions were chosen according to the melting temperature of the primers used. The annealing temperature was 2°C below the lowest melting temperature.

MEST

95°C 3 minutes

95°C 1 minute
55°C 1 minute } 25 cycles
72°C 1 minute

72°C 15 minutes

4°C 5 minutes

S100A2

95°C 3 minutes

95°C 1 minute
57°C 1 minute } 30 cycles
72°C 1 minute

72°C 15 minutes

4°C 5 minutes

4.2.4.3.2. The SuperTaq Protocol

The following reagents were added together in a PCR tube on ice. 6.25µl of SuperTaq buffer, 2µl of 2.5mM dNTPs, 5µl of ERCC1 sense primer, 5µl of ERCC1 antisense primer, 5µl of β-actin sense primer, and 5µl of β-actin antisense primer, 18.75µl of $dH_20$, 2µl of cDNA and 1µl of SuperTaq (5 units). The cycling conditions for ERCC1 are listed below.

ERCC1

95°C 3 minutes

95°C 1 minute
62°C 1 minute } 25 cycles
72°C 1 minute

72°C 15 minutes

4°C 5 minutes

4.2.4.4. Agarose Gel Electrophoresis Analysis of RT-PCR Products.

1.5% agarose gel was produced by heating 1.5g of agarose (Sigma) until melted in 100ml of 1xTAE. When the agarose had cooled 3µl of ethidium bromide was added. The agarose was poured and allowed to gel before being placed in the electrophoresis tank. 1xTAE buffer was poured over the gel, until it was submerged, the gel comb was then gently removed before the samples were loaded. Samples were prepared in PCR tubes on ice. 10µl of PCR product was added to 2µl of blue/orange 6X loading dye (Supplied with the 100bp DNA ladder, from Promega), containing xylene cyanol

FF (4kb), bromophenol blue (300bp) and Orange G (50bp) to facilitate loading of samples into gel electrophoresis wells, as well as tracking migration during electrophoresis. 2µl of 100bp DNA ladder (Promega) was added to 2µl of loading buffer and loaded in to the gel. The electrophoresis was run at 100V. Results were visualized using an ultraviolet light box (Jencons) and Scion Imager programme, Scion Corporation, Maryland USA (version 1.62). The relative band intensities were analysed using the Gel-Pro Analyzer for the Macintosh (version 2.0) software (Media Cybernetics, MD 20910), and were normalized to the control β-actin band intensities, to account for any differences in sample loading into the gel.

## 4.3. Results

Frozen stocks of the human ovarian cancer cell line A2780 and its cisplatin-resistant derivative cell line A2780cisR were thawed and grown in DMEM with 10%FCS and 2mM glutamine. After 10 passages, RNA was extracted from exponentially growing cells using a Qiagen kit.

### 4.3.1. RNA Extraction Results.

The purity of RNA samples was checked by measuring the $A_{260}/A_{280}$ ratio, values between 1.9 and 2.1 indicated pure samples. Samples were also analysed using agarose gel electrophoresis. Pure samples showed two distinct bands at 1.9Kb and 5.0Kb corresponding with the human ribosomal RNA subunits 18S and 28S, respectively. Figure 4.1. shows the analysis of RNA extraction products using agarose gel electrophoresis, an RNA ladder was used to verify the size of the RNA fragments visualized on the gel.

### 4.3.2. Microarray Results

Microarray experiments were carried out using Research Genetics (ResGen) nylon gene filters. For each cell line 3 technical repeats were conducted, using the same

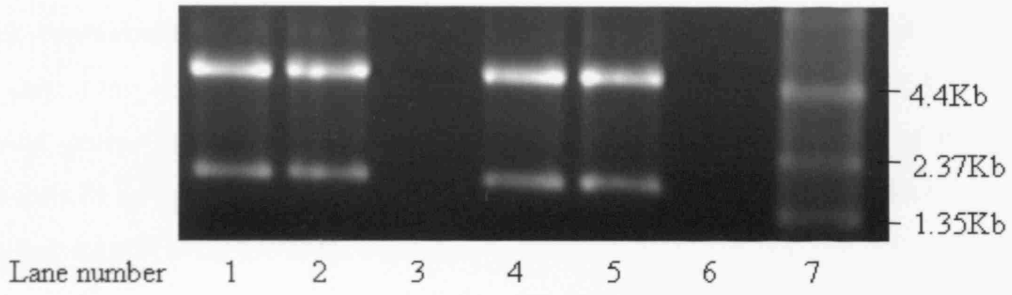


Figure 4.1. Analysis of RNA extraction products using agarose gel electrophoresis, ethidium bromide staining and UV light visualisation. Lanes 1, 2, 4 and 5 contain 1μg of sample RNA, lane 7 contains the RNA ladder.

RNA sample, and 5 biological repeats were conducted using RNA samples from different cell culture stock samples. In total, therefore, 8 microarray experiments were carried out for each cell line. Microarray data was only collected when the internal control on each nylon filter indicated that the filter had been correctly hybridised. This was assessed by referring to the 'total genomic control' spots on each filter. When correctly used these spots showed consistently high levels of hybridisation and $^{33}P$ signal. Clear and consistent hybridisation of sample probe to these control spots was a prerequisite for filter data to be processed.

Each experiment produced expression data in the form of raw intensity readings, indicating the level of binding of a radioactive probe for each of over 4 thousand known genes, indicating the expression level of the mRNA of each of the genes represented on the filter. These data were analysed in an attempt to select the genes that had significantly different expression levels between the two cell lines. This was achieved by quantile-quantile normalising the data to the array with the mean average signal, then using the limma package (part of the Bioconductor suite of bioinformatic packages, for the R statistical programming language) and finally by applying a 'false discovery rate' (FDR) algorithm (Benjamini *et al.* 1995).

In total 141 genes were found to be significantly different comparing P vs C (where P represents A2780 samples, and C represents A2780cisR samples. Where the value for the Log Odds for the Bayesian test were above 0.5, the genes were considered to be siginificantly altered between the two cell lines tested. Figure 4.2 presents the heatmap of the microarray data for each filter used. Each of the most differentially expressed genes is represented with coloured boxes, indicating the relative level of expression of that gene in each microarray experiment. Strong red and green coloured boxes represent relatively high and relatively low expression, respectively. Completely black boxes represent similar expression of that gene between the two data sets (A2780 and A2780cisR). Therefore, the shade of the box directly reflects the relative expression of that gene within the microarray experiments.


Figure 4.2. Heatmap of Microarray data, Red signifying high expression and Green low expression. Columns representing individual filters, and rows individual genes. A2780=P A2780cisR=C.

84 genes display higher expression in A2780 compared to A2780cisR, and 57 genes show higher expression in A2780cisR versus A2780. Tables A3 and A4 in the Appendix present the Microarray data ordered according to M value (Log2 of expression intensity data) in Table A3, and according to B value (Log odds for the Bayesian test) in Table A4. The largest fold difference in expression was 53-fold higher expression of MEST (mesoderm specific transcript homolog (mouse)) in A2780. In A2780cisR the largest increase in expression was for the gene ARL4 (ADP-ribosylation factor-like 4) at 11.7-fold. Categorising the genes in terms of fold difference in expression in A2780cisR, 39 genes showed >2-fold lower expression, 11 genes showed >4-fold lower expression and 7 genes showed >8-fold lower expression compared with expression levels in A2780, 57 genes in total. 21 genes showed >2-fold higher expression, 4 genes showed >4-fold higher expression, and 2 genes showed >8-fold higher expression in A2780cisR, compared with expression levels in A2780.

The 141 genes listed according to their cellular function are presented in Table 4.1. Functions were allocated by referencing each protein using the GeneCard web site (Weizmann Institute, Israel, http://bioinfo.weizmann.ac.il/cards/index.shtml) and the GenAtlas reference site (Université René Descartes, France, http://www.dsi.univparis5.fr/genatlas/). Genes representing a wide range of functional groups appear in Table 4.1. Genes involved in the cell cycle, signal transduction and cellular detoxification appear to show altered expression in the cisplatin resistant cell line, in line with the known cellular effects of cisplatin. Interestingly, only one DNA repair gene (ERCC1) is featured in Table 4.1. The large variety of functional groups represented in the list of significantly altered gene expression between A2780 and A2780cisR, suggests that the serial exposure of A2780 cells to increasing concentrations of cisplatin has had a large effect on the expression patterns of proteins involved in many processes throughout the cell.

### 4.3.3. RT-PCR Results

In order to confirm differences in RNA expression between the two cell lines, four genes were selected to undergo further investigations using reverse transcription

| Functional Group | Gene | Full Gene Name | P/C |
|---|---|---|---|
| Actin and actin binding proteins | CASK | Calcium/calmodulin-dependent serine protein kinase | P |
| | ACTA2 | Actin, alpha 2 | P |
| | ACTN3 | Actinin, alpha 3 | P |
| | CAPZB | Capping protein (actin filament) muscle Z line beta | P |
| | TMSB4X | Thymosin beta 4 X-linked | P |
| | TMSB10 | Thymosin beta 10 | C |
| | MARCKS | Myristolated alanine-rich protein kinase C substrate | C |
| | PTK9 | Protein tyrosine kinase 9 | C |
| | CNN1 | Calponin 1 (basic smooth muscle) | P |
| Antiapoptotic | TAX1BP1 | Tax1 (human Tcell leukaemia virus type1) binding protein 1 | C |
| | NOTCH3 | Notch homolog 3 (Drosophila) | P |
| ATP binding cassette protein | ABCF1 | ATP binding cassette sub-family F | P |
| Calcium binding/metabolism proteins | S100A11 | S100 calcium binding protein A11(calgizzarin) | P |
| | S100A2 | S100 calcium binding protein A2 | C |
| Cell cycle proteins | CDKN1B | Cyclin dependent kinase inhibitor 1 B (p27, Kip1) | P |
| | CCND2 | Cyclin D2 | P |
| | CDKN3 | Cyclin dependent kinase inhibitor 3 | C |
| | CDKN2A | Cyclin dependent kinase inhibitor 2A ($p14^{ARF}$) | C |
| | MARK3 | MAP/microtubule affinity-regulating kinase 3 | C |
| | UCHL1 | Ubiquitin carboxy-terminal esterase L1 | P |
| | BTG3 | BTG family member 3 | C |
| Cytoskeletal proteins | VIM | Vimentin | C |
| | ANK3 | Ankyrin 3, node of Ranvier (ankyrin G) | P |
| | DMD | Dystrophin | P |

Table 4.1. List of the 141 genes found to have significantly different expression levels between the cisplatin-sensitive human ovarian cancer cell line A2780, and the cisplatin-resistance sub-line A2780cisR. Listed according to functional group. Key: P indicates higher gene expression in A2780, C indicates higher gene expression in A2780cisR.

Table 4.1 continued

| Functional Group | Gene | Full Gene Name | P/C |
|---|---|---|---|
| Detoxification proteins | GSTT2 | Glutathione S-transferase theta 2 | C |
| | MT1X | Metallothionein 1X | C |
| Developmental proteins | MEOX2 | Mesenchyme homeobox 2 | P |
| | SNCA | Synuclein alpha | P |
| DNA repair | ERCC1 | Excision repair cross-complementing rodent repair deficiency, complementation group 1 | C |
| DNA Helicase | CHD2 | Chromodomain helicase DNA binding protein 2 | P |
| Extracellular matrix/cell adhesion proteins | MFAP2 | Microfibrillar-associated protein 2 | P |
| | COL11A1 | Collagen type XI alpha 1 | P |
| | COL1A2 | Collagen type I alpha 2 | C |
| | COL6A3 | Collagen type VI alpha 3 | C |
| | COL6A1 | Collagen type VI alpha 1 | C |
| | NID2 | Nidogen 2 (osteonidogen) | P |
| | SPP1 | Secreted phosphoprotein 1 | P |
| | CDH2 | Cadherin 2 type1, neuronal, N-cadherin | C |
| | POSTN | Periostin, osteoblast specific factor | C |
| | HAPLN1 | Hyaluronan and proteoglycan link protein 1 | P |
| | SPARC | Secreted protein, acidic, cysteine rich (osteonectin) | P |
| | CSPG2 | Chondroitin sulfate proteoglycan 2 (versican) | P |
| Focal Adhesion proteins | PXN | Paxillin | C |
| | ITGB1BP1 | Integrin beta 1 binding protein 1 | C |
| Glucose metabolism | GYG | Glycogenin | C |
| | GYG2 | Glycogenin 2 | P |
| | PFKP | Phosphofructokinase, platelet | C |
| | SLC2A3 | Solute carrier family 2, member 3 | P |

Table 4.1 continued

| Functional Group | Gene | Full Gene Name | P/C |
|---|---|---|---|
| Growth factors and receptors | VEGFC | Vascular endothelial growth factor C | P |
| | GPC3 | Glypican 3 | P |
| | PDGFRL | Platelet derived growth factor receptor-like | P |
| | PDGFRA | Platelet derived growth factor receptor, alpha polypeptide | P |
| | IGFBP2 | insulin-like growth factor binding protein 2 | P |
| Histones | HIST1H2AC | Histone 1, H2ac | P |
| | HIST1H1C | Histone 1, H1c | P |
| | HIST1H2BC | Histone 1, H2bc | P |
| | H2A.1 | Histone 2A.1 | P |
| | HIST2H2BE | Histone 2, H2be | P |
| Interferon related proteins | IFIT1 | Interferon induced protein with tetratricopeptide repeats 1 | P |
| | IFIT2 | Interferon induced protein with tetratricopeptide repeats 2 | P |
| | IFITM1 | Interferon induced transmembrane protein 1 (9-27) | P |
| | IFITM2 | Interferon induced transmembrane protein 2 (1-8D) | P |
| | IFITM3 | Interferon induced transmembrane protein 3 (1-8U) | P |
| | GIP2 | Interferon alpha inducible protein | P |
| | IFI30 | Interferon gamma inducible protein 30 | C |
| | MX1 | Myxovirus resistance 1 (interferon inducible protein p78) | P |
| | ISGF3G | Interferon stimulated transcription factor 3, gamma. | P |
| Immune response related proteins | FCER1G | Fc fragment of IgE high affinity 1 receptor for;gamma polypeptide | P |
| | HFL1 | H factor (complement)-like 1 | C |
| | FHR3 | Complement H related 3 | C |
| | CD59 | CD59 antigen p18-20 | C |
| | CD8B1 | CD 8 antigen, beta polypeptide 1 (p37) | C |
| | CD9 | CD9 antigen (p24) | C |

Table 4.1 continued

| Functional Group | Gene | Full Gene Name | P/C |
|---|---|---|---|
| Lysosomal proteins | CTSC | Cathepsin C | C |
| | CTSL | Cathepsin L | C |
| | GGH | Gamma glutamyl hydrolase | C |
| | LIPA | Lipase A, lysosomal acid,cholestarol esterase | P |
| Matrix proteases | MMP3 | Matrix metalloproteinase 3 (stromelysin 1, progelatinase) | P |
| | MMP10 | Matrix metalloproteinase 10 (stromelysin 2) | P |
| Metabolic proteins | FABP4 | Fatty acid binding protein 4 | P |
| | PCMT1 | Protein-L-isoaspartate (D-aspartate) O-methyltransferase | C |
| | CDO1 | Cysteine dioxygenase type 1 | P |
| | BLVRB | Biliverdin reductase B | P |
| Metabolic proteins continued | GAD1 | glutamate decarboxylase 1, brain | P |
| Signal transduction proteins | RGS1 | Regulator of G-protein signaling 1 | P |
| | RGS16 | Regulator of G-protein signaling 16 | P |
| | DUSP6 | Dual specificity phosphatase 6 | P |
| | DDR2 | Discoid domain receptor family member 2 | P |
| | EVI1 | Ectropic viral integration site 1 | C |
| | CCR1 | Chemokine (C-C motif) receptor 1 | P |
| | SPRY2 | Sprouty homolg 2 (Drosophila) | P |
| | EDG1 | Endothelial differentiation sphingolipid-G protein coupled receptor | P |
| | SOCS2 | Suppressor of cytokine signaling 2 | P |
| | CAMK1 | Calcium/calmodulin dependent protein kinase 1 | C |
| | F2R | Coagulation factor 2 (thrombin) receptor | P |
| | PTPRK | Protein tyrosine phosphatase receptor type K | C |
| | CRIP2 | Cysteine-rick protein 2 | C |
| | STK24 | Serine/threonine kinase 24 | P |
| | PPP2R2B | Protein phosphatase 2 | P |
| | TM4SF1 | Transmembrane 4, superfamily member 1 | C |
| | ARL4 | ADP-ribosylation factor-like 4 | C |

Table 4.1 continued

| Functional Group | Gene | Full Gene Name | P/C |
|---|---|---|---|
| Signal transduction proteins continued | PROCR | Protein C receptor endothelial | P |
| | BAI3 | Brain specific angiogenesis inhibitior 3 | P |
| Regulators of transcription | ID2 | Inhibitor of DNA binding 2 | C |
| | ID3 | Inhibitor of DNA binding 3 | C |
| | STAT1 | Signal transducer and activator of transcription 1 | P |
| | CITED2 | Cbp/p300-interacting transactivator 2 | C |
| | SREBF2 | Sterol regulatory element binding factor 2 | P |
| | FOSL2 | FOS-like antigen 2 | C |
| | TCF4 | Transcription factor 4 | P |
| | MID1 | Midline 1 (Opitz/BBB syndrome) | C |
| | LMO4 | LIM domain only 4 | P |
| | ARNT | Aryl hydrocarbon receptor nuclear translocator | P |
| | GTF2E1 | General transcription factor IIE, polypeptide 1 alpha | P |
| | PBX3 | Pre-B-cell leaukaemia transcription factor 3 | P |
| | CREM | cAMP responsive element modulator | C |
| | MEF2D | MADS box transcription enhancer factor 2, polypeptide D | P |
| Miscellaneous | A2M | Alpha-2-macroglobulin | P |
| | PTGDS | Prostaglandin D2 synthase | C |
| | SH3GL3 | SH3- domain GRB2-like 3 | P |
| | BST2 | Bone marrow stromal cell antigen 2 | P |
| | COPS8 | COP9 constitutive photomorphogenic homolog subunit 8 | C |
| | TOMM34 | Translocase of outer mitochondrial membrane 34 | C |
| | EPHX1 | Epoxide hydrolase 1, microsomal (xenobiotic) | C |
| | PSMD12 | Proteasome (prosome, macropain) 26S subunit, non-ATPase 12 | C |
| | DPYSL2 | Dihydropyrimidinase-like 2 | C |
| | UCP2 | Uncoupling protein 2 | P |
| | CYB5 | Cytochrome B5 | P |
| | INDO | Indoleamine-pyrrole 2,3 dioxygenase | P |

Table 4.1 continued

| Functional Group | Gene | Full Gene Name | P/C |
|---|---|---|---|
| Miscellaneous continued | SLC16A3 | Solute carrier 16 member 3 | C |
| | MEST | Mesoderm specific transcipt homolog (mouse) | P |
| | TAC1 | tachykinin precursor 1 | P |
| Genes of unknown function | HRASLS3 | Hras-like suppressor 3 | C |
| | DP1 | Polyposis locus pprotein 1 | C |
| | TNRC3 | Trinucleotide repeat containing 3 | C |
| | DIPA | Hepatitis delta antigen-interacting protein A | C |
| | C1orf29 | Chromosome 1, open reading frame 29 | C |
| | CLUL1 | Clusterin like (retinal) | P |
| | LRBA | LPS-responsive vesicle tracking beach and anchor containing | P |
| | MEIS4 | Myeloid ecotropic viral integration site 1, homolog 4 | P |
| | OXCT5 | 3-oxoacid CoA transferase | C |

coupled with polymerase chain reaction (RT-PCR). RT-PCR provided a quality control method for assessing the reliability of the microarray data. Two genes were selected as displaying large differences in expression using the microarray data; MEST and S100A2. β-actin was selected as a positive control for the techniques, to be used as a normalizing factor when analyzing the data, in order to cancel out differences in band intensity due to differences in sample loading in to the agarose gel. The ERCC1 gene was also chosen because of its implicated involvement in cisplatin sensitivity (Altaha *et al.* 2004). The PCR techniques were optimized and repeated three times, using different starting RNA samples. Band intensities were measured as optical densities, using Gel-Pro Analyzer for the Macintosh (version 2.0) software (Media Cybernetics, MD 20910, USA), and normalized to β-actin, producing a final set of data reflecting the relative band intensities for samples from the two cell lines. Control experiments were carried out to ensure that no DNA contaminated the RNA stocks used. There was no evidence of DNA contamination within the RNA samples (data not shown).

Figure 4.3 shows the results of the RT-PCR reaction using the MEST primers. While there was consistent amplification of a MEST PCR product in RNA from the cell line A2780, no product was seen for the RNA from the cell line A2780cisR. Increasing the starting volume of RNA (up to five fold) failed to produce a MEST PCR product for the A2780cisR (data not shown). Increasing the starting quantity of cDNA five-fold failed to produce a MEST PCR-product in the A2780cisR samples (Figure 4.4, Lane 4).

Figure 4.5 represents the results of the RT-PCR experiments using the ERCC1 primers. There was consistently more ERCC1 PCR product for the A2780cisR cell line samples, than the A2780 cell line sample, indicating higher levels of ERCC1 RNA expression in the cisplatin resistant cell line (A2780cisR), than in the parental sensitive (A2780). Analysis of these results indicated an approximately two-fold difference in expression between the two cell lines. The results of the S100A2 RT-PCR experiments are summarized in Figure 4.6. The results indicate more S100A2 PCR product in the A2780cisR samples, than in the A2780 samples. Analysis of

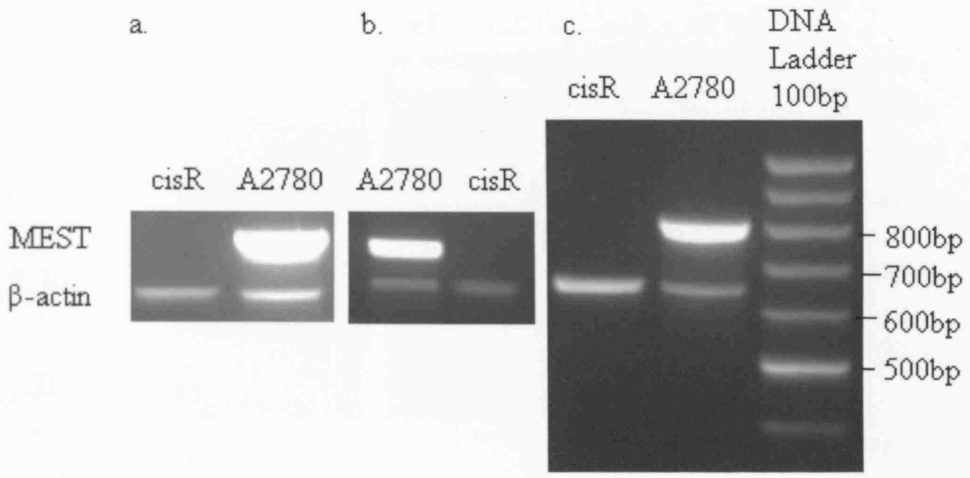


Figure 4.3. RT-PCR results using primers for the gene MEST. The β-actin fragment size was 636bp, the MEST fragment size was 794bp. Each image (4.3a-c) represents a separate experiment, using different RNA samples. Fragment sizes were verified at the time by running a 100bp DNA ladder control lane, as shown in 4.3c. (cisR represents A2780cisR).

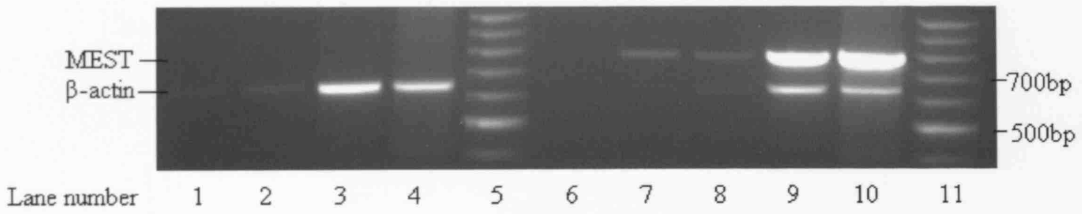


Figure 4.4. RT-PCR: Altering starting quantity of cDNA using MEST primers, and β-actin controls. The β-actin fragment size was 636bp, the MEST fragment size was 794bp. Lanes: 1. 0.02µl of A2780cisR cDNA, 2. 0.2µl of A2780cisR cDNA,3. 2µl of A2780cisR cDNA, 4. 10µl of A2780cisR cDNA, 5. 100bp DNA ladder (Promega), 7. 0.02µl A2780 cDNA, 8. 0.2µl A2780 cDNA, 9. 2µl A2780 cDNA, 10. 10µl A2780 cDNA, 11. 100bp DNA ladder.

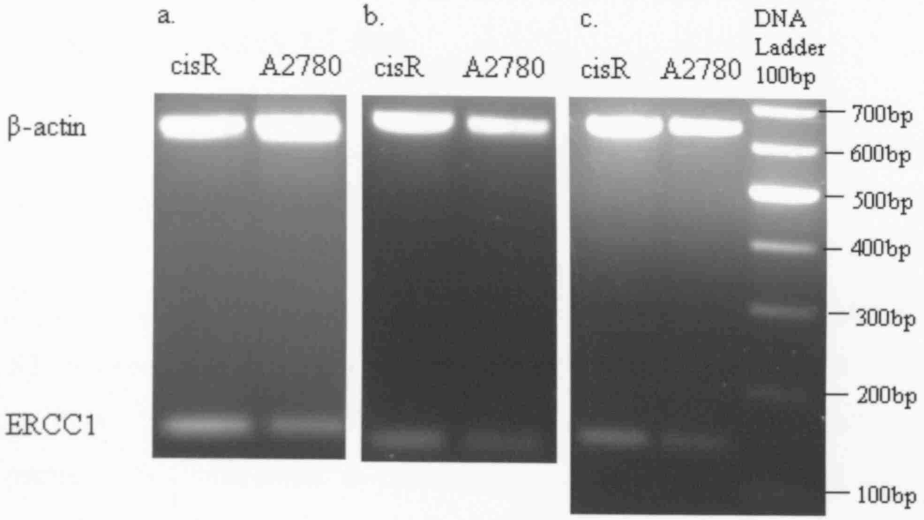


Figure 4.5. RT-PCR using primers for the gene ERCC1. The β-actin fragment was 636bp, the ERCC1 product was 143bp. Each image (4.5a-c) represents a separate experiment, using different RNA samples. 4.5c. includes a 100bp DNA ladder, to verify the size of the PCR fragments. (cisR represents A2780cisR).

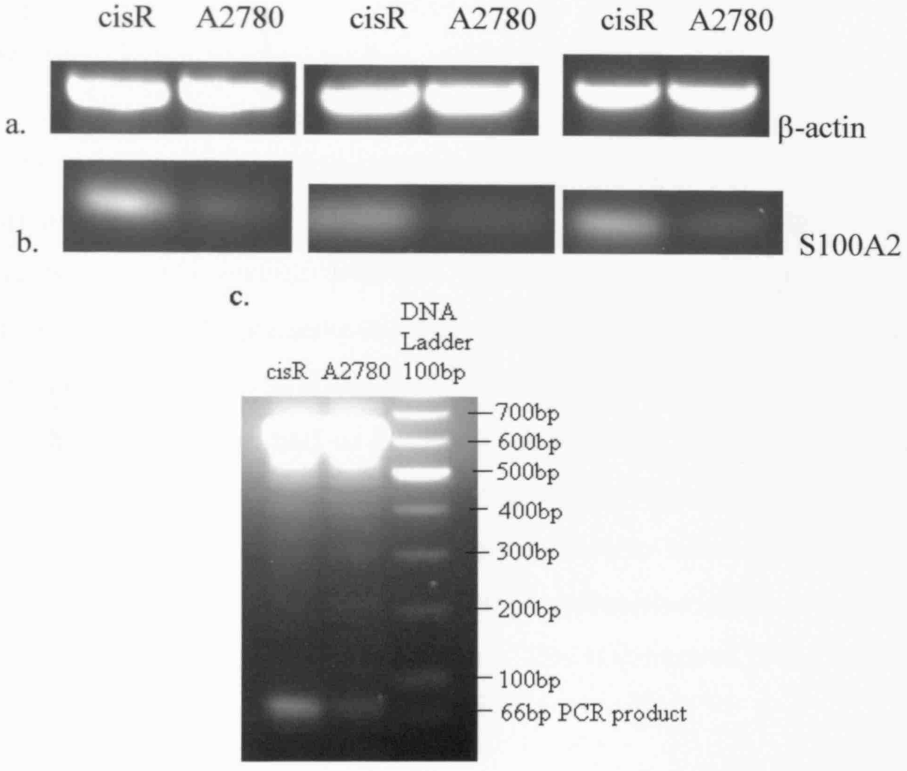


Figure 4.6. RT-PCR results using primers for the gene S100A2. The β-actin PCR products shown in 4.6a, correspond with the S100A2 PCR products directly below in 4.6b. with each of the three pairs representing a separate experiment, using different RNA samples. The exposure of the gels was manipulated to highlight the smaller S100A2 PCR product 4.6b. The size of the PCR products were confirmed using a 100bp DNA ladder, as shown in 4.6c, S100A2 fragment size at 66bp. (cisR represents A2780cisR).

band intensities, normalized to the β-actin controls indicates that the difference in expression was approximately 5.7-fold.

4.3.4. Comparison of RT-PCR and Microarray Estimates of Expression Differences for the Genes *S100A2*, *MEST* and *ERCC1*.

Table 4.2. compares the calculated fold difference in expression of S100A2, ERCC1, and MEST, between the cell lines A2780 and A2780cisR, using both RT-PCR and microarray data. Since no RT-PCR product was detected for A2780cisR using the MEST primers, this prevented a comparison between RT-PCR and microarray estimations of fold difference in expression of MEST between the paired cell lines. The data for S100A2 and ERCC1 from both techniques agreed with the cell line showing higher expression levels, and produced very similar estimates of fold difference in expression between the cell lines.

4.4. Discussion

Gene filter microarrays were used to identify differential gene expression between the two human ovarian cancer cell lines, A2780 and A2780cisR. In general, nylon microarrays were easily manipulated and did not require additional specialised equipment. Filters could be reused and easily stored at 4°C. The nylon microarrays, however, did not facilitate co-hybridisation of control and experimental sample at the same time. Instead samples had to be run separately and compared. Additional limitations included cross hybridisation within gene families, and using one blanket hybridisation temperature, although these limitations also occur using glass slide microarrays. Completely stripping each filter of radioactive probe after each use proved difficult, limiting each filter to four uses. This is compared to the other forms of array which are single use only.

The position of each of the 141 genes that showed significantly different expression between A2780 and A2780cisR following statistical analysis were mapped back to the position of each gene spot on the GF211 ResGen gene filter (Figure 4.7). This allowed for analysis of the distribution of the genes. Locations of gene spots are

Table 4.2. Comparison of calculated differences in expression of S100A2, ERCC1 and MEST, using RT-PCR and microarrays.

| Assay method | Fold Difference (A2780:A2780cisR) | | |
|---|---|---|---|
| | S100A2 | ERCC1 | MEST |
| RT-PCR | 0.175 | 0.46 | * |
| Microarray | 0.21 | 0.55 | 53 |

Values indicate fold differences in expression. *there was no PCR product for A2780cisR using the MEST primers.

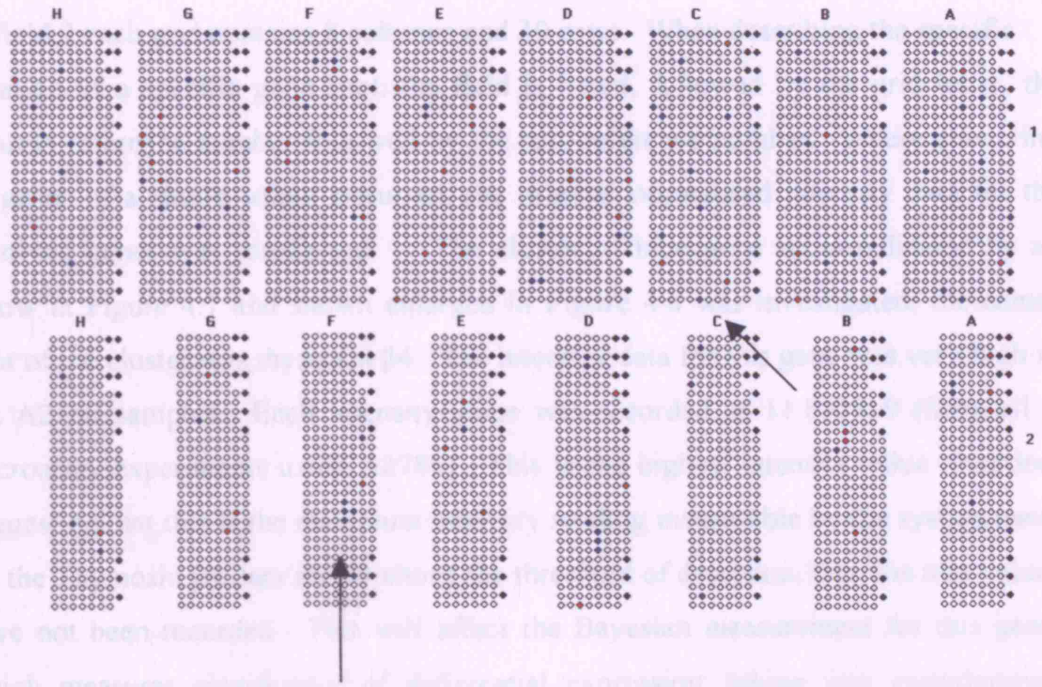


Figure 4.7. Map of Nylon Gene Filter GF211, showing the location of each of the 141 gene with significantly differential expression between A2780 and A2780cisR. The arrows indicate the gene spots locations of thymosin β4 (2 f 4 20) and vimentin (1 c 4 28). Black dots indicate total genomic DNA control spots. Blue dots represent the location of genes showing higher expression in A2780cisR, red dots represent the location of genes showing higher expression in A2780.

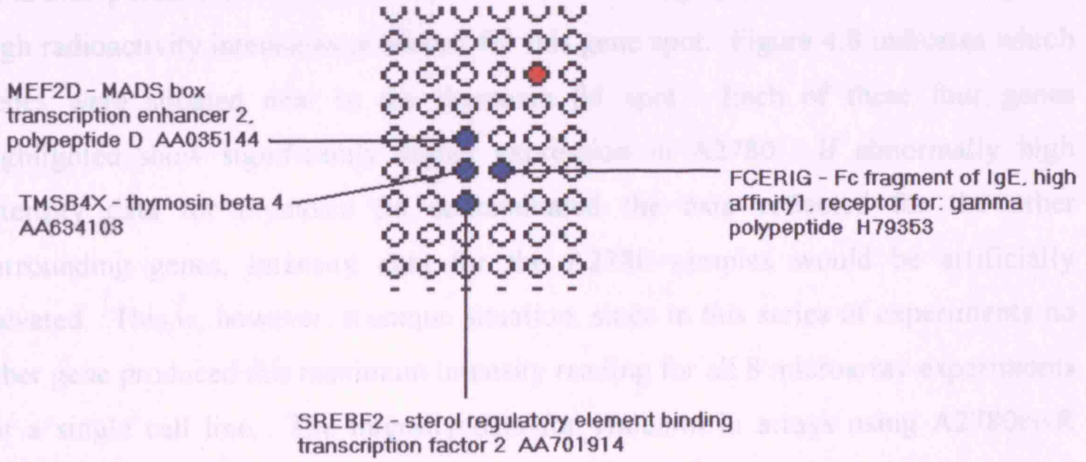


Figure 4.8. A magnified section of the GF211 gene filter, from field 2, grid F, including gene symbol, name and accession number.

either in the upper field indicated by a 1, or the lower field indicated by a 2; each field contains grids A-H. In field 1, each grid contains 12 columns and 30 rows and in field 2 each grid contains 8 columns and 30 rows. When describing the specific location of a specific gene spot, the field is listed, followed by the grid letter, the column reference number followed by the row reference number. Where clustering of genes of a single colour occurred, the original normalised intensity data for the involved genes was scrutinised. The cluster of blue gene spots indicated by an arrow in Figure 4.7 and shown enlarged in Figure 4.8 was investigated, the center spot of the cluster was thymosin β4. The intensity data for this gene was very high in the A2780 samples. Each intensity value was recorded as 11.833919 (from all 8 microarray experiments using A2780). This is the highest intensity value recorded, suggesting that this is the maximum intensity reading measurable by the system used. As the Thymosin β4 data are all above the threshold of detection, then the true values have not been recorded. This will affect the Bayesian measurement for this gene, which measures significance of differential expression, taking into consideration variation between individual intensity readings. Since each reading was the same, this predictor of significance will be incorrectly elevated. Thymosin β4 has the highest Bayesian value, at 24. It also means that the heatmap data for thymosin β4 is misleading. Interestingly, gene expression analysis carried out by Sherman-Baust at el. (2003) estimated a 95-fold reduction in thymosin β4 expression in their cisplatin resistant human ovarian cancer cell line.

It is also possible that the intensity of the surrounding spots is contaminated by the high radioactivity intensities produced for this gene spot. Figure 4.8 indicates which genes were situated near to the thymosin β4 spot. Each of these four genes highlighted show significantly higher expression in A2780. If abnormally high intensity data for thymosin β4 contaminated the data collected for the other surrounding genes, intensity data for the A2780 samples would be artificially elevated. This is, however, a unique situation, since in this series of experiments no other gene produced this maximum intensity reading for all 8 microarray experiments for a single cell line. The intensity data for vimentin in arrays using A2780cisR samples produced 6 of 8 data points as 11.833919 and 2 of 11.36483, but no clustering of red dots and hence no contamination of surrounding samples occur around this point (indicated with an arrow in Figure 4.7). It is, however, possible that

the intensity data for thymosin β 4 is considerably higher than the intensity data for vimentin, with both spots producing data above the maximum measurable intensity. The four blue spots in the bottom of field 2, grid D were also investigated. None of the intensity values were near the threshold (11.833919). This does not therefore appear to be a cluster of values influenced by a high intensity gene spot (Figure 4.7).

By analyzing the location of each of the 141 genes that showed significantly different expression between A2780 and A2780cisR the influence of physical factors affecting the gene filter data could be assessed. For example, if all of the genes showing significantly altered expression were in grid A in field 1, then the influence of the filter manufacturing process, or hybridisation process could be questioned. Ultimately the distribution of significant genes appears to be random, and not under the influence of external factors caused by the manufacture, handling and processing of the nylon gene filters.

The expression of several genes was also examined using reverse transcription-polymerase chain reaction (RT-PCR). Table 4.2. provided a comparison of calculated differences in expression using RT-PCR and microarrays between the cell lines; A2780 and A2780cisR. A2780cisR showed higher expression of the S100A2 gene, estimated as 5.7-fold and 4.8-fold using RT-PCR and microarrays, respectively. Higher expression of ERCC1 was observed in A2780cisR cells than A2780, calculated as 2.2-fold and 1.8-fold using RT-PCR and microarrays, respectively. Therefore, similar data were produced for both cell lines using the two different techniques.

The third gene tested, MEST, failed to produce a PCR product from A2780cisR cDNA, following the RT-PCR protocol, despite a five-fold increase in quantity of starting cDNA (Figure 4.4). The microarray data suggested approximately 53-fold higher expression in A2780 then in A2780cisR. In this instance therefore the gene filter protocol produced gene expression data that the RT-PCR protocol failed to produce. The failure to produce a MEST PCR-product for A2780cisR cDNA samples was not related to the primers, as the A2780 cDNA consistently produced an MEST PCR product, indicating that both MEST primers were functioning correctly.

Two genes appeared more than once on the list of genes with significantly altered expression between A2780 and A2780cisR. This occurred as these genes appeared more than once on the gene filter. Phosphofructokinase (platelet) (PFKP) and alpha-2-macroglobulin (A2M) both appeared three times on the GF211 gene filter, and occurred three times on the 'significant' list. An analysis of the three data sets for PFKP and A2M, comparing the size of the Log2 units, (a direct measurement of the difference in expression between the two cell lines, represented by column M in Tables A3 and A4 in the Appendix), and the Log Odds for the Bayesian test, (an indication of the significance of the expression data, represented by column B in Tables A3 and A4 in the Appendix) is presented in Table 4.3. In theory the three sets of data gathered for each gene should be the same, by analyzing the level of variation in the data collected an indication on inter-experimental error can be assessed.

The fact that two genes represented three times on the GF211 gene filter each appear three times on the list of significant genes, suggests that the microarray data is consistent. The small standard error values for the mean M (Log2 units) data, is a further indication of the consistency of results produced using the nylon gene filters. The larger standard errors produced by analyzing three B values for each gene (Log Odds for the Bayesian test) would suggest that this is a less consistent measurement, due to the variability between the three B values for a single gene.

Through a combination of analyzing the location of the significant genes on the GF211 ResGen gene filter, carrying out independent gene expression analysis using RT-PCR, and analysis of data collected for genes that appear more than once on the gene filter, the data collected using the GF211 nylon gene filter system appears to be an accurate representation of RNA expression, indicative of gene expression levels in the two human ovarian cancer cell lines tested.

An analysis was undertaken of some of the genes found to have significantly altered expression in the cisplatin resistant cell line, compared to the parental sensitive line, in an attempt to identify potential differences responsible for the cisplatin resistant phenotype.

Table 4.3. Comparison of data for two genes represented three times on the GF211 gene filter.

| | Gene name | Mean of three sets of data | Standard Error | Fold Difference* |
|---|---|---|---|---|
| M (Log2 units) | PFKP | -0.96 | ±0.12 | 1.9 |
| | A2M | 2.36 | ±0.18 | 5.1 |
| B (Bayesian test) | PFKP | 3.86 | ±2.42 | - |
| | A2M | 9.51 | ±1.84 | - |

* Fold difference represents the fold difference in expression between the cell lines A2780 and A2780cisR.

The cisplatin-resistant human ovarian cell line studied (A2780cisR) exhibited enhanced ERCC1 expression compared to the parental sensitive cell line (A2780). This result was confirmed using RT-PCR (Figure 4.5). The estimated differences in expression using microarray and RT-PCR were approximately 1.8- and 2.2-fold, respectively. As discussed in the introduction, ERCC1 forms a complex with XPF. XPF cross complements and corrects the repair defect of UV sensitive Chinese hamster mutant cells group 4, ERCC4 (Biggerstaff *et al.* 1993). The ERCC1-XPF heterodimer plays a key role in the NER resolution of bulky DNA adducts, and is believed to work in conjunction with homologous recombination in the resolution of interstrand crosslinks (Aboussekhra *et al.* 1995, Moggs *et al.* 1996, Araujo *et al.* 2000, Cole *et al.* 1973, Kuraoka *et al.* 2000, McHugh *et al.* 2001).

XPF and ERCC1 appear to be unstable outside of complex formation, because low levels of ERCC1 protein are detected in XPF mutant cells, despite normal mRNA levels (Yagi *et al.* 1997), transfection of wildtype XPF into these mutant cells restores ERCC1 protein levels (Yagi *et al.* 1998). Similarly, low XPF protein levels are detected in ERCC1 mutants and transfection with wildtype ERCC1 restores XPF to normal levels (Houtsmuller *et al.* 1999). In addition, ERCC1 mutations that interfere with complex formation led to rapid degradation of ERCC1 protein (Sijbers *et al.* 1996). The XPF gene was represented on the GF211 gene filter, and did not show a significant differential expression between the two cell lines tested. It would be prudent to assess ERCC1 protein levels in the two cell lines, as the expression of XPF appears to be the same in both cell lines.

The importance of ERCC1 in the processing of cisplatin damage was first highlighted when it was discovered that Chinese hamster ovary (CHO) cells lacking ERCC1 were hypersensitive to cisplatin treatment (Hoy *et al.* 1985, Damia *et al.* 1996). UV repair-deficient CHO cells lacking ERCC1 (43-3B), were incapable of CDDP DNA adduct repair (Lee *et al.* 1993). Following their stable transfection with ERCC1 (83-J5) cells exhibited proficient cisplatin-DNA adduct repair (measured using atomic absorption spectrometry), concurrent with a five-fold resistance to cisplatin (Lee *et al.* 1993).

Our results confirm data from Ferry *et al.* (2000), who analysed ERCC1 expression in cisplatin resistant human ovarian cancer cell lines derived from the parental A2780

line. They discovered a consistent increase in the steady state levels of ERCC1 within the cisplatin-resistant cell lines. Selvakumaran *et al.* (2003) used antisense-RNA methodologies to disrupt NER through the reduction of ERCC1. They were able to sensitise the relatively platinum-sensitive ovarian cancer cell line A2780 (from a platinum-naïve patient), and a relatively cisplatin resistant ovarian cancer cell line, OVCAR-10 (from a patient after platinum therapy and relapse) to cisplatin. Their host cell reactivation assay also indicated reduced DNA-damage repair capacity by the OVCAR-10 antisense ERCC1 cell lines. Interestingly, SCID mice injected i.p with the OVCAR-10 antisense ERCC1 cell lines showed significantly enhanced survival following cisplatin treatment compared with the OVCAR-10 xenographs (Selvakumaran *et al.* 2003).

Cisplatin exposure has also been shown to induce the expression of ERCC1 mRNA in human ovarian cancer cell lines, by over two-fold as early as six hours after treatment, leading to a peak level of four to six-fold 24 to 48 hours after exposure (Li *et al.* 1998b, Li *et al.* 1999). Treatment of the human ovarian cancer cell lines, A2780 and CP70 led to a six-fold increase in steady state ERCC1 mRNA (Li *et al.* 1998c). This increase was produced by both an increase in transcription and a 60% increase in the half life of ERCC1 mRNA.

When investigating the transcriptional control triggered by cisplatin Li *et al.* (1998b) discovered a four to five-fold increase in c-fos and c-jun mRNA, and a 14-fold increase in c-jun phosphorylation. The products of c-jun and c-fos form dimers making a transcription factor called activator protein 1 (AP-1), and the 5'-flanking region of ERCC1 contains an AP-1 like binding site, TGTGTCA situated between-361 and 367bp (Li *et al.* 1998b). The promoter elements TATA, CAAT and GC-boxes are absent from the promoter region of ERCC1 (van Duin *et al.* 1987). Fos-like antigen 2 (FOSL2) is a member of the FOS family capable of dimerizing with members of the Jun family to make AP-1 (Poirier *et al.* 1997). The cisplatin-resistant human ovarian cancer cell line studied here (A2780cisR) displayed elevated FOSL2 expression as measured using microarrays (approximately 1.7-fold). RT-PCR experiments to independently confirm this finding were not conducted. Blocking c-fos with cyclosporin A and c-jun with herbimycin A, respectively, blocked the cisplatin induced increase in ERCC1 expression, and led to enhanced cisplatin

cytotoxicity (Li *et al.* 1999). Blocking Jun function, by using a dominant negative non-phosphorylatable c-jun, inhibited cisplatin adduct repair and led to increased cisplatin sensitivity (Potapova *et al.* 1997). Potapova and colleagues discovered a ten-fold increase in JNK/SAPK (c-jun $NH_2$-terminal kinase/stress activated protein kinase) activity, leading to phosphorylation of c-jun at serines 63 and 73, stimulated by cisplatin treatment, but not following treatment with transplatin. Phosphorylation of c-jun at the serine residues 63 and 73 improves the transcriptional activity of the AP-1 binding sites (Smeal *et al.* 1992). Clearly the JNK/SAPK pathway is activated by cisplatin treatment, and involved in stimulating the repair of cisplatin-DNA adducts. Disrupting the functioning of Jun, by rendering it non-phosphorylatable, results in limited repair rates, and increased cisplatin cytotoxicity. Cisplatin exposure therefore leads to activation of JNK/SAPK, phosphorylation and activation of Jun and Fos, dimerisation and activation of AP-1 transcription factor, increased expression of ERCC1 and elevated cisplatin adduct repair. JNK also phosphorylates ATF2 which dimerises with Jun and activates genes controlled by ATF/CREB sites including DNA polymerase β, proliferating cell nuclear antigen (PCNA) and topoisomerase I (Hayakawa *et al.* 2003). DNA polymerase β and PCNA have been implicated in an increase in DNA repair associated with resistance (Zamble *et al.* 1995). Hayakawa *et al.* (2003) blocked ATF2 resulting in increased cisplatin sensitivity and inhibition of DNA repair.

Interestingly, transcription of γGCS, the rate limiting enzyme in GSH production, is also under the control of c-jun dimerisation and AP-1 binding (Yao *et al.* 1995). Treatment of the cisplatin resistant human ovarian cancer cell line with antisense-DNA directed against c-jun resulted in reduced γGCS mRNA expression, and decreased cellular GSH (Pan *et al.* 2002). Transfection of A2780 with c-jun, resulting in a nine-fold increase in c-jun protein level, led to a ten-fold increase in GSH content, and a two-fold increase in cisplatin resistance (Pan *et al.* 2002).

ERCC1 exists in at least two forms, the full-length gene product, and an alternatively spliced form that lacks exon VIII (Reed, 1998). Analysis of ERCC1 splicing has revealed a further control mechanism. Yu *et al.* (1998) correlated increased levels of alternatively spliced ERCC1 mRNA and protein with a reduction in cisplatin-DNA

adduct repair. In this case the splice variant appears to exert inhibition of function of the full length gene product.

Other compounds that prevent the cisplatin-induced elevation in ERCC1 result in increased cytotoxicity, for example, lactacystin (Li *et al.* 2001), IL-1α (Li *et al.* 1998a) and SU5416 (Zhong *et al.* 2003). These results further emphasize the relevance of ERCC1 status to cellular response to cisplatin.

Clinical studies have correlated elevated ERCC1 expression with poor response to platinum-based chemotherapy in non-small cell lung cancer (NSCLC) (Rosell *et al.* 2001) and ovarian cancer (Dabholkar *et al.* 1992 and 1994). Clear cell ovarian carcinoma, which is inherently resistant to cisplatin, expresses elevated ERCC1 and XPB compared with the other forms of ovarian cancer (Reed *et al.* 2003). Interestingly, Colella *et al.* (2001) reported no difference in ERCC1 mRNA or protein levels in A2780 and A2780CP8 (another name for A2780cisR).

In summary, the elevated ERCC1 level measured in the cisplatin-resistant cell line A2780cisR could contribute to the acquired resistant phenotype, possibly through the enhanced repair of cisplatin-induced ICL. If this was the case then it would correlate with the elevated ICL removal measured in A2780cisR, compared with the cisplatin-sensitve parental line A2780 detailed in Chapter 3 of this thesis. The elevated FOS2L in A2780cisR, a protein capable of dimerising with c-jun to produce AP-1 (Poirier *et al.* 1997) the transcription factor that appears to be responsible for controlling ERCC1 expression, could be contributing to the elevated ERCC1 levels measured. Clearly the level of ERCC1 expression has an impact on cellular responses to cisplatin exposure, and is linked to the clinical efficacy of this compound.

Related DNA repair genes that were on the GF211 filter, but that did not show any difference in expression between A2780 and A2780cisR were XPF, XPB, XPA, XPC, P58-Hhr23b, XPD, XPG, PCNA, RFC4, RFC1, as well as XRCC3, XRCC4, XRCC1 and XRCC9.

The cisplatin resistant cell line A2780cisR cell line showed 4.8-fold higher S100A2 gene expression compared to A2780. This result was confirmed using RT-PCR.

This gene is a member of the S100 calcium binding protein family. Wicki *et al.* (1997) discovered that S100A2 was downregulated during breast cancer progression, suggesting that it could be a candidate tumour suppressor gene. S100A2 has been found to be overexpressed in ovarian cancer (Hough *et al.* 2001, Santin *et al.* 2004). This gene has also been implicated as part of a signaling pathway that mediates apoptosis in response to etoposide (Sun *et al.* 2000, Wang *et al.* 1999). The exact function of this protein is still being investigated.

53-fold higher expression of MEST was observed in A2780 compared with A2780cisR, indicating that this gene was extensively downregulated in the cisplatin resistant ovarian cancer cell line. RT-PCR was attempted, each time yielding a clear MEST PCR product for the A2780 cell line, and no product for A2780cisR RNA. The exact function of this protein has yet to be elucidated.

The cisplatin resistant cell line A2780cisR exhibited elevated expression of metallothionein IX by approximately 1.5-fold, compared to the parental cell line A2780. No RT-PCR experiments were conducted using this gene. As discussed previously, metallothionein is an intracellular thiol capable of binding to, and therefore detoxifying cisplatin molecules (Doz *et al.* 1993). Metallothionein content has been correlated with cisplatin resistance in both *in-vivo* and *in-vitro* models (Yang *et al.* 1994, Endresen *et al.* 1984).

Many publications have reported an increase in metallothionein expression in response to exposure to chemotherapeutics including cisplatin (Kelley *et al.* 1988, Perego *et al.* 1998, Kikuchi *et al.* 1997). When the formation of cisplatin interstrand crosslinks over time in the two cell lines was observed in Chapter 3, similar levels of crosslink formation occurred up to the peak of crosslinking in both cell lines, indicating that no upstream resistance mechanism was at work in the cisplatin resistant A2780cisR. This suggests that the influence of metallothionein 1X on cisplatin sensitivity was minimal.

Similar genes that were on the gene filter GF211, but which showed no significant difference in expression between the two cell lines A2780 and A2780cisR were, metallothioneins, IB, IG, IL, IE, and IH. Metallothionein IIA did not appear on the

filter, and a comparison of expression of this mRNA between the two cell lines was therefore not carried out. Considering the importance of this particular metallothionein, a simple RT-PCR protocol using MTIIA specific primers might provider further useful information as to the importance of this protein in cisplatin resistance in A2780cisR. Testing A2780 and A2780cisR for sensitivity to cadmium chloride would provide evidence of the influence of metallothionein on cellular response to some cytotoxics and specifically cisplatin.

The microarray data indicated an approximate 1.9-fold increase in glutathione S-transferase theta (θ) 2 expression in the cisplatin-resistant human ovarian cancer cell line A2780cisR, compared to the sensitive parental cell line A2780. No RT-PCR experiments were carried out using this gene. Glutathione S-transferase theta (θ)2 is a member of the glutathione S-transferase superfamily of dimeric phase II metabolic enzymes. These enzymes protect the cell from damage through catalysing the reaction of reduced glutathione with a range of electrophilic toxic compounds. As previously discussed, glutathione S-transferases react with intracellular glutathione resulting in the formation of a glutathione thiolate anion (GS-) which acts as a nucleophile to attract electrophiles. Glutathione thiolate anions can then react with cisplatin, producing a conjugate bis-(glutathionato)-platinum, which is then effluxed through ATP-binding cassette transporters (ABCs) such as multispecific organic anion transporter (cMOAT) (also known as MRP2) and multidrug resistance-associated protein 1 (MRP1). Enhanced expression of cMOAT has been reported in response to cisplatin exposure (Schrenk *et al.* 2001). Cisplatin resistance in ovarian tumour cell lines has been closely correlated with GSH content (Hamilton *et al.* 1985, Godwin *et al.* 1992, Hamaguchi *et al.* 1993, Kudoh *et al.* 1994) and overexpression of GST (Oguchi *et al.* 1994). Immunocytochemical analysis of samples from human ovarian tumours produced a strong correlation between high GST expression, and clinical resistance to chemotherapy (Mayr *et al.* 2000). Another clinical study linked malignancy, poor prognosis and recurrence in ovarian cancer to elevated GST expression (Boss *et al.* 2001). Nishimura *et al.* (1996) discovered that human head and neck cancers with low GST activity were 4.7 times more likely to respond to platinum based chemotherapy.

Mammalian soluble GSTs can be subdivided into different classes termed Alpha (α), Mu (μ), Pi (π), Theta (θ), Kappa (κ ), Sigma (σ) and Omega (ω) (Coggan *et al.* 2002). Unlike the other classes of GST isoenzymes, the theta class genes are highly conserved, showing expression in humans, rats and mice, but also in fish, shrimp, plants, unicellular algae and bacteria (Landi *et al.* 2000). The Theta class of isoenzymes is therefore considered the most ancient, representing the early progenitor GST gene. Where the Alpha, Mu and Pi GST's function via a tyrosine residue in the active site of the molecule (Stenburg *et al.* 1991, Pennington *et al.* 1992, Kolm *et al.* 1992), theta GSTs catalytic activity has been linked to a serine residue (serine-11) within the active site, which stabilizes the glutathione bound in the active site as a thiolate anion (Board *et al.* 1995). Elucidation of the crystal structure of the Theta-class GST from the Australian sheep blowfly, *Lucilia cuprina* revealed that it was this serine residue near the N-terminus that forms a hydrogen bond with the glutathionyl sulphur atom. Mutation of ser-9 to alanine resulted in a loss of catalytic activity of this *L.cuprina* GST (Board *et al.* 1995). This serine was found to be conserved in all theta GSTs so far discovered. The rate of enzymatic activity for theta class GSTs is approximately ten times higher than for alpha, mu and pi classes (Landi *et al.* 2000). Theta GSTs also exhibit a lower affinity towards GSH-conjugates. Theta class GSTs therefore process substrates more quickly, and release the products of the conjugation faster then other GST classes (Landi *et al.* 2000).

While GST theta 2 remains largely uninvestigated, there is considerable evidence as to the importance of the glutathione S-transferase enzymes in the glutathione detoxification pathway, which itself, is very influential in preventing in the cytotoxicity of electrophilic chemotherapeutics, like cisplatin. Further research is needed to dissect out fully the role of GSTT2 in cisplatin resistance in A2780cisR, for instance inserting anti-sense sequences to knock out GSTT2 expression in A2780cisR, then retesting sensitivity to cisplatin. The formation of cisplatin interstrand crosslinks over time in the A2780 and A2780cisR was reported in Chapter 3, describing similar levels of crosslink formation occurring up to the peak of crosslinking in both cell lines, indicating that no upstream resistance mechanism was at work in the cisplatin resistant A2780cisR. This suggests that the influence of GSTT2 on cisplatin ICL formation is minimal.

Similar genes represented on the GF211 gene filter but showing no significant difference in expression between A2780 and A2780cisR, were the related proteins GST alpha 2, 3 and 4, Mu 1, 2, 3, 4 and 5, pi 1, theta 1 and 2, zeta 1. Glutathione was not present on the filter GF211 so expression could not be compared using our microarray data. Although Behrens *et al.* (1987) reported higher levels of GSH in A2780cisR cells compared to A2780 cells.

Expression of vimentin was 2.2-fold higher in A2780cisR compared to A2780. Six of the eight microarray raw intensity readings for the A2780cisR sample experiments produced the maximum possible reading using this experimental system. It can be assumed that the intensity data for this gene was above the upper threshold of detection, so that the actual difference in expression between A2780 and A2780cisR was greater than the calculated difference. This also means that the Bayesian data point for this gene is unreliable. No RT-PCR experiments were carried out using this gene.

Vimentin is an intermediate filament found in mesenchymal cells, and not normally found in epithelium-derived cancer cells (Steinert and Roop, 1988). While there is a lack of research linking vimentin expression with cisplatin resistance, it is a gene whose expression has been correlated with resistance in cancer cell lines to an array of different compounds. Increased levels of vimentin and cytokeratin 8 were correlated with increasing levels of doxorubicin resistance in human ovarian cancer cell lines, using indirect immunofluorescence (Moran *et al.* 1997). Conforti *et al.* (1995) and Meschini *et al.* (2000) found elevated vimentin expression in doxorubicin-resistant LoVo (human colon cancer) cell lines. Multi-drug resistant human breast cancer cell lines (Bichat *et al.* 1997) as well as adriamycin resistant and vinblastine-resistant human breast cancer cell lines (Sommers *et al.* 1992) also all exhibited elevated vimentin compared to the sensitive parental cell lines. There is evidence that exposure to chemotherapeutics, and the subsequent development of resistance to these agents is often associated with inappropriate expression of this mesenchymal intermediate filament. Interestingly, vimentin is also involved in apoptosis. Grzanka *et al.* (2003) linked the reorganisation of cytoskeletal proteins (F-actin, vimentin and tubulin) with the formation of apoptotic bodies in leukemia cell lines. Multiple caspases cleave vimentin at distinct sites during apoptosis induced by many stimuli

(Byun *et al.* 2001). This cleavage has two functions, firstly to dismantle the intermediate filaments and secondly to create a pro-apoptosis cleavage product which then amplifies the apoptotic signal. Interesting research by Belichenko and colleagues (2001) found that apoptosis could be suppressed in Jurkat cells by caspase-resistant vimentin (i.e. vimentin that was immune to caspase cleavage), this group concluded that the presence of full length vimentin was responsible for this inhibition. At higher doses of their apoptotic stimulus (photodynamic treatment with silicon phthalocyanide) this affect was cancelled out (Belichenko *et al.* 2001).

It could be that the elevation in expression of vimentin seen in our resistant cell line and echoed in many others, is a mechanism to prevent apoptosis upon drug treatment. This increase in vimentin might quench the caspase cleavage process, leading to a larger proportion of full-length protein, effectively diluting out the pro-apoptotic signal, thus rendering the cascade sub-lethal.

Approximately two-fold higher expression of a gene called ectropic viral integration site 1(EVI-1) was detected in A2780cisR samples compared to those from A2780. Evi-1 is an inhibitor of c-jun-N-terminal kinase (JNK) a mitogen–activated protein kinase (Kurokawa *et al.* 2000). Interestingly, a dominant negative inhibitor of JNK was found to delay the onset of apoptosis in response to cisplatin (Krilleke *et al.* 2003).

Expression of the gene LIM-domain only 4 (LMO4) was over 20-fold higher in A2780, compared to A2780cisR. Down-regulation of LMO4 expression has occurred in A2780cisR. This protein is a transcription regulator. LMO4 has been found to bind to BRCA1, with another protein CtIP, leading to the repression of BRCA1 mediated transcription (Sum *et al.* 2002). A reduction in the expression of this BRCA1-repressor could lead to an increase in functioning BRCA1 in A2780cisR. This is of potential interest as Quinn *et al.* (2003) demonstrated that BRCA1 abrogates the apoptotic phenotype induced by cisplatin and other DNA damaging agents. Reduced BRCA1 levels using antisense inhibition led to a decreased repair proficiency and enhanced apoptosis in response to cisplatin (Husain *et al.* 1998).

High BRCA1 mRNA levels correlated with poorer outcome in lung cancer patient that had previously been treated with gemcitabine/cisplatin neoadjuvant chemotherapy (Taron *et al.* 2004). A study of 71 Jewish women with epithelial ovarian cancer found that 34 patients had germ-line BRCA mutations (BRCA heterozygotes). These patients had higher response rates to platinum primary therapy than the patients with sporadic tumours, and BRCA heterozygotes with advanced stage disease had improved survival when compared to patients who has advanced stage sporadic disease (91 months versus 54 months, respectively p= 0.046) (Cass *et al.* 2003).

BRCA1-/- mouse embryonic cells were five-fold more sensitive to cisplatin than wild-type cells (Bhattacharyya *et al.* 2000). Interestingly, these BRCA1-/- cells were defective in Rad51 focus formation following exposure to x-rays and cisplatin, but they exhibited normal NER functioning (Bhattacharyya *et al.* 2000). Therefore, BRCA1 appears to be essential for the resolution of cisplatin-induced ICL via Rad51 focus formation. Downregulation of LMO4 in A2780cisR effectively increases BRCA1 expression, possibly contributing to the cisplatin resistant phenotype of A2780cisR. However, Yuan *et al.* (1999) failed to detect defective Rad51 foci formation in a BRCA1-/- human tumour cell line.

Actin is such an important protein, not only through its role as a key cytoskeletal protein, but also by providing a means by which a cell responds to extracellular and intracellular signaling. Constant cycles of actin polymerisation and depolymerisation facilitate movement, formation of a leading edge, anchorage to the extracellular matrix (ECM) and neighbouring cells via focal contacts and cell:cell junctions, and key stages in apoptosis and self destruction (Lodish *et al.* 1995). Several actin associated proteins appeared on the list of genes highlighted by the microarray experiments as exhibiting significantly altered expression rates between the cisplatin sensitive and resistant human ovarian cancer cell lines tested summarized in Table 4.1.

CAPZB is an actin capping protein involved in stabilizing actin filaments. It functions by preventing actin subunits from dissociating from actin filaments (Caldwell *et al.* 1989). Capped actin filaments usually exist where the organisation

of the cytoskeleton is unchanged, an example of this is the z-line in muscle cells where this molecule was first identified. The cisplatin-resistant cell line has significantly lower levels of this protein than the parental sensitive (approximately 1.6-fold), suggesting that the actin modeling within the cisplatin resistant cell line is more dynamic than in the sensitive cell line, requiring faster cycling between actin polymerisation and depolymerisation, rendering the need for an actin capping protein less important.

Another two proteins intricately involved in the functioning of actin within cells were selected using the microarray technology. Thymosin β4 was expressed at lower levels in the cisplatin-resistant cell line (approximately 21.5-fold). This protein again is involved in the formation of actin filaments, however this time the protein binds to sequestered actin monomers, to prevent the polymerisation of actin filaments. Thymosin β4 was the gene exhibiting the largest difference in expression level between A2780 and A2780cisR cells, with the raw intensity data collected for this gene in the A2780 cell line being all above the upper level of detection. This gene was the most downregulated gene reported by Sherman-Baust *et al.* (2003) when they compared gene expression in A2780, and their own cisplatin-resistant daughter ovarian cancer cell line. They found a 95-fold difference in the expression of this protein. Both studies used A2780 as the cisplatin sensitive comparison. This is convincing evidence that this gene is important in the development of cisplatin resistance in human ovarian cancer cell lines. Interesting follow-up research would be to artificially reduce thymosin β4 expression, perhaps using an antisense RNA approach, and then observe the affect on CDDP sensitivity. If reduced expression mediated a resistant response, then this protein must play an active role in resistance.

Several studies have investigated the effect of altered thymosin β4 expression. Artificially elevating the cytosolic concentration of thymosin β4 short term, by microinjecting excessive synthetic β4 into living epithelial cells and fibroblasts, resulted in actin depolymerisation and the loss of actin stress fibres (Sanders *et al.* 1992) as would be predicted with the reduction in free monomeric G-actin to form F-actin filaments. Golla *et al.* (1997) found that long term elevation of thymosin β4 in NIH 3T3 cells resulted in the predicted increase in G-actin pools, but that this effect did not lead on to a reduction in F-actin, as the cells compensated for the change in

equilibrium by increasing expression of actin, which actually led to a two-fold increase in F-actin. This led to an increase in focal adhesions and spreading of the transfected cells. The opposite to what would be expected occurred as the cells altered actin expression to overcome the shortfall in available G-actin.

Interestingly, thymosin β10, an isoform of thymosin β4, was significantly upregulated in our cisplatin-resistant cell line (approximately 3.85-fold). Elevated thymosin β 10 expression in NIH3T3 cells resulted in enhanced actin polymerisation and increased actin bundles, these cells also exhibited enhanced motility and spreading, with higher chemotactic and wound healing activity (Sun *et al.* 1996). As with the Golla *et al.* (1997) study, the opposite to what would be predicted occurred, perhaps this again was the result of altered gene expression to overcome the reduction in available G-actin. Transfection of thymosin β4 into NIH 3T3 cells, resulted in an increase in stress fiber associated proteins; myosin IIA, α-actinin and tropomyosin, and in focal adhesion associated proteins; vinculin, talin and α5 integrin (Golla *et al.* 1997). Figure 4.9 presents a schematic of focal adhesion and interacting proteins, as well as summarizing some of the results discussed.

Sherman-Baust *et al.* (2003) reported filamin A to be downregulated in their cisplatin-resistant ovarian cancer cell line. Filamin primarily functions within platelets anchoring the actin cytoskeleton to the integral membrane glycoprotein Gplb-IX, which is involved in binding to blood clots (Lodish *et al.* 1995). It is of interest as it is an actin-crosslinking protein, having two actin binding sites. Our microarray results included three other actin-crosslinking proteins also showing reduced expression in the cisplatin-resistant cell line, namely α-actinin, MARCKS and dystrophin.

Prior cisplatin exposure therefore seems to have had a dramatic effect on the actin interactions within the treated cells. It is interesting to note that the two cell lines had a very different physical appearance. A2780 grow bundled together resembling grapes, whereas A2780cisR stretch out and flatten to the plastic surface of a tissue culture flask more efficiently. Many of the genes that were selected as being significant according to the microarray data are involved in the cytoskeleton and

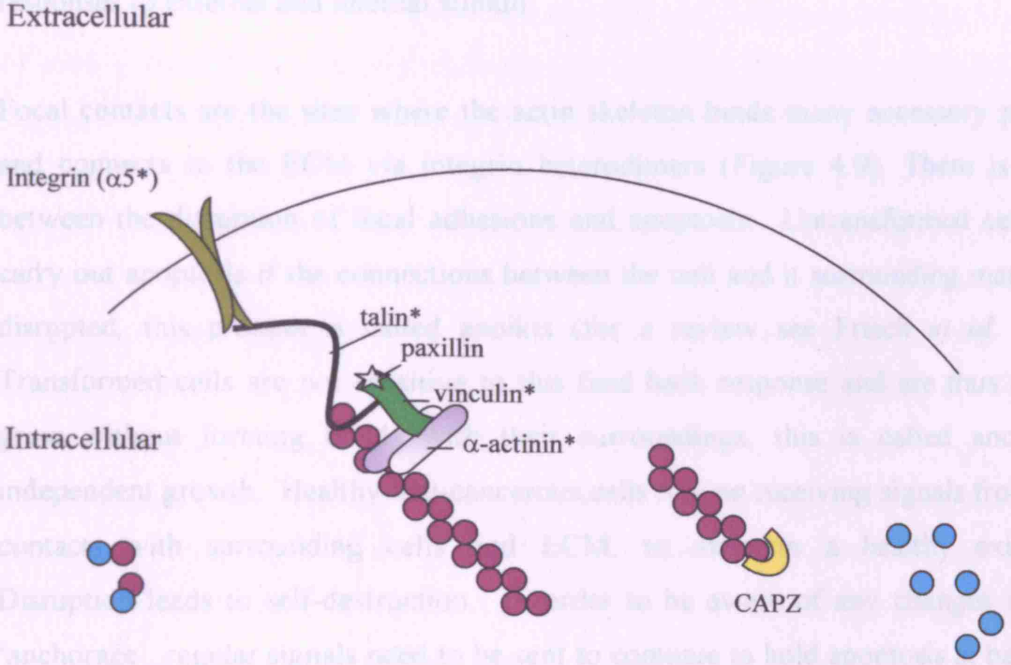


Key

- Thymosin β4/10
- G-actin (monomer)
- F-actin

| Significantly altered gene expression: | (Approx. Fold Diff.) |
|---|---|
| Paxillin | Upregulated in A2780cisR (1.5) |
| Thymosin β10 | Upregulated in A2780cisR (3.8) |
| Thymosin β4 | Downregulated in A2780cisR (1.5) |
| α-actinin 3 | Downregulated in A2780cisR (1.7) |

Figure 4.9. Focal Adhesion and Interacting Proteins. Also included is a list of gene showing significantly altered expression between A2780 and the cisplatin resistant cell line A2780cisR. Schematic of the focal adhesion adapted from Lodish *et al.* 1995, Molecular Cell Biology, third edition. * the expression of these genes was induced by transfecting cells with thymosin β4.
(Golla *et al.* 1997)

cellular adhesion. Research continues to consider the link between the extracellular matrix (ECM) and the network of molecules shaping the cell, and co-coordinating responses to external and internal stimuli.

Focal contacts are the sites where the actin skeleton binds many accessory proteins and connects to the ECM via integrin heterodimers (Figure 4.9). There is a link between the disruption of focal adhesions and apoptosis. Untransformed cells will carry out apoptosis if the connections between the cell and it surrounding matrix are disrupted, this process is called anoikis (for a review see Frisch *et al.* 2001). Transformed cells are not sensitive to this feed back response and are thus able to grow without forming bonds with their surroundings, this is called anchorage independent growth. Healthy non-cancerous cells rely on receiving signals from their contacts with surrounding cells and ECM, to maintain a healthy existence. Disruption leads to self-destruction. In order to be aware of any changes in their 'anchorage', regular signals need to be sent to continue to hold apoptosis at bay. For example focal adhesion kinase (FAK) is activated upon integrin binding with the ECM, it then interacts with a variety of other molecules as a protein tyrosine kinase, including paxillin and Src. Microinjection of peptides that interrupt the FAK integrin interaction, and anti-Fak antibodies induce apoptosis in fibroblasts (Hungerford *et al.* 1996). Permanent overexpression of active FAK prevents anoikis (Frisch *et al.* 1996). These constant signals act as a negative regulator of apoptosis. Increasingly evidence is suggesting that cancer cells can utilize these anti-apoptotic signals, mediated through contact with ECM proteins, via integrins and focal contacts, to prevent chemically induced apoptosis. Cell adhesion mediated drug resistance (or CAM-DR) is beginning to be recognized as an important factor in cancer drug resistance (Damiano *et al.* 1999). Hazelhurst *et al.* (2003) researched the impact on fibronectin-adherence to cellular sensitivity of myeloma cells to melphalan. Interestingly, adhesion inhibited melphalan induced apoptosis, by reducing melphalan induced mitochondrial depolarisation and caspase activation (Hazelhurst *et al.* 2003). No difference in melphalan-induced crosslinks was observed between the melphalan sensitive cells in suspension, and the relatively resistant cells adhered to fibronectin, assessed using the comet assay (Hazelhurst *et al.* 2003).

Expression of collagen type VI α1, type VI α 3 and type I α 2, was found to be significantly elevated in A2780cisR, while collagen type XI α1 was detected in higher levels in the parental cisplatin sensitive A2780. Collagen VI alpha 3 was one of many extracellular matrix proteins found to be the highly upregulated in other cisplatin-resistant human ovarian cancer cells (Sherman-Baust *et al.* 2003). When cisplatin sensitive cells were grown in the presence of collagen VI protein they became resistant (Sherman-Baust *et al.* 2003). Growing sensitive cells on plates pre-coated with collagen type I also induced a refractory response but to a lesser extent (Sherman-Baust *et al.* 2003). This is interesting as genes encoding both collagen type 1 and 6 (COL1A2, COL6A3, COL6A1) were found to be significantly up-regulated in the cisplatin-resistant A2780cisR cell line by, 3.7, 3.2 and 1.6-fold, respectively. The same publication was able to correlate an increase in collagen VI expression with increasing tumour grade. Low grade (highly or moderately differentiated) tumours expressed lower levels of COL6A3 than higher grade (poorly differentiated) tumours. Tumour grade is correlated with survival in ovarian cancer, and is a prognostic factor for the disease (Ozols *et al.* 1980). Patients with lower grade ovarian tumours, (and therefore lower COL6A3 expression), have higher survival rates, than patients with higher grade tumours (Ozols *et al.* 1980, Sherman-Baust *et al.* 2003).

The extracellular matrix (ECM) has been reported to be involved in suppressing apoptosis in small cell lung cancer (SCLC). Research published by Rintoul *et al.* (2002), found that SCLC cells exhibited enhanced expression of fibronectin, laminin and collagen IV, compared to normal lung tissue. They also found SCLC cells adhered to fibronectin, laminin or collagen IV were 'markedly protected' from apoptosis induced by the chemotherapeutics etoposide, adriamycin and cyclophosphamide. This protection was dependent on the interaction between the ECM proteins and β1 integrins on the surface of the cancer cells. Binding of the ECM to β1 integrins on the cell surface, activated a intracellular protein tyrosine kinase which blocked drug-induced caspase 3 signaling and the propagation of the death signal, alleviating apoptosis. Interestingly this effect was found to be downstream of DNA damage (Rintoul *et al.* 2002). Laminin has also been reported to mediate chemoresistance in SCLC (Fridman *et al.* 1990). Paradoxically, Sakamoto *et al.* (2001) in a three-fold cisplatin resistant human ovarian cancer cell line, showed

significantly reduced integrin β1 expression. Sherman-Baust *et al.* (2003) reports reduced integrin β 1 expression in their cisplatin-resistant human ovarian cancer cell line. β1 integrin clustering and enhanced tyrosine phosphorylation has been observed in human lung cancer cells (A549) in response to irradiation and cytotoxics including cisplatin (Cordes *et al.* 2004).

Further evidence as to the importance of the ECM in the apoptotic pathway came from Boudreau *et al.* (1995), who found that they could induce apoptosis in CIP-9 mammary epithelial cells by antibodies to β1 integrins and by the overexpression of stromelysin-1. Stromelysin-1 degrades ECM proteins, and expression of stromelysin 1 and stromelysin 2 was found to be significantly reduced, approximately 2.4- and 5.3-fold, respectively, in the cisplatin-resistant ovarian cancer cell line A2780cisR in this project. RT-PCR was not used to verify this result. As stromelysin promotes apoptosis, reduced expression would correlate with the development of a resistant phenotype. Another gene involved in the interface between the ECM and the actin cytoskeleton was significantly upregulated in A2780cisR. Paxillin is a multi-domain adaptor protein that processes adhesion and growth factor related signals.

While we observed no change in β1 integrin expression, results did show an increase in integrin β1 binding protein 1, ITGB1BP1 (also known as ICAP-1) in the cisplatin resistant cell line A2780cisR (approximately 1.8-fold). Initially this protein was identified as associating with the cytoplasmic tail of the β1 integrin binding to the COOH-terminal 13 amino acids (Chang *et al.* 2002). This protein has been shown to bind to the human metastatic suppressor protein NM23-H2. Together these proteins co-localise and precede focal adhesion formation in the leading edge and lamellipodia during the early stages of cell spreading, on fibronectin or collagen, ECM protein which interact with the β1 integrin. This is of interest because elevated NM23 has been correlated with increased cisplatin sensitivity in murine melanoma, human ovarian and breast carcinoma cell lines transfectants (Ferguson *et al.* 1996). They also reported increased formation of cisplatin ICLs in a NM23-H1 transfected breast carcinoma cell line (Ferguson *et al.* 1996). Conversely, elevated NM23 protein expression is correlated with diminished progression free survival in patients with ovarian cancer, treated with cisplatin-based chemotherapy (Srivatsa *et al.* 1996). It

has been suggested that NM23 proteins belong to a novel family of repair enzymes, after analysis of NM23-H2 revealed the active amino acid of the nuclease is a conserved lysine residue, the characteristic nucleophile of a class of repair proteins (Postel *et al.* 2000). NM23-H2 is predicted to be either a mismatch repair protein or a base excision repair protein (Postel *et al.* 2003).

Our cisplatin-resistant ovarian cancer cell line A2780cisR showed significantly lower p27 expression than the parental sensitive (approximately two-fold). p27 regulates a cells progression through the cell cycle, via the inhibition of the activity of cyclin-cyclin dependent kinase complexes. p27 is involved in inducing G1 arrest in response to DNA damage. A reduction in p27 leads to cell proliferation, and is correlated with increased tumour aggressiveness and poor prognosis in cancer patients (Ishihara *et al.* 1999). Elevated p27 protein levels have been linked with higher sensitivity to cisplatin in head and neck squamous cell carcinoma cell lines (Taguchi *et al.* 2004). Increased expression levels of p27 correlate with good responses to platinum-based chemotherapy in non-small cell lung cancer (Oshita *et al.* 2000). Both of these results confirm a link between higher p27 expression and sensitivity to platinum.

However over-expression of p27 in human colon carcinoma cells by transfection resulted in a loss of sensitivity to cisplatin (Dimanche-Boitrel *et al.* 1998). Hazelhurst *et al.* (2000) found that adhesion of myeloma cells to fibronectin via β1 integrins resulted in cell adhesion mediated drug resistance (CAM-DR) to the drug etoposide. Adhesion resulted in G1 arrest associated with increased p27 protein levels. Disruption of the cell-fibronectin contacts resulted in movement of the cells into S phase and a reduction in p27 levels and a drug-sensitive phenotype. Disruption of p27 alone, through antisense oligonucleotides also resulted in a drug sensitive phenotype without affecting fibronectin adhesion. This pinpoints the drug resistance to the induction of p27 via the fibronectin binding by β1 integrins.

Teicher *et al.* reported interesting findings in 'Science' journal in 1990. They exposed animals carrying EMT-6 murine mammary tumours to either; cisplatin, carboplatin, cyclophosphamide or thiotepa to develop *in-vivo* resistance. When these

tumour cells were exposed to the same agents *in-vitro*, no significant resistance was observed (Teicher *et al.* 1990). Follow up experiments found that drug resistance could be fully recapitulated *in-vitro* by growing these cells as 3-dimensional multicellular tumour spheroids, as opposed to monolayers (Kobayashi *et al.* 1993). These findings suggest drug resistance mechanisms that are operative only *in-vivo*.

Elevated p27 has been linked to resistance to γ–irradiation and chemotherapeutics in cancer cell lines (St Croix *et al.* 1996). St Croix and colleagues transferred cancer cells from monolayer to a 3D spheroid culture, and reported a significant elevation in p27 protein expression (up to 15-fold) in a panel of mouse and human carcinoma cell lines. When EMT-6 mammary tumour cell spheroids were treated with antisense oligonucleotides to reduce p27 expression, they reported reduced intercellular adhesion, increased cell proliferation, and sensitivity to 4-hydroperoxycyclophosphamide, and restored drug or radiation-induced cell-cycle arrest repressed in spheroid culture (St Croix et al. 1996). Xing *et al.* (2005) grew human ovarian cancer cell lines as multicellular spheroids, they reported elevated p27 protein expression. Antisense oligodeoxynucleotide (ASON) mediated downregulation of p27 resulted in reduced intracellular adhesion, increased cell proliferation and sensitised cells to paclitaxel (Xing *et al.* 2005). These results again link increased intercellular adhesion with elevated p27, and drug resistance.

Eymin *et al.* (1999) suggest that p27 overexpression leads to drug resistance by blocking apoptosis upstream of cytochrome C release and procaspase-3 activation. In two human hepatoma cell lines low dose cisplatin was shown to induce a modest increase in p27 expression after 72hrs, however high dose cisplatin treatment resulted in a reduction in p27 in both p53 wildtype and p53 negative cell lines (Qin *et al.* 2002).

Ubiquitin carboxy-terminal esterase L1 (UCHL1) is a protein implicated in p27 transportation and degradation, via its interaction with JAB1, a Jun activation domain binding protein that can bind to p27, and is involved in its cytoplasmic transportation for degradation (Caballero *et al.* 2002). UCHL1 expression was over 3.5-fold higher in A2780 than in A2780cisR. In effect, the elevated UCHL1 could reduce the

functional intracellular p27 levels in A2780, so that despite having higher p27 expression, having higher UCHL1 expression might negate the difference between the two cell lines.

To summarise, p27 is an important protein that regulates cellular behaviour, and mediates cell cycle arrest. Elevated p27 leads to G1 arrest and can result from integrin binding to the ECM and cell:cell binding via E-cadherin molecules (St Croix *et al.* 1998). When a cell is *in situ* and positioning itself within the 3D matrix that constitutes its surroundings it would be prudent for those interactions to prevent cell suicide (anoikis) and regulate progression through the cell cycle. This provides a stable environment maintained through complex feed-back loops.

Contradictory findings linking both the increase and the decrease in p27 with cancer drug resistance suggest that further research is required to elucidate the complicated role of p27 in cancer drug resistance.

Elevated expression of the genes inhibitor of DNA binding 2 (*ID2*) (approximately two-fold) and 3 (*ID3*) (approximately 4.2-fold) was observed in A2780cisR compared to A2780. RT-PCR experiments were not conducted. Cisplatin induced a transient upregulation in ID3 mRNA in the human sarcoma cell line MG-63 (Koyama *et al.* 2004), but no change in ID2 was observed. Cells with an enforced elevation in ID3 were more sensitive to cisplatin, through caspase 3 activation and generation of reactive oxygen species (ROS). It was concluded that ID3 was involved in cisplatin-induced cell death (Koyama *et al.* 2004).

Large scale comparative genomic hybridisation (CGH) analysis has been carried out into cisplatin-induced chromosomal changes (Wasenius *et al.* 1997, Kudoh *et al.* 1999, Takano *et al.* 2001, Yasui *et al.* 2004). CGH identifies regions of chromosomes that have undergone an increase or decrease in DNA copy number. It is possible that identified alterations in gene copy number could be associated with cisplatin resistance. The chromosomal location (cytogenetic band), of each of the 141 genes identified as being significantly altered between A2780 and A2780cisR was identified using LocusLink via the GeneCards web site (http://bioinfo.weizmann.ac.il/cards/index.shtml). Table 4.4 lists the genes in order

of chromosomal location. Gene location was analysed to reveal possible areas of loss or gain in DNA copy number.

Genomic losses or gains were predicted from the data presented in Table 4.4, by selecting localised chromosomal regions that contained at least three upregulated or downregulated genes in A2780cisR within a tight region of the chromosome. Once a list was produced, it was compared with published alterations in gene copy number associated with cisplatin resistance. This data is summarized in Table 4.5. There are several correlations between the predicted list and the published CGH data on cisplatin resistance. These correlations include evidence of gains in 3q21-26, 6q22-25 and 12p13, these regions contain the following genes 3q (TM4SF1, GYG, EVI1), 6q (MARCKS, PTPRK, CITED2, PCMT1) and 12p (CCND2, CDKN1B (p27), SLC2A3, A2M). Interestingly a gain in 12p12-13 would include the cell cycle proteins p27 and cyclin D2. Further study into altered copy number in relation to cisplatin resistance is needed to fully understand the importance of these results

Table 4.4. 141 genes listed according to chromosomal location. Red data indicates the gene was upregulated in A2780cisR, black data indicates the gene was down regulated in A2780cisR.

| Accession | Symbol | Name | Gene Location |
|---|---|---|---|
| R31701 | COL11A1 | Collagen type XI alpha 1 | 1p21 |
| R20666 | EDG1 | endothelial differentiation, sphingolipid G-protein-coupled receptor, 1 | 1p21 |
| AA410188 | C1orf29 | chromosome 1 open reading frame 29 | 1p22.3 |
| H27986 | LMO4 | LIM domain only 4 | 1p22.3 |
| AA430524 | CAPZB | capping protein (actin filament) muscle Z-line, beta | 1p36.1 |
| AA482119 | ID3 | inhibitor of DNA binding 3 | 1p36.13-p36.12 |
| N67487 | MFAP2 | microfibrillar-associated protein 2 | 1p36.1-p35 |
| AA406020 | G1P2 | interferon, alpha-inducible protein (clone IFI-15K) | 1p36.33 |
| AA035144 | MEF2D | MADS box transcription enhancer factor 2, polypeptide D | 1q12-q23 |
| AA458884 | S100A2 | S100 calcium binding protein 2 | 1q21 |
| T67552 | ARNT | aryl hydrocarbon receptor nuclear translocator | 1q21 |
| AA464731 | S100A11 | S100 calcium binding protein A11 (calgizzarin) | 1q21 |
| AA456298 | HIST2H2BE | histone 2, H2be | 1q21-q23 |
| H79353 | FCER1G | Fc fragment of IgE, high affinity I, receptor for; gamma | 1q23 |
| AA243749 | DDR2 | discoidin domain receptor family, member 2 | 1q23.3 |
| AA453774 | RGS16 | regulator of G-protein signalling 16 | 1q25-q31 |
| AA017544 | RGS1 | regulator of G-protein signalling 1 | 1q31 |
| T74567 | FHR-3 | complement factor H related 3 | 1q31.3 |
| AA703392 | HFL1 | H factor (complement)-like 1 | 1q32 |
| AA838691 | EPHX1 | epoxide hydrolase 1, microsomal (xenobiotic) | 1q42.1 |
| AA486085 | TMSB10 | Thymosin beta 10 | 2p11.2 |
| AA293671 | CD8B1 | CD8 antigen, beta polypeptide 1 (p37) | 2p12 |
| T58873 | FOSL2 | FOS-like antigen 2 | 2p23-p22 |
| H82442 | ID2 | inhibitor of DNA binding 2, | 2p25 |
| AA457038 | ITGB1BP1 | integrin beta 1 binding protein 1 | 2p25.2 |
| AA018457 | GAD1 | glutamate decarboxylase 1 (brain, 67kDa) | 2q31 |
| AA488075 | STAT1 | signal transducer and activator of transcription 1, 91kDa | 2q32.2 |
| H79047 | IGFBP2 | insulin-like growth factor binding protein 2 | 2q33-q34 |
| R62603 | COL6A3 | Collagen type VI alpha 3 | 2q37 |
| AA489699 | COPS8 | COP9 constitutive photomorphogenic homolog subunit 8 | 3p14.3 |
| AA036881 | CCR1 | chemokine (C-C motif) receptor 1 | 3p21 |
| H29322 | CAMK1 | calcium/calmodulin-dependent protein kinase I | 3p25.2 |
| AA455964 | GTF2E1 | general transcription factor IIE, polypeptide 1, alpha 56kDa | 3q21-q24 |
| AA487893 | TM4SF1 | transmembrane 4 superfamily member 1 | 3q21-q25 |
| AA411679 | GYG | Glycogenin | 3q24-q25.1 |
| AA181023 | EVI1 | ecotropic viral integration site 1 | 3q26.2 |
| AA670438 | UCHL1 | ubiquitin carboxyl-terminal esterase L1 | 4p14 |
| H23235 | PDGFRA | platelet-derived growth factor receptor, alpha polypeptide | 4q11-q13 |
| AA455067 | SNCA | synuclein, alpha | 4q21 |

| | | | |
|---|---|---|---|
| AA775616 | SPP1 | Secreted phosphoprotein 1 | 4q21-q25 |
| N57754 | TNRC3 | Trinucleotide repeat containing 3 | 4q28.3 |
| AA041400 | LRBA | LPS-responsive vesicle trafficking, | 4q31.23 |
| H07899 | VEGFC | Vascular endothelial growth factor C | 4q34.1-q34.3 |
| R40897 | OXCT5 | 3-oxoacid CoA transferase | 5p13 |
| AA455910 | F2R | coagulation factor II (thrombin) receptor | 5q13 |
| AA101875 | CSPG2 | chondroitin sulfate proteoglycan 2 (versican) | 5q14.3 |
| AA427801 | HAPLN1 | hyaluronan and proteoglycan link protein 1 | 5q14.3 |
| H99681 | DP1 | polyposis locus protein 1 | 5q22-q23 |
| AA497033 | CDO1 | cysteine dioxygenase, type I | 5q22-q23 |
| H95960 | SPARC | secreted protein, acidic, cysteine-rich (osteonectin) | 5q31.3-q32 |
| H15677 | PPP2R2B | protein phosphatase 2 regulatory subunit B (PR 52), beta | 5q31-q33 |
| AA452933 | HIST1H2AC | histone 1, H2ac | 6p21.3 |
| H70775 | HIST1H2BC | histone 1, H2bc | 6p21.3 |
| T66815 | HIST1H1C | histone 1, H1c | 6p21.3 |
| AA485752 | ABCF1 | ATP-binding cassette, sub-family F (GCN20), member 1 | 6p21.33 |
| AA426352 | H2A.1 | Histone H2A.1 | 6p22.1 |
| H17398 | BA13 | brain specific angiogenesis inhibitor | 6q12 |
| AA482231 | MARCKS | myristoylated alanine-rich protein kinase C substrate | 6q22.2 |
| R79082 | PTPRK | protein tyrosine phosphatase, receptor type, K | 6q22.2-23.1 |
| AA115076 | CITED2 | Cbp/p300-interacting transactivator, 2 | 6q23.3 |
| T68453 | PCMT1 | protein-L-isoaspartate (D-aspartate) O-methyltransferase | 6q24-q25 |
| AA598483 | TAX1BP1 | Tax1 binding protein 1 | 7p15 |
| AA779165 | ARL4 | ADP-ribosylation factor-like 4 | 7p21-p15.3 |
| H25223 | MEOX2 | mesenchyme homeo box 2 | 7p22.1-p21.3 |
| AA446659 | TAC1 | tachykinin, precursor 1 | 7q21-q22 |
| AA490172 | COL1A2 | collagen, type I, alpha 2 | 7q22.1 |
| AA598610 | MEST | mesoderm specific transcript homolog (mouse) | 7q32 |
| AA478279 | INDO | indoleamine-pyrrole 2,3 dioxygenase | 8p12-p11 |
| AA487460 | DPYSL2 | dihydropyrimidinase-like 2 | 8p22-p21 |
| AA454868 | PDGFRL | platelet-derived growth factor receptor-like | 8p22-p21.3 |
| AA456621 | GGH | gamma-glutamyl hydrolase | 8q12.1 |
| AA464417 | IFITM3 | interferon induced transmembrane protein 3 (1-8U) | 8q13.1 |
| N92901 | FABP4 | fatty acid binding protein 4, adipocyte | 8q21 |
| AA877595 | CDKN2A | cyclin-dependent kinase inhibitor 2A (p16) | 9p21 |
| W73874 | CTSL | cathepsin L | 9q21-q22 |
| AA778198 | PBX3 | pre-B-cell leukemia transcription factor 3 | 9q33-q34 |
| R59579 | PTGDS | prostaglandin D2 synthase 21kDa (brain) | 9q34.2-q34.3 |
| AA464861 | CREM | cAMP responsive element modulator | 10p12.1-p11.1 |
| AA486321 | VIM | Vimentin | 10p13 |

| | | | |
|---|---|---|---|
| AA608558 | PFKP | phosphofructokinase, platelet | 10p15.3-15.2 |
| R38433 | PFKP | phosphofructokinase, platelet | 10p15.3-p15.2 |
| R38433 | PFKP | phosphofructokinase, platelet | 10p15.3-p15.2 |
| AA677185 | ANK3 | ankyrin 3, node of Ranvier (ankyrin G) | 10q21 |
| AA630104 | LIPA | lipase A, lysosomal acid, cholesterol esterase | 10q23.2-q23.3 |
| AA634006 | ACTA2 | actin, alpha 2, smooth muscle, aorta | 10q23.3 |
| N63988 | IFIT2 | interferon-induced protein with tetratricopeptide repeats 2 | 10q23.31 |
| AA489640 | IFIT1 | interferon-induced protein with tetratricopeptide repeats 1 | 10q25-q26 |
| H60549 | CD59 | CD59 antigen p18-20 | 11p13 |
| AA862371 | IFITM2 | interferon induced transmembrane protein 2 (1-8D) | 11p15.5 |
| AA476438 | HRASLS3 | HRAS-like suppressor 3 | 11q12.3 |
| H61243 | UCP2 | uncoupling protein 2 (mitochondrial, proton carrier) | 11q13 |
| N94820 | DIPA | hepatitis delta antigen-interacting protein A | 11q13.1 |
| AA196000 | ACTN3 | actinin, alpha 3 | 11q13-q14 |
| AA644088 | CTSC | cathepsin C | 11q14.1-q14.3 |
| AA419251 | IFITM1 | interferon induced transmembrane protein 1 (9-27) | 11q15.5 |
| W51794 | MMP3 | matrix metalloproteinase 3 (stromelysin 1, progelatinase) | 11q22.3 |
| AA857496 | MMP10 | matrix metalloproteinase 10 (stromelysin 2) | 11q22.3 |
| AA412053 | CD9 | CD9 antigen (p24) | 12p13 |
| H84154 | CCND2 | cyclin D2 | 12p13 |
| AA630082 | CDKN1B | cyclin-dependent kinase inhibitor 1B (p27, Kip1) | 12p13.1-p12 |
| AA406552 | SLC2A3 | solute carrier family 2, member 3 | 12p13.3 |
| H06516 | A2M | alpha-2-macroglobulin | 12p13.3-p12.3 |
| H06516 | A2M | alpha-2-macroglobulin | 12p13.3-p12.3 |
| AA775447 | A2M | alpha-2-macroglobulin | 12p13.3-p12.3 |
| AA137031 | SOCS2 | suppressor of cytokine signaling 2 | 12q |
| AA019459 | PTK9 | PTK9 protein tyrosine kinase 9 | 12q12 |
| AA630374 | DUSP6 | dual specificity phosphatase 6 | 12q22-q23 |
| AA430574 | PXN | Paxillin | 12q24 |
| AA598653 | POSTN | periostin, osteoblast specific factor | 13q13.3 |
| AA453759 | SPRY2 | sprouty homolog 2 (Drosophila) | 13q22.2 |
| AA425401 | STK24 | serine/threonine kinase 24 (STE20 homolog, yeast) | 13q31.2-q32.3 |
| AA291389 | ISGF3G | interferon-stimulated transcription factor 3, gamma 48kDa | 14q11.2 |
| AA479199 | NID2 | nidogen 2 (osteonidogen) | 14q21-q22 |
| AA284072 | CDKN3 | cyclin-dependent kinase inhibitor 3 | 14q22 |
| AA485427 | CRIP2 | cysteine-rich protein 2 | 14q32.3 |
| H09721 | MARK3 | MAP/microtubule affinity-regulating kinase 3 | 14q32.3 |
| H50251 | SH3GL3 | SH3-domain GRB2-like 3 | 15q24 |
| N49703 | CHD2 | chromodomain helicase DNA binding protein 2 | 15q26 |
| N80129 | MT1X | metallothionein 1X | 16q13 |
| AA703449 | MEIS4 | Meis1, myeloid ecotropic viral integration site 1 homolog 4 | 17p11.1 |

| | | | |
|---|---|---|---|
| AA497055 | PSMD12 | proteasome 26S subunit, non-ATPase, 12 | 17q24.2 |
| H91647 | CLUL1 | clusterin-like 1 (retinal) | 18p11.32 |
| W49619 | CDH2 | cadherin 2, type 1, N-cadherin (neuronal) | 18q11.2 |
| AA669136 | TCF4 | transcription factor 4 | 18q21.1 |
| R91950 | CYB5 | cytochrome b-5 | 18q23 |
| AA630800 | IFI30 | interferon, gamma-inducible protein 30 | 19p13.1 |
| T63511 | NOTCH3 | Notch homolog 3 (Drosophila) | 19p13.12 |
| AA485371 | BST2 | bone marrow stromal cell antigen 2 | 19p13.2 |
| AA398400 | CNN1 | calponin 1, basic, smooth muscle | 19p13.2-p13.1 |
| N76927 | BLVRB | biliverdin reductase B (flavin reductase (NADPH)) | 19q13.1-q13.2 |
| T95289 | ERCC1 | excision repair cross-complementing group 1 | 19q13.2-q13.3 |
| T47443 | PROCR | protein C receptor, endothelial (EPCR) | 20q11.2 |
| AA457118 | TOMM34 | translocase of outer mitochondrial membrane 34 | 20q13.12 |
| N52496 | BTG3 | BTG family, member 3 | 21q21.1 |
| H99676 | COL6A1 | collagen, type VI, alpha 1 | 21q22.3 |
| AA457042 | MX1 | myxovirus (influenza virus) resistance 1, | 21q22.3 |
| AA490208 | GSTT2 | glutathione S-transferase theta 2 | 22q11.23 |
| AA129777 | SLC16A3 | solute carrier family 16, member 3 | 22q12.3-q13.2 |
| AA701914 | SREBF2 | sterol regulatory element binding transcription factor 2 | 22q13 |
| AA045965 | CASK | calcium/calmodulin-dependent serine protein kinase | Xp11.4 |
| AA461118 | DMD | dystrophin | Xp21.2 |
| AA598640 | MID1 | midline 1 (Opitz/BBB syndrome) | Xp22 |
| H04789 | GYG2 | glycogenin 2 | Xp22.3 |
| AA775872 | GPC3 | glypican 3 | Xp26.1 |
| AA634103 | TMSB4X | thymosin, beta 4, X-linked | Xq21.3-q22 |

| Number of Genes | Chromosomal Location | Correlation with previous Research Publications |
|---|---|---|
| **Gains** | | |
| 5 genes | 2p11.2-25.2 | |
| 3 genes | 3q21-26 | Gains 3q13-24 cisplatin resistant human bladder cancer cell line (T24/DDP10). Yasui *et al.* 2004 |
| 4 genes | 6q22-25 | Gains 6q13-16 cisplatin resistant human ovarian cancer cell lines. Wasenius *et al.* 1997<br>Gains 6q21-25 cisplatin resistant human ovarian cancer cell lines. Takano *et al.* 2001<br>Gains 6q24-27 cisplatin resistant human bladder cancer cell line (KK47/DDP10).<br>Yasui *et al.* 2004. |
| 4 genes | 12p12-13 | Gains 12p13 in samples from ovarian cancer patients that did not respond to cisplatin/doxorubicin/cyclophosphamide, as opposed to the patients that responded to cisplatin therapy, who showed no gain in this region. Kudoh *et al.* 1999. |
| **Losses** | | |
| 7 genes | 1q21-31 | Gains 1q31-32 cisplatin resistant human colonic cancer cell line (HT-29/cDDP).<br>Yasui *et al.* 2004.<br>Gains 1q21-22 cisplatin resistant ovarian cancer patients. Kudoh *et al.* 1999, Takano *et al.* 2001 |
| 3 genes | 2q31-34 | Loss 2 cisplatin resistant human ovarian cancer cell line (A2780/CP). Wasenius et al 1997<br>Gains 2q14.1-33 cisplatin resistant human ovarian cancer cell lines. Wasenius *et al.* 1997 |
| 5 genes | 6p21.3-22.1 | |
| 5 genes | 10q21-26 | Loss 10q12-15 cisplatin resistant human ovarian cancer cell lines. Takano *et al.* 2001 |
| 3 genes | 19p13.1-13.2 | |

Table 4.5. Correlation of microarray results of genomic locations with clusters of three or more genes showing similar patterns of expression, with genomic gains and loses associated with cisplatin resistance

## Chapter 5: Discussion

### 5.1. Discussion of Results Chapters

While much work in the past has focused on the effect of cisplatin intrastrand crosslinks in relation to clinical outcome (Reed *et al.* 1986, 1987, 1988, Poirier *et al.* 1993), limited research has been published into cisplatin interstrand crosslinking. Clinical research into cisplatin-ICL formation and unhooking was previously limited by an inability to measure sensitively this critical lesion using a low cell number. The conventional technique used to assess ICL levels, alkaline elution (Rudd *et al.* 1995), has been overtaken by a technique used previously to measure DNA single strand breaks (Ostling *et al.* 1984, Fairbairn *et al.* 1995). The single cell gel electrophoresis 'comet' assay has facilitated the effective measurement of ICL levels at a single cell level in a number of clinical settings (Spanswick *et al.* 2002, Webley *et al.* 2001).

Utilising the comet assay, the novel work presented in this thesis examines two models of the effect of cisplatin exposure on human ovarian tumour cells. The first model reflects *in-vivo* exposure to cisplatin, whereby CDDP-ICL formation and repair are examined *in-vitro* using tumour cells from patients previously treated with platinum-based chemotherapy (cisplatin or carboplatin). This data is compared to the ICL formation and repair kinetics from tumour cells from platinum-naïve patients. The second model reflects *in-vitro* cisplatin exposure, utilising a human ovarian cancer cell line from a platinum-naïve patient (A2780), and a cisplatin-resistant sub-line (A2780cisR), produced when A2780 cells were exposed to increasing doses of cisplatin over time.

Tumour, and where possible, mesothelial cells, were harvested from ascites, and from primary tumour tissue, isolated from ovarian cancer patients. As discussed in Chapter 2, there was no significant difference in cisplatin-ICL formation up to the peak of crosslinking, nine-hours after exposure, between ovarian tumour cells from patients previously treated with platinum (carboplatin or cisplatin) and platinum-naïve patients ($p=0.256$). This would suggest insignificant upstream resistance activity in our nineteen human ovarian tumour samples, implying that in the clinic these resistance mechanisms were not significant. This is interesting, as a number of

publications have reported a correlation between key upstream resistance proteins and response to platinum chemotherapy in human ovarian cancer patients (Cheng *et al.* 1997, Kigawa *et al.* 1998, Lewandowicz *et al.* 2002).

As reviewed in Chapter 2, where ovarian cancer patients have a history of treatment with platinum-based chemotherapeutics (cisplatin and carboplatin), their tumour cells generally showed enhanced cisplatin-ICL unhooking, when assessed *ex-vivo*. Platinum-naïve patients yield tumour samples that are generally only capable of limited cisplatin-ICL unhooking, whereby the majority of ICLs tend to persist after the peak of crosslinking ($p=0.04$). This is of interest as clinical research has previously correlated enhanced ICL repair in clinical samples with a patient's previous exposure to crosslinking chemotherapeutics (Spanswick *et al.* 2002). Our results found that enhanced ICL unhooking in a patient's ovarian tumour cells was always independent of any elevated ICL unhooking in the comparative mesothelial cell sample.

In conclusion, the clinical research presented in Chapter 2, identifies a significant difference in ICL repair capability between tumour cells from patients previously exposed to cisplatin or carboplatin, and tumour cells from platinum-naïve patients. This could be explained by the active selection of tumour cells with this ability from a heterogeneous tumour cell population, during the patient's initial exposure to platinum. The survival of these clones and the subsequent repopulation, as these clones divided, could explain this result. This would provide a direct link between the ability of cells to unhook platinum ICLs, and presumably to better survive a cytotoxic onslaught, and patient relapse, as the tumour tissue survives and repopulates. Evidence towards this selection pressure theory was illustrated by the results gained from one patient, who provided tumour tissue before platinum treatment, in the form of ascites, and then after several doses of carboplatin, during interval debulking surgery. While the initial tumour sample showed limited cisplatin-ICL repair, the sample collected at surgery showed significantly enhanced cisplatin ICL unhooking, repairing approximately 80% more crosslinks. This is of interest as the initial doses of chemotherapy would presumably have killed the platinum-sensitive tumour tissue, leaving the inherently refractive tumour tissue to be surgically removed. This patient received three doses of combined

carboplatin/paclitaxel between mid-June until interval debulking surgery in early September of the same year. The question arises, would this provide enough time for this patient's tumour tissue to become significantly resistant to cisplatin? Interesting research by Di Nicolantonio *et al.* (2005) provides a possible answer to this question. Their data suggest that human tumour tissue exhibits altered expression of key drug-resistance genes following six-days of *ex-vivo* exposure to a wide range of chemotherapeutics. This research reported elevated ERCC1 expression in both ovarian and breast tumour cells following a six-day *in-vitro* exposure to cisplatin.

Examining clinical platinum resistance in relation to ICL unhooking *in-vitro* proved complicated. For example, two patients were clinically resistant to platinum at the time that tissue samples were collected during treatment, indicated by tumour progression while undergoing treatment. Tumour samples from these patients showed no evidence of elevated ICL unhooking, or altered ICL formation. This implies that other resistance mechanisms were functioning within these patient's tumour tissue, for instance, replicative bypass (translesion synthesis) or an altered apoptotic response. A more extensive study with a larger sample number would be necessary to fully examine the relationship between platinum-ICL unhooking capability and patient prognosis following platinum chemotherapy.

Chapter 3 presented the results generated using the *in-vitro* cell line model of cisplatin resistance. A human ovarian cancer cell line, developed from a chemo-naïve patient, was exposed over-time to increasing doses of cisplatin, producing the cisplatin resistant cell line A2780cisR (Louie *et al.* 1985, Behrens *et al.* 1987). When cisplatin ICL formation and unhooking was examined over time using the comet assay, following an equimolar dose of cisplatin, both cell lines showed similar ICL formation, leading to a peak level nine-hours after exposure. There was, therefore, no evidence of any upstream resistance mechanisms inhibiting ICL formation in the resistant cell line compared to the sensitive cell line. This is interesting as a large number of research publications using paired sensitive and resistant human ovarian cancer cell lines have shown evidence of enhanced upstream resistance mechanisms linked to resistance to crosslinking agents (Horton *et al.* 1999), and specifically to cisplatin (Hamilton *et al.* 1985, Godwin *et al.* 1992, Hamaguchi *et al.* 1993, Kudoh *et*

*al.* 1994, Shellard *et al.* 1991, Oguchi *et al.* 1994, Kikuchi *et al.* 1997, Perego *et al.* 1998, Holford *et al.* 2000).

Two upstream resistance mechanisms have been previously reported in the A2780cisR cells compared to the parental A2780 cells, including reduced cisplatin accumulation, following cisplatin exposure (Holford *et al.* 1998), and elevated glutathione (GSH) level (Behrens *et al.* 1987). Several publications have reported increased cisplatin sensitivity in A2780cisR cells pre-treated with BSO, suggesting that reduction of GSH results in increased cytotoxicity (Perez *et al.* 2001, Jansen *et al.* 2002). Our data suggests that the reported elevated GSH and reduced CDDP accumulation in A2780cisR cells had little impact on ICL formation within this model system. It is possible that GSH is causing cisplatin resistance by supporting or facilitating DNA repair processes, as several publications have reported a link between GSH level and platinum-DNA repair capacity (Lai *et al.* 1989, Meijer *et al.* 1990, Alaoui-Jamali *et al.* 1994).

In the time period following the peak of crosslinking between the nine-hour and 48-hour time points, the cisplatin-resistant cells unhooked significantly more cisplatin-ICLs (~80%) than the sensitive cells (~26%), measured using the comet assay. This suggests that the cisplatin resistant A2780cisR cells have an enhanced cisplatin-ICL repair pathway, compared to the parental cells, this would therefore be an adapted capability, induced by the prolonged exposure of A2780 cells to cisplatin. Previous cell line research into cisplatin ICL-repair has shown enhanced overall genomic and gene specific ICL repair in cisplatin-resistant cell lines, compared to parental sensitive cell lines (Zhen *et al.* 1992, Johnson *et al.* 1994a and b, Petersen *et al.* 1996, Esaki *et al.* 1996)).

In order to pinpoint the process in the resistant cells, that enabled these cells to unhook the cisplatin-ICLs more efficiently than the parental cells, the responses of both cell lines to another interstrand crosslinking agent, namely mechlorethamine, were tested using the comet assay. Our cytotoxicity data, produced using the SRB assay showed that A2780cisR cells were approximately 1.5-fold resistant to mechlorethamine compared to A2780 cells. Interestingly, both cell lines showed similar ICL formation at the peak of crosslinking, which occurred immediately after a

one-hour drug exposure. Following the peak of crosslinking, both cell lines rapidly and efficiently unhooked approximately 60% of mechlorethamine-ICLs by the nine-hour time point. A2780cisR cells were slightly more efficient at unhooking the remaining ICL, so that by the 48-hour time point, A2780 cells had unhooked approximately 76% of all induced ICL, and A2780cisR cells had unhooked approximately 88% of all induced ICL. These results indicate that both cells lines process and repair mechlorethamine-induced ICLs in a similar fashion. These findings suggest that the enhanced ICL unhooking observed in A2780cisR cells treated with cisplatin is specific to cisplatin-induced ICL rather than to repair of all types of ICL.

As discussed, the interstrand crosslinks formed by mechlorethamine and cisplatin differ significantly, with the cisplatin-ICL forming between guanines in the sequence d(GpC), and mechlorethamine-ICL forming at the sequence d(GpNpC). The cisplatin lesion has a half-life of approximately 29 hours, with the peak of crosslinking occurring approximately nine-hours after a one-hour drug exposure (Dronkert and Kanaar, 2001, and data from Chapter 3). The mechlorethamine ICL has a half-life of approximately two hours, with the peak of crosslinking occurring immediately after a one-hour drug exposure (Dronkert and Kanaar, 2001, and data from Chapter 3). Differences in the repair of these lesions in mammalian cells have also been suggested. For example, research using CHO cell line mutants showed that only ERCC1 and XPF are required for the initial unhooking of the mechlorethamine-induced ICL, whereas cisplatin ICL unhooking required the additional XPB, XPG and XRCC3 proteins, as well as ERCC1/XPF (DeSilva *et al.* 2000 and 2002b). Also, DNA double strand breaks have been detected as an intermediate in the repair of mechlorethamine-ICL in exponentially growing yeast (McHugh *et al.* 2000) and in CHO cells (DeSilva *et al.* 2000), but not in the processing of cisplatin-ICL in CHO cells (DeSilva *et al.* 2002b).

The UV sensitivity experiments revealed that both cell lines had very similar $IC_{50}$ values. This suggests little difference in NER function between the two cell lines, as the cytotoxic DNA lesions induced by UV exposure, the cyclobutane pyrimidine dimer (CPD) and the pyrimidine (6-4) photoproducts (6-4PPs) are repaired by NER (Thoma, 1999, Aboussekhra *et al.* 1995, Batty *et al.* 2000). This is interesting as

there is still debate as to which type of cisplatin-DNA adduct is lethal (Eastman, 1999). As discussed in the introduction, cisplatin intrastrand crosslinks have been suggested to be the major cytotoxic lesion induced by this compound (Fichtinger-Schepman *et al.* 1995). Cells repair cisplatin-intrastrand crosslinks via NER (Moggs *et al.* 1996, 1997, Szymkowski *et al.* 1992, Huang *et al.* 1994 and Visse *et al.* 1994). Therefore the lack of any evidence for differential NER repair function between the two cell lines, implies no difference in the repair of cisplatin intrastrand crosslinks either. When Colella and colleagues (2001) investigated cisplatin-DNA adduct repair in the N-*ras* gene using the A2780 and A2780cisR cell lines and quantitative PCR, which essentially gauges the repair of bifunctional cisplatin adducts, they reported similar kinetics of formation and repair by both cell types. Approximately 90% of bifunctional cisplatin-DNA lesions are intrastrand crosslinks, this technique therefore reflects the repair of this type of lesion in A2780 and A2780cisR cells (Fichtinger-Schepman *et al.* 1987). As our research into the formation and repair of cisplatin-interstrand crosslinks, using the comet assay, showed clearly enhanced ICL repair in the resistant A2780cisR cells compared to A2780 cells, we can postulate that the cellular processing of this type of lesion is the most important factor in cisplatin sensitivity in our human ovarian cancer cell lines.

In summary, the cell lines research presented in Chapter 3, demonstrates that the *in-vitro* exposure of A2780 human ovarian cancer cells to increasing doses of cisplatin, has produced cells which are cisplatin resistant and capable of enhanced cisplatin-ICL unhooking, but show little difference in the unhooking of another type of ICL, induced by the nitrogen mustard compound mechlorethamine. These cisplatin-resistant cells (A2780cisR) show no major difference in UV sensitivity, implicating similar NER by both cell lines, which has implications for the possible repair of the cisplatin intrastrand crosslinks by both cell lines, as these lesions are repaired via NER.

Importantly, the *in-vitro* exposure of A2780 cells to cisplatin to produce A2780cisR cells has produced the same phenotype as the exposure of human ovarian tumour cells to cisplatin *in-vivo* reported in Chapter 2, namely enhanced cisplatin-ICL unhooking. These paired cell lines therefore provide an excellent *in-vitro* model for the situation observed in the clinic, they are also easily manipulated and abundant.

Therefore, as A2780cisR cells were produced from A2780 cells via exposure to increasing doses of cisplatin, any difference in gene expression between the two cell lines should be directly linked to cisplatin exposure. A full genetic analysis of the two cell lines was carried out using nylon microarrays, and the expression of several genes was confirmed using RT-PCR. The aim of this research was to identify stable genetic differences between the two cell lines caused by the prolonged cisplatin exposure, which could be responsible for the observed cisplatin resistance, and enhanced cisplatin-ICL unhooking capability. These results were presented in Chapter 4.

Microarray experiments were designed using three technical repeats (using the same RNA sample) and five biological repeats (using different RNA samples) for each cell line. All of the data generated was processed by a bioinformatisist (Dr. Stephen Henderson, The Wolfson Institute, UCL), in order to clarify the genes displaying a significant difference in expression between A2780 and A2780cisR cells. In total our microarray experiments and statistical analysis revealed 141 genes showing significantly altered levels of expression between A2780 cells and A2780cisR cells.

The expression of genes from many different functional groups appeared to be altered in the resistant cell line, implicating the wide-ranging effect of cisplatin on cellular functioning.

By analysing the position of each of the genes displaying significantly altered expression between the two cell lines and mapping back to the blueprint of the GF211 filter, by analysing the expression of genes featured more that once on the filter and on the 'significant' list, and through directed RT-PCR verification of the results, it became clear that the data produced using this method of expression analysis was consistently reproducible and accurate in terms of what was actually occurring at a cellular level. Having successfully carried out these 'quality control' tests the results produced using this technique were taken to represent actual differences in gene expression between the two human ovarian cancer cell lines A2780 and A2780cisR.

Specifically there was elevated expression of the NER protein, ERCC1, in the resistant cell line. ERCC1 is known to be an important protein involved in mediating

cellular response to cisplatin exposure (Altaha *et al.* 2004). As previously discussed, CHO cells lacking this protein are hypersensitive to cisplatin (Hoy *et al.* 1985, Damia *et al.* 1996). Transfection of ERCC1 into CHO cells lacking this protein, facilitated cisplatin-DNA adduct repair, assessed using atomic absorption spectroscopy (Lee *et al.* 1993). Ferry *et al.* (2000) analysed ERCC1 expression in cisplatin-resistant cell lines derived from A2780 cells, they reported a consistent increase in the steady state levels of ERCC1 in the resistant cell lines.

Clinical studies also underline the importance of ERCC1 in cellular response to cisplatin. Breast and ovarian tumour cells harvested from patients, and subsequently exposed *ex-vivo* to cisplatin for six days showed significantly elevated ERCC1 expression, $p=0.02$ and $p=0.01$, respectively (Di Nicolantonio *et al.* 2005). Clinical research using human tissue samples has revealed that elevated ERCC1 expression correlates with poor response to platinum-based chemotherapy in non-small cell lung cancer (NSCLC) (Rosell *et al.* 2001), gastric cancer (Metzger *et al.* 1998) and ovarian cancer (Dabholkar *et al.* 1992 and 1994). Interestingly, clear cell ovarian carcinoma is inherently resistant to cisplatin, and expresses elevated ERCC1 and XPB compared to other forms of ovarian cancer (Reed *et al.* 2003).

Another interesting result produced using microarrays was the significantly altered expression of actin and actin associated proteins (especially thymosin β4), focal adhesion proteins, cytoskeletal proteins and ECM proteins. Initially focusing on the higher levels of collagen types I and VI in the resistant cell line compared to the sensitive cell line, elevated collagen VI alpha 3 (COL6A3) levels were detected in another cisplatin resistant cell line derived from A2780, using serial analysis of gene expression (SAGE) profiling (Sherman-Baust *et al.* 2003). This group also grew A2780 cells in tissue culture plates pre-coated with human collagen VI, and reported significantly elevated cisplatin resistance (Sherman-Baust *et al.* 2003). Semi-quantitative RT-PCR and immunofluorescence experiments correlated COL6A3 expression with tumour grade, with lower levels of expression in low grade (highly to moderately differentiated) tumours, and higher levels in high grade (poorly differentiated) tumours (Sherman-Baust *et al.* 2003). Tumour grade has been closely related to a patient's prognosis in ovarian cancer with higher-grade tumours correlating with reduced survival (Ozols *et al.* 1980).

When analysing tumour cell expression of ECM molecules, it is relevant that non-transformed cells receive signals produced through contacts formed to the ECM and to neighbouring cells, that reassure the cell that it is existing within a healthy environment (Raff, 1992, Frisch *et al.* 2001). Disruption of these contacts results in cell death via apoptosis, in a process known as anoikis (Frisch *et al.* 1994 and 2001). Transformed cells do not rely on these maintenance signals and so can exist without adhering to their surroundings, this is known as anchorage independent growth (Stoker *et al.* 1968).

Hazelhurst *et al.* (2003) reported reduced melphalan-induced apoptosis in myeloma cells adhered to fibronectin. No difference in melphalan-induced crosslinks was observed between the sensitive cells grown in suspension and the resistant cells grown adhered to fibronectin (Hazelhurst *et al.* 2003). Adhesion of myeloma cells to fibronectin via β1 integrins resulted in etoposide resistance (Hazelhurst *et al.* 2000). Enhanced expression of the ECM proteins fibronectin, laminin and collagen IV was detected in small cell lung cancer cells compared to normal lung tissue (Sethi *et al.* 1999, Rintoul and Sethi, 2002). Sethi *et al.* (1999) found that SCLC cells adhered to each of the aforementioned ECM components were markedly protected from apoptosis induced by etoposide, adriamycin and cyclophosphamide. Binding of ECM proteins to β1 integrins was found to activate an intracellular protein tyrosine kinase which effectively blocked drug induced caspase 3 signalling and apoptosis, and this effect was found to be downstream of DNA damage formation (Rintoul and Sethi, 2002).

Therefore tumour cells appear to be remodelling their surrounding microenvironment, via the enhanced expression of certain ECM proteins, and altered focal adhesion sites in order to stimulate continuous anti-apoptotic signalling that reduces cellular sensitivity to a variety of chemical agents (Morin *et al.* 2003). This cell adhesion mediated drug resistance (CAM-DR) functions downstream of DNA damage.

There are two additional points to be considered when reviewing the cisplatin-resistance microarray results that put the results into context. Firstly, while the genes listed in the 'significantly altered' gene expression list provide useful information about the molecular and cellular events involved in cisplatin resistance, the genes not

featured on the list also provide insight. Where genes featured on the GF211 gene filter, but did not occur on the 'significantly altered expression' list, it can be assumed that the expression of those genes remained unaltered following prolonged cisplatin exposure. Therefore, the microarray data is useful for selecting altered as well as unaltered gene expression patterns between the two cell lines tested. Lists of interesting 'unaltered' genes are featured within the discussion section of Chapter 4. Secondly, the microarray data in Chapter 4 only represents differences in gene expression between the two cell lines, it does not definitively describe differences in protein levels or activity between the two cell lines. Sulfation, glycosylation and phosphorylation are examples of post-translational modifications that control protein activity (Hudelist *et al.* 2005). Variable mRNA half-life and the binding of accessory proteins that stabilise proteins and prevent ubiquitination are just two further examples of post-translational control, that alter the activity of a gene product, that would remain undetected by microarray-gene expression analysis. While the gene expression data gathered together in Chapter 4 is informative, it is part of a larger picture that also needs to be investigated. Proteomic research using western blots, 2-dimensional gel electrophoresis and mass spectrometry, ELISAs, immunocytochemistry and protein microarrays could all be used to further research the important differences between our cisplatin-sensitive and resistant cell lines (Hudelist *et al.* 2005, Stein *et al.* 2003).

Future research into cisplatin-resistance in human ovarian cancer could include microarray experiments using A2780 and A2780cisR before and after cisplatin exposure. This data would provide information about the cisplatin-inducible changes in gene expression between the two cell lines. Specifically examining the difference in gene expression between both cell lines following a one-hour cisplatin exposure and a nine-hour and a 12-hour post-treatment incubation would illuminate the changes in gene expression coinciding with the differential response of both cell lines to cisplatin-induced ICL. This data could help answer the question: Why do cisplatin-ICL persist in the sensitive cell line, and are efficiently excised in the resistant cell line?

Cisplatin-induced intrastrand crosslinks could be examined in both cell lines using the ELISA technique detailed in DeSilva *et al.* (2002b). This data could be compared

to the Collela *et al.* (2001) data and to the UVC cytotoxicity data. RT-PCR experiments could be used to check the difference in gene expression of the genes implicated in CAM-DR. Microarray experiments could be carried out to examine the altered gene expression of A2780 cells grown on collagen, to those grown in the absence of collagen. RT-PCR experiments could specifically investigate the expression of key signal transduction proteins involved in focal adhesions and integrin binding to the ECM, for instance FAK. Pre-treatment of cells with various integrin antagonists (especially against integrinβ1) followed by cisplatin exposure, could provide information about the nature of the suggested CAM-DR observed in the A2780cisR cells.

The clinical work could be continued by carrying out comprehensive microarray experiments using clinical material from previously platinum-exposed patients, and platinum-naïve patients. Is ERCC1 expression elevated in the tumour cells from previously exposed patients, as predicted? This could be easily checked using RT-PCR and the same primers that were used for the cell line investigations.

## 5.2. Conclusion and Future Directions

The evidence presented in Chapters 2 and 3 showed that ovarian cancer cells exposed to cisplatin *in-vivo* and *in-vitro* exhibited enhanced ICL unhooking within the overall genome. These results contribute to the ongoing debate as to which cisplatin-induced DNA lesion is responsible for cytotoxicity (Eastman, 1999). As research has unveiled altered cellular processing of both intrastrand and interstrand crosslinks within resistance models, depending on the particular cellular model being studied, it appears likely that both types of lesion contribute to the cytotoxicity of this agent (Hill *et al.* 1994a, Jones *et al.* 1991, Romanet *et al.* 1999, Zhen *et al.* 1992, Johnson *et al.* 1994a and b, Petersen *et al.* 1996). Our results imply that cisplatin exposure results in the selective survival of cells capable of unhooking cisplatin-ICLs, cells without this ability do not seem to survive treatment.

Having assessed the results collated within this thesis, the question now is; how can this novel information improve the prognosis of ovarian cancer sufferers? What is clear from chemotherapy-resistance research and from other areas of cancer research

is that a heterogeneous tumour cell population, which is inherently genetically unstable, will adapt to its surroundings, and evolve according to its environmental stresses. The importance of devastating a tumour population with an initial cancer treatment is highlighted by the fact that only a single cells needs to survive in order to repopulate and induce a patient's relapse. Whether or not a patient responds to a second treatment with the same chemotherapeutic depends on whether or not the surviving tumour population stably expresses certain behavioural traits to overcome and resist the mechanism of action of that particular agent. Therefore treatment techniques that can maximise the opportunity to destroy chemonaïve tumour tissue before it has had an opportunity to become resilient, are one of the best chances to prevent the development of clinical drug resistance.

Tumour cells from platinum-naïve patients were less able to unhook cisplatin-ICLs than normal cells from the same patient. This suggests that initially ovarian tumour cells would be hypersensitive to platinum chemotherapy, compared to normal tissue, causing the selective destruction of tumour cells at doses that would be sub-toxic to normal cells. As tumour cells from previously exposed patients show the opposite tendency, it appears that the best time to utilise platinum chemotherapy in ovarian cancer is initially before the tumour cells have adapted to unhook the lesion.

The use of high-dose chemotherapy and of targeted chemotherapy such as antibody-directed enzyme pro-drug therapy (ADEPT), with its associated bystander effect, could make the most of the first chance that an oncologist has to cure their patient with their initial choice of treatment. It may turn out that the use of combination chemotherapy and of especially designed chemotherapeutics that specifically sidestep known resistance mechanisms, could aid in achieving this treatment ideal.

SJG-136, a pyrrolo[2,1-*c*][1,4]benzodiazepine dimer (PBD) is a rationally designed interstrand crosslinking agent that has been developed to avoid detection by the cell's repair machinery, by lying within the minor groove and causing minimal distortion to the DNA helix (Hartley *et al.* 2004). These lesions therefore persist and avoid effective removal, resulting in increased cytotoxicity, SJG-136 is >100 times more cytotoxic than the mustard melphalan, and is presently being used in phase I clinical trials (Hartley *et al.* 2004, Clingen *et al.* 2005).

More specifically the work presented in this thesis suggests that one significant marker associated with platinum resistance in human ovarian cancer is elevated ERCC1 expression. Attempting to reduce the effect of elevated ERCC1 expression within a tumour, could increase the sensitivity of the tumour tissue to platinum-based chemotherapeutic regimes. Interestingly, gemcitabine and cisplatin exhibit synergistic cytotoxicity, this synergism was abrogated following antisense down-regulation of ERCC1 (Yang *et al.* 2000). Pre-treatment of human ovarian tumour cells with gemcitabine, followed by cisplatin exposure resulted in inhibition of intrastrand and interstrand crosslink repair, compared to the repair rates achieved when cells we incubated with cisplatin alone (Moufarij *et al.* 2003). Also of interest is the novel compound F11782, which is a dual catalytic inhibitor of topoisomerases. This compound is believed to inhibit the initial incisional event of NER, through the inhibition of the ERCC1/XPF complex (Barret *et al.* 2002).

Another approach might be to biopsy tumour tissue, before therapy, and to examine ERCC1 expression. Patients whose tumours exhibit elevated ERCC1 could have their therapy tailored to account for the fact that first-line treatment with platinum chemotherapy might not be the optimal approach needed to maximise the initial cytotoxic onslaught against the initially sensitive tumour tissue.

Future research into cisplatin-resistance in human ovarian cancer could include microarray experiments using A2780 and A2780cisR before and after cisplatin exposure. This data would provide information about the cisplatin-inducible changes in gene expression between the two cell lines. Specifically examining the difference in gene expression between both cell lines following a one-hour cisplatin exposure and a nine-hour and a 12-hour post-treatment incubation would illuminate the changes in gene expression coinciding with the differential response of both cell lines to cisplatin-induced ICL.

Cisplatin-induced intrastrand crosslinks could be examined in both cell lines using the ELISA technique detailed in DeSilva *et al.* (2002b). This data could be compared to the Collela *et al.* (2001) data and to the UVC cytotoxicity data. RT-PCR experiments could be used to check the difference in gene expression of the genes implicated in CAM-DR. Microarray experiments could be carried out to examine the

altered gene expression of A2780 cells grown on collagen, to those grown in the absence of collagen. RT-PCR experiments could specifically investigate the expression of key signal transduction proteins involved in focal adhesions and integrin binding to the ECM, for instance FAK. Pre-treatment of cells with various integrin antagonists (especially β1) followed by cisplatin exposure, could provide information about the nature of the suggested CAM-DR observed in the A2780cisR cells.

The clinical work could be continued by carrying out comprehensive microarray experiments using clinical material from previously platinum-exposed patients, and platinum-naïve patients. Where possible, multiple samples could be collected from individual patients during their treatment. Gene expression analysis could be carried out on the same patient's samples before and after they were treated with platinum, and compared.

Ultimately the work presented in this thesis increases our knowledge of the responses of human ovarian tumour cells to platinum. In the future this knowledge could contribute to the improved efficacy of cancer treatments, until they can effectively target and destroy tumour cells without a resistant response.

**Chapter 6: References in Alphabetical Order**

Aabo K, Adams M, Adnitt P, Alberts DS, Athanazziou A, Barley V, Bell DR, Bianchi U, Bolis G, Brady MF, Brodovsky HS, Bruckner H, Buyse M, Canetta R, Chylak V, Cohen CK, Colombo N, Conte PF, Crowther D, EdmonsonJH, Gennatas C, Gilbey E, Gore M, Guthrie D, Yeap BY, *et al.*
Chemotherapy in advanced ovarian cancer; four systematic meta-analyses of individual patient data from 37 randomised trials. Advanced Ovarian Cancer Trialists' Group.
British Journal of Cancer 1998;78(11):1479-87

Abeles RH, Walsh CT,
Acettylenic enzyme inactivators. Inactivation of gamma-cystathionase, in vitro and in vivo by propargylglycine.
J. Am. Chem. Soc. 1973;95:6124-5

Aboussekhra A, Biggerstaff M, Shivji MKK, Vilpo JA, Moncollin V, Podust VN, Protic M, Hubscher U, Egly J-M, Wood RD.
Mammalian DNA nucleotide excision repair reconstituted with purified protein components.
Cell 1995;80:859-68

Aebi S, Kurdi-Haidar B, Gordon R, Cenni B, Zheng H, Fink D, Christen RD, Boland CR, Koi M, Fishel R, Howell SB.
Loss of mismatch repair in acquired resistance to cisplatin.
Cancer Research 1996;56:3087-90

Agami R, Blandino G, Oren M, Shaul Y.
Interaction of c-Abl and p73alpha and their collaboration to induce apoptosis.
Nature 1999;399:809-13

Agarwal R, Kaye SB.
Ovarian cancer: Strategies for overcoming resistance to chemotherapy.
Nature Cancer Reviews 2003;3:502-515.

Akaboshi M, Kawai K, Maki H, Akuta K, Ujeno Y, Miyahara T.
The number of platinum atoms binding to DNA, RNA and protein molecules of HeLa cells treated with cisplatin at its mean lethal concentration.
Jpn. J. Cancer Research 1992; 83:522-26

Alaoui-Jamali MA, Panasci L, Centurioni GM, Schecter R, Lehnert S, Batist G.
Nitrogen mustard DNA interaction in melphalan-resistant mammary carcinoma cells with elevated intracellular glutathione and glutathione S-transferase activity.
Cancer Chemother. Pharmacol. 1992;30(5):341-7

Alaoui-Jamali M, Loubaba BB, Robyn S, Tapiero H, Batist G.
Effect of DNA repair enzyme modulators on cytotoxicity of L-phenylalanine mustard and cis-diamminedichloroplatinum(II) in mammary carcinoma cells resistant to alkylating drugs.
Cancer Chemother. Pharmacol. 1994;34(2):153-8

Albertella MR, Green CM, Lehmann AR, O'Connor MJ.
A role for polymerase eta in the cellular tolerance to cisplatin-induced damage.
Cancer Research 2005;65(21):9799-806

Alici S, Saip P, Eralp Y, Aydiner A, Topuz E.
Oral etoposide (VP-16) in platinum-resistant epithelial ovarian cancer.
American Journal of Clinical Oncology 2003;26(4):358-62

Ali-Osman F, Rairkar A, Young P.
Formation and repair of 1,3-bis-(2-chloroethyl)-1-nitrosourea and cisplatin induced total genomic DNA interstrand crosslinks in human glioma cells.
Cancer Biochem Biophys. 1995 Jan;14(4):231-41.

Allen JD, Schinkel AH.
Multidrug resistance and pharmacological protection mediated by the breast cancer resistance protein (BCRP/ABCG2).
Mol Cancer Ther. 2002 Apr;1(6):427-34

Aloyz R, Zhi-Yuan X, Bello V, Bergeron J, Han F-Y, Yan Y, Malapetsa A, Alaoui-Jamali MA, Duncan AMV, Panasci L.
Regulation of cisplatin resistance and homologous recombination repair by the TFIIH subunit XPD.
Cancer Research 2002;62:5457-62

Altaha R, Liang X, Yu JJ, Reed E.
Excision repair cross complementing-group 1: gene expression and platinum resistance (Review).
International Journal of Molecular Medicine 2004;14:959-70

American Cancer Society 2004, Cancer Facts and Figures. (Atlanta, GA).
http://www.cancer.org/downloads/STT/CAFF_finalPWSecured.pdf

American Cancer Society: Ovarian cancer detailed guide, 2004.
http://www.cancer.org/docroot/CRI/CRI_2_3x.asp?dt=33

Anderson DG, Kowalczykowski SC.
The translocating RecBCD enzyme stimulates recombination by directing RecA protein onto ssDNA in a chi-regulated manner.
Cell. 1997 Jul 11;90(1):77-86.

Andre T, Bensmaine MA, Louvet C, Francois E, Lucas V, Desseigne F, Beerblock K, Bouche O, Carola E, Merrouche Y, Morvan F, Dupont-Andre G, de Gramont A.
Multicenter phase II study of bimonthly high-dose leucovorin, fluorouracil infusion, and oxaliplatin for metastatic colorectal cancer resistant to the same leucovorin and fluorouracil regimen.
J Clin Oncol. 1999 Nov;17(11):3560-8.

Andre T, Boni C, Mounedji-Boudiaf L, Navarro M, Tabernero J, Hickish T, Topham C, Zaninelli M, Clingan P, Bridgewater J, Tabah-Fisch I, de Gramont A; Multicenter International Study of Oxaliplatin/5-Fluorouracil/Leucovorin in the Adjuvant Treatment of Colon Cancer (MOSAIC) Investigators.

Oxaliplatin, fluorouracil, and leucovorin as adjuvant treatment for colon cancer.
N Engl J Med. 2004 Jun 3;350(23):2343-51.

Andrews PA, Schiefer MA, Murphy MP, Howell SB.
Enhanced potentiation of cisplatin cytotoxicity in human ovarian cancer cells by prolonged glutathione depletion.
Chem. Biol. Interaction. 1988;65(1):51-8

Antonini I, Polucci P, Kelland LR, Menta E, Pescalli N and Martelli S.
2,3-Dihyrdo-1*H*,7*H*-pyrimido[5,6,1-*de*]acridine-1,3,7-trione Derivatives, a Class of Cytotoxic Agents Active on Multi-drug Resistant Cell Lines: Synthesis, Biological Evaluation, and Structure-Activity Relationships.
J. Med. Chem. 1999 ; 42 :2535-41

Araujo SJ, Tirode F, Coin F, Pospiech H, Syvaoja JE, Stucki M, Hubscher U, Egly J-M, Wood RD.
Nucleotide excision repair of DNA with recombinant human proteins: definition of the minimum set of factors, active forms of TFIIH, and modulation by CAK.
Genes and Development 2000;14:349-59

Ashkenazi A, Dixit VM.
Death receptors: Signaling and modulation.
Science 1998;281:1305-8

Baekelandt MM, Holm R, Nesland JM, Trope CG, Kristensen GB.
P-glycoprotein expression is a marker for chemotherapy resistance and prognosis in advanced ovarian cancer.
Anticancer Res. 2000 Mar-Apr;20(2B):1061-7.

Bagby GC Jr.
Genetic basis of Faconi anaemia.
Curr. Opin. Hematol. 2003;10(1):68-76

Bailly V, Sommers CH, Sung P, Prakash L, Prakash S.

Specific complex formation between proteins encoded by the yeast DNA repair and recombination gene *RAD1* and *RAD10*
PNAS 1992;89:8273-8277

Ban N, Takahashi Y, Takayama T, Kura T, Katahira T, Sakamaki S, Niitsu Y.
Transfection of glutathione s-transferase (GST)-pi antisense aomplementary DNA increases the sensitivity of a colon cancer cell line to adriamycin, cisplatin, melphalan and etoposide.
Cancer Research 1996;56(15):3577-82

Bancroft DP, Lepre CA, Lippard SJ.
195Pt NMR kinetic and mechanistic studies of cis- and trans-diamminedichloroplatinum(II) binding to DNA.
J. Am. Chem. Soc. 1990 ; 112:6860-71

Barnes DE, Tomkinson AE, Lehmann AR, Webster AD, Lindahl T.
Mutations in the DNA ligase I gene of an individual with immunodeficiencies and cellular hypersensitivity to DNA-damaging agents.
Cell 1992;69(3):495-503

Barnham KJ, Berners-Price SJ, Frenkiel TA, Frey U, Sadler PJ.
Platination pathways for reactions of cisplatin with GG single-stranded and double-stranded decanucleotides.
Angewandte Chemie, International Edition in English 1995;34(17):1874-77.

Barret JM, Calsou P, Larsen AK, Salles B.
A cisplatin-resistant murine leukemia cell line exhibits increased topoisomerase II activity.
Molecular Pharmacology 1994;46(3):431-6

Barret JM, Cadou M, Hill BT.
Inhibition of nucleotide excision repair and sensitisation of cells to DNA cross-linking anticancer drugs by F 11782, a novel fluorinated epipodophylloid.
Biochem Pharmacol. 2002 Jan 15;63(2):251-8.

Barton-Burke M.
Gemcitabine: a pharmacologic and clinical overview.
Cancer Nursing 1999;22(2):176-83.

Bast RC Jr. Feeney M, Lazarus H, et al.
Reactivity of a monoclonal antibody with human ovarian carcinoma.
Journal of Clinical Investigation 1981;68:1331-37

Batty DP, Wood RD.
Damage recognition in nucleotide excision repair of DNA.
Gene 2000;241:193-204

Bauer GB, Povirk LF.
Specificity and kinetics of interstrand and intrastrand bifunctional alkylation by nitrogen mustards at a G-G-C sequence.
Nucleic Acids Res. 1997 Mar 15;25(6):1211-8.

Bedford P, Walker MC, Sharma HL, Perera A, McAuliffe CA, Masters JRW, Hill BT.
Factors influencing the sensitivity of two human bladder carcinoma cell lines to CDDP(II),
Chem-Biol. Interact. 1987;61:1-15

Behrens BC, Hamilton TC, Masuda H, Grotzinger KR, Whang-Peng J, Louie KG, Knutsen T, McKoy WM, Young RC, Ozols RF.
Characterisation of a cis-diamminedichloroplatinum(II)-resistant human ovarian cancer cell line and its use in evaluation of platinum analogues.
Cancer Research 1987 Jan 15;47(2):414-8

Beith J, Hartley J, Darling J, Souhami R.
DNA interstrand crosslinking and cytotoxicity induced by chloroethylnitrosoureas and cisplatin in human glioma cell lines which vary in cellular concentration of O6-alkylguanine-DNA alkyltransferase.
British Journal of Cancer 1997;75(4):500-5

Belichenko I, Morishima N, Separovic D.
Caspase-resistant vimentin suppresses apoptosis after photodynamic treatment with a silicon phthalocyanine in Jurkat cells.
Arch Biochem Biophys. 2001 Jun 1;390(1):57-63.

Bell DA.
Origins and molecular pathology of ovarian cancer.
Modern Pathology 2005;18:S19-S32

Bellon SF, Coleman JH, Lippard SJ.
DNA unwinding produced by site specific intrastrand crosslinks of the antitumour drug *cis*-diamminedichloroplatinum(II).
Biochemistry 1991;30:8026-35

Benchekroun MN, Parker R, Reed E, Sinha BK.
Inhibition of DNA repair and sensitisation of cisplatin in human ovarian carcinoma cells by interleukin-1 alpha.
Biochem Biophys Res Commun. 1993 Aug 31;195(1):294-300.

Benchekroun MN, Parker R, Dabholkar M, Reed E, Sinha BK.
Effects of interleukin 1 alpha on DNA repair in human ovarian carcinoma (NIH-OVCAR-3) cells: implications in the mechanism of sensitisation of cis-diamminedichloroplatinum(II).
Mol. Pharmacol. 1995 Jun;47(6):1255-60

Benjamini Y, and Hochberg Y.
Controlling the false discovery rate: a practical and powerful approach to multiple testing.
Journal of the Royal Statistical Society. Series_B 1995;57(1): 289-300

Berardini M, Mackay W, Loechler EL.
Evidence for a recombination-independent pathway for the repair of DNA interstrand

cross-links based on a site-specific study with nitrogen mustard.
Biochemistry. 1997 Mar 25;36(12):3506-13.

Berardini M, Foster PL, Loechler EL.
DNA polymerase II (polB) is involved in a new DNA repair pathway for DNA interstrand cross-links in Escherichia coli.
J Bacteriol. 1999 May;181(9):2878-82.

Bergoglio V, Canitrot Y, Hogarth L, Minto L, Howell SB, Cazaux C, Hoffman JS.
Enhanced expression and activity of DNA polymerase β in human ovarian tumour cells: impact on sensitivity towards antitumour agents.
Oncogene 2001 Sept 27;20(43):6181-7

Bessho T, Mu D, Sancar A.
Initiation of DNA interstrand cross-link repair in humans: the nucleotide excision repair system makes dual incisions 5' to the cross-linked base and removes a 22- to 28- nucleotide-long damage-free strand.
Molecular and Cellular Biology 1997;17(12):6822-30

Bhattacharyya A, Ear US, Koller BH, Weichselbaum RR, Bishop DK.
The breast cancer susceptibility gene BRCA1 is required for subnuclear assembly of Rad51 and survival following treatment with the DNA crosslinking agent Cisplatin.
The Journal of Biological Chemistry 2000;275(31):23899-903

Bichat F, Mouawad R, Solis-Recendez G, Khayat D, Bastian G.
Cytoskeleton alteration in MCF7R cells, a multidrug resistant human breast cancer cell line.
Anticancer Res. 1997 Sep-Oct;17(5A):3393-401.

Biggerstaff M, Szymkowski DE, Wood RD.
Correction of the ERCC1, ERCC4 and xeroderma pigmentosum group F DNA repair defects in vitro.
EMBO J. 1993;12:3685-3692

Bishop DK, Ear U, Bhattacharyya A, Calderone C, Beckett M, Weichselbaum RR, Shinohara A.
Xrcc3 is required for assembly of Rad51 complexes in-vivo.
The Journal of Biological Chemistry 1998;273(34):21482-88

Black SM, Beggs JD, Hayes JD, Bartoszek A, Muramatsu M, Sakai M, Wolf CR.
Expression of human glutathione S-transferases in Saccharomyces cerevisiae confers resistance to the anticancer drugs adriamycin and chlorambucil.
Biochem. J. 1990;268(2):309-15

Blommaert FA, van Dijk-Knijnenburg HC, Dijt FJ, den Engelse L, Baan RA, Berends F, Fichtinger-Schepman AM.
Formation of DNA adducts by the anticancer drug carboplatin: different nucleotide sequence preferences in vitro and in cells.
Biochemistry. 1995 Jul 4;34(26):8474-80.

Board PG, Coggan M, Wilce MC, Parker MW
Evidence for an essential serine residue in the active site of the Theta class glutathione transferases.
Biochem J. 1995 Oct 1;311 ( Pt 1):247-50.

Bolton MG, Hilton J, Robertson KD, Streeper RT, Colvin OM, Noe DA.
Kinetic analysis of the reaction of melphalan with water, phosphate and glutathione.
Drug Metab. Dispos. 1993;21(6):986-96

Bosl GJ, Motzer RJ.
Testicular germ-cell cancer.
N. Engl. J. Med. 1997;337(4):242-53

Boss EA, Peters WH, Roelofs HM, Boonstra H, Steegers EA and Massuger LF.
Glutathione S-transferases P1-1 and A1-1 in ovarian cyst fluids.
Eur. J. Gynaecol. Oncol. 2001;22(6):427-32

Boudreau N, Sympson CJ, Werb Z, Bissell MJ.
Suppression of ICE and apoptosis in mammary epithelial cells by extracellular matrix.
Science. 1995 Feb 10;267(5199):891-3.

Brabec V, Kasparkova J.
Modifications of DNA by platinum complexes. Relation to resistance of tumors to platinum antitumor drugs.
Drug Resist Updat. 2005 Jun;8(3):131-46.

Bramson J, McQuillan A, Aubin R, Alaoui-Jamali M, Batist G, Christodoulopoulos G, Panasci LC.
Nitrogen mustard drug resistance in B-cell chronic lymphocytic leukaemia as an in-vivo model for crosslinking agent resistance.
Mutation Research 1995a;336(3):269-78

Bramson J, McQuillan A, Panasci LC.
DNA repair enzyme expression in chronic lymphocytic leukaemia vis-à-vis nitrogen mustard drug resistance.
Cancer Letters 1995b;90(2):139-48.

Bristow RE, Tomacruz RS, Armstrong DK, Trimble EL, Montz FJ.
Survival effect of maximal cytoreductive surgery for advanced ovarian carcinoma during the platinum era: a meta-analysis.
Journal of Clinical Oncology 2002;20(5):1248-59

Brown R, Hirst GL, Gallagher WM, McIlwrath AJ, Margison GP, van der Zee AG, Anthoney DA.
hMLH1 expression and cellular responses of ovarian tumour cells to treatment with cytotoxic anticancer agents.
Oncogene. 1997 Jul 3;15(1):45-52.

Bungo M, Fujiwara Y, Kasahara K, Nakagawa K, Ohe Y, Sasaki Y, Irino S, Saijo N.
Decreased accumulation as a mechanism of resistance to cis-diamminedichloroplatinum(II) in human non small cell lung cancer cell lines: Relation to DNA damage and repair.
Cancer Research 1990;50:2549-53

Bunting KD, Lindahl R, Townsend AJ.
Oxazaphophorine-specific resistance in human MCF-7 breast carcinoma cell lines expressing transfected rat class 3 aldehyde dehydrogenase.
Journal of Biological Chemistry 1994;269(37):23197-203

Burden DA, Osheroff N.
Mechanism of action of eukaryotic topoisomerase II and drugs targeted to the enzyme.
Biochim Biophys Acta. 1998 Oct 1;1400(1-3):139-54.

Byun Y, Chen F, Chang R, Trivedi M, Green KJ, Cryns VL.
Caspase cleavage of vimentin disrupts intermediate filaments and promotes apoptosis.
Cell Death Differ. 2001 May;8(5):443-50.

Caballero OL, Resto V, Patturajan M, Meerzaman D, Guo MZ, Engles J, Yochem R, Ratovitski E, Sidransky D, Jen J.
Interaction and colocalisation of PGP9.5 with JAB1 and p27(Kip1).
Oncogene. 2002 May 2;21(19):3003-10.

Cadron I, Amant F, Van Gorp T, Nevem P, Leunen K, Vergote I.
The management of borderline tumours of the ovary.
Current Opinion in Oncology 2006;18(5):488-93

Caldecott K, Jeggo P.
Cross-sensitivity of gamma-ray-sensitive hamster mutants to crosslinking agents.
Mutat. Res. 1991;255(2):111-21

Caldwell JE, Heiss SG, Mermall V, Cooper JA.
Effects of CapZ, an actin capping protein of muscle, on the polymerisation of actin.
Biochemistry 1989 ;28(21):8506-14

Calsou P, Frit P, Salles B.
Repair synthesis by human cell extracts in cisplatin-damaged DNA is preferentially determined by minor adducts.
Nucleic Acids Research 1992;20(23):6363-8

Calvert AH, Harland SJ, Newell DR, Siddik ZH, Jones AC, McElwain TJ, Raju S, Wiltshaw E, Smith IE, Baker JM, Peckham MJ, Harrap KR.
Early clinical studies with cis-diammine-1,1-cyclobutane dicarboxylate platinum II.
Cancer Chemother. Pharamacol. 1982;9(3):140-7

Calvert H, Judson I, can der Vijgh WJ.
Platinum complexes in cancer medicine: pharmacokinetics and pharmadynamics in relation to toxicity and therapeutic activity.
Cancer Surv. 1993;17:189-217

Campos L, Rouault JP, Sabido O, Oriol P, Roubi N, Vasselon C, Archimbaud E, Magaud JP, Guyotat D.
High expression of Bcl-2 protein in acute myeloid leukaemia cells associated with poor response to chemotherapy.
Blood 1993;81(11):3091-6

CancerStats Monograph, CancerStats Incidence UK, Published by Cancer Research UK, Feb. 2004.
http://www.cancerresearchuk.org/aboutcancer/statistics/cancerstatsreport/

CancerStats Monograph, CancerStats Mortaliy UK, Published by Cancer Research UK, Feb. 2004.
http://www.cancerresearchuk.org/aboutcancer/statistics/cancerstatsreport/

Cass I, Baldwin RL, Varkey T, Moslehi R, Narod SA, Karlan BY.
Improved survival in women with BRCA-associated ovarian carcinoma.
Cancer 2003;97(9):2187-95

Castagna A, Antonioli P, Astner H, Hamdan M, Righetti SC, Perego P, Zunino F and Righetti PG.
A proteomic approach to cisplatin resistance in the cervix squamous cell carcinoma cell line A431.
Proteomics 2004;4:3246-67

Chaney SG, Campbell SL, Bassett E, Wu Y.
Recognition and processing of cisplatin- and oxaliplatin-DNA adducts.
Crit Rev Oncol Hematol. 2005 Jan;53(1):3-11.

Chang L-C, Sheu H-M, Huang Y-S, Tsai T-R, Kuo K-W.
A novel function of emodin: Enhancement of the nucleotide excision repair of UV- and cisplatin-induced DNA damage in human cells.
Biochemical Pharmacology 1999 ;58: 49-57

Chang DD, Hoang BQ, Liu J, Springer TA.
Molecular basis for interaction between Icap1α PTB domain and β1 integrin.
The Journal of Biological Chemistry 2002; 277(10): 8140-5

Chen G, and Zeller WJ.
Augmentation of cisplatin (DDP) cytotoxicity in-vivo by DL-buthionine sulfoximine (BSO) in DDP sensitive and resistant rat ovarian tumours and its relation to DNA interstrand crosslinks.
Anticancer Research 1991;11(6):2231-7

Chen G, Hutter KJ, Teller WJ.
Positive correlation between cellular glutathione and acquired cisplatin resistance in human ovarian cancer cells.
Cell. Biol. Toxicol. 1995;11(5):273-81

Chen ZP, Malapetsa A, Marcantonio D, Mohr G, Brien S, Panasci LC.
Correlation of chloroethylnitrosourea resistance with ERCC2 expression in human tumour cell lines as determined by quantitative competitive polymerase chain reaction.
Cancer Research 1996;56(11):2475-8

Chen ZP, Malapetsa A, McQuillan A, Marcantonio D, Bello V, Mohr G, Remack J, Brent TP, Panasci LC.
Evidence for nucleotide excision repair as a modifying factor of $O^6$-Methylguanine-DNA-methyltransferase-mediated innate chloroethylnitrosourea resistance in human tumour cell lines.
Molecular Pharmacology 1997;52:815-20

Chen J, Yang R, Liu F.
Establishment of cisplatin-induced multidrug resistant human epithelial ovarian cancer cell line 3AO/cDDP and its expressions of multidrug resistance proteins
Zhonghua Fu Chan Ke Za Zhi. 2000 Oct;35(10):617-20.

Chen ZP, Malapetsa A, Monks A, Myers TG, Mohr G, Sausville EA, Scudiero DA, Panasci LC.
Nucleotide excision repair protein levels vis-à-vis anticancer drug resistance in 60 human tumour cell lines.
Ai Zheng 2002;21(3):233-9

Chen Q, Van der Sluis PC, Boulware D, Hazelhurst LA, Dalton WS.
The FANC/BRCA pathway is involved in melphalan induced DNA interstrand crosslink repair and accounts for melphalan resistance in multiple myeloma.
Blood First Edition Paper, prepublished on-line March 31, 2005.

Cheng X, Kigawa J, Minagawa Y, Kanamori Y, Itamochi H, Okada M, Terakawa N.
Glutathione S-transferase-pi expression and glutathione concentration in ovarian carcinoma before and after chemotherapy.
Cancer. 1997 Feb 1;79(3):521-7.

Cheng G, Li Y, Tian F.
Comparison of stepwise and pulse induced cisplatin-resistant ovarian cancer cell sublines]
Zhonghua Zhong Liu Za Zhi. 2001 Jul;23(4):305-8.

Cho Y, Gorina S, Jeffrey PD, Pavletich NP.
Crystal structure of a p53 tumour suppressor-DNA complex: understanding tumourigenic mutations.
Science 1994;265:346-54

Choi CH.
ABC transporters as multidrug resistance mechanisms and the development of chemosensitizers for their reversal.
Cancer Cell Int. 2005 Oct 4;5:30.

Choudhuri S.
Microarrays in biology and medicine.
J Biochem Mol Toxicol. 2004;18(4):171-9

Clingen PH, De Silva IU, McHugh PJ, Ghadessy FJ, Tilby MJ, Thurston DE, Hartley JA.
The XPF-ERCC1 endonuclease and homologous recombination contribute to the repair of minor groove DNA interstrand crosslinks in mammalian cells produced by the pyrrolo[2,1-c][1,4]benzodiazepine dimer SJG-136.
Nucleic Acids Res. 2005 Jun 8;33(10):3283-91. Print 2005.

Codegoni AM, Broggini M, Pitelli MR, Pantarotto M, Torri V, Mangioni C, D'Incalci M.
Expression of genes of potential importance in the response to chemotherapy and DNA repair in patients with ovarian cancer.
Gynecol Oncol. 1997 Apr;65(1):130-7.

Coggan M, Flanagan JU, Parker MW, Vichai V, Pearson WR, Board PG.

Identification and characterisation of GSTT3, a third murine theta class glutathione transferase.
Biochem. J. 2002;366:323-32

Cole RS.
Repair of DNA containing interstrand crosslinks in *Escherchia coli*: sequential excision and recombination.
Proc. Natl. Acad. Sci. USA 1973;70:1064-68

Colella G, Pennati M, Bearzatto A, Leone R, Colangelo D, Manzotti C, Daidone MG, Zaffaroni N
Activity of a trinuclear platinum complex in human ovarian cancer cell lines sensitive and resistant to cisplatin: cytotoxicity and induction and gene specific repair of DNA lesions.
British Journal of Cancer 2001;84(10):1387-90

Colombo N.
Randomised trail of paclitaxel (PTX) and carboplatin (CBDCA) versus a control arm of carboplatin or CAP (cyclophosphamide, doxorubicin and cisplatin): The Third International Collaborative Ovarian Neoplasm study (ICON3).
Proc. ASCO 2000;19:379a.

Conforti G, Codegoni AM, Scanziani E, Dolfini E, Dasdia T, Calza M, Caniatti M, Broggini M.
Different vimentin expression in two clones derived from a human colocarcinoma cell line (LoVo) showing different sensitivity to doxorubicin.
Br J Cancer. 1995 Mar;71(3):505-11

Connell PP, Siddiqui N, Hoffman S, Kuang A, Khatipov E-A, Weichselbaum RR, Bishop DK.
A hot spot for RAD51C Interactions revealed by a peptide that sensitises cells to cisplatin.
Cancer Research 2004;64:3002-5

Cordes N, Beinke C, Plasswilm L, van Beuningen D.
Irradiation and various cytotoxic drugs enhance tyrosine phosphorylation and beta (1) integrin clustering in human A549 lung cancer cells in a substratum-dependent manner in vitro.
Strahlenther Onkol. 2004; 180(3):157-64

Crul M, van Waardenburg RC, Beijnen JH, Schellens JH.
DNA-based drug interactions of cisplatin.
Cancer Treat Rev. 2002 Dec;28(6):291-303

Cullen KJ, Newkirk KA, Schmaker LM, Aldosari N, Rone JD, Haddad BR.
Glutathione S-transferase π amplification is associated with cisplatin resistance in head and neck squamous cell carcinoma cell lines and primary tumours.
Cancer Research 2003;63:8097-8102

Cullinane C, Mazur SJ, Essigmann JM, Phillips DR, Bohr VA.
Inhibition of RNA polymerase II transcription in human cell extracts by cisplatin DNA damage.
Biochemistry 1999;38(19):6204-12

Cummings J, Anderson L, Willmott N, Smyth JF.
The molecular pharmacology of doxorubicin in-vivo.
The European Journal of Cancer 1991;27(5): 532-5

Cummings J, Spanswick VJ, Smyth JF.
Re-evaluation of the molecular pharmacology of mitomycin C.
Eur J Cancer. 1995 Nov;31A(12):1928-33.

Dabholkar M, Bostick-Bruton F, Weber C, Bohr VA, Egwuagu C and Reed E.
ERCC1 and ERCC2 expression in malignant tissues from ovarian cancer patients.
Journal of the National Cancer Institute 1992:84(19);1512-7

Dabholkar M, Vionnet J, Bostick-Bruton F, Yu JJ, Reed E.

Messenger RNA levels of XPAC and ERCC1 in ovarian cancer tissue correlates with response to platinum-based chemotherapy.
The Journal of Clinical Investigations 1994:94;703-8

Damia G, Imperatori L, Stefanini M, D'Incalci M.
Sensitivity of CHO mutant cell lines with specific defects in nucleotide excision repair to different anti-cancer agents.
International Journal of Cancer 1996;66(6):779-83

Damia G, D'Incalci M.
Mechanisms of resistance to alkylating agents.
Cytotechnology 1998;27:165-73

Damiano JS, Cress AE, Hazelhurst LA, Shtil AA, Dalton WS.
Cell adhesion mediated drug resistance (CAM-DR): role of integrins and resistance to apoptosis in human myeloma cell lines.
Blood 1999;93(5):1658-67

De Bruin WCC, Wagenmans MJM, Board PG, Peters WHM.
Expression of glutathione S transferase θ class isozymes in human colorectal gastric cancers.
Carcinogenesis 1999;20(8):1453-7

De Laat WL, Appeldoorn E, Jaspers NGJ, Hoeijmakers JHJ.
DNA structural elements required for ERCC1-XPF endonuclease activity.
Journal of Biological Chemistry 1998;273:7835-42

De Silva IU, McHugh PJ, Clingen PH, Hartley JA.
Defining the roles of nucleotide excision repair and recombination in the repair of DNA Interstrand crosslinks in mammalian cells.
Molecular and Cellular Biology 2000;20(21):7980-90

De Silva, IU.

Mechanism of repair of DNA damage produced by antitumour drugs
PhD Thesis, University College London 2002a

De Silva IU, McHugh P, Clingen PH, Hartley JA.
Defects in interstrand crosslink uncoupling do not account for the extreme sensitivity of ERCC1 and XPF cells to cisplatin.
Nucleic Acid Research 2002b, Vol. 30 No. 17 pp 3848-56

Diadone MG, Luisi A, Veneroni S, Benini E, Silvestrini R.
Clinical studies of Bcl-2 and treatment benefit in breast cancer patients.
Endocr. Relat. Cancer 1999;6(1):61-8

Dimanche-Boitrel MT, Micheau O, Hammann A, Haugg M, Eymin B, Chauffert B, Solary E.
Contribution of the cyclin-dependent kinase inhibitor p27KIP1 to the confluence-dependent resistance of HT29 human colon carcinoma cells.
Int J Cancer. 1998 Aug 31;77(5):796-802.

Di Nicolantonio F, Mercer SJ, Knight LA, Gabriel FG, Whitehouse PA, Sharma S, Fernando A, Glaysher S, Di Palma S, Johnson P, Somers SS, Toh S, Higgins B, Lamont A, Gulliford T, Hurren J, Yiangou C, Cree IA.
Cancer cell adaptation to chemotherapy.
BMC Cancer. 2005 Jul 18;5:78.

DiPaola RS, Aisner J.
Overcoming bcl-2 and p53-mediated resistance in prostate cancer.
Semin. Oncol. 1999;26(1Suppl.2):112-6

Dixon B. (Editorial)
Microarray technology: an array of applications that is far from micro.
Biotechnology advances 2002;20:361-62

Doglioni C, Angelo D, Laurino L, Iuzzolino P, Chiarelli C, Celio M, Viale G.
Calretinin: A novel immunocytochemical marker for mesothelioma.
American Journal of Surgical Pathology 1996; 20(9):1037-46



Dole M, Nunez G, Merchant AK, Maybaum J, Rode CK, Bloch CA, Castle VP.

Dronkert ML, Kanaar R.
Repair of DNA interstrand cross-links.
Mutat Res. 2001 Sep 4;486(4):217-47.

Drummond JT, Anthoney A, Brown R, Modrich P.
Cispatin and adriamycin resistance are associated with MutLα and mismatch repair deficiency in an ovarian tumour cell line.
The Journal of Biological Chemistry 1996;271(33):19645-8

Duckett DR. Drummond JT, Murchie AIH, Readon JT, Sancar A, Lilley DMJ, Modrick P.
Human MutSα recognizes DNA base pairs containing $O^6$-methylguanine, O6-methylthymine or the cisplatin d(GpG) adduct.
PNAS 1996; 93: 6443-7

Ducore JM, Erickson LC, Zwelling LA, Laurent G, Kohn KW.
Comparative studies of DNA cross-linking and cytotoxicity in Burkitt's lymphoma cell lines treated with cis-diamminedichloroplatinum(II) and L-phenylalanine mustard.
Cancer Res. 1982 Mar;42(3):897-902.

Duxbury MS, Ito H, Zinner MJ, Ashley SW, Whang EE.
Focal adhesion kinase gene silencing promotes anoikis and suppresses metastasis of human pancreatic adenocarcinoma cells.
Surgery. 2004 May;135(5):555-62.

Eastman A, Barry MA.
Interaction of trans-diamminedichloroplatinum(II) with DNA: formation of monofunctional adducts and their reaction with glutathione.
Biochemistry. 1987 Jun 16;26(12):3303-7.

Eastman A, Jennerwein MM, Nagel DL.

Characterisation of bifunctional adducts produced in DNA by trans-diamminedichloroplatinum(II).
Chem Biol Interact. 1988;67(1-2):71-80.

Eastman A.
The mechanism of action of cisplatin: from adduct to apoptosis.
In, Cisplatin: Chemistry and Biochemistry of a leading anticancer drug, ed. Bernhard Lippert, 1999

Ebadi M, Iversen PL.
Metallothionein in carcinogenesis and cancer chemotherapy.
Gen. Pharmacol. 1994;25(7):1297-310

Edwards MS, Levin VA, Wilson CB.
Brain tumor chemotherapy: an evaluation of agents in current use for phase II and III trials.
Cancer Treat Rep. 1980;64(12):1179-205.

Endresen L, Schjerven L, Rugstad HE.
Tumours from a cell strain witth a high content of metallothionein show enhanced resistance against cis-dichlorodiammineplatinum.
Acta. Pharmacol. Toxicol. (Copenh). 1984;55(3):183-7

Epenetos AA, Canti G, Taylor-Papadimitriou J, Curling M, Bodmer WF.
Use of two epithelium-specific monoclonal antibodies for diagnosis of malignancy in serous effusions.
Lancet. 1982 Nov 6;2(8306):1004-6.

Erickson LC, Zwelling LA, Ducore JM, Sharkey NA, Kohn KW.
Differential cytotoxicity and DNA cross-linking in normal and transformed human fibroblasts treated with cis-diamminedichloroplatinum(II).
Cancer Res. 1981 Jul;41(7):2791-4.

Esaki T, Nakano S, Masumoto N, Fujishima H, Niho Y

Schedule-dependent reversion of acquired cisplatin resistance by 5-fluorouracil in newly established cisplatin resistant HST-1 human squamous carcinoma cell line.
Int. J. Cancer. 1996 Feb 8;65(4): 479-84

Esteller M, Garcia-Foncillas J, Andion E, et al.
Inactivation of the DNA repair gene *MGMT* and the clinical response of gliomas to alkylating agents.
New England Journal of Medicine 2000;343:1350-4

Evans E, Moggs J, Hwang J, Egly J, Wood RD.
Mechanisms of open complex and dual incision formation by human nucleotide excision repair factors.
EMBO J. 1997;16:6559-73

Ewig RAG, and Kohn KW.
DNA damage and repair in mouse leukaemia L1210 cells treated with nitrogen nustard, 1,3-Bis(2-chloroethyl)-1-nitrosourea and other nitrosoureas.
Cancer Research 1977;37:2114-22

Eymin B, Haugg M, Droin N, Sordet O, Dimanche-Boitrel MT, Solary E.
p27Kip1 induces drug resistance by preventing apoptosis upstream of cytochrome C release and pro-caspase-3 activation in leukemic cells.
Oncogene 1999 ; 18(7):1411-8

Fairbairn D.W, Olive PL, O'Neil KL.
The comet assay: a comprehensive review.
Mutat. Res. 1995;339:37-59

Fan S, El-Deiry WS, Bae I, Freeman J, Jandle D, Bhatia K, Fornace Jr AJ, Magrath I, Kohn KW, O'Connor PM.
*p53* gene mutations are associated with decreased sensitivity of human lymphoma cells to DNA damaging agents.
Cancer Research 1994;54: 5824-30

Ferguson AW, Flatow U, MacDonald NJ, Larminat F, Bohr VA, Steeg PS.
Increased sensitivity to cisplatin by nm23-transfected tumor cell lines.
Cancer Research 1996; 56(13):2931-5

Ferry KV, Hamilton TC, Johnson SW.
Increased nucleotide excision repair in cisplatin resistant ovarian cancer cells. Role of ERCC1-XPF.
Biochemical Pharmacology 2000;60;1305-13

Fichtinger-Schepman AM, van der Veer JL, den Hartog JH, Lohman PH, Reedijk J.
Adducts of the antitumour drug cis-diamminedichloroplatinum(II) with DNA: formation, identification and quantitation.
Biochemistry 1985 ; 24(3):707-13

Fichtinger-Schepman AM, van Oosterom AT, Lohman PH and Berends F.
Cis-Diamminedichloroplatinum(II)-induced DNA adducts in peripheral leukocyte from seven cancer patients: quantitative immunochemical detection of the adduct induction and removal after a single dose of cis-diamminedichloroplatinum(II).
Cancer Research 1987 ; 47(11):3000-4

Fichtinger-Schepman AM, van Dijk-Knijenenburg HC, van der Velde-Visser SD, Berends F, Baan RA.
Cisplatin- and carboplatin-DNA adducts: is PT-AG the cytotoxic lesion?
Carcinogenesis 1995 Oct;16(10):2447-53

FIGO Guidelines, 2004
International Federation of Gynecology and Obstetrics (FIGO), London, UK.
http://www.igcs.org/guidelines/guideline_staging-booklet.pdf

Fisch MJ, Howard KL, Einhirn LH, Sledge GW.
Relationship between platinum-DNA adducts in leukocytes of patients with advanced germ cell cancer and survival.
Clinical Cancer Research 1996;2(6):1063-6

Fishel R.
Signaling mismatch repair in cancer.
Nature Medicine 1999;5(11):1239-41

Fishman-Lobell J, Harber JE.
Removal of non-homologous DNA ends in double strand break recombination: the role of the yeast ultraviolet repair gene RAD1.
Science 1992;258:480-484

Fojo T, Bates S.
Strategies for reversing drug resistance.
Oncogene 2003;22(47):7512-23

Fram RJ, Woda BA, Wilson JM, Robichaud N.
Characterisation of acquired resistance to CDDP(II) in BE human colon cancer cells.
Cancer Research 1990;50:72-7

Fridman R, Giaccone G, Kanemoto T, Martin GR, Gazdar AF, Mulshine JL.
Reconstituted basement membrane (matrigel) and laminin can enhance the tumorigenicity and the drug resistance of small cell lung cancer cell lines.
Proc Natl Acad Sci U S A. 1990 Sep;87(17):6698-702.

Frisch SM, Francis H.
Disruption of epithelial cell-matrix interactions induces apoptosis.
J Cell Biol. 1994 Feb;124(4):619-26.

Frisch SM, Vuori K, Ruoslahti E, Chan-Hui PY.
Control of adhesion-dependent cell survival by focal adhesion kinase.
Cell Biol. 1996 Aug;134(3):793-9.

Frisch SM, Screaton RA.
Anoikis mechanisms.

Curr Opin Cell Biol. 2001 Oct;13(5):555-62.

Furuta T, Ueda T, Aune G, Sarasin A, Kraemer KH, Pommier Y.
Transcription-coupled nucleotide excision repair as a determinant of cisplatin sensitivity of human cells.
Cancer Res. 2002 Sep 1;62(17):4899-902.

Galmarini CM, Mackey JR, Dumontet C.
Nucleoside analogues and nucleobases in cancer treatment.
Lancet Oncol. 2002 Jul;3(7):415-24.

Garcia-Carbonero R, Supko JG.
Current perspectives on the clinical experience, pharmacology, and continued development of the camptothecins.
Clin Cancer Res. 2002 Mar;8(3):641-61.

Garcia-Hiquera I, Taniguchi T, Gaesan S, Meyn MS, Timmers C, Hejna J, Grompe M, and D'Andrea AD.
Interaction of the Fanconi anaemia proteins and BRCA1 in a common pathway.
Mole. Cell. 2001;7:249-62

Gasior SL, Olivares H, Ear U, Hari DM, Weichselbaum R, Bishop DK.
Assembly of RecA like recombinases: Distinct roles for mediator proteins in mitosis and meiosis.
PNAS 2001;98(15):8411-8

Geleziunas R, McQuillan A, Malapetsa A, Hutchinson M, Kopriva D, Wainberg MA, Hiscott J, Bramson J, Panasci L.
Increased DNA synthesis and repair-enzyme expression in lymphocytes from patients withchronic lymphocytic leukaemia resistant to nitrogen mustards.
Journal of the National Cancer Institute 1991;83(8):557-64

Gerson, SL.
Clinical relevance of MGMT in the treatment of cancer.

Journal of Clinical Oncology 2002;20(9):2388-99

Ghazal-Aswad S, Hogarth L, Hall AG, George M, Sinha DP, Lind M, Calvert AH, Sunter JP, Newell DR.
The relationship between tumour glutathione concentration, glutathione S-transferase isoenzyme expression and response to single agent carboplatin in epithelial ovarian cancer patients.
Br J Cancer. 1996 Aug;74(3):468-73.

Gibson LF, Fortney J, Magro G, Ericson SG, Lynch JP, Landreth KS.
Regulation of Bax and Bcl-2 expression in breast cancer cells by chemotherapy.
Breast Cancer Res. Treat. 1999;55(2):107-17

Gilman A, and Phillips FS.
The biological actions and therapeutic applications of the B-chloroethylamines and sulfides.
Science 1946;103(2675):409-15,436

Gligorov J, Lotz JP.
Preclinical pharmacology of the taxanes: implications of the differences.
Oncologist. 2004;9 Suppl 2:3-8.

Glisson B, Gupta R, Hodges P, Ross W.
Cross-resistance to intercalating agents in an epipodophyllotoxin-resistant Chinese hamster ovary cell line: evidence for a common intracellular target.
Cancer Res. 1986 Apr;46(4 Pt 2):1939-42.

Godwin AK, Meister A, O'Dwyer PJ, Huang CS, Hamilton TC, Anderson ME.
High resistance to cisplatin in human ovarian cancer cell lines is associated with a marker increase in glutathione synthesis.
PNAS 1992;89:3070-4

Golla R, Philp N, Safer D, Chintapalli J, Hoffman R, Collins L, Nachmias VT.

Co-ordinate regulation of the cytoskeleton in 3T3 cells overexpressing thymosin-beta4. Cell Motil Cytoskeleton. 1997;38(2):187-200.

Gong J, Constanzo A, Yang H-Q, Melino G, Kaelin Jr WG, Levrero M, Wang JYJ.
The tyrosine kinase c-Abl regulates p73 in apoptotic response to cisplatin-induced damage.
Nature 1999;399:806-9

Gonzalez VM, Fuertes MA, Alonso C, Perez JM.
Is cisplatin-induced cell death always produced by apoptosis?
Molecular Pharmacology 2001;59(4):657-63

Gordon AN, Granai CO, Rose PG, Hainsworth J, Lopez A, Weissman C, *et al.*
Phase II study of liposomal doxorubicin in platinum- and paxlitaxel- refractory epithelial ovarian cancer.
Journal of Clinical Oncology 2000;18:3093-100

Gordon AN, Fleagle JT, Guthrie D, Parkin DE, Gore ME, Lacave AJ.
Recurrent epithelial ovarian carcinoma: a randomized phase III study of pegylated liposomal doxorubicin versus topotecan.
J Clin Oncol. 2001 Jul 15;19(14):3312-22.

Gore ME, Fryatt I, Wiltshaw E, Dawson T, Robinson BA, Calvert AH.
Cisplatin/carboplatin cross-resistance in ovarian cancer.
Br J Cancer. 1989 Nov;60(5):767-9.

Goto S, Iida T, Cho S, Oka M, Kohno S, Kondo T.
Overexpression of glutathione s-transferase pi enhances the adduct formation of cisplatin with glutathione in human cancer cells.
Free Radical Research 1999;31(6):549-58

Goto S, Kamada K, Soh Y, Ihara Y and Kondo T.
Significance of nuclear glutathione s-transferase π in resistance to anti-cancer drugs.

Jpn. J. Can. Res. 2002;93:1047-56

Greenbaum M, Letourneau S, Assar H, Schecter RL, Batist G, Cournoyer D.
Retrovirus mediated gene transfer of rat glutathione S-transferase Yc confers alkylating drug resistance in NIH3T3 mouse fibroblasts.
Cancer Research 1994;54(16):4442-7

Grzanka A, Grzanka D, Orlikowska M.
Cytoskeletal reorganisation during process of apoptosis induced by cytostatic drugs in K-562 and HL-60 leukemia cell lines.
Biochem Pharmacol. 2003 Oct 15;66(8):1611-7.

Haldar S, Basu A, Croce CM.
Bcl2 is the guardian of microtubule integrity.
Cancer Res. 1997 Jan 15;57(2):229-33.

Hamaguchi K, Godwin AK, Yokushiji M, O'Dwyer PJ, Ozols RF, Hamilton TC.
Cross resistance to diverse drugs is associated with primary cisplatin resistance in ovarian cancer cell lines.
Cancer Research 1993;53:5225-32

Hamilton TC, Winker MA, Louie KG, Batist G, Behrens BC, Tsuro T, Grotzinger KR, McKoy WM, Young RC and Ozols RF.
Augmentation of adriamycin, melphalan and cisplatin cytotoxicity in drug resistant and sensitive human ovarian cancer cell lines by buthionine sulphoximine (BSO) mediated glutathione depletion.
Biochemical Pharmacology 1985;34(14):2583-6

Hanawalt PC.
Controlling the efficiency of excision repair.
Mutat Res. 2001 Feb 25;485(1):3-13.

Hanigan MH, Ricketts WA.

Extracellular GSHis a source of cysteine for cells that express gamma-glutamyl transpeptidase.
Biochemistry 1993;32:6302-6

Hanigan MH, Frierson HF Jr, Abeler VM, Kaern J, Taylor PT Jr.
Human germ cell tumours: expression of gamma-glutamyl transpeptidase and sensitivity to cisplatin.
British Journal of Cancer 1999;81(1):75-9

Hansson J, Lewensohn R, Ringborg U, Nilsson B.
Formation and removal of DNA crosslinks induced by melphalan and nitrogen mustard in relation to drug induced cytotoxicity in human melanoma cells.
Cancer Research 1987 May 15;47(10): 2631-7

Hansson J, Edgren MR, Egyhazi S, Hao XY, Mannervik B, Ringbork U.
Increased cisplatin sensitivity of human fibroblasts from a subject with an inherent glutathione deficiency.
Acta Oncol. 1996;35(6):683-90

Harder HC, Rosenberg B.
Inhibitory effects of anti-tumor platinum compounds on DNA, RNA and protein syntheses in mammalian cells in virtro.
Int J Cancer. 1970 Sep 15;6(2):207-16.

Hardiman G.
Microarray platforms--comparisons and contrasts.
Pharmacogenomics. 2004 Jul;5(5):487-502.

Harris CC.
P53: at the crossroad of molecular carcinogenesis and risk assessment.
Science 1993;262(5142):1980-1

Hartley JA.

Selectivity in Alkylating agent-DNA interactions.
In, Molecular aspects of Anticancer Drug-DNA Interactions, Volume I, eds. Neidle S, Waring M. 1993, CRC Press, USA.

Hartley JM, Spanswick VJ, Gander M, Giacomini G, Whelan J, Souhami R and Hartley JA.
Measurement of DNA crosslinks in patients on ifosfamide therapy using the single cell gel electrophoresis (comet) assay.
Clinical Cancer Research 1999;5:507-12

Hartley JA, Spanswick VJ, Brooks N, Clingen PH, McHugh PJ, Hochhauser D, Pedley RB, Kelland LR, Alley MC, Schultz R, Hollingshead MG, Schweikart KM, Tomaszewski JE, Sausville EA, Gregson SJ, Howard PW, Thurston DE.
SJG-136 (NSC 694501), a novel rationally designed DNA minor groove interstrand cross-linking agent with potent and broad spectrum antitumor activity: part 1: cellular pharmacology, in vitro and initial in vivo antitumor activity.
Cancer Res. 2004 Sep 15;64(18):6693-9.

Hashimoto Y, Shudo K.
Chemical modification of DNA with muta-carcinogens. III. Reductive alkylation of DNA with mitomycin C.
Environ Health Perspect. 1985 Oct;62:219-22.

Hashimoto H, Chattejee S, Berger NA.
Inhibition of etoposide (VP-16)-induced DNA recombination and mutant frequency by Bcl-2 protein overexpression.
Cancer Research 1995;55(18)4029-35

Hayakawa J, Depatie C, Ohmichi M, Mercola D.
The activation of c-jun $NH_2$-terminal kinase (JNK) by DNA-damaging agents serves to promote drug resistance via activating transcription factor 2 (ATF2)-dependent enhanced DNA repair.
The Journal of Biological Chemistry 2003; 278(23): 20582-92

Hayes D, Cvitkovic E, Goldberg R, Scheiner E and Krakoff IH.
Amelioration of renal toxicity of high dose cis-platinum diammine dichloride (CPDD) by mannitol induced diuresis.
Proc. Am. Assoc. Cancer Res. 1976; 67: p169.

Hazelhurst LA, Damiano JS, Buyuksal I, Pledger WJ and Dalton WS.
Adhesion to fibronectin via beta-1 integrins regulates p27kip1 levels and contributes to cell adhesion mediated drug resistance (CAM-DR).
Oncogene 2000;19:4319-27

Hazelhurst LA, Enkemann SA, Beam CA, et al.
Genotypic and phenotypic comparisons of de-novo and acquired melphalan resistance inan isogenic multiple myeloma cell line model.
Cancer Research 2003;63:7900-6

Henriques JAP, Moustacchi E.
Isolation and characterisation of *pso* mutants sensitive to photo-addition of psoralen derivatives in *Saccharomyces cerevisiae*.
Genetics 1980;95:273-88

Henriques JAP, Brozmanova J, Brendel M.
Role of *PSO* genes in the repair of photoinduced interstrand crosslinks and photooxidative damage in the DNA of the yeast *Saccharomyces cerevisiae*.
Journal of Photochemistry and Photobiology B: Biology 1997;39:185-96

Herod JJO, Eliopoulos AG, Warwick J, Niedobitek G, Young LS, Kerr DJ.
The prognostic significance of Bcl-2 and p53 expression in ovarian carcinoma.
Cancer Research 1996;56:2178-84

Herzog TJ.
Clinical experience with topotecan in relapsed ovarian cancer.
Gynecological Oncology 2003;90 (3pt2):S3-7

Hickman JA.

Apoptosis and chemotherapy resistance.
European Journal of Cancer 1996;32A(6):921-6

Higby DJ, Wallace HJ Jr, Albert D et al.
Diamminodichloroplatinum in the chemotherapy of testicular tumours.
Journal of Urology 1974; 112:100-4

Hill BT, Shellard SA, Fichtinger-Schepman AM, Schmoll HJ and Harstick A.
Differential formation and enhanced removal of specific cisplatin DNA adducts in two cisplatin-selected resistant human testicular teratome sublines.
Anticancer Drugs 1994a, Jun;5(3):321-8

Hill BT, Scanlon KJ, Hansson J, Harstrick A, Pera M, Fichtinger-Schepman AM, Shellard SA.
Deficient repair of cisplatin-DNA adducts identified in human testicular teratoma cell lines established from tumours from untreated patients.
Eur J Cancer. 1994b;30A(6):832-7.

Hilton J.
Role of aldehyde dehydrogenase in cyclophosphamide-resistant L1210 leukaemia.
Cancer Research 1984;44(11):5156-60

Hirazono K, Shinozuka T, Kuroshima Y, Itoh H, Kawai K.
Immunohistochemical expression of glutathione S-transferase pi (GST-pi) and chemotherapy response in malignant ovarian tumors.
J Obstet Gynaecol. 1995 Jun;21(3):305-12.

Hishikawa Y, Abe S, Kinugasa S, Yoshimura H, Monden N, Igarashi M, Tachibana M, Nagasue N.
Overexpression of metallothionein correlates with chemoresistance to cisplatin and prognosis in oesophageal cancer.
Oncology 1997;54(4):342-7

Hochwald SN, Harrison LE, Rose DM, Anderson M, Burt ME.

Gamma glutamyl transpeptidase mediation of tumour GSH utilisation in-vivo.
Journal of the National Cancer Institute 1996;88:193-7

Holford J, Sharp SY, Murrer BA, Abrams M, Kelland LR.
In vitro circumvention of cisplatin resistance by the novel sterically hindered platinum complex AMD473.
British Journal of Cancer 1998;77(3):366-73

Holford J, Beale PJ, Boxall FE, Sharp SY, Kelland LR.
Mechanism of drug resistance to the platinum complex ZD0473 in ovarian cancer cell lines.
European Journal of Cancer 2000;36:1984-90

Hollstein M, Sidransky D, Vogelstein B, Harris CC.
P53 mutations in human cancers.
Science 1991;253(5015):49-53

Holzer A, Samimi G, Katano K, Naedermann W, Howell SB.
The role of human copper transporter hCTR1 in cisplatin uptake in human ovarian cancer cells.
Proc. Am. Assoc. Cancer Res. 2003;44:923

Hong JH, Lee E, Shin HYJ, Ahn H.
Antisense Bcl-2 oligonucleotide in cisplatin-resistant bladder cancer cell lines.
BJU Unternational 2002;90:113-7

Horton JK, Roy G, Piper JT, Van Houten B, Awasthi YC, Mitra S, Alaoui-Jamali MA, Boldogh I, Singhal SS.
Characterisation of a chlorambucil-resistant human ovarian carcinoma cell line overexpressing glutathione S-transferase μ.
Biochemical Pharmacology 1999;58:693-702

Hospers GAP, Mulder NH, de Jong B, de Ley L, Uges DRA, Fichtinger-Schepman AMJ, Scheper RJ, de Vries EGE.

Characterisation of a human small cell lung carcinoma cell line with acquired resistance to CDDP(II) *in-vitro*.
Cancer Research 1988;48:6803-7

Hough CD, Cho KR, Zonderman AB, Schwartz DR, Morin PJ.
Coordinately up-regulated genes in ovarian cancer.
Cancer Res. 2001 May 15;61(10):3869-76.

Houtsmuller AD, Rademakers S, Nigg AI, Hoogstraten D, Hoeijmakers JHJ and Vermeulen W.
Action of DNA repair endonuclease ERCC1/XPF in living cells.
Science 1999;284:958-61

Howle JA, Gale GR.
Cis-dichlorodiammineplatinum (II). Persistent and selective inhibition of deoxyribonucleic acid synthesis in vivo.
Biochem Pharmacol. 1970 Oct;19(10):2757-62.

Howlett NG, Taniguchi T, Olson S, Cox B, Waisfisz Q, De Die-Smulders C, Persky N, Grompe M, Joenje H, Pals G, Ikeda H, Fox EA, D'Andrea AD.
Biallelic inactivation of BRCA2 in Fanconi Anemia.
Science 2002;297(5581):606-9

Hoy CA, Thompson LH, Mooney CL, Salazar EP.
Defective DNA crosslink removal in Chinese hamster cell mutants hypersensitive to bifunctional alkylating agents.
Cancer Research 1985 ;45 (4): 1737-43

Huang J-C, Svoboda DL, Reardon JT, Sancar A.
Human nucleotide excision nuclease removes thymine dimers from DNA by incising the 22$^{nd}$ phosphodiester bond 5' and the 6$^{th}$ phosphodiester bond 3' to the photodimer.
Proc. Natl. Acad. Sci. USA 1992;89:3664-8

Huang CS, Anderson M, Meister A.
Amino acid sequence and function of the light subunit of rat kidney gamma-glutamylcysteine synthetase.
Journal of Biological Chemistry 1993;268:20578-83

Huang J-C, Zamble DB, Reardon JT, Lippard SJ, Sancar A.
HMG-domain proteins specifically inhibit the repair of the major DNA adduct of the anticancer drug cisplatin by human excision nuclease.
Proc. Natl. Acad. Sci. USA 1994;91:10394-8

Hudelist G, Singer CF, Kubista E, Czerwenka K.
Use of high-throughput arrays for profiling differentially expressed proteins in normal and malignant tissues.
Anticancer Drugs. 2005 Aug;16(7):683-9.

Huizing MT, Misser VH, Pieters RC, ten Bokkel Huinink WW, Veenhof CH, Vermorken JB, Pinedo HM, Beijnen JH.
Taxanes: a new class of antitumour agents.
Cancer Invest. 1995;13(4):381-404

Hungerford JE, Compton MT, Matter ML, Hoffstrom BG, Otey CA.
Inhibition of pp125FAK in cultured fibroblasts results in apoptosis.
J Cell Biol. 1996 Dec;135(5):1383-90

Husain A, He G, Venkatraman ES, Spriggs DR.
BRCA1 up-regulation is associated with repair-mediated resistance to cis-diamminedichloroplatinum(II).
Cancer Res. 1998 Mar 15;58(6):1120-3.

Ishida S, Lee J, Thiele DJ, Herskowitz I.
Uptake of the anticancer drug cisplatin mediated by the copper transporter Ctr1 in yeast and mammals.
Proc Natl Acad Sci U S A. 2002 Oct 29;99(22):14298-302

Ishihara S, Minato K, Hoshino H, Saito R, Hara F, Nakajima T and Mori M.
The cyclin-dependent kinase inhibitor p27 as a prognostic factor in advanced non-small cell lung cancer: its immunohistochemical evaluation using biopsy specimens.
Lung Cancer 1999; 26:187-94

Ivanov EL, Harber JE.
*RAD1* and *RAD10* but no other excision repair genes are required for double strand break induced recombination in *Saccharomyces cerevisiae.*
Mol. Cell Biol. 1995;15:2245-51

Iyer L. and Ratain MJ.
Pharmacogenetics and Cancer Chemotherapy.
European Journal of Cancer 1998, 34 (10): 1493-99.

Jamieson ER, and Lippard SJ.
Structure, recognition and processing of cisplatin–DNA adducts.
Chem. Rev. 1999;99:2467-98

Jansen BAJ, Brouwer J, Reedijk J.
Glutathione induces cellular resistance against cationic dinuclear platinum anticancer drugs.
Journal of Inorganic Biochemistry 2002;89:197-202

Jennerwein MM, Eastman A, Khokhar A.
Characterisation of adducts produced in DNA by isomeric 1,2-diaminocyclohexaneplatinum(II) complexes.
Chem Biol Interact. 1989;70(1-2):39-49.

Jiricny J.
Mediating mismatch repair.
Nature Genetics 2000;24:6-8

Johnson IS, Armstrong JG, Gorman M, Burnett JP Jr.

The Vinca Alkaloids: A new class of oncolytic agents.
Cancer Research 1963;23:1390-427

Johnson SW, Perez RP, Godwin AK, Yeung AT, Handel LM, Ozols RF, Hamilton TC.
Role of platinum-DNA adduct formation and removal in cisplatin resistance in human ovarian cancer cell lines.
Biochem Pharmacol. 1994a Feb 11;47(4):689-97.

Johnson SW, Swiggard PA, Handel LM, Brennan JM, Godwin AK, Ozols RF, Hamilton TC.
Relationship between platinum-DNA adduct formation and removal and cisplatin cytotoxicity in cisplatin-sensitive and -resistant human ovarian cancer cells.
Cancer Res. 1994b Nov 15;54(22):5911-6.

Jolles CJ.
Ovarian cancer: histogenic classification, histologic grading, diagnosis, staging and epidemiology.
Clin. Obstet. Gynecol. 1985;28(4):787-99

Jones JC, Zhen WP, Reed E, Parker RJ, Sancar A, Bohr VA.
Gene-specific formation and repair of cisplatin intrastrand adducts and interstrand cross-links in Chinese hamster ovary cells.
J Biol Chem. 1991 Apr 15;266(11):7101-7.

Jones CJ, Wood RD.
Preferential bindng of the xeroderma pigmentosum group A complementing protein to damaged DNA.
Biochemistry 1993;32(45):12096-104

Jones PA, and Laird PW.
Cancer epigenetics comes of age.

Nature Genetics 1999;21:163-7

Jordan MA.
Mechanism of action of antitumor drugs that interact with microtubules and tubulin.
Curr Med Chem Anti-Canc Agents. 2002 Jan;2(1):1-17.

Junor EJ, Hole DJ, McNulty L, Mason M, Young J.
Specialist gynaecologists and survival outcome in ovarian cancer: a Scottish national study of 1866 patients.
Br. J. Obstet. Gynaecol. 1999;106:1130-6

Kamesaki S, Kamesaki H, Jorgensen TJ, Tanizawa A, Pommier Y, Cossman J.
Bcl-2 protein inhibits etoposide-induced apoptosis through its effects on events subsequent to topoisomerase II-induced DNA strand breaks and their repair.
Cancer Research 1993;53(18):4251-6

Kartalou M, Essigman JM.
Mechanisms of resistance to cisplatin.
Mutation Research 2001;478:23-43

Kasparkova J, Brabec V.
Recognition of DNA interstrand cross-links of cis-diamminedichloroplatinum(II) and its trans isomer by DNA-binding proteins.
Biochemistry. 1995 Sep 26;34(38):12379-87.

Kasparkova J, Novakova O, Farrell N, Brabec V.
DNA binding by antitumour trans-[PtCL2(NH3)thiazole)]. Protein recognition and nucleotide excision repair of monofunctional adducts.
Biochemistry 2003 Jan 28;42(3): 792-800

Katano K, Kondo A, Safaei R, Holzer A, Samimi G, Mishima M, Kuo YM, Rochdi M, Howell SB.
Acquisition of resistance to cisplatin is accompanied by changes in the cellular pharmacology of copper.

Cancer Res. 2002 Nov 15;62(22):6559-65.

Katsumata N.
Docetaxel: an alternative taxane in ovarian cancer.
British Journal of Cancer 2003;89 Suppl. 3;S9-S15.

Katz ME, Schwartz PE, Kapp DS, Luikart S.
Epithelial carcinoma of the ovary: current strategies.
Ann. Intern. Med. 1981;91(1):98-111

Kavallaris M, Kuo DY, Burkhart CA, Regl DL, Norris MD, Haber M, Horwitz SB.
Taxol-resistant epithelial ovarian tumours are associated with altered expression of specific beta-tubulin isotypes.
Journal of Clinical Investigation 1997;100(5):1282-93

Kelland LR, Abel G, McKeage MJ, Jones M, Goddard PM, Valenti M, Murrer BA, Harrap KR.
Preclinical antitumour evaluation of Bis-acetato-ammine-dichloro-cyclohexylamine platinum (IV): an orally active platinum drug.
Cancer Research 1993;53:2581-6

Keller KL, Overbeck-Carrick TL, Beck DJ.
Survival and induction of SOS in Escherichia coli treated with cisplatin, UV-irradiation, or mitomycin C are dependent on the function of the RecBC and RecFOR pathways of homologous recombination.
Mutat Res. 2001 Jun 5;486(1):21-9.

Kelley SI, Basu A, Teicher BA, Hacker MP, Hamer DH, Lazo JS.
Overexpression of metallothionein confers resistance to anticancer drugs.
Science 1988;241(4874): 1813-5.

Khan AS.

Genomics and microarray for detection and diagnostics.
Acta Microbiol Immunol Hung. 2004;51(4):463-7.

Kigawa J, Minagawa Y, Kanamori Y, Itamochi H, Cheng X, Okada M, Oishi T, Terakawa N.
Glutathione concentration may be a useful predictor of response to second-line chemotherapy in patients with ovarian cancer.
Cancer. 1998 Feb 15;82(4):697-702.

Kikuchi Y, Hirata J, Yamamoto K, Ishii K, Kita T, Kudoh K, Tode T, Nagata I, Taniguchi K, Kuwano M.
Altered expression of gamma-glutamylcysteine synthetase, metallothionein and topoisomerase I or II during acquisition of drug resistance to cisplatin in human ovarian cancer cells.
Jpn. J. Cancer Res. 1997;88(2):213-7

Kim JK, Patel D, Choi BS.
Contrasting structural impacts induced by cis-syn cyclobutane dimmer and (6-4) adduct in DNA duplex decamers: implication in mutagenesis and repair activity.
Photochem. Photobiol. 1995;62(1):44-50

Kitada S, Andersen J, Akar S, Zapata JM, Takayama S, Krajewski S, Wang HG, Zhang X, Bullrich F, Croce CM, Rai K, Hines J, Reed JC.
Expression of apoptosis –regulating proteins in chronic lymphocytic leukaemia: correlations with in vitro and in vivo chemoresponses.
Blood 1998;91(9):3379-89

Knox RJ, Friedlos F, Lydall DA, Roberts JJ.
Mechanism of cytotoxicity of anticancer platinum drugs: evidence that cis-diamminedichloroplatinum(II) and cis-diammine-(1,1-cyclobutanedicarboxylato)platinum(II) differ only in the kinetics of their interaction with DNA.
Cancer Res. 1986 Apr;46(4 Pt 2):1972-9.

Knox RJ, Lydall DA, Friedlos F, Basham C, Roberts JJ.
The effect of monofunctional or difunctional platinum adducts and of various other associated DNA damage on the expression of transfected DNA in mammalian cell lines sensitive or resistant to difunctional agents.
Biochim Biophys Acta. 1987 Apr 29;908(3):214-23.

Kobayashi H, Man S, Graham CH, Kapitain SJ, Teicher BA, Kerbel RS.
Acquired multi-cellular mediated resistance to alkylating agents in cancer.
PNAS 1993;90(8):3294-8

Kobayashi S, Kohda T, Miyoshi N, Kuroiwa Y, Aisaka K, Tsutsumi O, Kaneko-Ishino T, Ishino F.
Human PEG1/MEST, an imprinted gene on chromosome 7.
Hum Mol Genet. 1997 May;6(5):781-6.

Kobayashi T, Ruan S, Clodi K, Kliche KO, Shiku H, Andreeff M, Zhang W.
Overexpression of Bax gene sensitised K562 erythroleukaemia cells to apoptosis induced by selective chemotherapeutic agents.
Oncogene 1998;16(12):1587-91

Koberle B, Grimaldi KA, Sunters A, Hartley JA, Kelland LR, Masters RW.
DNA repair capacity and cisplatin sensitivity of human testis tumour cells.
International Journal of Cancer 1997;70:551-5

Koberle B, Masters JRW, Hartley JA, Wood RD.
Defective repair of cisplatin-induced DNA damage caused by reduced XPA protein in testicular germ cell tumours.
Current Biology 1999;9:273-6

Kociba RJ, Sleight SD, Rosenberg B.
Inhibition of Dunning asc itic leukemia and Walker 256 carcinosarcoma with cis-diamminedichloroplatinum (NSC-119875).
Cancer Chemother Rep. 1970 Oct;54(5):325-8.

Kocjan G, Sweetney E, Miller KD, Bobrow L.
AUA1: New immunocytochemical marker for detecting epithelial cells in body cavity fluids.
J Clin. Pathol. 1992; 45: 358-9

Kohler T, Schill C, Deininger MW, Krahl R, Borchert S, Hasenclever D, Leiblein S, Wagner O, Neiderwieser D.
High Bad and Bax mRNA expression correlate with negative outcomein acute myeloid leukaemia (AML).
Leukaemia 2002;16(1):22-9

Kohn K, Ewig R, Erickson L, and Zwelling L.
Measurement of strand breaks and cross links by alkaline elution. In: E.C. Friedberg and P.C. Hanawalt (eds.). DNA Repair. A Laboratory Manual of Research Procedures. Volume 1, Part B, pp379-402 (Marcel Dekker) 1981.

Kohn KW,
Biological aspects of DNA damage by crosslinking agents.
In, Molecular aspects of anti-cancer drug action, ed. Neidle and Waring. 1983

Koike K, Kawabe T, Tanaka T, Toh S, Uchiumi T, Wada M, Akiyama S, Ono M, Kuwano M.
A canalicular multispecific organic anion transporter (cMOAT) antisense cDNA enhances drug sensitivity in human hepatic cancer cells.
Cancer Res. 1997 Dec 15;57(24):5475-9.

Kolm RH, Groga SE,Mannervik B.
Participation of the phenolic hydroxyl group of Try-8 in the catalytic mechanism of human glutathione transferase P1-1.
Biochem. J. 1992;285:537-40

Komatsu M, Sumizawa T, Mutoh M, Chen ZS, Terada K, Furukawa T, Yang XL, Gao H, Miura N, Sugiyama T, Akiyama S.

Copper-transporting P-type adenosine triphosphatase (ATP7B) is associated with cisplatin resistance.
Cancer Res. 2000 Mar 1;60(5):1312-6.

Komiya S, Gebhardt MC, Mangham DC, Inoue A.
Role of glutathione in cisplatin resistance in osteosarcoma cell lines.
Journal of Orthop. Res. 1998;16(1):15-22

Kondo S, Yin D, Takeuchi J, Morimura T, Oda Y, Kikuchi H.
Bcl-2 gene enables rescue from in-vitro myelosuppression (bone marrow cell death) induced by chemotherapy.
British Journal of Cancer 1994;70(3):421-6

Kondo Y, Woo ES, Michalska AE, Choo KH, Lazo JS.
Metallothionein null cells have increased sensitivity to anti-cancer drugs.
Cancer Research 1995;55(10):2021-3

Konopa J.
Adriamycin and daunomycin induce interstrand DNA crosslinks in Hela S3 Cells.
Biochem Biophys Res Commun. 1983 Feb 10;110(3):819-26.

Kool M, de Haas M, Scheffer GL, Scheper RJ, van Eijk MJ, Juijn JA, Baas F, Borst P.
Analysis of expression of cMOAT (MRP2), MRP3, MRP4, and MRP5, homologues of the multidrug resistance-associated protein gene (MRP1), in human cancer cell lines.
Cancer Res. 1997 Aug 15;57(16):3537-47.

Kostanova-Poliakova D, Sabova L.
Anti-apoptotic proteins-targets for chemosensitisation of tumour cells and cancer treatment.
Neoplasma 2005;52(6):441-9

Kotecha MT, Afghan RK, Vasilikopoulou E, Wilson E, Marsh P, Kast WM, Davies DH, Caparros-Wanderley W.
Enhanced tumour growth after DNA vaccination against human papilloma virus E7 oncoprotein: evidence for tumour-induced immune deviation.
Vaccine. 2003 Jun 2;21(19-20):2506-15.

Koyama T, Suzuki H, Imakiire A, Yanase N, Hata K, Mizuguchi J.
Id3-mediated enhancement of cisplatin-induced apoptosis in a sarcoma cell line MG-63.
Anticancer Research 2004;24(3a):1519-24

Krilleke D, Ucur E, Pulte D, Schulze-Osthoff K, Debatin KM, Herr I.
Inhibition of JNK signaling diminishes early but not late cellular stress-induced apoptosis.
Int J Cancer. 2003 Nov 20;107(4):520-7.

Kristensen GB, Trope C.
Epithelial ovarian carcinoma.
Lancet 1997;349:113-7

Kudoh K, Kita T, Hirata J, Ishii K, Hiramatsu H, Kikuchi Y, Nagata I.
Potentiation of cisplatin sensitivity of cisplatin resistant human ovarian cancer cell lines by buthionine sulphoximine.
Nippon Sanka Fujinka Gakkai Zasshi 1994;46(6):525-32

Kudoh K, Kita K, Hirata J, Ishii K, Hiramatsu H, Kikuchi Y, Nagata I.
Potentiation of cisplatin sensitivity of cisplatin resistant human ovarian cancer cell lines by buthionine sulphoximine.
Journal of Orthop. Res. 1998;16(1):15-22

Kudoh K, Takano M, Koshikawa T, Hirai M, Yoshida S, Mano Y, Yamamoto K, Ishii K, Kita T, Kikuchi Y, Nagata I, Miwa M, Uchida K.
Gains of 1q21-q22 and 13q12-q14 are potential indicators for resistance to cisplatin-based chemotherapy in ovarian cancer patients.
Clinical Cancer Research 1999;5:2526-31

Kuhn W, Rutke S, Spathe K. Schmalfeldt B, Florack G, von Hundelshausen B, Pachyn D, Ulm K, Graeff H .
Neoadjuvant chemotherapy followed by tumour debulking prolongs survival for patients with poor prognosis in International Federation of Gyecology and Obstetrics stage IIIC ovarian carcinoma.
Cancer 2001;92:2585-91

Kuraoka I, Kobertz WR, Ariza RR, Biggerstaff M, Essigmann JM, Woods RD.
Repair of an interstrand DNA crosslink initiated by ERCC1-XPF repair/recombination nuclease.
The Journal of Biological Chemistry 2000;275(34):26632-36

Kurian KM, Watson CJ, Wyllie AH.
DNA Chip Technology
Journal of Pathology 1999;187:267-71

Kurokawa M, Mitani K, Yamagata T, Takahashi T, Izutsu K, Ogawa S, Moriguchi T, Nishida E, Yazaki Y, Hirai H.
The evi-1 oncoprotein inhibits c-jun N-terminal kinase and prevents stress-induced cell death.
EMBO J. 2000 Jun 15;19(12):2958-68.

Lai GM, Ozols RF, Smyth JF.
Enhanced DNA repair and resistance to CDDP(II) in human ovarian cancer cell lines.
Biochemical Pharmacology 1988;37:4597-600

Lai GM, Ozols RF, Young RC, Hamilton TC.
Effect of glutathione on DNA repair in cisplatin-resistant human ovarian cancer cell lines.
Journal of the National Cancer Institute 1989;81(7):535-9

Lan L, Hayashi T, Rabeya RM, Nakajima S, Kanno S, Takao M, Matsunaga T, Yoshino M, Ichikawa M, Riele H, Tsuchiya S, Tanaka K. Yasui A.
Functional and physical interactions between ERCC1 and MSH2 complexes for resistance to cis-diamminedichloroplatinum (II) in mammalian cells.
DNA Repair (Amst.) 2004;3(2):135-43

Landi S.
Mammalian class theta GST and differential susceptibility to carcinogens: a review.
Mutation Research 2000;463:247-83

Larminat F, Zhen W, Bohr VA.
Gene-specific repair of interstrand crosslinks induced by chemotherapeutic agents can be preferential.
The Journal of Biological Chemistry 1993;268(4):2649-54

Larsen AK, Escargueil AE, Skladanowski A.
Catalytic topoisomerase II inhibitors in cancer therapy.
Pharmacol Ther. 2003 Aug;99(2):167-81.

Lawley PD, Phillips DH.
DNA adducts from chemotherapeutic agents.
Mutation Research 1996;355:13-40

Leadon SA.
DNA Repair '99: Transcription coupled repair of DNA damage: unanticipated players, unexpected complexities.
Am. J. Hum. Genet. 1999;64:1249-63

Leadon SA, and Lawrence DA,
Preferential repair of DNA damage on the transcribed strand of the human metallothionein genes requires RNA polymerase II.
Mutation Research 1991;255:67-78

Lebwohl D and Canetta R.

Clinical Development of platinum complexes in cancer therapy: an historical perspective and an update.
European Journal of Cancer 1998; 34(10): 1522-34

Lee KS, Kim HK, Moon AS, Hong YS, Kang JH, Kim DJ, Park JG.
Effects of BSO treatment on glutathione levels and cytotoxicities of cisplatin, carboplatin and radiation in human stomach and ovarian cancer cell lines.
Korean Journal of Internal Medicine 1992;7(2):111-7

Lee KB, Parker RJ, Bohr V, Cornelison T, and Reed E.
Cisplatin sensitivity/resistance in UV repair-deficient Chinese hamster ovary cells of complementation groups 1 and 3.
Carcinogenesis 1993;14(10): 2177-80

Lee JH, Park CJ, Shin JS, Ikegami T, Akutsu H, Choi BS.
NMR structure of the DNA decamer duplex containing double T*G mismatches of cis-syn cyclobutane pyrimidine dimer: implications for DNA damage recognition by the XPC-hHR23B complex.
Nucleic Acids Research 2004;32(8):2474-81

Legendre F, Bas V, Kozelka J, Chottard JC.
A complete kinetic study of GG versus AG platination suggests that the doubly aquated derivatives of cisplatin are the actual DNA binding species.
Chemistry 2000;6(11):2002-10

Lehmann AR.
DNA repair-deficient diseases, xeroderma pigmentosum, Cockayne syndrome and trichothiodystrophy.
Biochimie 2003;85(11):1101-11

Leonard GD, Fojo T, Bates SE.
The role of ABC transporters in clinical practice.
Oncologist. 2003;8(5):411-24.

Lepre CA, Strothkamp KG, Lippard SJ.
Synthesis and 1H NMR spectroscopic characterisation of trans-[Pt(NH3)2[d(ApGpGpCpCpT)-N7-A(1), N7-G(3)]].
Biochemistry, 1987, 26, 5651-5657

Leslie EM, Deeley RG, Cole SP.
Multidrug resistance proteins: role of P-glycoprotein, MRP1, MRP2, and BCRP (ABCG2) in tissue defense.
Toxicol Appl Pharmacol. 2005 May 1;204(3):216-37.

Levesque MA, Katsaros D, Massobrio M, Genta F, Yu H, Richiardi G, Fracchioli S, Durando A, Arisio R, Diamandis EP.
Evidence for a dose-response effect between p53 (but not $p21^{WAF1\ Cip1}$) protein concentrations, survival, and responsiveness in patients with epithelial ovarian cancer treated with platinum-based chemotherapy.
Clinical Cancer Research 2000;6:3260-70

Levi F, Franceschi S, La Vecchia C, Ruzicka J, Gloor E, Randimbison L.
Epidemiologic pathology of ovarian cancer from the Vaud Cancer Registry, Switzerland.
Ann. Oncol. 1993;4(4):289-94

Lewandowicz GM, Britt P, Elgie AW, Williamson CJ, Coley HM, Hall AG, Sargent JM.
Cellular glutathione content, in vitro chemoresponse, and the effect of BSO modulation in samples derived from patients with advanced ovarian cancer.
Gynecol Oncol. 2002 May;85(2):298-304.

Leyland-Jones BR, Townsend AJ, Tu CP, Cowan KH, Goldsmith ME.
Antineoplastic drug sensitivity of human MCF-7 breast cancer cells stably transfected with a human alpha class glutathione S-transferase gene.
Cancer Research 1991;51(2):587-94

Li P, Nijhawan D, Budihardjo J, Srinivasula SM, *et al.*

Cytochrome c and dATP-dependent formation of Apaf-1/caspase complex initiates an apoptotic protease cascade.
Cell 1997;91:479-89.

Li Q, Bostick-Bruton F, Reed E.
Effect of interleukin-1 alpha and tumour necrosis factor-alpha on cisplatin-induced ERCC-1 mRNA expression in a human ovarian carcinoma cell line.
Anticancer Res. 1998a Jul-Aug;18(4A):2283-7.

Li Q, Gardner K, Zhang L, Tsang B, Bostick-Bruton F, Reed E.
Cisplatin induction of ERCC-1 mRNA expression in A2780/CP70 human ovarian cancer cells.
J Biol Chem. 1998b Sep 4;273(36):23419-25.

Li Q, Ding L, Yu JJ, Mu C, Tsang B, Bostick-Bruton F, Reed E.
Cisplatin and phorbol ester independently induce ERCC-1 protein in human ovarian carcinoma cells.
Int J Oncol. 1998c Nov;13(5):987-92.

Li Q, Tsang B, Bostick-Bruton F, Reed E.
Modulation of excision repair cross complementation group 1 (ERCC-1) mRNA expression by pharmacological agents in human ovarian carcinoma cells.
Biochem Pharmacol. 1999 Feb 15;57(4):347-53.

Li QQ, Ding L, Reed E.
Proteasome inhibition suppresses cisplatin-dependent ERCC-1 mRNA expression in human ovarian tumor cells.
Res Commun Mol Pathol Pharmacol. 2000 May-Jun;107(5-6):387-96.

Li QQ, Yunmbam MK, Zhong X, Yu JJ, Mimnaugh EG, Neckers L, Reed E.
Lactacystin enhances cisplatin sensitivity in resistant human ovarian cancer cell lines via inhibition of DNA repair and ERCC-1 expression.
Cell Mol Biol (Noisy-le-grand). 2001;47 Online Pub:OL61-72.

Li L, Luan Y, Wang G, Tang B, Li D, Zhang W, Li X, Zhao J, Ding H, Reed E, Li QQ.
Development and characterisation of five cell models for chemoresistance studies of human ovarian carcinoma.
International Journal of Molecular Medicine 2004;14(2):257-64

Liedert B, Materna V, Schadendorf D, Thomale J, Lage H.
Overexpression of cMOAT (MRP2/ABCC2) is associated with decreased formation of platinum-DNA adducts and decreased G2-arrest in melanoma cells resistant to cisplatin.
J Invest Dermatol. 2003 Jul;121(1):172-6.

Lipponen P, Pietilainein T, Kosma VM, Aaltomaa S, Eskelinen M, Syrjanen K.
Apoptosis suppressing protein Bcl-2 is expressed in well-differentiated breast carcinomas with favourable prognosis.
Journal of Pathology 1995;177(1):49-55

Liu N, Lamerdin JE, Tebbs RS, Schild D, Tucker JD, Shen MR, Brookman KW, et al.
XRCC2 and XRCC3, new human Rad51-family members, promote chromosome stability and protect against DNA crosslinks and other damages.
Molecular Cell 1998:1:783-93

Lodish et al. Molecular Cell Biology, 1995 third edition. Scientific American Books, NY, USA.

Lohrer H, Robson T.
Overexpression of metallothionein in CHO cells and its effect on cell killing by ionizing radiation and alkylating agents.
Carcinogenesis 1989;10(12):2279-84

Louie KG, Behrens BC, Kinsella TJ, Hamilton TC, Grotzinger KR, McKoy WM, Winker MA, Ozols RF.

Radiation survival parameters of antineoplastic drug-sensitive and -resistant human ovarian cancer cell lines and their modification by buthionine sulfoximine.
Can. Res. 1985 May;45(5):2110-5

Lowe SW, Lin AW.
Apoptosis in cancer.
Carcinogenesis 2000;21(3):485-95

Lown JW.
The chemistry of DNA damage by antitumour drugs.
Molecular Aspects of Anticancer Drug Action, ed. Weidle and Waring, 1983

Ludlum DB.
Reaction of nitrogen mustard with synthetic polynucleotides.
Biochim. Biophys. Acta. 1967;142(1):282-4

MacKay HJ, Cameron D, Rahilly M, MacKean MJ, Paul J, Kaye SB, Brown R.
Reduced MLH1 expression in breast tumours after primary chemotherapy predicts disease free survival.
Journal of Clinical Oncology 2000;18:87-93

MacKean MJ, Millan D, Paul J, Kaye SB, and Brown R.
The clinical relevance of mismatch repair protein immunochemistry in ovarian cancer.
Proc. Am. Assoc. Cancer Research 1999;40:498

Magnaldo T, Sarasin A.
Xeroderma pigmentosum: from symptoms and genetics to gene-based skin therapy.
Cells Tissues Organs. 2004;177(3):189-98.

Makar AP, Baekelandt M, Trope CG, Kristensen GB.
The prognostic significance of residual disease, FIGO substage, tumour histology, and grade in patients with FIGO stage III ovarian cancer.
Gynecologic Oncology 1995;56:175-80

Mantripragada KK, Buckley PG, de Stahl TD, Dumanski JP.
Genomic microarrays in the spotlight.
Trends Genet. 2004;20(2):87-94

Markman M, Rothman R, Hakes T, Reichman B, Hoskins W, Rubin S, Jones W, Almadrones L, Lewis JL Jr.
Second-line platinum therapy in patients with ovarian cancer previously treated with cisplatin.
J Clin Oncol. 1991 Mar;9(3):389-93.

Masson JY, Tarsounas MC, Stasiak AZ, Stasiak A, Shah R, McIlwraith MJ, Benson FE, West SC.
Identification and purification of two distinct complexes containing the five Rad51 paralogs.
Genes Dev. 2001;15(24):3296-307

Masuda H, Ozols RF, Lai GM, Fojo A, Rothenberg M, Hamilton TC.
Increased DNA repair as a mechanism of acquired resistance to cis-diamminedichloroplatinum(II) in human ovarian cancer cells.
Cancer Research 1988 Oct 15;48(20):5713-6

Masuda H, Tanaka T, Masuda H, Kusaba I.
Increased removal of DNA bound platinum in a human ovarian cancer cell line resistant to cis-diamminedichloroplatinum(II).
Cancer Research 1990; 50:1863-1866

Materna V, Liedert B, Thomale J, Lage H.
Protection of platinum-DNA adduct formation and reversal of cisplatin resistance by anti-MRP2 hammerhead ribozymes in human cancer cells.
Int J Cancer. 2005 Jun 20;115(3):393-402.

Matsumoto Y, Oka M, Sakamoto A, Narasaki F, Fukuda M, Takatani H, Terashi K, Ikeda K, Tsurutani J, Nagashima S, Soda S, Kohno S.
Enhanced expression of metallothionein in human non-small-cell lung carcinomas following chemotherapy.
Anticancer Research 1997;17(5B):3777-80

Matsunaga T, Mu D, Park C-H, Reardon JT, Sancar A.
Human DNA repair excision nuclease.
The Journal of Biological Chemistry 1995;270(35):20862-9

Mattes WB, Hartley JA, Kohn KW.
DNA sequence selectivity of guanine-N7 alkylation by nitrogen mustards.
Nucleic Acids Resarch 1986;14(7):2971-87

Mayne LV and Lehmann AR.
Failure of RNA synthesis to recover after UV irradiation: an early defect in cells from individuals with Cockayne's syndrome and xeroderma pigmentosum.
Cancer Research 1982;42:1473-78

Mayr D, Pannekamp U, Baretton GB, Gropp M, Meier W, Flens MJ, Scheper R, Diebold J.
Immunohistochemical analysis of drug resistance-associated proteins in ovarian carcinomas.
Pathol. Res. Pract. 2000; 196(7):469-75

McGuire WP, Hoskins WJ, Brady MF, Kucera PR, Partridge EE, Look KY, Clarke-Pearson DL, Davidson M.
Cyclophosphamide and cisplatin compared with paclitaxel and cisplatin in patients with stage III and stage IV ovarian cancer.
The New England Journal of Medicine 1996;334:1-6

McHugh PJ, Sones WR, Hartley JA.

Repair of intermediate structures produced at DNA interstrand crosslinks in *Saccharomyces cerevisiae*.
Molecular and Cellular Biology 2000;20(10):3425-33

McHugh PJ, Spanswick VJ, Hartley JA.
Repair of DNA interstrand crosslinks: molecular mechanisms and clinical relevance.
The Lancet, Oncology 2001;2:483-90

McLean GW, Carragher NO, Avizienyte E, Evans J, Brunton VG, Frame MC.
The role of focal-adhesion kinase in cancer - a new therapeutic opportunity.
Nat Rev Cancer. 2005 Jul;5(7):505-15.

Meijer C, Mulder NH, Hospers GAP, Uges DRA, de Vries EGE.
The role of glutathione in resistance to cisplatin in a human small cell lung cancer cell line.
British Journal of Cancer 1990;62(1):72-7

Meijer C, Mulder NH, Trimmer-Bosscha H, Sluiter WJ, Meersma GJ, de Vries EGE.
Relatioship of cellular glutathione to the cytotoxicity and resistance of seven platinum compounds.
Cancer Research 1992;52:6885-9

Mellon I, Spivak G, Hanawalt PC.
Selective removal of transcription blocking DNA damage from the transcribed strand of the mammalian DHFR gene.
Cell 1987;51:241-9

Merrin C
A new method to prevent toxicity with high doses of cis diammine platinum (therapeutic efficacy in previously treated widespread and recurrent testicular tumours).
Proc. Am. Soc. Clin. Oncol. 1976 ; 12: p243

Meschini S, Calcabrini A, Monti E, Del Bufalo D, Stringaro A, Dolfini E, Arancia G.

Intracellular P-glycoprotein expression is associated with the intrinsic multidrug resistance phenotype in human colon adenocarcinoma cells.
Int. J. Cancer 2000; 87:615-28

Mese H, Sasaki A, Nakayama S, Yokoyama S, Sawada S, Ishikawa T, Matsumura T.
Analysis of cellular sensitisation with cisplatin-induced apoptosis by glucose-starved stress in cisplatin-sensitive and -resistant A431 cell line.
Anticancer Res. 2001;21(2A):1029-33

Mestdagh N, Pommery N, Saucier J-M, Hecquet B, Fournier C, Slomianny C, Teissier E, Henichart J-P.
Chemoresistance to doxorubicin and cisplatin in a murine cell line. Analysis of P-glycoprotein, topoisomerase II activity, glutathione and related enzymes.
Anticancer Research 1994;14:869-74

Metzger R, Leichman CG, Danenberg KD, Danenberg PV, Lenz HJ, Hayashi K, Groshen S, Salonga D, Cohen H, Laine L, Crookes P, Silberman H, Baranda J, Konda B, Leichman L.
ERCC1 mRNA levels complement thymidylate synthase mRNA levels in predicting response and survival for gastric cancer patients receiving combination cisplatin and fluorouracil chemotherapy.
J Clin Oncol. 1998 Jan;16(1):309-16.

Mignotte B, Vayssiere JL.
Mitochondria and apoptosis.
European Journal of Biochemistry 1998;252(1):1-15

Miller ML, Ojima I.
Chemistry and chemical biology of taxane anticancer agents.
Chem Rec. 2001;1(3):195-211.

Mistry P, Kelland LR, Abel G, Sidhar S, Harrap KR.
The relationship between glutathione, glutathione-S-transferase and cytotoxicity of platinum drugs and melphalan in eight human ovarian carcinoma cell lines.

BJC 1991;64:215-20

Mitchell DL, Nairn RS.
The biology of the (6-4) photoproduct.
Photochem. Photobiol. 1989;49:805-19

Miyake H, Hanada N, Nakamura H, Kagawa S, Fujiwara T, Hara I, Eto H, Gohji K, Arakawa S, Kamidono S, Saya H.
Overexpression of Bcl-2 in bladder cancer cells inhibits apoptosis induced by cisplatin and adenoviral –mediated p53 gene transfer.
Oncogene 1998;16(7):933-43

Miyashita T, Harigai M, Hanada M, Reed JC.
Identification of a p53-dependent negative response element in the *bcl-2* gene.
Cancer Research 1994;54:3131-5

Miyazaki T, Kato H, Faried A, Sohda M, Nakajima M, Fukai Y, Masuda N, Manda R, Fukuchi M, Ojima H, Tsukada K, Kuwano H.
Predictors of response to chemo-radiotherapy and radiotherapy for esophageal squamous cell carcinoma.
Anti-cancer Research 2005;25(4):2749-55

Moggs JG, Yarema KJ, Essigmann JM, Wood RD.
Analysis of incision sites produced by human cell extracts of purified proteins during nucleotide excision repair of a 1,3-intrastrand d(GpTpG)-cisplatin adduct.
The Journal of Biological Chemistry 1996;271(12):7177-86

Moggs JG, Szymkowski DE, Yamada M, Karran P, Wood RD.
Differental human nucleotide excision repair of paired and mispaired cisplatin-DNA adducts.
Nucleic Acids Research 1997:25(3):480-90

Montgomery JA, Struck RF.
The relationship of the metabolism of anticancer agents to their activity.

Prog. Drug Res. 1973;17:320-409

Moran E, Cleary I, Larkin AM, Nic Amhlaoibh R, Masterson A, Scheper RJ, Izquierdo MA, Centre M, O'Sullivan F, Clynes M.
Co-expression of MDR associated markers, including P-170, MRP and LRP and cytoskeletal proteins, in three resistant variants of the human carcinoma cell line OAW42.
European Journal of Cancer 1997: 33(4);652-660

Morin PJ.
Drug resistance and the microenvironment: nature and nurture.
Drug Resist Updat. 2003 Aug;6(4):169-72.

Moscow JA, Townsend AJ and Cowan KH.
Elevation of pi class glutathione S-transferase activity in human breast cancer cells by transfection of the GST-pi gene and its affect on sensitivity to toxins.
Molecular Pharmacology 1989;36:22-28

Moss C, and Kaye SB.
Review: Ovarian cancer: progress and continuing controversies in management.
European Journal of Cancer 2002;38:1701-7

Moufarij MA, Phillips DR, Cullinane C.
Gemcitabine potentiates cisplatin cytotoxicity and inhibits repair of cisplatin-DNA damage in ovarian cancer cell lines.
Mol Pharmacol. 2003 Apr;63(4):862-9.

Mu D, Hsu DS, Sancar A.
Reaction mechanism of human DNA repair excision nuclease.
The Journal of Biological Chemistry 1996;271(14):8285-94

Mu D, Bessho T, Nechev LV, Chen DJ, Harris TM, Hearst JE, Sancar A.
DNA interstrand cross-links induce futile repair synthesis in mammalian cell extracts.
Molecular and Cellular Biology 2000;20(7):2446-54

Muggia FM, Hainsworth JD, Jeffers S, Miller P, Groshen S, Tan M, *et al.*
Phase II study of liposomal doxorubicin in refractory ovarian cancer: antitumour activity and toxicity modification by liposomal encapsulation.
J. Clin. Oncol. 1997;15:987-93

Muggia FM, Braly PS, *et al.*
Phase III randomized study of cisplatin versus paclitaxel versus cisplatin and paclitaxel in patients with suboptimal stage III or IV ovarian cancer: a gynecologic oncology group study.
Journal of Clinical Oncology 2000;18:106-15

Murayama I, Otsuji N.
Mutation by mitomycins in the ultraviolet light-sensitive mutant of Escherichia Coli.
Mutat. Res. 1973;18(1):117-9

Murphy D, McGown AT, Hall A, Cattan A, Crowther D, Fox BW.
Glutathione S-transferase activity and isoenzyme distribution in ovarian tumour biopsies taken before or after cytotoxic chemotherapy.
Br J Cancer. 1992 Nov;66(5):937-42.

Mutch DG.
Surgical management of ovarian cancer.
Semin. Oncol. 2002;29:3-8

Nagel H, Hemmerlein B, Ruschenburg I, Huppe K, Droese M.
The value of anti-calretinin antibody in the differential diagnosis of normal and reactive mesothelia versus metastatic tumors in effusion cytology.
Pathol Res Pract. 1998;194(11):759-64.

Nakayama K, Takebayashi Y, Nakayama S, Hata K, Fujiwaki R, Fukumoto M, Miyazaki K.
Prognostic value of overexpression of p53 in human ovarian carcinoma patients receiving cisplatin.

Cancer Letters 2003;192:227-35

Naser LJ, Pinto AL, Lippard SJ, Essigmann JM.

Chemical and biological studies of the major DNA adduct of cis-diamminedichloroplatinum(II), cis-[Pt(NH3)2(d(GpG]], built into a specific site in a viral genome.
Biochemistry. 1988 Jun 14;27(12):4357-67.

National Institute for Clinical Excellence, July 2002.
Technology Appraisal Guidance 45: Guidance on the use of pegylated liposomal doxorubicin hydrochloride (PLDH) for the treatment of advanced ovarian cancer.
London UK.

Nicoletto MO, Falci C, Pianalto D, Artioli G, Azzoni P, De Masi G, Ferrazzi E, Perin A, Donach M, Zoli W.
Phase II study of pegylated liposomal doxorubicin and oxaliplatin in relapsed advanced ovarian cancer.
Gynecol Oncol. 2005 Oct 17;

Niedernhofer LJ, Odijk H, Budzowska M, van Drunen E, Maas A, Theil AF, de Wit J, Jaspers NGJ, Beverloo HB, Hoeijmakers JHJ, Kanaar R.
The structure-specific endonuclease Ercc1-Xpf is required to resolve DNA interstrand cross-link-induceddouble-strand breaks.
Molecular and Cellular Biology 2004;24(13):5776-87

Nielsen D, Maare C, Skovsgaard T.
Cellular resistance to anthracyclines.
Gen Pharmacol. 1996 Mar;27(2):251-5.

Nigro JM, Baker SJ, Preisinger AC, Jessup JM, Hostetter R, Cleary K, Bigner SH, Davidson N, Baylin S, Devilee P, *et al.*
Mutations in the p53 gene occur in diverse human tumour types.
Nature 1989;342(6250):705-8

Nishimura T, Newkirk K, Sessions RB, Andrews PA, Trock BJ, Rasmussen AA, Montgomery EA, Bischoff EK, Cullen KJ.
Immunohistochemical staining for glutathione s-transferase predicts response to platinum-based chemotherapy in head and neck cancer.
Clin. Can. Res. 1996;2(11):1859-65

Nishimura T, Newkirk K, Sessions RB, Andrews PA, Trock BJ, Rusmussen AA, Montgomery EA, Bischoff EK, Hanigan MH, Cullen KJ.
Association between expression of glutathione-associated enzymes and response to platinum-based chemotherapy in head and neck cancer.
Chem. Biol. Interact. 1998;111-2:187-98

O'Brien ML, Tew KD.
Glutathione and related enzymes in multidrug resistance.
European Journal of Cancer 1996;32A(6):967-78

O'Connor PM, Kohn KW.
Comparative pharmacokinetics of NDA lesion formation and removal following treatment of L1210 cells with nitrogen mustards.
Cancer Communication 1990;2:387-94

O'Dwyer PJ, Stevenson JP
Chemotherapy of advanced colorectal cancer.
Cancer Treat Res. 1998;98:111-52.

Oguchi H, Kikkawa F, Kojima M, Maeda O, Mizuno K, Suganuma N, Kawai M, Tomoda Y.
Glutathione related enzymes in cis-diamminedichloroplatinum(II)-sensitive and -resistant human ovarian carcinoma cells.
Anticancer Research 1994;14(1A):193-200

Ohashi A, Zdzienicka MZ, Chen J, Couch FJ.

Fanconi Anemia complementation group D2 (FANCD2) functions independently of BRCA2- and RAD51- associated homologous recombination in response to DNA damage.
J. Biol. Chem. 2005;280(15)14877-83

Ohmori T, Podack ER, Nishio K, Takahashi M, Miyahara Y, Takeda Y, Kubota N, Funayama Y, Ogasawara H, Ohira T, Ohta S, Saijo N.
Apoptosis of lung cancer cells caused by some anti-cancer agents (MMC, CPT-11, ADM) is inhibited by BCL-2.
Biochemical and Biophysical Research Communications 19931;192(1):30-36

Okuyama T, Maehara Y, Endo K, Baba H, Adachi Y, Kuwano M, Sugimachi K.
Expression of glutathione s transferase-pi and sensitivity of human gastric cancer cells to cisplatin.
Cancer 1994;74(4):1230-6

Olive PL, Banath JP, Durand RE.
Heterogeneity in radiation-induced DNA damage and repair in tumour and normal cells measured using the 'comet' assay.
Radiation Research 1990;122:86-94.

Ortega JA, Nesbit ME Jr, Donaldson MH, Hittle RE, Weiner J, Karon M, Hammond D.
L-Asparaginase, vincristine, and prednisone for induction of first remission in acute lymphocytic leukemia.
Cancer Res. 1977 Feb;37(2):535-40.

Oshita F, Kameda Y, Nishio K, Tanaka G, Yamada K, Nomura I, Nakayama H and Noda K.
Increased expression levels of cyclin-dependent kinase inhibitor p27 correlate with good responses to platinum based chemotherapy in non-small cell lung cancer.
Oncol Rep. 2000; 7(3):491-5

Ostling O, Johanson KJ,

Microelectrophoretic study of radiation-induced DNA damages in individual mammalian cells.
Biochem. Biophys. Res. Commun. 1984;123:291-8

Ozalp SS, Yalcin OT, Tanir M, Kabukcuoglu S, Etiz E.
Multidrug resistance gene-1 (Pgp) expression in epithelial ovarian malignancies.
Eur J Gynaecol Oncol. 2002;23(4):337-40.

Ozols RF, Garvin AJ, Costa J, Simon RM, Young RC.
Advanced ovarian cancer: correlation of histologic grade with response to therapy and survival.
Cancer 1980;45(3):572-81

Ozols RF, Bundy BN, Greer BE, Fowler JM, Clarke-Pearson D, Burger RA, Mannel RS, DeGeest K, Hortenbach EM, BaergenR.
Phae III trial of carboplatin and paclitaxel compared with cisplatin and paclitaxel in patients with optimally resected stage III ovarian cancer: A gynecologic oncology group study.
Journal of Clinical Oncology 2003;21(17):3194-200

Pan B, Yao K-S, Monia BO, Dean NM, McKay R, Hamilton TC and O'Dwyer PJ.
Reversal of cisplatin resistance in human ovarian cancer cell lines by a c-jun antisense oligodeoxynucleotide (ISI 10582): evidence for the role of transcription factor overexpression in determining resistant phenotype.
Biochemical Pharmacology 2002;63:1699-1707

Parker RJ, Eastman A, Bostick-Bruton F, Reed E
Acquired cisplatin resistance in human ovarian cell lines is associated with enhanced repair of cisplatin-DNA lesions and reduced drug accumulation.
J Clin. Invest. 1991a Mar;87(3): 772-7

Parker RJ, Gill I, Tarone R, Vionnet JA, Grunberg S, Muggia FM, Reed E.
Platinum-DNA damage in leukocyte DNA of patients receiving carboplatin and cisplatin chemotherapy, measured by atomic absorption spectrometry.

Carcinogenesis 1991b ;12(7):1253-8

Pennington CJ, Rule GS.
Mapping the substrate binding of a human class mu glutathione transferase using nuclear magnetic resonance spectroscopy.
Biochemistry 1992;31:2912-20

Perego P, Giarola M, Righetti SC, Supino R, Caserini C, Delia D, Pierotti MA, Miyashita, Reed JC, Zunino F.
Association between cisplatin resistance and mutation of *p53* gene and reduced Bax expression in ovarian carcinoma cell systems.
Cancer Research 1996;56:556-62

Perego P, Pomanelli S, Carenini N, Magnani I, Leone R, Bonetti A, Paolicchi A, Zunino F.
Ovarian cancer cisplatin-resistant cell lines: multiple changes including collateral sensitivity to Taxol.
Ann. Oncol. 1998;9(4):423-30

Perego P, Caserini C, Gatti L, Carenini N, Romanelli S, Supino R, Colangelo D, Viano I, Leone R, Spinelli S, Pezzoni G, Manzotti C, Farrell N and Zunino F.
A novel trinuclear platinum complex overcomes cisplatin resistance in an osteosarcoma cell system.
Molecular Pharmacology 1999;55:528-34

Perez JM, Cerrillo V, Matesanz AI, Millan JM, Navarro P, Alonso C, Souza P.
DNA interstrand cross-linking efficiency and cytotoxic activity of novel cadmium(II)-thiocarbodiazone complexes.
Chembiochem 2001;2:119-123

Pestell KE, Hobbs SM, Titley JC, Kelland LR, Walton MI.
Effect of p53 status on sensitivity to platinum compleses in a human ovarian cancer cell line.
Molecular Pharmacology 2000;57:503-11

Petersen LN, Mamenta EL, Stevnsner T, Chaney SG, Bohr VA.
Increase gene specific repair of cisplatin induced interstrand crosslinks in cisplatin resistant cell lines, and studies on carrier ligans specificity.
Carcinogenesis 1996 Dec;17(12): 2597-602

Pettersson F
Annual Report on the results of treatment in gynaecological cancer, Volume 22.
Stockholm: Radiumhemmet, 1995

Phillips DR, White RJ, Cullinane C.
DNA sequence-specific adducts of adriamycin and mitomycin C.
FEBS Letters 1989;246(1,2):233-40

Piette J, Gamper HB, van de Vorst A, Hearst JE.
Mutagenesis induced by site specifically placed 4'-hydroxymethyl-4,5',8-trimethylpsoralen adducts.
Nucleic Acids Res. 1988 Nov 11;16(21):9961-77.

Pil PM, Lippard SJ.
Specific binding of chromosomal protein HMG1 to DNA damaged by the anticancer drug cisplatin.
Science. 1992 Apr 10;256(5054):234-7.

Podust LM, Podust VN, Floth C, Hubscher U.
Assembly of DNA polymerase δ and ε holoenzymes depends on the geometry of the DNA template.
Nucleic Acids Research 1994;22(15):2970-75

Poirier MC, Reed E, Shamkhani H, Tarone RE, Gupta-Burt S.
Platinum drug-DNA interactions in human tissues measured by cisplatin-DNA enzyme-linked immnuosorbent assay and atomic absorbance spectroscopy.
Environ. Health Perspect. 1993;99:149-54

Poirier C, Lalouette A, Foletta VC, Cohen DR, Guenet JL.
The gene encoding Fos-related antigen 2 (Fosl2) maps to mouse chromosome 5.
Mammalian Genome 1997; 8 : 223

Pollack JR, Perou CM, Alizadeh AA, Eisen MB, Pergamenschikov A, Williams CF, Jeffrey SS, Botstein D, Brown PO.
Genome-wide analysis of DNA copy-number changes using cDNA microarrays.
Nat Genet. 1999 Sep;23(1):41-6.

Pommier Y, Pourquier P, Fan Y, Strumberg D.
Mechanism of action of eukaryotic DNA topoisomerase I and drugs targeted to the enzyme.
Biochimica et Biophysica Acta 1998; 1400:83-106

Pommier Y, Sordet O, Antony S, Hayward R, Kohn K.
Apoptosis defects and chemotherapy resistance: molecular interaction maps and networks.
Oncogene 2004, 23:2934-49.

Postel EH, Abramczyk BM, Levit MN, Kyin S.
Catalysis of DNA cleavage and nucleoside triphosphate synthesis by NM23-H2/NDP kinase share an active site that implies a DNA repair function.
Proc Natl Acad Sci U S A. 2000 Dec 19;97(26):14194-9.

Postel EH.
Multiple biochemical activities of NM23/NDP kinase in gene regulation.
J Bioenerg Biomembr. 2003 Feb;35(1):31-40.

Potapova O, Haghighi A, Bost F, Liu C, Birrer MJ, Gjerset R, Mercola D.
The Jun kinase/stress activated protein kinase pathway functions to regulate DNA repair and inhibition of the pathway sensitizes tumour cells to cisplatin.
The Journal of Biological Chemistry 1997; 272(22): 14041-44

Povirk LF, Shuker DE.
DNA damage and mutagenesis induced by nitrogen mustards.
Mutat. Res. 1994;318(3):205-26

Pratt WB, Ruddon RW, Ensminger WD, Maybaum J.
The anticancer drugs.
Oxford University Press, Second Edition, 1994.

Priestman TJ,
Cancer Chemotherapy: An introduction
Springer-Verlag (Berlin), Third Edition, 1989.

Pu QQ, Bezwoda WR.
Induction of alkylator (melphalan) resistancein HL60 cells isaccompanied by
increasd levels of topoisomerase II expression and function.
Molecular Pharmacology 1999;56(1):147-53

Pu QQ, Bezwoda WR.
Alkylator resistance in human B lymphoid cell lines:(2). Increased levels of
topoisomerase II expression and function in a melphalan-resistant B-CLL cell line.
Anticancer Research 2000;20(4):2569-78

Puchalski RB and Fahl WE.
Expression of recombinant glutathion S-transferase $\pi$ , Ya or $Yb_1$ confers resistance
to alkylating agents.
PNAS 1990;87:2443-7.

Pullman A, and Pullman B.
Molecular electrostatic potential of the nucleic acids.
Quart. Rev. Biophys. 1981;14:289-380

Pusztai L, Krishnamurti S, Perez Cardona J, Sneige N, Esteva FJ, Volchenok M, Breitenfelder P, Kau SW, Takayama S, Krajewski S, Reed JC, Bast RC Jr, Hortobagyi GN.
Expression of Bag-1 and Bcl-2 proteins before and after neoadjuvant chemotherapy of locally advanced breast cancer.
Cancer Invest. 2004;22(2): 248-56

Qin LF, Ng IOL.
Induction of apoptosis by cisplatin and its affect on cell cycle related proteins and cell cycle changes in hepatoma cells.
Cancer Letters 2002; 175:27-38

Quinn JE, Kennedy RD, Mullan PB, Gilmore PM, Carty M, Johnston PG, Harkin DP.
BRCA1 functions as a differential modulator of chemotherapy-induced apoptosis.
Cancer Res. 2003 Oct 1;63(19):6221-8.

Raff MC.
Social controls on cell survival and cell death.
Nature. 1992 Apr 2;356(6368):397-400.

Raff M.
Cell suicide for beginners.
Nature 1998;396:119-968

Rapkiewicz AV, Espina V, Petricoin III EF, Liotta LA.
Biomarkers of ovarian tumours.
European Journal of Cancer 2004;40:2604-12

Reed E, Yuspa SH, Zwelling LA, Ozols RF, Poirier MC.
Quantitation of cis-diamminedichloroplatinumII (cisplatin)-DNA-intrastrand adducts in testicular and ovarian cancer patients receiving cisplatin chemotherapy.
Journal of Clinical Investigation 1986;77(2):545-50

Reed E, Ozols RF, Tarone R, Yuspa SH, Poirier MC.
Platinum-DNA adducts in leukocyte DNA correlate with disease response in ovarian cancer patients receiving platinum-based chemotherapy.
Proc. Natl. Acad. Sci. USA 1987;84:5024-28

Reed E, Ozols RF, Tarone R, Yuspa SH, Poirier MC.
The measurement of cisplatin-DNA adduct levels in testicular cancer patients.
Carcinogenesis 1988;9(10):1909-11

Reed E, Parker RJ, Gill I, Bicher A, Dabholkar M, Vionnet JA, Bostick-Bruton F, Tarone R, Muggia FM.
Platinum-DNA adducts in leukocyte DNA of a cohort of 49 patients with 24 different types of malignancies.
Cancer Research 1993;53(16):3694-9

Reed E.
Platinum-DNA adduct, nucleotide excision repair and platinum based anti-cancer chemotherapy.
Cancer Treatment Review 1998a Oct;24(5):331-44

Reed E.
Nucleotide excision repair and anti-cancer chemotherapy.
Cytotechnology 1998b ;27:187-201

Reed E, Yu JJ, Davies A, Gannon J, Armentrout SL.
Clear cell tumours have higher mRNA levels of ERCC1 and XPB than other histological types of epithelial ovarian cancer.
Clinical Cancer Research 2003;9:5299-305

Reles A, Wen WH, Schmider A, Gee C, Runnebaum IB, Kilian U, Jones LA, El-Naggar A, Minguillon C, Schonborn I, Reich O, Kreienberg R, Lichtenegger W, Press MF.
Correlation of *P53* mutations with resistance to platinum-based chemotherapy and

shortened survival in ovarian cancer.
Clinical Cancer Research 2001;7;2984-97

Reslova S.
The induction of lysogenic strains of Escherichia coli by cis-dichloro-diammineplatinum (II).
Chem Biol Interact. 1971 Dec;4(1):66-70.

Rintoul RC, Sethi T.
Extracellular matrix regulation of drug resistance in small-cell lung cancer.
Clin Sci (Lond). 2002 Apr;102(4):417-24.

Robichaud NJ, Fram RJ.
Schedule dependence on BSO in reversing cisplatin resistance.
Chem. Biol. Interactions 1990;76(3):333-42

Rogers J, Khan M, Ellis J,
Calretinin and other CaBPs in the nervous system.
Adv. Exp. Med. Biol. 1990;269:195-203

Romanet T, Re JL, De Meo M, Serre-Debeauvlais F, Lavielle JP, Reyt E, Riva C.
Detection of hypoxia by measurement of DNA damage and repair in human lymphocytes (comet assay): a predictive variable for tumour response during chemotherapy in patients with head and neck squamous cell carcinoma.
In Vivo 1999;13(4):343-8

Rooseboom M, Commandeur JNM, Vermeulen NPE.
Enzyme-catalysed activation of anticancer prodrugs.
Pharmacological Reviews 2004;56(1):53-102

Rose WC, Schurig JE.
Preclinical antitumour and toxicological profile of carboplatin.
Cancer Treatment Reviews 1985;12 Suppl. A:1-19.

Rose PG.
Pegylated Liposomal Doxorubicin: Optimizing the Dosing Schedule in Ovarian Cancer.
The Oncologist 2005;10:205-14

Rosell R, Danenberg K, Gandara D et al.
Altered ERCC1 expression correlates with response to cisplatin (DDP) and gemcitabine (GEM) in non-small-cell lung cancer (NSCLC) patients (pts).
Proc Am Soc Clin Oncol 2001:20;326a (abst. 1300)

Rosenberg B, Vancamp L, Krigas T.
Inhibition of cell division in Escherichia coli by electrolysis products from a platinum electrode.
Nature 1965;205:698-9

Rosenberg B, Renshaw E, Vancamp L, Hartwick J, Drobnik J.
Platinum induced filamentous growth in *Escherichia coli.*
Journal of Bacteriology 1967 ;93(2):716-21.

Rosenberg B, VanCamp L, Trosko JE, Mansour VH.Platinum compounds: a new class of potent antitumour agents.
Nature. 1969 Apr 26;222(191):385-6.

Rosenberg B, VanCamp L
The successful regression of large solid sarcoma 180 tumors by platinum compounds.
Cancer Res. 1970 Jun;30(6):1799-802.

Rosenkranz HS, Garro AJ, Levy JA, Carr HS.
Studies with hydroxyurea. I. The reversible inhibition of bacterial DNA synthesis and the effect of hydroxyurea on the bactericidal action of streptomycin.
Biochim Biophys Acta. 1966 Mar 21;114(3):501-15.

Ross WE, Ewig RA, Kohn KW.
Differences between melphalan and nitrogen mustard in the formation and removal of DNA crosslinks.
Cancer Research 1978;38:1502-6

Rothfuss A, Grompe M.
Repair kinetics of genomic interstrand DNA crosslinks: evidence for double strand break-dependent activation of the fanconi anaemia/BRCA pathway.
Molecular and Cellular Biology 2004;24(1):123-34

Rowinsky EK, Donehower RC.
The clinical pharmacology and use of antimicrotubule agents in cancer chemotherapeutics.
Pharmacol Ther. 1991 Oct;52(1):35-84.

Rubbi Cp, Milner J.
P53 is a chromatin accessibility factor for nucleotide excision repair of DNA damage.
EMBO J. 2003;22(4):975-86

Rudd GN, Hartley JA, Souhami RL.
Persistence of cisplatin-induced DNA interstrand crosslinking in peripheral blood mononuclear cells from elderly and young individuals.
Cancer Chemotherapy and Pharmacology 1995;35(4):323-6

Rudin CM, Yang Z, Schumaker LM, VanderWeele DJ, Newkirk K, Egorin MJ, Zuhowski EG, Cullen KJ.
Inhibition of glutathione synthesis reverses Bcl-2-mediated cisplatin resistance.
Cancer Research 2003;63(2):312-8

Saburi Y, Nakagawa M, Ono M, Sakai M, Muramatsu M, Kohno K and Kuwano M.
Increased expression of glutathione S-transferase gene in cis-diamminedichloroplatinum(II)-resistant variants of a Chinese hamster ovary cell line.
Cancer Research 1989;49:7020-5

Safaei R, Howell SB.
Copper transporters regulate the cellular pharmacology and sensitivity to platinum drugs.
Crit. Rev. Oncol. Hematol. 2005;53(1):13-23

Saga Y, Hashimoto H, Yachiku S, Iwata T and Tokumitsu M.
Reversal of acquired cisplatin resistance by modulation of metallothionein in transplanted murine tumours.
International Journal of Urology 2004;11:407-15

Saijo M, Kuoraoka I, Masutani C, Hanaoka F, Tanaka K.
Sequential binding of DNA repair proteins RPA and ERCC1 to XPA in vitro.
Nucleic Acids Research 1996;24:4719-4724

Sakamoto M, Kondo A, Kawasaki K, Goto T, Sakamoto H, Miyake K, Koyamatsu Y, Akiya T, Iwabuchi H, Muroya T, Ochiai K, Tanaka T, Kikuchi Y, Tenjin Y.
Analysis of gene expression profiles associated with cisplatin resistance in human ovarian cancer cell lines and tissues using cDNA microarrays.
Human Cell 2001; 14 (4): 305-315

Salles B, Butour JL, Lesca C, Macquet JP.
Cis-Pt(NH3)2CL2 and trans-Pt(NH3)2CL2 inhibit DNA synthesis in cultured L1210 leukaemia cells.
Biochem. Biophys. Res. Commun. 1983;112(2):555-63

Samimi G, Fink D, Varki NM, Husain A, Hoskins WJ, Alberts DS, Howell SB.
Analysis of MLH1 and MSH2 expression in ovarian cancer before and after platinum-drug-based chemotherapy.
Clinical Cancer Research 2000;6(4):1415-21

Samimi G, Varki NM, Wilczynski S, Safaei R, Alberts DS, Howell SB.
Increase in expression of the copper transporter ATP7A during platinum drug-based treatment is associated with poor survival in ovarian cancer patients.

Clin Cancer Res. 2003 Dec 1;9(16 Pt 1):5853-9.

Sancar A.
Mechanisms of DNA excision repair.
Science 1994;266:1954-56

Sanchez-Zamorano LM, Salazar-Martinez E, Escudero-De Los Rios P, Gonzalez-Lira G, Flores-Luna L, Lazcano-Ponce EC.
Factors associatec with non-epithelial ovarian cancer among Mexican women: A matched case-control study.
International Journal of Gynecological Cancer 2003;13:756-63

Sanders MC, Goldstein AL, Wang YL.
Thymosin β4 (Fx peptide) is a potent regulator of actin polymerisation in living cells.
PNAS 1992; 89: 4678-82

Santin AD, Zhan F, Bellone S, Palmieri M, Cane S, Bignotti E, Anfossi S, Gokden M, Dunn D, Roman JJ, O'Brien TJ, Tian E, Cannon MJ, Shaughnessy J Jr, Pecorelli S.
Gene expression profiles in primary ovarian serous papillary tumors and normal ovarian epithelium: identification of candidate molecular markers for ovarian cancer diagnosis and therapy.
Int J Cancer. 2004 Oct 20;112(1):14-25.

Sargent JM, Elgie AW, Williamson CJ, Taylor CG.
Aphidicolin markedly increases the platinum sensitivity of cells from primary ovarian tumours.
Br J Cancer. 1996 Dec;74(11):1730-3.

Sargent GR, Meservy JL, Perkins BD, Kilburn AE, Intody Z, Adair GM, Nairn RS, Wilson JH.
Role of the nucleotide excision repair gene ERCC1 in formation of recombination-dependent rearrangements in mammalian cells.

Nucleic Acids Research 2000;28(19):3771-8

Sartorelli AC, Hodnick WF, Belcourt MF, Tomasz M, Haffty B, Fischer JJ, Rockwell S.
Mitomycin C: a prototype bioreductive agent.
Oncol Res. 1994;6(10-11):501-8.

Satoh M, Kloth DM, Kadhim SA.
Modulation of both cisplatin nephrotoxicity and drug resistance in murine bladder tumour by controlling metallothionein synthesis.
Cancer Research 1993;53:1829-32

Sawa H, Kobayashi T, Mukai K, Zhang W, Shiku H.
Bax overexpression enhances cytochrome C release from mitochondria and sensitises KATOIII gastric cells to chemotherapeutic agent-induced apoptosis.
International Journal of Oncology 2000;16(4):745-9

Schellens JH, Ma J, Planting AS, van der Burg ME, van Meerten E, de Boer-Dennert M, Schmitz PI, Stoter G, Verweij J.
Relationship between the exposure to cisplatin, DNA-adduct formation in leukocytes and tumour response in patients with solid tumours.
British Journal of Cancer 1996;73(12):1569-75

Schiff PB, Horwitz SB.
Taxol stabilizes microtubules in mouse fibroblast cells.
Proc Natl Acad Sci U S A. 1980 Mar;77(3):1561-5.

Schilder RJ, Hall L, Monks A, Handel LM, Fornace AJ Jr.,Ozols RF, Fojo AT, Hamilton TC.
Metallothionein gene expression and resistance to cisplatin in human ovarian cancer.
Int. J.Cancer 1990;45(3):416-22.

Schmitt E, Cimoli G, Steyaert A, Bertrand R.
Bcl-xL modulates apoptosis induced by anticancer drugs and delays DEVDase and

DNA fragmentation-promoting activities.
Exp. Cell. Res. 1998;240(1):107-21

Schrenk D, Baus PR, Ermel N, Klein C, Vorderstemann B, Kauffmann HM.
Up-regulation of transporters of the MRP family by drugs and toxins.
Toxicol Lett. 2001 Mar 31;120(1-3):51-7.

Selvakumaran M, Pisarcik DA, Bao R, Yeung AT, Hamilton TC.
Enhanced cisplatin cytotoxicity by disturbing the nucleotide excision repair pathway in ovarian cancer cell lines.
Cancer Research 2003;63:1311-6

Sethi T, Rintoul RC, Moore SM, MacKinnon AC, Salter D, Choo C, Chilvers ER, Dransfield I, Donnelly SC, Strieter R, Haslett C.
Extracellular matrix proteins protect small cell lung cancer cells against apoptosis: a mechanism for small cell lung cancer growth and drug resistance in vivo.
Nat Med. 1999 Jun;5(6):662-8.

Sheibani N, Jennerwein MM, Eastman A.
DNA repair in cell sensitive and resistant to cis-diamminedichloroplatinum(II):host cell reactivation of damaged plasmid DNA.
Biochemistry 1989 Apr 4;28(7):3120-4

Shellard SA, Hosking LK, Hill BT.
Anomalous relationship between cisplatin sensitivity and the formation and removal of platinum-DNA adducts in two human ovarian cancer cell lines *in-vitro*.
Cancer Research 1991;51:4557-64

Sherman-Baust CA, Weeraratna AT, Rangel LBA, Pizer ES, Cho KR, Schwartz DR, Shock T and Morin P.
Remodeling of the extracellular matrix through overexpression of collagen IV contributes to cisplatin resistance in ovarian cancer cells.
Cancer Cell 2003 ; 3: 377-86

Shiga H, Heath EI, Rasmussen AA, Trock B, Johnston PG, Forastiere AA, Langmacher M, Baylor A, Lee M, Cullen KJ.
Prognostic value of p53, glutathione S-transferase π, and thymidylate synthase for neoadjuvant cisplatin-based chemotherapy in head and neck cancer.
Clinical Cancer Research 1999;5:4097-104.

Shivji MK, Kenny MK, Wood RD.
Proliferating cell nuclear antigen is required for DNA excision repair.
Cell 1992;69:367-74

Sijbers AM, de Laat WL, Ariza RR, Biggerstaff M, Wei Y-F, Moggs JG, Carter KC, Shell BK, Evans E, de Jong MC, Rademakers S, de Rooij J, Jaspers NGJ, Hoeijmakers JHJ, Wood RD.
Xeroderma pigmentosum group F caused by a defect in a structure-specific DNA repair endonuclease.
Cell 1996;86:811-22

Simonian PL, Grillot DAM, Nunez G.
Bcl-2 and Bcl-XL can differentially block chemotherapy-induced cell death.
Blood 1997;90(3):1208-16

Siu LL, Banerjee D, Khurana RJ, Pan X, Pflueger R, Tannock IF, Moore MJ.
The prognostic role of p53, metallothionein, P-glycoprotein, and MIB-1 in muscle-invasive urothelial transitional cell carcinoma.
Clin. Cancer Res. 1998;4(3):559-65

Skehan P, Storeng R, Scudiero D, Monks A, McMahon J, Vistica D, Warren JT, Bokesch H, Kenney S, Boyd MR.
New colorimetric cytotoxicity assay for anticancer-drug screening.
J Natl Cancer Inst. 1990 Jul 4;82(13):1107-12.

Skladanowski A, Konopa J.
Interstrand DNA crosslinking induced by anthracyclines in tumour cells.

Biochem Pharmacol. 1994a Jun 15;47(12):2269-78.

Skladanowski A, Konopa J.
Relevance of interstrand DNA crosslinking induced by anthracyclines for their biological activity.
Biochem Pharmacol. 1994b Jun 15;47(12):2279-87.

Sladek FM, Munn MM, Rupp WD, Howard-Flanders P.
In vitro repair of psoralen-DNA cross-links by RecA. UvrABC, and the 5'-exonuclease of DNA polymerase I.
Journal of Biological Chemistry 1989;264(12):6755-65

Smeal T, Binetruy B, Mercola D, Grover-Bardwick A, Heidecker G, Rapp UR, Karin
Oncoprotein-mediated signalling cascade stimulates c-Jun activity by phosphorylation of serines 63 and 73.
Mol Cell Biol. 1992 Aug;12(8):3507-13

Smolewski P, Robak T, Krykowski E, Blasinska-Moraweic M, Niewiadomska H, Pluzanska A, Chmielowska E, Zambrano O.
Prognostic factors in Hodgkin's disease: multivariate analysis of 327 patients from a single institution.
Clinical Cancer Research 2000;6(3):1150-60

Smyth G.K.
Linear models and empirical bayes method for assessing differential expression in microarray experiments.
Statistical Applications in Genetics and Molecular Biology 2004;3(1), Article 3.
http://www.stasci.org/smyth/pubs/ebayes.pdf

Sommers CL, Heckford SE, Skerker JM, Worland P, Torri JA, Thompson EW, Byers SW, Gelmann EP.
Loss of epithelial markers and acquisition of vimentin expression in adriamycin- and

vinblastine-resistant human breast cancer cell lines.
Cancer Res. 1992 Oct 1;52(19):5190-7.

Sorenson CM, Eastman A.

Influence of cis-diamminedichloroplatinum(II) on DNA synthesis and cell cycle progression in excision repair proficient and deficient Chinese hamster ovary cells.
Cancer Res. 1988 Dec 1;48(23):6703-7.

Souliotis VL, Meletios A D, Sfikakis PP.
Gene specific formation and repair of DNA monoadducts and interstrand crosslinks after therapeutic exposure to nitrogen mustards.
Clinical Cancer Research 2003;9(12):4465-74

Spanswick VJ, Hartley JM, Ward TH, Hartley JA.
Measurement of drug-induced DNA interstrand crosslinking using the single cell gel electrophoresis (Comet) assay.
In: Brown R, Boger-Brown U, eds. Methods in Molecular Medicine: Cytotoxic Drug Resistance Mechanisms. Volume 28. Totowa, NJ: Humana Press; 1999: 143-54

Spanswick VJ, Craddock C, Sekhar M, Mahendra P, Shankaranarayana P, Hughes G, Hochhauser D, Hartley JA.
Repair of DNA interstrand crosslinks as a mechanism of clinical resistance to melphalan in multiple myeloma
Blood 2002 July;100(1):224-229.

Spurdle AB, Webb PM, Purdie DM, Chen X, Green A, Chenevix-Trench G.
Polymorphisms at the glutathione S-transferase GSTM1, GSTT1 and GSTP1 loci: risk of ovarian cancer by histological subtype.
Carcinogenesis 2001;22(1):67-72

Srivatsa PJ, Cliby WA, Keeney GL, Dodson MK, Suman VJ, Roche PC, Podratz KC.

Elevated nm23 protein expression is correlated with diminished progression-free survival in patients with epithelial ovarian carcinoma.
Gynecol Oncol. 1996 Mar;60(3):363-72.

Strandberg MC, Bresnick E, Eastman A.
The significance of DNA crosslinking to cis-diamminedichloroplatinum(II)-induced cytotoxicity in sensitive and resistant lines of murine leukaemia L1210 cells.
Chem. Biol. Interact. 1982;39(2):169-80

Strathdee G, MacKean MJ, Illand M, Brown R.
A role for methylation of the hMLH1 promoter in loss of hMLH1 expression and drug resistance in ovarian cancer.
Oncogene 1999;18(14):2335-41

St Croix B, Florenes VA, Rak JW, Flanagan M, Bhattacharya N, Slingerland JM, Kerbel RS.
Impact of the cyclin dependent kinase inhibitor p27kip1 on resistance of tumour cells to anti-cancer agents.
Nat. Med. 1996;2(11):1204-10

St Croix B, Sheehan C, Rak JW, Florenes VA, Slingerland JM, Kerbel RS.
E-cadherin-dependent growth suppression is mediated by the cyclin dependent kinase inhibitor $p27^{kip1}$.
The Journal of Cell Biology 1998; 142(2): 557-71

Stein RC, Zvelebil MJ.
The application of 2D gel-based proteomics methods to the study of breast cancer.
J Mammary Gland Biol Neoplasia. 2002 Oct;7(4):385-93.

Steinert PM, Roop DR.
Molecular and cellular biology of intermediate filaments.
Annu Rev Biochem. 1988;57:593-625.

Stenberg G, Board PG, Mannervik B.
Mutation of an evolutionary conserved tyrosine residue in the active site of a human

class alpha glutathione transferase.
FEBS Lett. 1991;293:153-5.

Stoker M, O'Neill C, Berryman S, Waxman V.
Anchorage and growth regulation in normal and virus-transformed cells.
Int J Cancer. 1968 Sep 15;3(5):683-93.

Stryer L, Biochemistry, Fourth Edition, 1995, Stanford University, W.H. Freeman and company, New York, US.

Su F, Hu X, Jia W, Gong C, Song E, Hamar P.
Glutathione S-transferase π indicates chemotherapy resistance in breast cancer.
Journal of Surgical Research 2003;113:102-8

Sugasawa K, Ng JMY, Masutani C, Iwai S, van der Spek PJ, Eker APM, Hanoaka F, Bootsma D, Hoeijmakers JHJ.
Xeroderma pigmentosum group C protein complex is the initiator of global nucleotide excision repair.
Molecular Cell 1998;2:223-32.

Sugawara N, Haber JE.
Characterisation of double strand break induced recombination: homology requirements and single stranded DNA formation.
Mole. Cell Biol. 1992;12:563-75

Sugiyama T, Kamura T, Kigawa J, Terakawa N, Kikuchi Y, Kita T, Suzuki M, Sato I, Taguchi K.
Clinical characteristics of clear cell carcinoma of the ovary: a distinct histologic type with poor prognosis and resistance to platinum-based chemotherapy.
Cancer. 2000 Jun 1;88(11):2584-9.

Sum EY, Peng B, Yu X, Chen J, Byrne J, Lindeman GJ, Visvader JE.

The LIM domain protein LMO4 interacts with the cofactor CtIP and the tumor suppressor BRCA1 and inhibits BRCA1 activity.
J Biol Chem. 2002 Mar 8;277(10):7849-56. Epub 2001 Dec 18.

Sun H-Q, Kwiatkowska K, Yin HL.
β-thymosins are not simple actin monomer buffering proteins.
The Journal of Biological Chemistry 1996; 271(16): 9223-30

Sun Y.
Identification and characterisation of genes responsive to apoptosis: application of DNA chip technology and mRNA differential display.
Histol Histopathol. 2000 Oct;15(4):1271-84.

Sung P, and Robberson DL.
DNA strand exchange mediated by a Rad51-ssDNA nucleoprotein filament with polarity opposite to that of RecA.
Cell 1995;82:453-61

Sunters A, Springer CJ, Bagshawe KD, Souhami RL, Hartley JA.
The cytotoxicity, DNA crosslinking ability and DNA sequence selectivity of the aniline mustards melphalan, chlorambucil and 4-[bis(2-chloroethyl)amino] benzoic acid.
Biochemical Pharmacology 1992;44(1):59-64

Suzuki H, Pangborn J and Kilgore WW.
Filamentous cells of Escherichia coli formed in the presence of Mitomycin.
Journal of Bacteriology 1967 ;93(2):683-8

Suzuki Y, Imai Y, Nakayama H, Takahashi K, Takio K, Takahashi R.
A serine protease, HtrA2, is released from the mitochondria and interacts with XIAP, inducing cell death.
Mol. Cell 2001;8:613-21

Svoboda DL, Taylor J-S, Hearst JE, Sancar A.
DNA repair by eukaryotic nucleotide excision nuclease.
The Journal of Biological Chemistry 1993;268(3):1931-6

Szymkowski DE, Yarema K, Essigmann JM, Lippard SJ, Wood RD.
An intrastrand d(GpG) platinum crosslink in duplex M13 DNA is refractory to repair by human cell extracts.
Proc Natl Acad Sci U S A. 1992 Nov 15;89(22):10772-6.

Szymkowski DE, Lawrence CW, Wood RD.
Repair by human cell extracts of single (6-4) and cyclobutane thymine-thymine photoproducts in DNA.
Proc. Natl. Acad. Sci. USA 1993;90(21):9823-7

Taguchi T, Kato Y, Baba Y, Nishimura G, Tanigaki Y, Horiuchi C, Mochimatsu I and Tsukuda M.
Protein levels of p21, p27, cyclin E and Bax predict sensitivity to cisplatin and paclitaxel in head and neck squamous cell carcinomas.
Oncol Rep.2004:11(2):421-6

Takahashi T, Nau MM, Chiba I, Birrer M, Rosenberg RK, Vinocour M, Levitt M, Pass H, Gazdor AF, Minna JD.
P53: a frequent target for genetic abnormalities in lung cancer.
Science 1989;246(4929):491-4

Takano M, Kudo K, Goto T, Yamamoto K, Kita T, Kikuchi Y.
Analyses by comparative genomic hybridisation of genes relating with cisplatin-resistance in ovarian cancer.
Hum Cell. 2001 Dec;14(4):267-71.

Takata M, Saski MS, Tachiiri S, Fukushima T, Sonoda E, Schild D, Thompson LH, Takeda S.
Chromosome instability and defective recombinational repair in knockout mutants of the five Rad51 paralogs.

Mole. Cell Biol. 2001;21(8):2858-66

Tan KB, Mattern MR, Boyce RA, Hertzberg RP, Schein PS.
Elevated topoisomerase II activity and altered chromatin in nitrogen mustard-resistant human cells.
NCI Monogr. 1987a;4:95-8

Tan KB, Mattern MR, Boyce RA, Schein PS.
Elevated DNA topoisomerase II activity in nitrogen mustard-resistant human cells.
Proc. Natl. Acad. Sci. USA 1987b;84(21):7668-71

Taniguchi K, Wada M, Kohno K, Nakamura T, Kawabe T, Kawakami M, Kagotani K, Okumura K, Akiyama S, Kuwano M.
A human canalicular multispecific organic anion transporter (cMOAT) gene is overexpressed in cisplatin-resistant human cancer cell lines with decreased drug accumulation.
Cancer Res. 1996 Sep 15;56(18):4124-9.

Taniguchi T, Garcia-Higuera I, Andreassen PR, Gregory RC, Grompe M, D'Andrea AD.
S-phase specific interaction of the fanconi anaemia protein FANCD2, with BRCA1 and Rad51.
Blood 2002;100:2414-20

Taniguchi T, Tischkowitz M, Ameziane N, Hodgson SV, Mathew CG, Joenje H, Mok SC, D'Andrea DA.
Disruption of Fanconi anemia-BRCA pathway in cisplatin-sensitive ovarian tumours.
Nature Medicine 2003;9(5):568-74

Taron M, Rosell R, Felip E, Mendez P, Souglakos J, Ronco MS, Queralt C, Majo J, Sanchez JM, Sanchez JJ, Maestre J.
BRCA1 mRNA expression levels as an indicator of chemoresistance in lung cancer.
Hum Mol Genet. 2004 Oct 15;13(20):2443-9.

Tashiro T, Kawada Y, Sakurai Y, Kidani Y.
Antitumor activity of a new platinum complex, oxalato (trans-l-1,2-diaminocyclohexane)platinum (II): new experimental data.
Biomed Pharmacother. 1989;43(4):251-60.

Tebbs RS, Zhao Y, Tucker JD, Scheerer JB, Siciliano MJ, Hwang M, Liu N, Legerski RJ, Thompson LH.
Correction of chromosome instability and sensitivity to diverse mutagens by a cloned cDNA of the XRCC3 DNA repair gene.
Proc. Natl. Acad. Sci. USA. 1995;92(14):6354-8

Teicher BA, Holden Sa, Kelley MJ, Shea TC, Cucchi CA, Rosowsky A, Henne WD, Frei III E.
Characterisation of a human squamous carcinoma cell line resistant to CDDP (II).
Cancer Research 1987;47:388-93

Teicher BA, Herman TS, Holden SA, Wang YY, Pfeffer MR, Crawford JW, Frei E 3rd.
Tumour resistance to alkylating agents conferred by mechanisms operative only in-vivo.
Science 1990;247:(4949 Pt 1):1457-61.

Theocharis SE, Margeli AP, Koutselinis A.
Metallothionein: a multifunctional protein from toxicity to cancer.
Int. J. Biol. Markers. 2003;18(3):162-9

Thigpen JT, Blessing JA, Ball H, Hummel SJ, Barrett RJ.
Phase II trial of paclitaxel in patients with progressive ovarian carcinoma after platinum-based chemotherapy: a Gynecologic Oncology Group study.
Journal of Clinical Oncology 1994 Sept;12(9):1748-53

Thigpen JT, Aghajanian CA, Alberts DS, Campos SM, Gordon AN, Markman M, McMeekin DS, Monk BJ, Rose PG.

Role of pegylated liposomal doxorubicin in ovarian cancer.
Gynaecologic Oncology 2005;96:10-18

Thoma F,
Light and dark in chromatin repair: repair of UV-induced DNA lesions by photolyase and nucleotide excision repair.
The EMBO Journal 1999;18(23):6585-98

Thomas H, Coley HM.
Overcoming multidrug resistance in cancer: an update on the clinical strategy of inhibiting p-glycoprotein.
Cancer Control. 2003 Mar-Apr;10(2):159-65.

Tingulstad S, Skjeldestad FE, Halvorsen TB, Hagen B.
Survival and prognostic factors in patients with ovarian cancer.
Obstetrics and Gynecology 2003:101(5):885-91

Tomasz M, Lipman R, Chowdary D, Pawlak J, Verdine GL, Nakanishi K.
Isolation and structure of a covalent cross-link adduct between mitomycin C and DNA.
Science. 1987 Mar 6;235(4793):1204-8.

Tomasz M, Chawla AK, Lipman R.
Mechanism of monofunctional and bifunctional alkylation of DNA by mitomycin C.
Biochemistry. 1988 May 3;27(9):3182-7.

Tomasz M.
Mitomycin C: small, fast and deadly (but very selective).
Chem Biol. 1995 Sep;2(9):575-9.

Tomida A, Tsuruo T.
Drug resistance mediated by cellular stress response to the microenvironment of solid tumours.
Anticancer Drug Design 1999;14(2):169-77

Tomkinson AE, Levin DS.
Mammalian DNA ligases.
Bioessays 1997;19:893-901

Tonato M, Mosconi AM, Martin C.
Safety profile of gemcitabine.
Anticancer Drugs. 1995 Dec;6 Suppl 6:27-32.

Toney JH, Donahue BA, Kellet PJ, Bruhn SL, Essigman JM and Lippard S.
Isolation of cDNAs encoding a human protein that binds selectively to DNA modified by the anticancer drug *cis*-diammine-dichloroplatinum (II).
PNAS 1989, 86. 8328-32.

Tong WP, Ludlum DB.
Formation of the cross-linked base, diguanylethane, in DNA treated with N,N'-bis(2-chloroethyl)-N-nitrosourea.
Cancer Res. 1981 Feb;41(2):380-2.

Tong WP, Kirk MC, Ludlum DB.
Formation of the cross-link 1-[N3-deoxycytidyl),2-[N1-deoxyguanosinyl]ethane in DNA treated with N,N'-bis(2-chloroethyl)-N-nitrosourea.
Cancer Res. 1982 Aug;42(8):3102-5.

Tornaletti S, Patrick SM, Turchi JJ, Hanawalt PC.
Behaviour of T7 RNA polymerase and mammalian RNA polymerase II at site specific cisplatin adducts in the template DNA.
Journal of Biological Chemistry 2003;278(37):35791-7

Torres-Garcia SJ, Cousineau L, Caplan S, Panasci L.
Correlation of resistance to nitrogen mustards in chronic lymphocytic leukaemia with enhanced removal of melphalan-induced DNA crosslinks.
Biochemical Pharmacology 1989;38(18):3122-3

Toso RJ, Jordan MA, Farrell KW, Matsumoto B, Wilson L.
Kinetic stabilisation of microtubule dynamic instability in vitro by vinblastine.
Biochemistry. 1993 Feb 9;32(5):1285-93.

Townsend AJ, Tu CP, Cowan KH.
Expression of human mu or alpha class glutathione S-transferases in stably transfected human MCF-7 breast cancer cells: effects on cellular sensitivity to cytotoxic agents.
Molecular Pharmacology 1992;41(2):230-6

Troelstra C, Vangool A, Dewit J, Vermeulen W, Bootsma D, Hoeijmakers JHJ.
ERCC6 a member of a subfamily of putative helicases, is involved in Cockayne's Syndrome and preferential repair of active genes.
Cell 1992;71:939-53

Tsao YP, Russo A, Nyamuswa G, Silber R, Liu LF.
Interaction between replication forks and topoisomerase I-DNA cleavable complexes: studies in a cell-free SV40 DNA replication system.
Cancer Res. 1993 Dec 15;53(24):5908-14.

Umezu K, Kolodner RD.
Protein interactions in genetic recombination in Escherichia coli. Interactions involving RecO and RecR overcome the inhibition of RecA by single-stranded DNA-binding protein.
J Biol Chem. 1994 Nov 25;269(47):30005-13.

Van der Burg ME, van Lent M, Buyse M, Kobierska A, Colombo N, Favalli G, Lacave AJ, Nardi M, Renard J, Pecorelli S.
The effect of debulking surgery after induction chemotherapy on the prognosis in advanced epithelial ovarian cancer. Gynecological Cancer Co-operative Group of the European Organisation for Research and Treatment of Cancer.
The New England Journal of Medicine 1995;322:629-34

van der Burg ME, de Wit R, van Putten WL, Logmans A, Kruit WH, Stoter G, Verweij J.
Weekly cisplatin and daily oral etoposide is highly effective in platinum pretreated ovarian cancer.
British Journal of Cancer 2002;86(1):19-25

van der Zee AG, van Ommen B, Meijer C, Hollema H, van Bladeren PJ, de Vries EG.
Glutathione S-transferase activity and isoenzyme composition in benign ovarian tumours, untreated malignant ovarian tumours, and malignant ovarian tumours after platinum/cyclophosphamide chemotherapy.
Br J Cancer. 1992 Nov;66(5):930-6.

Van Duin MJ, de Wit J, Odijk H, Westerveld A, Yasui A, Koken HM, Hoeijmakers JH and Bootsma D.
Molecular characterisation of the human excision gene ERCC1: cDNA cloning and amino acid homology with the yeast DNA repair gene RAD10.
Cell 1986;44:913-23

Van Duin M, Koken MHM,van der Tol J, ten Dijke P, Odijk H, Westerveld A, Bootsma D, Hoeijmakers JHJ.
Genomic characterisation of the human excision repair gene ERCC1.
Nucleic Acids Research 1987;15(22):9195-9213

Van Houten B, Gamper H, Holbrook SR, Hearst JE, Sancer A.
Action mechanism of ABC excision nuclease on a DNA substate containing a psoralen crosslink at a defined position.
Proc. Natl. Acad. Sci. USA 1986;83:8077-81

Van Slooten HJ, Clahsen PC, van Dierendonck JH, Duval C, Pallud C, Mandard AM, Delobelle-Deroide A, van de Velde CJ, van de Vijver MJ.
Expression of Bcl-2 in node-negative breast cancer is associated with various prognostic factors, but does not predict response to one course of perioperative chemotherapy.
British Journal of Cancer 1996;74(1):78-85

Vasak M, Hasler DW.
Metallothioneins: new functional and structural insights.
Current Opinion in Chemical Biology 2000;4:177-83

Vasey PA, McMahon L, Paul J, Reed N, Kaye SB.
A phase II trial of capecitabine (Xeloda) in recurrent ovarian cancer.
British Journal of Cancer 2003;89(10):1843-8.

Verhagen AM, Ekert PG, Pakusch M, Silke J, Connolly LM *et al.*
Identification of DIABLO, a mammalian protein that promotes apoptosis by binding to and antagonising IAP proteins.
Cell 2000;102:43-53

Vikhanskaya F, Marchini S, Marabese M, Galliera E, Broggini M.
P73alpha overexpression is associated with resistance to treatment with DNA damaging agents in a human ovarian cancer cell line.
Cancer Research 2001;61:935-938

Visse R, van Gool AJ, Moolenaar GF, de Ruijter M, van de Putte P.
The actual incision determines the efficiency of repair of cisplatin damaged DNA by the Escherichia coli UvrABC endonuclease.
Biochemistry 1994;33(7):1804-11

Vogelstein B.
Cancer: A deadly inheritance.
Nature 1990;348(6303):681-2

Volker M, Mone MJ, Karmakar P, van Hoffen A, Schul W, Vermeulen W, Hoeijmakers JHJ, van Driel R, van Zeeland AA, Mullenders LHF.
Sequential assembly of nucleotide excision repair factors in vivo.
Molecular Cell 2001;8:213-24

Volpato M, Seargent J, Loadman PM, Phillips RM.

Formation of DNA interstrand cross-links as a marker of Mitomycin C bioreductive activation and chemosensitivity.
Eur J Cancer. 2005 Jun;41(9):1331-8.

Von Hoff DD, Schilsky R, Reichert CM, Reddick RL, Rozencweig M, Young RC, Muggia FM.
Toxic effects of cis-dichlorodiammineplatinum(II) in man.
Cancer Treat Rep. 1979 Sep-Oct;63(9-10):1527-31.

Wakai S, Marumo H, Tomioka K, Shimizu M, Kato E, Kamada H, Kudo S, Fujimoto Y.
Purification and isolation study on gancidins.
J Antibiot (Tokyo). 1958 Jul;11(4):150-5.

Walko CM, Lindley C.
Capecitabine: a review.
Clin. Ther. 2005;27(1):23-44

Walton MI, Whysong D, O'Connor PM, Hockenbery D, Korsmeyer SJ, Kohn KW.
Constitutive expression of human Bcl-2 modulates nitrogen mustard and camptothecin induced apoptosis.
Cancer Research 1993;53(8):1853-61

Wang YY, Teicher BA, Shea TC, Holden SA, Rosbe KW, al-Achi A, Henner WD.
Cross-resistance and glutathione S-transferase-pi levels among four human melanoma cell lines selected for alkylating agent resistance.
Cancer Research 1989;49(22):6185-92

Wang K, Lu J and Li R.
The events that occur when cisplatin encounters cells.
Coordination Chemistry Reviews 1996 ; 151:53-88

Wang Y, Rea T, Bian J, Gray S, Sun Y.

Identification of the genes responsive to etoposide-induced apoptosis: application of DNA chip technology.
FEBS Lett. 1999 Feb 26;445(2-3):269-73

Wang X, Peterson CA, Zheng H, Nairn RS, Legerski RJ, Li L.
Involvement of nucleotide excision repair in the recombination-independent repair and error-prone pathway of DNA interstrand crosslink repair.
Mole. Cell. Biol. 2001a:21(3):713-20

Wang Z-M, Chen Z-P, Xu Z-Y, Christodoulopoulos G, Bello V, Mohr G, Alozy R, Panasci LC.
In-vitro evidence for homologous recombinational repair in resistance to melphalan.
Journal of the National Cancer Institute 2001b;93(19):1473-8

Wani MC, Taylor HL, Wall ME, Coggon P, McPhail AT.
Plant antitumor agents. VI. The isolation and structure of taxol, a novel antileukemic and antitumor agent from Taxus brevifolia.
J Am Chem Soc. 1971 May 5;93(9):2325-7.

Wasenius VM, Jekunen A, Monni O, Joensuu H, Aebi A, Howell SB, Knuutila S.
Comparative genomic hybridisation analysis of chromosomal changes occurring during development of acquired resistance to cisplatin in human ovarian carcinoma cell lines.
Genes, Chromosomes and Cancer 1997;18:286-91

Webley SD, Francis RJ, Pedley RB, Sharma SK, Begent RH, Hartley JA, Hochhauser D.
Measurement of the critical DNA lesions produced by antibody-directed enzyme prodrug therapy (ADEPT) in vitro, in vivo and in clinical material.
Br J Cancer. 2001 Jun 15;84(12):1671-6.

Welsch CW.

Growth inhibition of rat mammary carcinoma induced by cis-platinum diamminodichloride-II.
J Natl Cancer Inst. 1971 Nov;47(5):1071-8.

Westerveld A, Hoeijmakers JHJ, de Wit J, Odijk H, Pastink A, Wood RD, Bootsma D.
Molecular cloning of a human DNA repair gene.
Nature 1984;310:425-9

Wicki R, Franz C, Scholl FA, Heizmann CW, Schafer BW.
Repression of the candidate tumor suppressor gene S100A2 in breast cancer is mediated by site-specific hypermethylation.
Cell Calcium. 1997 Oct;22(4):243-54.

Wikborn C, Pettersson F, Moberg PJ.
Delay in diagnosis of epithelial ovarian cancer.
International Journal of Gyecology and Obstetrics 1996;52:263-7

Williams J, Lucas PC, Griffith KA, Choi M, Pogoros S, Hu YY, Liu JR.
Expression of Bcl-xL in ovarian carcinoma is associated with chemoresistance and recurrent disease.
Gynecol. Oncol. 2005;96:287-95

Wiltshaw E, Carr B.
Cis-platinumdiamminedichloride
In Connors TA, Roberts JJ. eds
Platinum co-ordination complexes in cancer chemotherapy.
Heidelberg, Springer, 1974: 178-82

Witkin EM.
The radiation sensitivity of Escherichia coli B: a hypothesis relating filament formation and prophage induction.
Proc Natl Acad Sci U S A. 1967 May;57(5):1275-9. 4.

Wood RD, Shivji MKK.
Which DNA polymerases are used for DNA repair in eukaryotes?
Carcinogenesis 1997;18:605-610

Woynarowski JM, Faivre S, Herzig MC, Arnett B, Chapman WG, Trevino AV, Raymond E, Chaney SG, Vaisman A, Varchenko M, Juniewicz PE.
Oxaliplatin-induced damage of cellular DNA.
Mol Pharmacol. 2000 Nov;58(5):920-7.

Wrigley EC, McGown AT, Buckley H, Hall A, Crowther D.
Glutathione-S-transferase activity and isoenzyme levels measured by two methods in ovarian cancer, and their value as markers of disease outcome.
Br J Cancer. 1996 Mar;73(6):763-9.

Xing H, Wang S, Hu K, Tao W, Li J, Gao Q, Yang X, Weng D, Lu Y, Ma D.
Effect of the cyclin-dependent kinase inhibitor p27 on resistance of ovarian cancer multicellular spheroids to anticancer therapy.
J. Cancer Res. Clin. Oncol. 2005;131(8):511-19

Xu ZY, Loignon M. Han FY, Panasci L, Aloyz R.
Xrcc3 induces cisplatin resistance by stimulation of Rad51-related recombinational repair, s-phase checkpoint activation, and reduced apoptosis.
J. Pharmacol. Exp. Ther. 2005;314(2):495-505

Yagi T, Wood RD, Takebe H.
A low content of ERCC1 and 120kDa protein is a frequent feature of group F xeroderma pigmentosum fibroblast cells.
Mutagenesis 1997;12:41-44

Yagi Y, Matsumura Y, Sato M, Nishigori C, Mori T, Sijbers AM, and Takebe H.
Complete restoration of DNA repair characteristics in group F xeroderma pigmentosum cells by overexpression of transfected XPF cDNA.
Carcinogenesis 1998;19:55-60.

Yamada M, O'Regan E, Brown R, Karran P.
Selective recognition of a cisplatin-DNA adduct by human mismatch repair proteins.
Nucleic Acids Research 1997;25(3):491-5

Yang WZ, Begleiter A, Johnston JB, Israels LG, Mowat MR.
Role of glutathione and glutathione S-transferase in chlorambucil resistance.
Molecular Pharmacology 1992;41(4):625-30

Yang YY, Woo ES, Reese CE, Bahnson RR, Saijo N, Lazo JS.
Human metallothionein isoform expression in cisplatin-sensitive and resistant cells.
Mol. Pharm. 1994;45(3):453-60

Yang LY, Li L, Jiang H, Shen Y, Plunkett W.
Expression of ERCC1 antisense RNA abrogates gemicitabine-mediated cytotoxic synergism with cisplatin in human colon tumor cells defective in mismatch repair but proficient in nucleotide excision repair.
Clin Cancer Res. 2000 Mar;6(3):773-81.

Yang X, Zheng F, Xing Hm Gao Q, Wei W, Lu Y, Wang S, Zhou J, Hu W, Ma D.
Resistance to chemotherapy-induced apoptosis via decrease caspase 3 activity and overexpression of anti-apoptotic proteins in ovarian cancer.
J. Cancer Res. Clin. Oncol. 2004;130:423-8

Yang X, Hing H, Gao Q, Chen G, Lu Y, Wang S, Ma D.
Regulation of HtrA2/Omi by X-linked inhibitor of apoptosis protein in chemoresistance in human ovarian cancer cells.
Gynecol. Oncol. 2005;97:413-21

Yao KS, Godwin AK, Johnson SW, Ozols RF, O'Dwyer PJ, Hamilton TC.
Evidence for altered regulation of γ-glutamyl cysteine synthetase gene expression among cisplatin sensitive and cisplatin resistant human ovarian cancer cell lines.
Cancer Research 1995;55:4367-74

Yarosh DB, Barnes D, Erickson LC.
Transfection of DNA from a chloroethylnitrosourea-resistant tumour cell line (MER+) to a sensitive tumour cell line (MER-) results in a tumour cell line resistant to MNNG and CNU that has increased O-6-methylguanine- DNA methyltransferase levels and reduced levels of DNA interstrand crosslinking.
Carcinogenesis 1986;7(9):1603-6

Yasui k, Mihara S, Zhao C, Okamoto H, Saito-Ohara F, Tomida A, Funato T, Yokomizo A, Naito S, Imoto O, Tsuruo T, Inazawa J.
Alteration of copy numbers of genes as a mechanism for acquired drug resistance.
Cancer Research 2004;64:1403-10

Yazlovitskaya EM, DeHaan RD, Persons DI.
Prolonged wild-type p53 protein accumulation and cisplatin resistance.
Biochem. Biophys. Res. Commun. 2001;283(4):732-7

Yin BWT, Dnistrian A, Lloyd KO.
Ovarian cancer antigen Ca125 is encoded by the MUC16 mucin gene.
International Journal of Cancer 2002;98:737-40

Yu JJ, Mu C, Dabholkar M, Guo Y, Bostick-Bruton F, Reed E.
Alternative splicing of ERCC1 and cisplatin-DNA adduct repair in human tumour cel lines.
International Journal of Molecular Medicine 1998;1(3):617-20

Yuan ZM, Smith PB, Brundrett RB, Colvin M, Fenselau C.
Glutathione conjugation with phosphoramide mustard and cyclophosphamide. A mechanistic study using tandem mass spectrometry.
Drug Metab. Dispos. 1991;19(3)-625-9

Yuan SS, Lee SY, Chen G, Song M, Tomlinson GE, Lee EY.
BRCA2 is required for ionizing radiation-induced assembly of Rad51 complex in-vivo.
Cancer Research 1999;59(15):3547-51

Yunmbam MK, Li QQ, Mimnaugh EG, Kayastha GL, Yu JJ, Jones LN, Neckers L, Reed E.
Effect of the proteasome inhibitor ALLnL on cisplatin sensitivity in human ovarian tumor cells.
Int J Oncol. 2001 Oct;19(4):741-8.

Zamble DB, Lippard SJ.
Cisplatin and DNA repair in cancer chemotherapy.
TIBS 1995 October; 20: 435-439

Zamble DB, Mu D, Reardon JT, Sancar A, Lippard SJ.
Repair of cisplatin-DNA adducts by the mammalian excision nuclease.
Biochemistry 1996;35(31):10004-13

Zdraveski, Z.Z., Mello, J.A., Marinus, M.G. and Essigmann, J.M.
Multiple pathways of recombination define cellular responses to cisplatin.
Chemistry & Biology 2000; 7, 39-50

Zeman SM, Phillips DR, Crothers DM.
Characterisation of covalent Adriamycin-DNA adducts.
PNAS 1998;95:11561-11565

Zhang K, Chew M, Yang EB, Wong KP, Mack P.
Modulation of cisplatin cytotoxicity and cisplatin induced DNA crosslinks in HepG2 cells by regulation of glutathione related mechanisms.
Molecular Pharmacology 2001;59(4):837-43

Zhang N, Lu X, Zhang X, Peterson CA, Legerski RJ.
hMutSβ is required for the recognition and uncoupling of psoralen interstrand crosslinks in vitro.
Molecular and Cellular Biology 2002;22(7):2388-97

Zhen W, Link Jr. CJ, O'Connor PM, Reed E, Parker R, Howell SB, Bohr VA.

Increased gene specific repair of cisplatin interstrand crosslinks in cisplatin resistant human ovarian cancer cell lines.
Molecular and Cellular Biology 1992;12(9):3689-98

Zheng H, Wang X, Warren AJ, Legerski RJ, Nairn RS, Hamilton JW, Li L.
Nucleotide excision repair- and polymerase η-mediated error-prone removal of mitomycin C interstrand crosslinks.
Molecular and Cellular Biology 2003;23(2):754-61

Zhong X, Li QQ, Reed E.
SU5416 sensitizes ovarian cancer cells to cisplatin through inhibition of nucleotide excision repair.
Cell Mol Life Sci. 2003 Apr;60(4):794-802.

Zhou J, Chen Y, Li C, Liu W.
The protein expression of Bcl-2, Bax, Fas/Apo-1 in acute myeloid leukaemia.
J. Tongji. Med. Univ. 1998;18(1):42-5

Zou H, Li Y, Liu X, Wang X.
An APAF-1 cytochrome c multimeric complex is a functional apoptosome that activated pro-caspase 9.
Journal of Biological Chemistry 1999;274:11549-54

Zwelling LA, Kohn KW, Ross WE, Ewig RAG, Anderson T.
Kinetics of formation and disappearance of a DNA cross-linking effect in mouse L1210 cells treated with cis- and trans-diammine-dichloroplatinum(II).
Cancer Research 1978;38:1762-8

Zwelling LA, Anderson T, Kohn KW.
DNA-protein and DNA interstrand cross-linking by cis- and trans-platinum(II) diamminedichloride in L1210 mouse leukemia cells and relation to cytotoxicity.
Cancer Res. 1979a Feb;39(2 Pt 1):365-9.

Zwelling LA, Bradley MO, Sharkey NA, Anderson T, Kohn KW.
Mutagenicity, cytotoxicity and DNA crosslinking in V79 Chinese hamster cells

treated with cis- and trans-Pt(II) diamminedichloride.
Mutat Res. 1979b Jul;67(3):271-80.

**Appendixes**

**A1 Patient Information Sheet**

UNIVERSITY COLLEGE HOSPITAL

Huntley Street
London WC1E 6AU
Telephone: 0171 387 9300 Ext:.....
0171 380 9566 (direct line)
Fax: 0171 380 9754

PATIENT INFORMATION SHEET

*Molecular Basis of Ovarian Diseases*

We would like you to help us study the causes of ovarian disease and the sensitivity and resistance of ovarian cancers to anti-cancer drugs by allowing us to take a small sample of your ovary, fluid in your abdomen and/or blood.

You are about to have surgical treatment for your ovarian disease. Most of the surgically removed tissue will be taken to the pathology laboratory for routine analysis. We are trying to find out why women develop ovarian disease as research in this area is still very limited. We would like to take a sample of tissue, which the pathologists do not need and which would otherwise be discarded, fluid or blood depending on the procedure you are about to undergo to look at the cells more closely. This may be a sample from your ovary, some of the fluid removed from your abdomen or chest, or tissue samples from the omentum (a fatty structure often removed by the surgeon), lymph nodes and blood. The amounts taken do not affect your treatment, or put you at any increased risk. The blood sample is an extra specimen. No extra procedures will be performed. We will perform studies on these samples in the laboratory. This will increase our understanding of the mechanisms involved in the development of cancer and may help us identify better therapies in the future. The samples will not be used for any other purpose, and any tissue over and above that needed for diagnosis is disposed of after 2 months by the pathology department.

The way in which the samples are taken will be explained to you, and your consent will be asked for the procedure. The use of these samples is entirely voluntary, and if you do not wish to take part, you may withdraw from the study at any time without giving a reason. This will in no way affect the medical care you receive from your doctors. The samples obtained will be coded anonymously but it would be helpful if information from your notes could be used to correlate the clinical and laboratory findings. This will be undertaken by a member of the clinical research team and will be treated in the strictest confidence.

If at any point you wish for further information you may contact:

Miss Tania Adib, Specialist Registrar
Wolfson Institute for Biomedical Research,
University College London.
The Cruciform Building,Gower Street,
London WC1E 6AE Tel. No: 020 7679 6857

or discuss this with your consultant Gynaecologist or Oncologist November 2000

UNIVERSITY COLLEGE HOSPITAL

Huntley Street
London WC1E 6AU
Telephone: 0171 387 9300 Ext:.....
0171 380 9566 (direct line)
Fax: 0171 380 9754

A2 Consent Form

# PATIENT CONSENT FORM

## *THE MOLECULAR BIOLOGY OF PREMALIGNANT AND MALIGNANT OVARIAN AND VULVAL DISEASES AND SENSITIVITY TO CYTOTOXIC DRUGS*

Patient name.....

Address.....

.....

I have received an explanation of the study and understand what the study involves. If I decide not to participate, my future treatment will not be affected in any way, and I may withdraw from the study at any time.
I agree to take part in the study.

Signature..... Date.....

I have been present whilst the study has been explained to the patient and have witnessed her consent to take part.

Signature..... Date.....

I have explained the study to the patient and I am content that she has given informed consent.

Signature..... Date.....

## A3. Microarray Data Ordered According to M value (Log2 of Expression Intensity Data) presented in Table A3.

## Table A3.

| Name | Symbol | Name | M | B |
|---|---|---|---|---|
| AA779165 | ARL4 | ADP-ribosylation factor-like 4 | -3 5187221 | 17 3540497 |
| AA487893 | TM4SF1 | transmembrane 4 superfamily member 1 | -3 0059224 | 9 4054046 |
| AA598640 | MID1 | midline 1 (Opitz/BBB syndrome) | -2 6993415 | 18 0621977 |
| AA598483 | TAX1BP1 | Tax1 (human T-cell leukemia virus type I) binding protein 1 | -2 299899 | 7 5802064 |
| AA458884 | S100A2 | S100 calcium binding protein 2 | -2 2626586 | 12 6309598 |
| AA482119 | ID3 | inhibitor of DNA binding 3 dominant negative helix-loop-helix protein | -2 0559957 | 7 8396983 |
| AA486085 | TMSB10 | Thymosin beta 10 | -1 9571253 | 5 3140883 |
| AA644088 | CTSC | cathepsin C | -1 9210414 | 16 0705404 |
| AA490172 | COL1A2 | collagen type I alpha 2 | -1 9076853 | 6 9470959 |
| AA630800 | IFI30 | interferon gamma-inducible protein 30 | -1 7533329 | 10 4799412 |
| AA703392 | HFL1 | H factor (complement)-like 1 | -1 7508811 | 9 0889797 |
| AA482231 | MARCKS | myristoylated alanine-rich protein kinase C substrate | -1 7253124 | 8 2630318 |
| R62603 | COL6A3 | Collagen type VI alpha 3 | -1 6635706 | 10 2447599 |
| AA464861 | CREM | cAMP responsive element modulator | -1 4277106 | 4 8766463 |
| AA412053 | CD9 | CD9 antigen (p24) | -1 3702724 | 0 7526075 |
| AA456621 | GGH | gamma-glutamyl hydrolase (conjugase folylpolygammaglutamyl hydrolase) | -1 2471388 | 4 0236273 |
| R59579 | PTGDS | prostaglandin D2 synthase 21kDa (brain) | -1 2470994 | 1 6799566 |
| AA476438 | HRASLS3 | HRAS-like suppressor 3 | -1 2315501 | 7 8637709 |
| AA115076 | CITED2 | Cbp/p300-interacting transactivator with Glu/Asp-rich carboxy-terminal domain 2 | -1 2123943 | 6 6438385 |
| AA608558 | PFKP | phosphofructokinase platelet | -1 1945265 | 8 7036163 |
| AA411679 | GYG | Glycogenin | -1 1567653 | 1 91832 |
| AA486321 | VIM | Vimentin | -1 1255786 | 9 9788437 |
| H99681 | DP1 | polyposis locus protein 1 | -1 0938159 | 1 5491351 |
| N57754 | TNRC3 | Trinucleotide repeat containing 3 | -1 0656046 | 9 2131253 |
| AA181023 | EVI1 | ecotropic viral integration site 1 | -1 0303124 | 7 2976806 |
| H60549 | CD59 | CD59 antigen p18-20 (antigen identified by monoclonal antibodies 16 3A5 EJ16 EJ30 EL32 and G344) | -1 0103923 | 2 3772821 |
| AA019459 | PTK9 | PTK9 protein tyrosine kinase 9 | -1 0099322 | 2 9086331 |
| AA489699 | COPS8 | COP9 constitutive photomorphogenic homolog subunit 8 (Arabidopsis) | -0 9848136 | 2 1501091 |
| H82442 | ID2 | inhibitor of DNA binding 2 dominant negative helix-loop-helix protein | -0 9691106 | 6 7360241 |
| AA284072 | CDKN3 | cyclin-dependent kinase inhibitor 3 (CDK2-associated dual specificity phosphatase) | -0 9484494 | 0 9679128 |
| T74567 | FHR-3 | complement factor H related 3 | -0 9353283 | 1 9641545 |
| AA485427 | CRIP2 | cysteine-rich protein 2 | -0 9351656 | 5 6042529 |
| AA490208 | GSTT2 | glutathione S-transferase theta 2 | -0 9295173 | 2 2761419 |
| N94820 | DIPA | hepatitis delta antigen-interacting protein A | -0 9235965 | 3 6162686 |
| H09721 | MARK3 | MAP/microtubule affinity-regulating kinase 3 | -0 9161254 | 1 2293674 |
| AA410188 | C1orf29 | chromosome 1 open reading frame 29 | -0 9156365 | 3 8285745 |
| N52496 | BTG3 | BTG family member 3 | -0 9093137 | 2 5052952 |
| AA129777 | SLC16A3 | solute carrier family 16 (monocarboxylic acid transporters) member 3 | -0 8846018 | 3 5949731 |
| T95289 | ERCC1 | excision repair cross-complementing rodent repair deficiency complementation group 1 (includes overlapping antisense sequence) | -0 8844539 | 2 8475761 |
| AA293671 | CD8B1 | CD8 antigen beta polypeptide 1 (p37) | -0 8814276 | 1 6805734 |
| R38433 | PFKP | phosphofructokinase platelet | -0 8788533 | 1 603848 |
| T68453 | PCMT1 | protein-L-isoaspartate (D-aspartate) O-methyltransferase | -0 8715628 | 4 330818 |
| AA457038 | ITGB1BP1 | integrin beta 1 binding protein 1 | -0 8697968 | 0 814672 |
| AA877595 | CDKN2A | cyclin-dependent kinase inhibitor 2A (melanoma p16 inhibits CDK4) | -0 8636089 | 1 3686615 |
| W73874 | CTSL | cathepsin L | -0 8514742 | 1 1268746 |
| AA497055 | PSMD12 | proteasome (prosome macropain) 26S subunit non-ATPase 12 | -0 8343878 | 0 5946626 |
| R38433 | PFKP | phosphofructokinase platelet | -0 8124395 | 5 5384606 |
| AA487460 | DPYSL2 | dihydropyrimidinase-like 2 | -0 8117585 | 1 2841634 |
| R79082 | PTPRK | protein tyrosine phosphatase receptor type K | -0 7920798 | 2 0985028 |
| AA838691 | EPHX1 | epoxide hydrolase 1 microsomal (xenobiotic) | -0 7452518 | 2 1752498 |
| T58873 | FOSL2 | FOS-like antigen 2 | -0 7370583 | 0 6271127 |
| W49619 | CDH2 | cadherin 2 type 1 N-cadherin (neuronal) | -0 7045605 | 2 3638834 |
| H29322 | CAMK1 | calcium/calmodulin-dependent protein kinase I | -0 702849 | 1 4670563 |
| R40897 | OXCT5 | 3-oxoacid CoA transferase | -0 7022003 | 1 9708812 |
| H99676 | COL6A1 | collagen type VI alpha 1 | -0 7017598 | 2 7887409 |
| AA430574 | PXN | Paxillin | -0 6325283 | 4 5576419 |
| AA457118 | TOMM34 | translocase of outer mitochondrial membrane 34 | -0 607676 | 1 2890304 |
| N80129 | MT1X | metallothionein 1X | -0 54165 | 0 9763709 |
| AA598653 | POSTN | periostin osteoblast specific factor | -0 5410685 | 1 5104019 |
| T67552 | ARNT | aryl hydrocarbon receptor nuclear translocator | 0 4724562 | 1 3005956 |
| AA456298 | HIST2H2BE | histone 2 H2be | 0 4870318 | 0 856575 |
| AA425401 | STK24 | serine/threonine kinase 24 (STE20 homolog yeast) | 0 4936649 | 1 2625757 |
| H17398 | BA13 | brain specific angiogenesis inhibitor | 0 5234054 | 0 6101628 |
| H04789 | GYG2 | glycogenin 2 | 0 5880985 | 1 6993231 |
| H91647 | CLUL1 | clusterin-like 1 (retinal) | 0 5947801 | 1 8211137 |

| | | | | |
|---|---|---|---|---|
| H15677 | PPP2R2B | protein phosphatase 2 (formerly 2A), regulatory subunit B (PR 52), beta isoform | 0 605832 | 2 1160705 |
| AA426352 | H2A 1 | Histone H2A 1 | 0 6191979 | 1 8616346 |
| AA485752 | ABCF1 | ATP-binding cassette, sub-family F (GCN20), member 1 | 0 6507542 | 2 6731432 |
| AA291389 | ISGF3G | interferon-stimulated transcription factor 3, gamma 48kDa | 0 6536164 | 3 5598407 |
| AA406552 | SLC2A3 | solute carrier family 2 (facilitated glucose transporter), member 3 | 0 6625057 | 2 9791724 |
| AA455964 | GTF2E1 | general transcription factor IIE, polypeptide 1, alpha 56kDa | 0 6851539 | 2 989638 |
| AA430524 | CAPZB | capping protein (actin filament) muscle Z-line, beta | 0 6928569 | 1 274187 |
| AA041400 | LRBA | LPS-responsive vesicle trafficking, beach and anchor containing | 0 700007 | 1 0071921 |
| N92901 | FABP4 | fatty acid binding protein 4, adipocyte | 0 7333144 | 6 5169975 |
| N49703 | CHD2 | chromodomain helicase DNA binding protein 2 | 0 7408736 | 2 0934191 |
| AA396400 | CNN1 | calponin 1, basic, smooth muscle | 0 7965682 | 1 1771523 |
| AA196000 | ACTN3 | actinin, alpha 3 | 0 8070318 | 0 9781952 |
| R31701 | COL11A1 | Collagen type XI alpha 1 | 0 8249685 | 1 7762696 |
| AA101875 | CSPG2 | chondroitin sulfate proteoglycan 2 (versican) | 0 8471592 | 4 9133187 |
| AA485371 | BST2 | bone marrow stromal cell antigen 2 | 0 8484171 | 1 8447095 |
| H50251 | SH3GL3 | SH3-domain GRB2-like 3 | 0 849815 | 2 8884528 |
| N76927 | BLVRB | biliverdin reductase B (flavin reductase (NADPH)) | 0 9251405 | 3 2770303 |
| H95960 | SPARC | secreted protein, acidic, cysteine-rich (osteonectin) | 0 9397248 | 2 3700383 |
| T47443 | PROCR | protein C receptor, endothelial (EPCR) | 0 9409731 | 8 8732896 |
| AA669136 | TCF4 | transcription factor 4 | 0 9639176 | 6 1645989 |
| N63988 | IFIT2 | interferon-induced protein with tetratricopeptide repeats 2 | 0 972553 | 3 908129 |
| AA703449 | MEIS4 | Meis1, myeloid ecotropic viral integration site 1 homolog 4 (mouse) | 0 9763917 | 2 305843 |
| AA497033 | CDO1 | cysteine dioxygenase, type I | 0 9962265 | 9 6941378 |
| AA446659 | TAC1 | tachykinin, precursor 1 (substance K, substance P, neurokinin 1, neurokinin 2, neuromedin L, neurokinin alpha, neuropeptide K, neuropeptide gamma) | 1 02516 | 1 2249505 |
| AA778198 | PBX3 | pre-B-cell leukemia transcription factor 3 | 1 0392748 | 5 2182723 |
| AA452933 | HIST1H2AC | histone 1, H2ac | 1 0579834 | 3 4579164 |
| AA630082 | CDKN1B | cyclin-dependent kinase inhibitor 1B (p27, Kip1) | 1 0670366 | 2 655694 |
| T63511 | NOTCH3 | Notch homolog 3 (Drosophila) | 1 0688179 | 2 7674576 |
| AA775616 | SPP1 | Secreted phosphoprotein 1 | 1 0780387 | 7 6811427 |
| AA018457 | GAD1 | glutamate decarboxylase 1 (brain, 67kDa) | 1 0965873 | 5 5113503 |
| AA045965 | CASK | calcium/calmodulin-dependent serine protein kinase (MAGUK family) | 1 1223994 | 5 8941123 |
| AA630104 | LIPA | lipase A, lysosomal acid, cholesterol esterase (Wolman disease) | 1 1294891 | 2 1703059 |
| AA677185 | ANK3 | ankyrin 3, node of Ranvier (ankyrin G) | 1 1336501 | 3 5721374 |
| AA455910 | F2R | coagulation factor II (thrombin) receptor | 1 1356436 | 2 306576 |
| H61243 | UCP2 | uncoupling protein 2 (mitochondrial, proton carrier) | 1 1702299 | 11 2983329 |
| AA634006 | ACTA2 | actin, alpha 2, smooth muscle, aorta | 1 2099962 | 5 739342 |
| AA137031 | SOCS2 | suppressor of cytokine signaling 2 | 1 2273334 | 2 7284861 |
| R91950 | CYB5 | cytochrome b-5 | 1 2304401 | 7 1655273 |
| H23235 | PDGFRA | platelet-derived growth factor receptor, alpha polypeptide | 1 2400575 | 11 5330898 |
| W51794 | MMP3 | matrix metalloproteinase 3 (stromelysin 1, progelatinase) | 1 2844807 | 4 7450252 |
| AA036881 | CCR1 | chemokine (C-C motif) receptor 1 | 1 2878569 | 7 2852174 |
| AA454868 | PDGFRL | platelet-derived growth factor receptor-like | 1 305222 | 3 9833491 |
| H70775 | HIST1H2BC | histone 1, H2bc | 1 3084527 | 0 7671713 |
| R20686 | EDG1 | endothelial differentiation, sphingolipid G-protein-coupled receptor, 1 | 1 3310001 | 2 9557119 |
| AA478279 | INDO | indoleamine-pyrrole 2,3 dioxygenase | 1 3413956 | 2 7809638 |
| AA775872 | GPC3 | glypican 3 | 1 3750138 | 6 6893125 |
| AA488075 | STAT1 | signal transducer and activator of transcription 1, 91kDa | 1 4125271 | 4 599423 |
| AA461118 | DMD | dystrophin (muscular dystrophy, Duchenne and Becker types) | 1 433172 | 9 2010794 |
| AA455067 | SNCA | synuclein, alpha (non A4 component of amyloid precursor) | 1 4508695 | 5 5622682 |
| N67487 | MFAP2 | microfibrillar-associated protein 2 | 1 56398 | 5 2158861 |
| AA862371 | IFITM2 | interferon induced transmembrane protein 2 (1-8D) | 1 5670594 | 6 8662539 |
| AA479199 | NID2 | nidogen 2 (osteonidogen) | 1 5737082 | 8 0359634 |
| AA453759 | SPRY2 | sprouty homolog 2 (Drosophila) | 1 5792712 | 1 9118831 |
| AA243749 | DDR2 | discoidin domain receptor family, member 2 | 1 5899782 | 6 2542057 |
| AA453774 | RGS16 | regulator of G-protein signalling 16 | 1 6221764 | 12 3587295 |
| AA464417 | IFITM3 | interferon induced transmembrane protein 3 (1-8U) | 1 7001448 | 9 3917219 |
| H84154 | CCND2 | cyclin D2 | 1 7181152 | 11 7201815 |
| AA457042 | MX1 | myxovirus (influenza virus) resistance 1, interferon-inducible protein p78 (mouse) | 1 8499457 | 13 8069758 |
| AA670438 | UCHL1 | ubiquitin carboxyl-terminal esterase L1 (ubiquitin thiolesterase) | 1 8551382 | 11 6225785 |
| H79047 | IGFBP2 | insulin-like growth factor binding protein 2 | 1 8706844 | 11 9185466 |
| AA701914 | SREBF2 | sterol regulatory element binding transcription factor 2 | 1 9185107 | 0 6534325 |
| AA035144 | MEF2D | MADS box transcription enhancer factor 2, polypeptide D (myocyte enhancer factor 2D) | 1 9447293 | 5 5549015 |
| H06516 | A2M | alpha-2-macroglobulin | 2 0596673 | 12 0013787 |
| H07899 | VEGFC | Vascular endothelial growth factor C | 2 1037325 | 9 9993034 |
| H25223 | MEOX2 | mesenchyme homeo box 2 (growth arrest-specific homeo box) | 2 1908432 | 10 0950923 |
| AA464731 | S100A11 | S100 calcium binding protein A11 (calgizzarin) | 2 2092134 | 8 1836539 |
| H06516 | A2M | alpha-2-macroglobulin | 2 3261025 | 5 9085015 |
| AA857496 | MMP10 | matrix metalloproteinase 10 (stromelysin 2) | 2 4130963 | 11 1880585 |
| AA406020 | G1P2 | interferon, alpha-inducible protein (clone IFI-15K) | 2 5839981 | 8 3012323 |
| H79353 | FCER1G | Fc fragment of IgE, high affinity I, receptor for, gamma polypeptide | 2 5904608 | 4 1393514 |
| AA775447 | A2M | alpha-2-macroglobulin | 2 7035764 | 10 6439095 |
| T66815 | HIST1H1C | histone 1, H1c | 2 7048116 | 7 7171909 |
| AA630374 | DUSP6 | dual specificity phosphatase 6 | 2 8552158 | 13 748576 |
| AA489640 | IFIT1 | interferon-induced protein with tetratricopeptide repeats 1 | 3 0853278 | 9 5309834 |
| AA419251 | IFITM1 | interferon induced transmembrane protein 1 (9-27) | 3 2843501 | 15 1130547 |
| AA017544 | RGS1 | regulator of G-protein signalling 1 | 3 3592192 | 14 4956949 |

| | | | | |
|---|---|---|---|---|
| AA427801 | HAPLN1 | hyaluronan and proteoglycan link protein 1 | 3.5537826 | 13.9047635 |
| AA634103 | TMSB4X | thymosin, beta 4, X-linked | 4.416513 | 24.0908146 |
| H27986 | LMO4 | LIM domain only 4 | 4.5679163 | 16.6284803 |
| AA598610 | MEST | mesoderm specific transcript homolog (mouse) | 5.7271485 | 16.2105297 |

## A4. Microarray Data Ordered According to B value (Log Odds for the Bayesian Test), listed in Table A4.

## Table A4.

| Name | Symbol | Name | M | B |
|---|---|---|---|---|
| AA634103 | TMSB4X | thymosin, beta 4, X-linked | 4.416513 | 24.0908146 |
| AA598640 | MID1 | midline 1 (Opitz/BBB syndrome) | -2.6993415 | 18.0621977 |
| AA779165 | ARL4 | ADP-ribosylation factor-like 4 | -3.5187221 | 17.3540497 |
| H27986 | LMO4 | LIM domain only 4 | 4.5679163 | 16.6284803 |
| AA598610 | MEST | mesoderm specific transcript homolog (mouse) | 5.7271485 | 16.2105297 |
| AA644088 | CTSC | cathepsin C | -1.9210414 | 16.0705404 |
| AA419251 | IFITM1 | interferon induced transmembrane protein 1 (9-27) | 3.2843501 | 15.1130547 |
| AA017544 | RGS1 | regulator of G-protein signalling 1 | 3.3592192 | 14.4956949 |
| AA427801 | HAPLN1 | hyaluronan and proteoglycan link protein 1 | 3.5537826 | 13.9047635 |
| AA457042 | MX1 | myxovirus (influenza virus) resistance 1, interferon-inducible protein p78 (mouse) | 1.8499457 | 13.8069758 |
| AA630374 | DUSP6 | dual specificity phosphatase 6 | 2.8552158 | 13.748576 |
| AA458884 | S100A2 | S100 calcium binding protein 2 | -2.2626586 | 12.6309598 |
| AA453774 | RGS16 | regulator of G-protein signalling 16 | 1.6221764 | 12.3587295 |
| H06516 | A2M | Alpha-2-macroglobulin | 2.0596673 | 12.0013787 |
| H79047 | IGFBP2 | insulin-like growth factor binding protein 2 | 1.8706844 | 11.9185466 |
| H84154 | CCND2 | Cyclin D2 | 1.7181152 | 11.7201815 |
| AA670438 | UCHL1 | ubiquitin carboxyl-terminal esterase L1 (ubiquitin thiolesterase) | 1.8551382 | 11.6225785 |
| H23235 | PDGFRA | platelet-derived growth factor receptor, alpha polypeptide | 1.2400575 | 11.5330898 |
| H61243 | UCP2 | uncoupling protein 2 (mitochondrial, proton carrier) | 1.1702299 | 11.2983329 |
| AA857496 | MMP10 | matrix metalloproteinase 10 (stromelysin 2) | 2.4130963 | 11.1880585 |
| AA775447 | A2M | Alpha-2-macroglobulin | 2.7035764 | 10.6439095 |
| AA630800 | IFI30 | interferon, gamma-inducible protein 30 | -1.7533329 | 10.4799412 |
| R62603 | COL6A3 | Collagen type VI alpha 3 | -1.8635706 | 10.2447599 |
| H25223 | MEOX2 | mesenchyme homeo box 2 (growth arrest-specific homeo box) | 2.1908432 | 10.0950923 |
| H07899 | VEGFC | Vascular endothelial growth factor C | 2.1037325 | 9.9993034 |
| AA486321 | VIM | vimentin | -1.1255786 | 9.9788437 |
| AA497033 | CDO1 | cysteine dioxygenase, type I | 0.9962265 | 9.6941378 |
| AA489640 | IFIT1 | interferon-induced protein with tetratricopeptide repeats 1 | 3.0853278 | 9.5309834 |
| AA487893 | TM4SF1 | transmembrane 4 superfamily member 1 | -3.0059224 | 9.4054046 |
| AA464417 | IFITM3 | interferon induced transmembrane protein 3 (1-8U) | 1.7001448 | 9.3917219 |
| N57754 | TNRC3 | Trinucleotide repeat containing 3 | -1.0656046 | 9.2131253 |
| AA461118 | DMD | dystrophin (muscular dystrophy, Duchenne and Becker types) | 1.433172 | 9.2010794 |
| AA703392 | HFL1 | H factor (complement)-like 1 | -1.7508811 | 9.0889797 |
| T47443 | PROCR | protein C receptor, endothelial (EPCR) | 0.9409731 | 8.8732896 |
| AA608558 | PFKP | phosphofructokinase, platelet | -1.1945265 | 8.7036163 |
| AA406020 | G1P2 | interferon, alpha-inducible protein (clone IFI-15K) | 2.5839981 | 8.3012323 |
| AA482231 | MARCKS | myristoylated alanine-rich protein kinase C substrate | -1.7253124 | 8.2630318 |
| AA464731 | S100A11 | S100 calcium binding protein A11 (calgizzarin) | 2.2092134 | 8.1836539 |
| AA479199 | NID2 | nidogen 2 (osteonidogen) | 1.5737082 | 8.0359634 |
| AA476438 | HRASLS3 | HRAS-like suppressor 3 | -1.2315501 | 7.8637709 |
| AA482119 | ID3 | inhibitor of DNA binding 3, dominant negative helix-loop-helix protein | -2.0559957 | 7.8396963 |
| T66815 | HIST1H1C | histone 1, H1c | 2.7048116 | 7.7171909 |
| AA775616 | SPP1 | Secreted phosphoprotein 1 | 1.0780387 | 7.6811427 |
| AA598483 | TAX1BP1 | Tax1 (human T-cell leukemia virus type I) binding protein 1 | -2.299899 | 7.5802064 |
| AA181023 | EVI1 | ecotropic viral integration site 1 | -1.0303124 | 7.2976806 |
| AA036881 | CCR1 | chemokine (C-C motif) receptor 1 | 1.2878569 | 7.2852174 |
| R91950 | CYB5 | cytochrome b-5 | 1.2304401 | 7.1655273 |
| AA490172 | COL1A2 | collagen, type I, alpha 2 | -1.9076653 | 6.9470959 |
| AA862371 | IFITM2 | interferon induced transmembrane protein 2 (1-8D) | 1.5670594 | 6.8662539 |
| H82442 | ID2 | inhibitor of DNA binding 2, dominant negative helix-loop-helix protein | -0.9691106 | 6.7360241 |
| AA775872 | GPC3 | glypican 3 | 1.3750138 | 6.6893125 |
| AA115076 | CITED2 | Cbp/p300-interacting transactivator, with Glu/Asp-rich carboxy-terminal domain, 2 | -1.2123943 | 6.6438385 |
| N92901 | FABP4 | fatty acid binding protein 4, adipocyte | 0.7333144 | 6.5169975 |
| AA243749 | DDR2 | discoidin domain receptor family, member 2 | 1.5899782 | 6.2542057 |
| AA669136 | TCF4 | transcription factor 4 | 0.9639176 | 6.1645989 |
| H06516 | A2M | Alpha-2-macroglobulin | 2.3261025 | 5.9085015 |
| AA045965 | CASK | calcium/calmodulin-dependent serine protein kinase (MAGUK family) | 1.1223994 | 5.8941123 |
| AA634006 | ACTA2 | Actin, alpha 2, smooth muscle, aorta | 1.2099962 | 5.739342 |
| AA485427 | CRIP2 | cysteine-rich protein 2 | -0.9351656 | 5.6042529 |
| AA455067 | SNCA | synuclein, alpha (non A4 component of amyloid precursor) | 1.4508695 | 5.5622682 |
| AA035144 | MEF2D | MADS box transcription enhancer factor 2, polypeptide D (myocyte enhancer factor 2D) | 1.9447293 | 5.5549015 |

| | | | | |
|---|---|---|---|---|
| R38433 | PFKP | phosphofructokinase platelet | -0 8124395 | 5 5384606 |
| AA018457 | GAD1 | glutamate decarboxylase 1 (brain 67kDa) | 1 0985873 | 5 5113503 |
| AA486085 | TMSB10 | Thymosin beta 10 | -1 9571253 | 5 3140883 |
| AA778198 | PBX3 | pre-B-cell leukemia transcription factor 3 | 1 0392748 | 5 2182723 |
| N87487 | MFAP2 | microfibrillar-associated protein 2 | 1 56398 | 5 2158861 |
| AA101875 | CSPG2 | chondroitin sulfate proteoglycan 2 (versican) | 0 8471592 | 4 9133187 |
| AA464861 | CREM | Camp responsive element modulator | -1 4277106 | 4 8766463 |
| W51794 | MMP3 | matrix metalloproteinase 3 (stromelysin 1 progelatinase) | 1 2844807 | 4 7450252 |
| AA488075 | STAT1 | signal transducer and activator of transcription 1 91kDa | 1 4125271 | 4 599423 |
| AA430574 | PXN | paxillin | -0 6325283 | 4 5576419 |
| T68453 | PCMT1 | protein-L-isoaspartate (D-aspartate) O-methyltransferase | -0 8715628 | 4 330818 |
| H79353 | FCER1G | Fc fragment of IgE high affinity I receptor for gamma polypeptide | 2 5904608 | 4 1393514 |
| AA456621 | GGH | gamma-glutamyl hydrolase (conjugase folylpolygammaglutamyl hydrolase) | -1 2471388 | 4 0236273 |
| AA454868 | PDGFRL | platelet-derived growth factor receptor-like | 1 305222 | 3 9633491 |
| N63988 | IFIT2 | interferon-induced protein with tetratricopeptide repeats 2 | 0 972553 | 3 908129 |
| AA410188 | C1orf29 | chromosome 1 open reading frame 29 | -0 9156365 | 3 8285745 |
| N94820 | DIPA | hepatitis delta antigen-interacting protein A | -0 9235965 | 3 6162686 |
| AA129777 | SLC16A3 | solute carrier family 16 (monocarboxylic acid transporters) member 3 | -0 8846018 | 3 5949731 |
| AA677185 | ANK3 | ankyrin 3 node of Ranvier (ankyrin G) | 1 1336501 | 3 5721374 |
| AA291389 | ISGF3G | interferon-stimulated transcription factor 3 gamma 48kDa | 0 6536164 | 3 5598407 |
| AA452933 | HIST1H2AC | histone 1 H2ac | 1 0579834 | 3 4579164 |
| N76927 | BLVRB | biliverdin reductase B (flavin reductase (NADPH)) | 0 9251405 | 3 2770303 |
| AA455964 | GTF2E1 | general transcription factor IIE polypeptide 1 alpha 56kDa | 0 6851539 | 2 989838 |
| AA406552 | SLC2A3 | solute carrier family 2 (facilitated glucose transporter) member 3 | 0 6625057 | 2 9791724 |
| R20666 | EDG1 | endothelial differentiation sphingolipid G-protein-coupled receptor 1 | 1 3310001 | 2 9557119 |
| AA019459 | PTK9 | PTK9 protein tyrosine kinase 9 | -1 0099322 | 2 9086331 |
| H50251 | SH3GL3 | SH3-domain GRB2-like 3 | 0 849815 | 2 8884528 |
| T95289 | ERCC1 | excision repair cross-complementing rodent repair deficiency complementation group 1 (includes overlapping antisense sequence) | -0 8844539 | 2 8475761 |
| H99676 | COL6A1 | collagen type VI alpha 1 | -0 7017598 | 2 7887409 |
| AA478279 | INDO | indoleamine-pyrrole 2 3 dioxygenase | 1 3413956 | 2 7809638 |
| T63511 | NOTCH3 | Notch homolog 3 (Drosophila) | 1 0688179 | 2 7674576 |
| AA137031 | SOCS2 | suppressor of cytokine signaling 2 | 1 2273334 | 2 7284861 |
| AA485752 | ABCF1 | ATP-binding cassette sub-family F (GCN20) member 1 | 0 6507542 | 2 6731432 |
| AA630082 | CDKN1B | cyclin-dependent kinase inhibitor 1B (p27 Kip1) | 1 0670366 | 2 655694 |
| N52496 | BTG3 | BTG family member 3 | -0 9093137 | 2 5052952 |
| H60549 | CD59 | CD59 antigen p18-20 (antigen identified by monoclonal antibodies 16 3A5 EJ16 EJ30 EL32 and G344) | -1 0103923 | 2 3772821 |
| H95960 | SPARC | secreted protein acidic cysteine-rich (osteonectin) | 0 9397248 | 2 3700383 |
| W49619 | CDH2 | cadherin 2 type 1 N-cadherin (neuronal) | -0 7045605 | 2 3638834 |
| AA455910 | F2R | coagulation factor II (thrombin) receptor | 1 1356436 | 2 306576 |
| AA703449 | MEIS4 | Meis1 myeloid ecotropic viral integration site 1 homolog 4 (mouse) | 0 9763917 | 2 305843 |
| AA490208 | GSTT2 | glutathione S-transferase theta 2 | -0 9295173 | 2 2761419 |
| AA838691 | EPHX1 | epoxide hydrolase 1 microsomal (xenobiotic) | -0 7452518 | 2 1752498 |
| AA630104 | LIPA | lipase A lysosomal acid cholesterol esterase (Wolman disease) | 1 1294891 | 2 1703059 |
| AA489699 | COPS8 | COP9 constitutive photomorphogenic homolog subunit 8 (Arabidopsis) | -0 9848136 | 2 1501091 |
| H15677 | PPP2R2B | protein phosphatase 2 (formerly 2A) regulatory subunit B (PR 52) beta isoform | 0 605832 | 2 1160705 |
| R79082 | PTPRK | protein tyrosine phosphatase receptor type K | -0 7920798 | 2 0985028 |
| N49703 | CHD2 | chromodomain helicase DNA binding protein 2 | 0 7408736 | 2 0934191 |
| R40897 | OXCT5 | 3-oxoacid CoA transferase | -0 7022003 | 1 9708812 |
| T74567 | FHR-3 | complement factor H related 3 | -0 9353283 | 1 9641545 |
| AA411679 | GYG | glycogenin | -1 1567653 | 1 91832 |
| AA453759 | SPRY2 | sprouty homolog 2 (Drosophila) | 1 5792712 | 1 9118831 |
| AA426352 | H2A 1 | Histone H2A 1 | 0 6191979 | 1 8616346 |
| AA485371 | BST2 | Bone marrow stromal cell antigen 2 | 0 8484171 | 1 8447095 |
| H91647 | CLUL1 | clusterin-like 1 (retinal) | 0 5947801 | 1 8211137 |
| R31701 | COL11A1 | Collagen type XI alpha 1 | 0 8249885 | 1 7762696 |
| H04789 | GYG2 | glycogenin 2 | 0 5880985 | 1 6993231 |
| AA293671 | CD8B1 | CD8 antigen beta polypeptide 1 (p37) | -0 8814276 | 1 6805734 |
| R59579 | PTGDS | prostaglandin D2 synthase 21kDa (brain) | -1 2470994 | 1 6799566 |
| R38433 | PFKP | phosphofructokinase platelet | -0 8788533 | 1 603848 |
| H99681 | DP1 | polyposis locus protein 1 | -1 0938159 | 1 5491351 |
| AA598653 | POSTN | periostin osteoblast specific factor | -0 5410685 | 1 5104019 |
| H29322 | CAMK1 | calcium/calmodulin-dependent protein kinase I | -0 702849 | 1 4670563 |
| AA877595 | CDKN2A | cyclin-dependent kinase inhibitor 2A (melanoma p16 inhibits CDK4) | -0 8636069 | 1 3686615 |
| T67552 | ARNT | aryl hydrocarbon receptor nuclear translocator | 0 4724562 | 1 3005956 |
| AA457118 | TOMM34 | translocase of outer mitochondrial membrane 34 | -0 607676 | 1 2890304 |
| AA487460 | DPYSL2 | dihydropyrimidinase-like 2 | -0 8117585 | 1 2841634 |
| AA430524 | CAPZB | capping protein (actin filament) muscle Z-line beta | 0 6928569 | 1 274167 |
| AA425401 | STK24 | serine/threonine kinase 24 (STE20 homolog yeast) | 0 4936649 | 1 2625757 |
| H09721 | MARK3 | MAP/microtubule affinity-regulating kinase 3 | -0 9161254 | 1 2293674 |
| AA446659 | TAC1 | tachykinin precursor 1 (substance K substance P neurokinin 1 neurokinin 2 neuromedin L neurokinin alpha neuropeptide K neuropeptide gamma) | 1 02516 | 1 2249505 |
| AA398400 | CNN1 | calponin 1 basic smooth muscle | 0 7965682 | 1 1771523 |
| W73874 | CTSL | cathepsin L | -0 8514742 | 1 1268746 |
| AA041400 | LRBA | LPS-responsive vesicle trafficking beach and anchor containing | 0 700007 | 1 0071921 |
| AA196000 | ACTN3 | actinin alpha 3 | 0 8070318 | 0 9781952 |
| N80129 | MT1X | metallothionein 1X | -0 54165 | 0 9763709 |

| | | | | |
|---|---|---|---|---|
| AA284072 | CDKN3 | cyclin-dependent kinase inhibitor 3 (CDK2-associated dual specificity phosphatase) | -0 9484494 | 0 9679128 |
| AA456298 | HIST2H2BE | histone 2 H2be | 0 4870318 | 0 856575 |
| AA457038 | ITGB1BP1 | integrin beta 1 binding protein 1 | -0 8697968 | 0 814672 |
| H70775 | HIST1H2BC | histone 1 H2bc | 1 3084527 | 0 7671713 |
| AA412053 | CD9 | CD9 antigen (p24) | -1 3702724 | 0 7528075 |
| AA701914 | SREBF2 | sterol regulatory element binding transcription factor 2 | 1 9185107 | 0 6534325 |
| T58873 | FOSL2 | FOS-like antigen 2 | -0 7370583 | 0 6271127 |
| H17398 | BA13 | Brain specific angiogenesis inhibitor | 0 5234054 | 0 6101628 |
| AA497055 | PSMD12 | proteasome (prosome macropain) 26S subunit non-ATPase 12 | -0 8343878 | 0 5946626 |

A5. Mean Variance Pairs (MVA) Before and After Data Normalisation. Presented in Figure A5.

a.

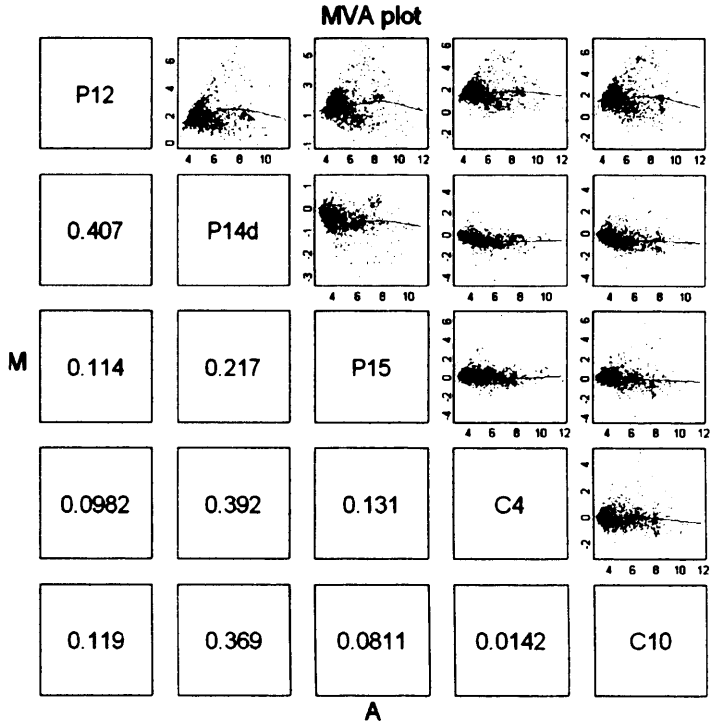


b.

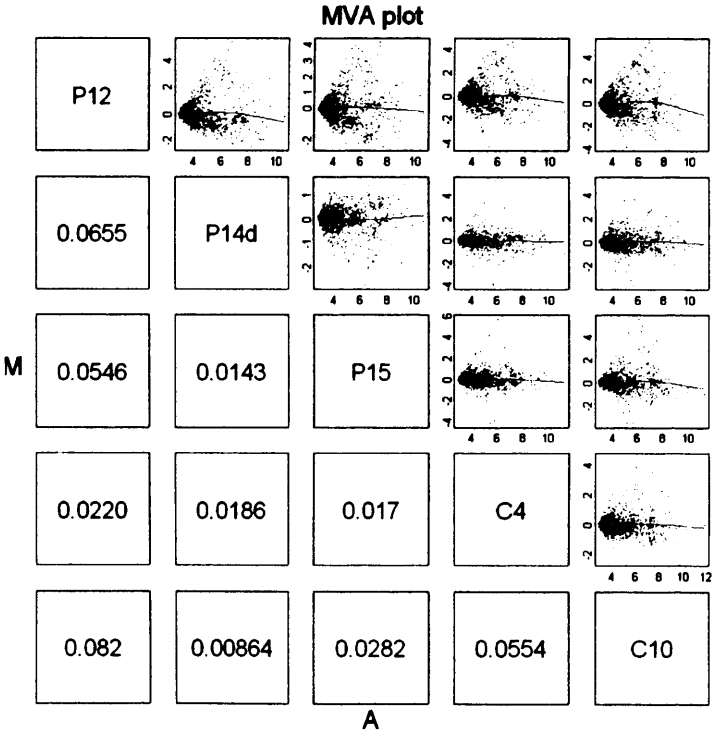


Figure A5. Mean variance (MVA) pairs. The red line is a loess fit and the numbers are the average variance of each scatter plot. a. MVA pairs before normalisation. b. MVA pairs after normalisation.